Netrin-1 and neurons in hepatocellular carcinoma

Ievgeniia Chicherova

N°d'ordre NNT : 2022LYSE1060

THESE de DOCTORAT DE L'UNIVERSITE DE LYON
opérée au sein de
l'Université Claude Bernard Lyon 1

Ecole Doctorale N° 340
Biologie Moléculaire Intégrative et Cellulaire (BMIC)

Spécialité de doctorat : Maladies chroniques du foie
Discipline : Pharmacologie et recherche translationnelle

Soutenue publiquement le 19/04/2022, par :
Ievgeniia CHICHEROVA

Netrin-1 and neurons in hepatocellular carcinoma

Nétrine-1 et neurones dans le carcinome hépatocellulaire

Devant le jury composé de :

Mr. Pr. **Fabien ZOULIM**, PU-PH, CRCL - HCL	Président, examinateur
Mme. Dr. **Valérie PARADIS**, PU-PH, Paris VII – Inserm	Rapporteure
Mme. Dr. **Sandra REBOUISSOU**, CR, Inserm	Rapporteure
Mr. Dr. **Arnaud MILLET,** CR, IAB	Examinateur
Mr. Dr. **Romain PARENT**, CR, CRCL	Directeur de thèse
Mr. Dr. **Thomas DECAENS**, PU-PH, IAB - CHU Grenoble	Co-directeur de thèse

Université Claude Bernard – LYON 1

Président de l'Université	M. Frédéric FLEURY
Président du Conseil Académique	M. Hamda BEN HADID
Vice-Président du Conseil d'Administration	M. Didier REVEL
Vice-Président du Conseil des Etudes et de la Vie Universitaire	Mme Céline BROCHIER
Vice-Président de la Commission de Recherche	M. Petru MIRONESCU
Directeur Général des Services	M. Pierre ROLLAND

COMPOSANTES SANTE

Département de Formation et Centre de Recherche en Biologie Humaine	Directrice : Mme Anne-Marie SCHOTT
Faculté d'Odontologie	Doyenne : Mme Dominique SEUX
Faculté de Médecine et Maïeutique Lyon Sud - Charles Mérieux	Doyenne : Mme Carole BURILLON
Faculté de Médecine Lyon-Est	Doyen : M. Gilles RODE
Institut des Sciences et Techniques de la Réadaptation (ISTR)	Directeur : M. Xavier PERROT
Institut des Sciences Pharmaceutiques et Biologiques (ISBP)	Directeur : M. Claude DUSSART

COMPOSANTES & DEPARTEMENTS DE SCIENCES & TECHNOLOGIE

Département Génie Electrique et des Procédés (GEP)	Directrice : Mme Rosaria FERRIGNO
Département Informatique	Directeur : M. Behzad SHARIAT
Département Mécanique	Directeur M. Marc BUFFAT
Ecole Supérieure de Chimie, Physique, Electronique (CPE Lyon)	Directeur : Gérard PIGNAULT
Institut de Science Financière et d'Assurances (ISFA)	Directeur : M. Nicolas LEBOISNE
Institut National du Professorat et de l'Education	Directeur : M. Pierre CHAREYRON
Institut Universitaire de Technologie de Lyon 1	Directeur : M. Christophe VITON
Observatoire de Lyon	Directrice : Mme Isabelle DANIEL
Polytechnique Lyon	Directeur : Emmanuel PERRIN
UFR Biosciences	Administratrice provisoire : Mme Kathrin GIESELER
UFR des Sciences et Techniques des Activités Physiques et Sportives (STAPS)	Directeur : M. Yannick VANPOULLE
UFR Faculté des Sciences	Directeur : M. Bruno ANDRIOLETTI

Acknowledgments

To the members of the thesis jury

I would like to thank my supervisor **Romain PARENT** for the opportunity to start a PhD in the field of liver pathologies, for your availability and advice, for the trust and liberty that you gave me.

Our group leader professor **Fabien ZOULIM**, I am very grateful for your welcome. My PhD experience was scientifically rich and warm thanks to the well-equipped laboratory, efficacious mentoring and the positive human environment. Thank you for accepting to be the president of my jury.

My co-director **Thomas DECAENS**, thank you for your advice and support all along these 4 years of my PhD.

Professor **Valérie PARADIS**, **Sandra REBOUISSOU** and **Arnaud MILLET,** thank you for revising my thesis and participating in my thesis defense. I am very grateful to you for taking the time to evaluate my work.

Abstract

Chronic liver inflammation can lead to chronic liver diseases (CLD), including hepatitis, cirrhosis and hepatocellular carcinoma (HCC), which is the most common malignant primary liver tumor and is the 3rd deadliest cancer in terms of mortality worldwide. Regardless of the etiological factor, all CLDs share numerous common pathophysiological mechanisms, including unfolded protein response (UPR), chronic inflammation and fibrosis.

Using animal models and clinical samples we studied a potential common denominator of CLDs and HCC, which is the system of axonal guidance factor netrin-1 and its dependence receptors UNC5s. Netrin-1, known as pro-oncogenic in other solid tumors, is induced during hepatic inflammation, and the pro-apoptotic signal of UNC5 receptors is attenuated with overall increased ligand/receptor balance in cirrhosis and HCC.

Chronic inflammation is mediated by multiple actors of the immune system. The implication of the autonomic nervous system (ANS) in hepatic inflammation and CLD progression remains seldom addressed if any, and poorly understood. Looking at the dynamics of pre-synaptic and post-synaptic neuronal markers in cirrhosis and HCC, we observed the reshaping of the balance between intrahepatic sympathetic (adrenergic) and parasympathetic (cholinergic) nervous systems. *In vivo* models of cirrhosis-related HCC showed the progressive establishment of a cholinergic orientation throughout the different stages of disease evolution. The overall cholinergic orientation in HCC was associated with anti-inflammatory microenvironment and poorer survival in patients. The observed CLD-to-HCC progression *in vivo* was accompanied by the overexpression of immature neuronal markers. Altogether, we showed that the parasympathetic arm of the ANS is implicated in the pathophysiology of HCC, a notion grounding the interest of ANS-targeting drugs in HCC studies, many of which being clinically safe and well characterized.

Trying to establish the connection between pro-survival and chemotactic netrin-1 and intrahepatic ANS, we observed a positive association between netrin-1/UNC5s and cholinergic signal in HCC. Netrin-1 targeting by the monoclonal antibody NP137, currently studied in the clinical trials in the treatment of advanced solid tumors, showed remodeling of ANS orientation, confirming the sensitivity of ANS to netrin-1/UNC5 axis in the hepatic pathological context.

Some common molecular anomalies in HCC (*TERT* promoter and *CTNNB1* gene), showed an association with netrin-1/UNC5 system, whereas mutations in *TP53*, a known regulator of *NTN1* and *UNC5*s expression did not show any association with netrin-1/UNC5 axis reshuffling in clinical HCC samples, also unsensitive to the functionality status of p53. In average, *CTNNB1*-mutated clinical samples correlated with adrenergic polarity of HCC, whereas *TP53* mutations appear to be positively associated with cholinergic polarity of HCC.

Taken together, while causal relationships between these factors and HCC need be more documented, my thesis results suggest the putative pro-cancerogenic role of the netrin-1 and the implication of the neuroregulation via ANS in the CLD and HCC development.

Key words: Autonomic Nervous System (ANS), Chronic Liver Disease (CLD), cirrhosis, Hepatocellular Carcinoma (HCC), Netrin-1 (NTN1), UNC5.

Résumé

L'inflammation hépatique chronique peut entraîner des maladies chroniques du foie (MCF), notamment l'hépatite, la cirrhose et le carcinome hépatocellulaire (CHC), qui est la tumeur maligne primaire du foie la plus fréquente et le troisième cancer en termes de mortalité dans le monde. Indépendamment des facteurs étiologiques, toutes les MCFs partagent de nombreux mécanismes physiopathologiques communs : réponse aux protéines mal repliées (UPR), inflammation chronique et fibrose.

A l'aide d'un modèle animal et d'échantillons cliniques nous avons étudié un autre dénominateur commun des MCFs et du CHC : la molécule neurotrope de guidage axonal nétrine-1 et ses récepteurs à dépendance UNC5A, UNC5b et UNC5C. La nétrine-1, connue de ces propriétés pro-oncogéniques dans d'autres tumeurs solides, est induite pendant l'inflammation hépatique, alors que le signal pro-apoptotique des récepteurs UNC5 est atténué avec un équilibre ligand/récepteur globalement augmenté dans la cirrhose et le CHC.

L'inflammation chronique est médiée par de multiples acteurs du système immunitaire. L'implication du système nerveux autonome (SNA) dans l'inflammation hépatique et la progression du CLD reste mal comprise. En étudiant l'implication des signaux neuronaux pré-synaptiques et post-synaptiques dans la cirrhose et le CHC, nous avons observé le remaniement de l'équilibre entre les systèmes nerveux sympathique (adrénergique) et parasympathique (cholinergique) intra-hépatiques. Le modèle animal de CHC sur cirrhose a montré l'établissement progressif d'une orientation cholinergique à travers les différents stades de la fibrose. Le signal cholinergique global du CHC était associé à un microenvironnement anti-inflammatoire et à une survie plus faible chez les patients. La progression observée des MCFs vers le CHC *in vivo* était accompagnée de la surexpression de marqueurs neuronaux immatures dans le CHC. Dans l'ensemble, nous avons montré que le bras parasympathique du SNA est impliqué dans la physiopathologie du CHC, suggérant l'utilisation de médicaments ciblant le SNA, dont beaucoup sont cliniquement sûrs et bien caractérisés, dans les études sur le CHC.

En tentant d'établir le lien entre la nétrine-1 ayant des propriétés anti-apoptotiques et chimiotactiques et le SNA intrahépatique, nous avons identifié une corrélation positive entre le système nétrine-1/UNC5s et le signal cholinergique dans le CHC. Le ciblage de la nétrine-1 par l'anticorps monoclonal NP137, actuellement étudié dans des essais cliniques dans le traitement des tumeurs solides avancées, induit un remaniement de l'orientation du SNA, confirmant la sensibilité du SNA à l'axe nétrine-1/UNC5 dans le contexte hépatique pathologique. Les anomalies moléculaires les plus courantes dans le CHC au niveau du promoteur du gène *TERT* et au niveau du gène *CTNNB1*, ont montré une association avec le système nétrine-1/UNC5, alors que les mutations dans *TP53*, un régulateur de l'expression de *NTN1* et *UNC5*x n'ont pas montré d'association dans le remodelage de l'axe nétrine-1/UNC5 dans les échantillons cliniques de CHC, également insensibles au statut fonctionnel de la protéine p53. Globalement, les échantillons cliniques hébergeant une mutation dans le gène *CTNNB1* sont corrélés à la polarité adrénergique du CHC, tandis que les mutations dans le gène *TP53* apparaissent comme positivement associées à la polarité cholinergique du CHC.

Dans l'ensemble, bien que devant être enrichis en termes d'études de causalité impliquant différents facteurs modulables et le phénotype de la maladie, les résultats de ma thèse suggèrent

le rôle pro-cancérogène de la nétrine-1 et l'implication de la neuroregulation associée via l'orientation de SNA dans les MCFs et le CHC.

Mots clés : Système Nerveux Autonome (SNA), maladie chronique du foie, cirrhose, Carcinome Hépatocellulaire (CHC), Netrin-1 (NTN1), UNC5.

Résumé substantiel

Nétrine-1 et neurones dans le carcinome hépatocellulaire

Ce travail a été réalisé par Ievgeniia Chicherova au sein du Centre de Recherche en Cancérologie de Lyon (CRCL, UMR INSERM 1052, CNRS 5286, Centre Léon Berard, Dirigé par Patrick Mehlen).

Directeur de thèse : Romain Parent

Co-directeur de thèse : Thomas Decaens

Introduction

Les maladies chroniques du foie touchent environ 1.5 milliard personnes dans le monde. Elles représentent des facteurs de risque majeurs pour le développement du carcinome hépatocellulaire (CHC). Virales ou non-virales, les maladies chroniques du foie partagent les mêmes mécanismes pathologiques : inflammation et remaniement de la matrice extracellulaire évoluant vers la fibrose. Bien que la nétrine-1 soit normalement exprimée à de faibles niveaux dans les nerfs périphériques, cette molécule de guidage axonale surexprimée dans de nombreux cancers et plusieurs maladies inflammatoires, pourrait jouer un rôle dans la tumorigenèse en régulant l'apoptose. La nétrine-1 agit par le biais de la liaison aux "récepteurs à dépendance", tels que DCC et UNC5A-D. L'expression de l'un de ces récepteurs à la surface d'une cellule cancéreuse rend cette cellule dépendante de la disponibilité du ligand pour sa survie. Par conséquent, la perte de l'activité des récepteurs de dépendance confère un avantage sélectif aux cellules tumorales.

Notre groupe de recherche a étudié le rôle de la nétrine-1 et de ses récepteurs dans les pathologies chroniques hépatiques virales et en particulier dans le contexte de l'infection par le virus d'hépatite C (VHC). Il a été démontré que la nétrine-1 est surexprimée dans le foie cirrhotique et qu'elle protège les cellules dédifférenciées et cancéreuses de la mort cellulaire induite par l'UPR. Son récepteur UNC5A est régulé à la baisse en cas de stress du réticulum endoplasmique, surexprimé dans le foie fibrotique mais s'effondre chez les patients atteints de CHC, et de façon plus frappante chez les patients infectés par le VHC et essentiellement chez ceux qui présentent des stades avancés de fibrose (F2-F4), ce qui suggère que le VHC a un impact important sur la biogenèse de UNC5A chez les patients, en particulier dans le foie prénéoplasique. Il semblerait donc que le signal anti-apoptotique du système nétrine-1/UNC5 favorise la transformation maligne du foie cirrhotique en CHC, bien que ceci reste à démontrer causalement.

Les études récentes ont démontré que l'infiltration des nerfs du système nerveux autonome (SNA) favorise le développement des maladies chroniques du foie et du CHC. Malgré les résultats parfois contradictoires, le rôle exact des nerfs sympathiques et parasympathiques dans les pathologies chroniques du foie reste flou. À ce jour, il a été démontré que les récepteurs post-synaptiques des SNA, tant adrénergiques que cholinergiques, agissent défavorablement ou au contraire dans l'intérêt du patient dans certains modèles expérimentaux de cancer.

Dans ce contexte, les principaux objectifs de ma thèse consistaient à :

1) Etudier le rôle de nétrine-1 dans la cirrhose et le CHC, et tenter d'identifier la population des patients susceptibles de bénéficier de la thérapie ciblant la protéine nétrine-1.
2) Etudier le rôle du SNA dans la cirrhose et le CHC
3) Etudier la relation entre le système nétrine-1/UNC5 et l'innervation intrahépatique par le SNA.

4) Démontrer la possibilité de cibler le système nétrine-1/UNC5 dans le traitement et la prévention du CHC.

Matériel et méthodes

Nous avons utilisé les échantillons cliniques tumoraux et para-tumoraux de patients atteints de CHC afin de caractériser l'expression de nétrine-1 et ses récepteurs par qRT-PCR et de quantifier l'expression des protéines netrin-1 et UNC5B. Les Tumor Microarrays (TMA) ont été utilisés afin de quantifier l'expression protéique de nétrine-1 par immunohistochimie. Des tests pharmacologiques évaluant les effets de la modulation de la nétrine-1 sur la viabilité cellulaire ont été réalisées sur des lignées cellulaires humaines (lignées cellulaires de CHC Hep3B, CLP13, Huh7, Huh7.5, HepG2 et lignée de cellules progénitrices bipotentes prolifératives HepaRG) et sur des hépatocytes humains primaires, exprimant ou non la nétrine-1. Des rats traités au diethylnitrosamine (DEN) ont été utilisés pour mimer la physiopathologie du CHC cirrhotique dans l'étude de ciblage de nétrine-1 en monothérapie. Des souris transgéniques surexprimant la nétrine-1 ont été utilisées afin d'élucider le rôle de la nétrine-1 dans le développement du CHC, décrire la physiopathologie hépatique associée, étudier la composante immunitaire et nerveuse ainsi que leur relation dans le contexte de surexpression de nétrine-1.

Résultats

Nous avons démontré que les ratios ligand/récepteur *NTN1/UNC5A* et *NTN1/UNC5C* sont régulés à la hausse dans les tumeurs par rapport au foie cirrhotique, indépendamment de facteur étiologique. Bien que la surexpression de la nétrine-1 dans les pathologies chroniques du foie était connue pour conférer un avantage à l'infection par le VHC, favorisant l'infectivité du virus, notre étude a montré que le rôle pathologique de la nétrine-1 est étendu au contexte non viral du développement du CHC. De plus, nous avons illustré que l'axe nétrine-1/UNC5 présente une valeur pronostique dans l'apparition du CHC sur un terrain cirrhotique. De manière importante, la nétrine-1 a été identifiée comme un facteur de risque de la progression de la cirrhose vers le CHC. Par contre, l'analyse de corrélation de l'expression de la nétrine-1 (ARNm ou protéine) avec les paramètres clinico-biologiques des patients n'a pas identifié une éventuelle population cible susceptible d'être répondeurs au traitement ciblant la nértrine-1.

L'analyse des mutations dans le gène *TP53* n'a pas montré d'association entre le statut mutationnel du gène ou la fonctionnalité de la protéine p53 et l'expression de nétrine-1/UNC5 dans la cirrhose ou le CHC. Cependant, nous avons trouvé une association entre l'expression de ligand et des récepteurs et l'expression de *TERT*. *NTN1, UNC5A, UNC5B* et *UNC5C* sont positivement corrélés à l'induction de *TERT* dans le CHC. D'autre part, les ratios *NTN1/UNC5* semblent être négativement corrélés avec l'expression de *TERT* dans la cirrhose et ne montrent aucune corrélation dans les échantillons de CHC, en suggérant la dynamique différentielle du remodelage et de la transformation des tissus dans la cirrhose et les tumeurs. Des découvertes récentes ont démontré que la nétrine-1 régule la voie de signalisation Wnt classique par la stabilisation indirecte de la β-caténine, notamment par son récepteur UNC5B. Notre étude n'a pas montré de corrélation entre l'expression de la nétrine-1 (ARNm ou protéine) et le statut mutationnel *CTNBN1* chez les patients atteints de CHC, mais nous avons identifié une association négative entre les mutations *CTNNB1* et *UNC5A, UNC5B* et *UNC5C*, suggérant une relation entre la voie des récepteurs à dépendance et la voie de signalisation canonique de Wnt.

Nous avons ensuite considéré l'implication du SNA dans la cirrhose et le CHC dans des échantillons de patients et dans un modèle expérimental de CHC cirrhotique chez le rat. L'analyse bioinformatique a révélé que le nombre de voies immunitaires liées aux tumeurs adrénergiques

était plus élevé que celles liées aux tumeurs cholinergiques. De plus, les cellules $CD4^+$ naïves, les cellules γδ T, les cellules B et les cellules dendritiques myéloïdes étaient significativement enrichies dans les tumeurs cholinergiques, alors que les cellules souches hématopoïétiques, les cellules natural killers et les macrophages M2 étaient enrichis dans les tumeurs adrénergiques, ce qui suggère que la signalisation adrénergique est corrélée aux processus immunitaires qui peuvent mieux interférer avec la progression de la pathologie. De plus, la polarité adrénergique des tumeurs était associée aux mutations activatrices dans le gène *CTNNB1*, alors que la polarité cholinergique était associée aux mutations dans le gène *TP53.*

Nous avons étudié pour la première fois les effets du ciblage de la nétrine-1 dans le contexte des maladies chroniques du foie et HCC. Le ciblage de la nétrine-1 par l'anticorps monoclonal NP137, qui est actuellement étudié dans les études cliniques dans le traitement des tumeurs solides, n'a pas montré d'effet *in vitro*. Conscients de possibles discordances d'effets entre les études *in vitro* et *in vivo*, nous avons étudié les effets d'un anticorps anti-nétrine-1 humanisé utilisé en oncologie clinique en monothérapie chez le rat développant un CHC sur foie cirrhotique. L'étude chez des rats traités par DEN n'a pas révélé d'efficacité de la capture de la nétrine-1 par cet anticorps dans le traitement du CHC sur un fond cirrhotique.

Nous avons en revanche observé que chez les rats traités par DEN, la capture de la nétrine-1 induit la régulation à la baisse du signal adrénergique global dans les tissus cirrhotiques, mais n'affecte pas l'équilibre adrénergique/cholinergique dans les tumeurs. Le rapport adrénergique/cholinergique global était plus faible dans le tissu tumoral des rats traités avec DEN. La corrélation négative identifiée entre l'orientation adrénergique et l'axe netrin-1/UNC5 dans les tissues cirrhotiques et la corrélation positive avec, en revanche, les marqueurs cholinergiques dans les tissues tumoraux des patients suggèrent une régulation différentielle du SNA dans la cirrhose par rapport au CHC. Comme notre étude n'a montré aucune corrélation entre l'expression du ligand nétrine-1 et de ses récepteurs UNC5 dans les tumeurs, mais l'existence d'une telle corrélation positive dans la cirrhose, nous pouvons émettre l'hypothèse que la relation ANS-nétrine-1/UNC5 peut avoir aussi suivre une dynamique différentielle dans la cirrhose et dans les tumeurs.

Conclusion et perspectives

Les récepteurs à dépendance de type UNC5 peuvent transduire deux signaux opposés : lorsqu'ils ne sont pas liés au ligand, ils induisent un signal apoptotique, alors que lorsque liés au ligand, ils induisent la survie, et la migration cellulaire. L'axe nétrine-1/UNC5 semble avoir rôle pro-hépatocarcinogénique dans le contexte cirrhotique. L'étude chez les souris transgéniques surexprimant la nétrine-1 aidera à comprendre le rôle biologique de la nétrine-1 dans l'apparition et la progression du cancer du foie. Les résultats attendus aideront également à comprendre la modulation des composants immunitaires par l'analyse FACS, et la relation ANS - nétrine-1/UNC5 par immunomarquage dans les tumeurs et les tissus péri-tumoraux. Bien que le rôle du nerf vague dépende de l'organe et de la pathologie, la modulation de l'innervation hépatique dans les MCFs et le CHC pourrait susciter un intérêt croissant, et l'essai de médicaments anticholinergiques devenir une approche envisageable. Avec presque aucune donnée d'un effet clair de la vagotomie (chirurgicale ou pharmacologique) dans le contexte hépatique, tester des agents anti-cholinergiques, dont beaucoup sont cliniquement sûrs et bien caractérisés, en monothérapie ou en combinaison avec des médicaments anti-CHC, aidera à comprendre a minima les conséquences de la modulation pharmacologique du système cholinergique, mais aussi de l'équilibre adrénergique/cholinergique. A notre connaissance, la régulation du SNA (neuropathie et neurogenèse) dans le CHC n'a jamais été étudiée *in vivo* auparavant. Etant donné que le CHC survient sur un fond cirrhotique dans 90% des cas, nous avons montré que le modèle

animal de rats chroniquement traités par DEN, qui récapitule la physiopathologie humaine du CHC, peut constituer un outil d'étude pertinent de la neurorégulation dans le CHC.

Publications

1. **Neural features of hepatocellular carcinoma define targetable neuroclasses with distinct pathogenic and prognostic statuses**

Charlotte Hernandez°, Claire Verzeroli°, **Ievgeniia Chicherova**, Abud-José Farca-Luna, Laurie Tonon, Pascale Bellaud, Bruno Turlin, Alain Fautrel, Zuzana Macek-Jilkova, Thomas Decaens, Sandra Rebouissou, Alain Viari, Fabien Zoulim, Romain Parent

(Submitted on 2022-02-18, Cancer Cell)

2. **Hepatic inflammation elicits production proinflammatory netrin-1 through exclusive activation of translation**

Romain Barnault°, Claire Verzeroli°, Carole Fournier, Maud Michelet, Anna Rita Redavid, **Ievgeniia Chicherova,** Annie Adrait, Olga Khomich, Fleur Chapus, Mathieu Richaud, Veronika Reiterer, Federica Grazia Centonze, Julie Lucifora, Birke Bartosch, Michel Rivoire, Hesso Farhan, Yohann Couté, Valbona Mirakaj, Thomas Decaens, Patrick Mehlen, Benjamin Gibert, Fabien Zoulim, Romain Parent

(Published on 2022-03-07, Hepatology)

Table of contents

Figures

Tables

Abbreviations

AAV	Adeno-Associated Virus
ACh	AcetylCholine
AFB1	AFlatoxin B1
AFP	Alpha-FetoProtein
ALD	Alcoholic Liver Disease
ANCOVA	Analysis Of COVariance
ANOVA	ANalysis Of Variance
ANS	Autonomic Nervous System
ATF6	Activated Transcription Factor 6
APC	Antigen-Presenting Cell
AVGDG	Align - Grantham Variation - Grantham Variation
BAFs	BRG1- or HRBM-Associated factors
BCLC	Barcelona Clinic Liver Cancer
BMP-2	Bone Morphogenetic Protein 2
CCL2/3/5/8/19	chemokine (C-C motif) Ligand 2/3/5/8/19
CI	Confidence Interval
CLD	Chronic Liver Disease
CNS	Central Nervous System
CRC	ColoRectal Cancer
CRP	C-Reactive Protein
CXCL10	C-X-C motif chemokine Ligand 10
DAMPs	Danger-Associated Molecular Patterns
DAPK	Death-Associated Protein Kinase
DCs	Dendritic Cells
DCC	Deleted in Colorectal Cancer
DCX	Doublecortin
DNA	DeoxyriboNucleic Acid
DSCAM	Down Syndrome Cell Adhesion Molecule
EGF	Epidermal Growth Factor
EGFR	Epithelial Growth Factor Receptor
EMT	Epithelial-Mesenchymal Transition
ER	Endoplasmic Reticulum
ETS	Erythroblast Transformation Specific
FACS	Flow Cytometry or Fluorescence-Activated Cell Sorting
FGF	Fibroblast Growth Factor
FGFR	Fibroblast Growth Factor Receptor
FzD	FrizzleD
GSEA	Gene Set Enrichment Analysis
HBV	Hepatitis B Virus
HCC	HepatoCellular Carcinoma
HCV	Hepatitis C Virus
HGF	Hepatocyte Growth Factor
HR	Hazard Ratio
HSC	Hepatic Stellate Cells
HSPG	Heparan Sulfate Proteoglycans
IC50	Inhibitory Concentration 50
IGF-1	Insulin Growth Factor-1
IL-1/6/8/10	InterLeukin-1/6/8/10
INA	Alpha-InterNexin
JAK	Janus Kinases
KCs	Kupffer Cells
LARP1	LA-Related Protein 1
LGR5	Leucine-rich repeat-containing G-protein coupled Receptor 5

LSECs	Liver Sinusoidal Endothelial cells
MRI	Magnetic Resonance Imaging
NAFLD	Non-Alcoholic Fatty Liver Disease
nAG	newt Anterior Gradient protein
NASH	Non-Alcoholic SteatoHepatitis
NES	Normalized Enrichment Score
NKs	Natural Killer cells
NKTs	Natural Killers T cells
NTR	NeTRin-like module
NeuN	Neuronal Nuclear protein
NGF	Nerve Growth Factor
NGS	Next Generation Sequencing
NRA	Neutral Red Assay
NS5A	NonStructural Protein 5
NSCLC	Non-Small Cell Lung Cancer
OS	Overall Survival
PAMPs	Pathogen-Associated Molecular Patterns
PBS	Phosphate-Buffered Saline
PCA	Principal Component Analysis
PCOLCEs	ProCOLlagen C-proteinase Enhancer proteins
PDAC	Pancreatic Ductal AdenoCarcinoma
PEPCK	PhosphoEnolPyruvate CarboxyCinase
PERK	Protein Kinase RNA-like Endoplasmic Reticulum Kinase
PHHs	Primary Human Hepatocytes
PI3K	PhosphoInositide-3-Kinase
PNI	Peri-Neural Invasion
PFI	Progression-Free Interval
PTEN	Phosphatase and TENsin homolog
RET	Rearrangement During Transfection
RNA	RiboNucleic Acid
ROS	Reactive Oxygen Species
SFK	Src-Family Kinase
SIFT	Sorts Intolerant From Tolerant
SRB	SulfoRhodamine B
ssGSEA	Single Sample GSEA
STAT	Signal Transducer and Activator of Transcription protein
TACE	TransArterial EhemoEmbolization
TAMs	Tumor-Associated Macrophages
TERT	TElomerase Reverse Transcriptase
TGF-α/β	Tumor Growth Factor alpha/beta
TH	Tyrosine Hydroxylase
TIMPs	Tissue Inhibitors of Metallo-Proteinases
TKI	Tyrosine Kinase Inhibitor
TMA	Tumor MicroArray
TNM	Tumor-Node-Metastasis
Treg	regulatory T cells
TSC1/2	Tuberous Sclerosis 1/2
UNC5	UNCoordinated-5 homolog
UPR	Unfolded Protein Response
VAChT	Vesicular ACh Transporter
VEGF	Vascular Endothelial Growth Factor
VEGFR	Vascular Endothelial Growth Factor Receptor

Chapter 1: Background

1.1. Chronic liver diseases and hepatocellular carcinoma

1.1.1. The liver

Liver physiology

The liver is the largest internal organ of the body and is the center of multiple physiological processes: detoxification, synthesis, storage and metabolism (**Figure *1***).

The liver is an organ of detoxification, as it helps to eliminate toxins, drugs, alcohol and destroyed red blood cells' hemoglobin. Bilirubin is absorbed, stored and conjugated by the hepatocytes and then secreted into the bile or the urine. The blood concentration of bilirubin reflects the good operational status of the hepatocytes, while its accumulation in the bloodstream causes jaundice.

Also, liver has unique immunoregulatory functions with its local hepatic antigen-presenting cells (APCs), including myeloid and plasmacytoid dendritic cells, liver sinusoidal endothelial cells, Kupffer cells and hepatocytes. In case of infection, Kupffer cells are able to phagocyte and eliminate the bacteria coming from the digestive tract.

The liver is an important reservoir for minerals, vitamins (e.g., A, B12, D, E, K), glycogen and lipids storage. It is also a place of biosynthesis and secretion; it allows the production of albumin, most blood clotting factors (fibrinogen, prothrombin, factor V, VII - XII, proteins C and S, antithrombin, and von Willebrand factor), hormones (e.g., IGF-1, angiotensinogen), bile and electrolytes (e.g., Na^+, K^+, Cl^-, $HCO3^-$). Bile acids follow an enterohepatic cycle: they are synthesized in the liver, secreted in the bile, and reach the intestine to participate in digestion. The majority of bile acids is reabsorbed by the enterocytes, conveyed towards the bloodstream and captured by the hepatocytes again, completing the enterohepatic loop, to ensure continuously two fundamentally important functions – fat digestion and absorption as well as cholesterol homeostasis.

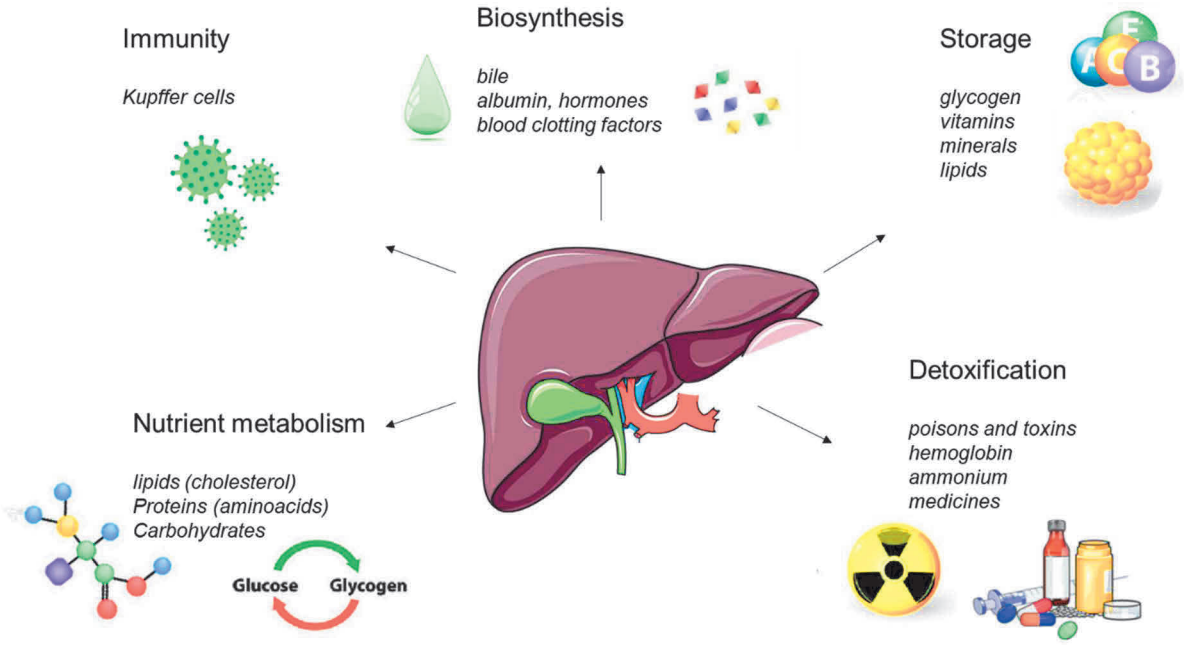

Figure 1. Schematic overview of liver function

Liver architecture

The liver is a structurally and functionally complex organ and is considered the second most complex organ after the brain[1]. It is composed of several main cell types: hepatocytes, cholangiocytes, stellate cells, Kupffer cells and sinusoidal epithelial cells. Each of these cell types, of varying embryonic origin, have unique functions that coordinately regulate liver function at several levels:

- **Hepatocytes**, about 60-80% of the liver mass, are the primary epithelial cells of the liver and are responsible for the vast majority of liver functions. They form the functional parenchyma tissue of the organ. Although hepatocytes are highly differentiated epithelial cells and are quiescent in physiological conditions, and are unique among differentiated parenchymal cells because they retain a stem cell-like ability to proliferate in case of acute injuries that diminish hepatic mass or as an adaptive response in chronic liver diseases[2].
- **Cholangiocytes** are the second major population of liver epithelial cells, representing less than 1% of liver cells, and line the lumen of the bile ducts. Their main physiological function consists in modification of hepatic canalicular bile as it is transported along the biliary tree[3].
- **Hepatic Stellate Cells** (HSC) are resident mesenchymal cells that retain patterns of resident fibroblasts and pericytes, and constitute nearly one-third of non-parenchymal cells and 15% of total resident cells in normal liver[1,4]. HSC, when quiescent, serve as a reservoir for vitamin A and, when activated, transdifferentiate into proliferative, migratory, and contractile myofibroblasts, progressively deplete the vitamin A stock and actively participate in the remodeling of the extracellular matrix of the injured liver by depositing and reorganizing collagen fibers. This process is involved in the healing of the liver, which can progress to cirrhosis.
- **Kupffer cells** are the resident macrophages of the liver, and their pro- or anti-inflammatory roles are finely tuned to the stimuli associated with injury repair.
- **Sinusoidal endothelial cells** line the lumen of sinusoidal capillaries and form 50-180 nm pores providing macromolecule exchange while maintaining barrier function[5].

Connective tissue, or **hepatic extracellular matrix**, represents only nearly 0.5% of the total liver mass but plays a key role in the scaffolding of the organ, giving it mechanical support and preserving hydration and homeostasis. Extracellular matrix is constituted mainly of water, collagenous (collagen) and non-collagenous proteins (e.g. elastin, fibrinogen, proteoglycans, fibrillins, matrix proteins), and free glycosaminoglycans[6,7].

Liver cells organize into functional units of livers - lobules, which organize into lobes. Surprisingly, regardless of the angle of liver section the same phenomenon, called "isotopic parenchyma" is observed: lobules with central veins in the middle surrounded by 4 to 6 portal triads[8]. The liver is irrigated by the hepatic artery and the portal vein which branch into arterioles and venules and bring blood into the sinusoids converging towards the centrilobular vein. The organization of the liver into lobules results from this vascular network (**Figure 2**).

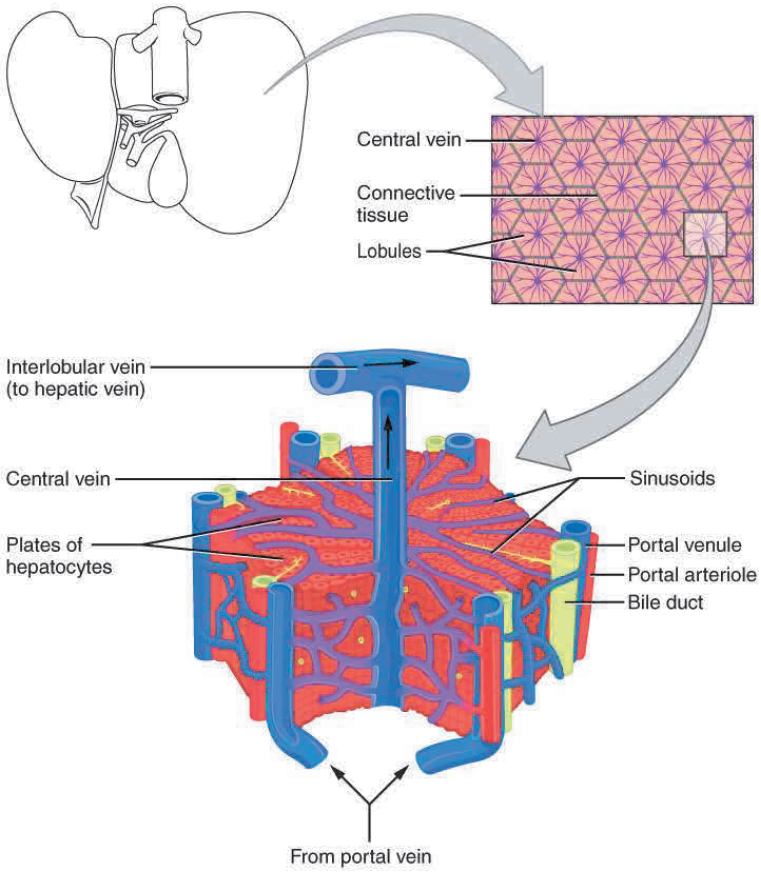

Figure 2. Hepatic functional unit: the hepatic lobule

Adapted from Laperche et al., 2003[9].

The lobule is centered on the centrolobular vein and bordered by the portal spaces (the portal vein), the hepatic artery and the bile ducts.

The liver is divided into four unequal lobes: the right lobe is the largest, the left lobe and the quadrate and caudate lobes. Each lobe is divided into segments (8 in total) according to the connection of the vessels and the bile ducts.

The vascularization (incoming and outgoing) is variable between the lobes. With two major vascular systems irrigating the liver, the portal vein and the hepatic artery, with 70% and 30% of blood flow, respectively, the liver contains approximately 25% of cardiac output. The portal vein is supplied by the mesenteric, gastric, splenic and pancreatic veins, and portal blood is distributed through the liver to the left and right. The distribution is not completely identical. For instance, blood draining the stomach and spleen tends to go into the left lobe. In addition, blood flow is regulated by nerve stimuli and stellate cells which could potentially explain the inter-lobular variation in liver disease. Inter-lobular variation has been documented in paracetamol hepatotoxicity, copper, iron and phosphorus distribution as well as in chemical carcinogenesis, cirrhosis and regeneration[1].

Intrahepatic immunoregulation

In the body, the liver is a central player in immunoregulation. Intrinsic hepatic immunoregulation is complex, with the presence of the multitude of innate and adaptive immune cells. Liver displays the largest population of resident macrophages in the whole body and a high density of natural killer T cells, γδ T cells and transiting lymphocytes with prevalent $CD8^+$ T cell population compared to that in other organs[10]. Natural Killers T cells (NKTs) directly kill target cells and release pro- and

anti-inflammatory factors (e.g., IL-4, IL-17 and IFN-γ). Liver immunotolerance operated by the multiple APCs results from the intricate interactions between hepatic resident cells and peripheral leukocytes, and through the tiny regulation of balance between pro-inflammatory signals (IFN-γ, IL-2, IL-6, IL-7, IL-12, IL-15) and anti-inflammatory signals (IL-10, IL-13, TGF-β). KCs express a range of Toll-like receptors (TLRs) wherein TLR3 and TLR9 empower KCs to become potent APCs to override immunotolerance and to induce robust T cell response. Potent $CD141^+$ DCs confers a strong T cells response too but are absent in the chronic inflammation. Some immune cell populations are associated with risk factors. For instance, myeloid-derived suppressor cells releasing anti-inflammatory IL-10 and TGF-β suppress T cell response during HBV infection. Deregulation of a such intricate and finely tuned immunological network inevitably leads to liver pathology (chronic infection, autoimmunity and hepatocarcinogenesis)[11].

Intrahepatic neurology

The liver receives efferent and afferent nerves of both arms of Autonomic Nervous System (ANS) - sympathetic (adrenergic signaling) and parasympathetic (cholinergic signaling) nerve systems, distributed in the portal tracts but also in intra-lobular. The liver is innervated by the parasympathetic craniosacral nervous system through the vagus nerve (X^{th} cranial nerve), and receives sympathetic fibers from the celiac plexus governed by the VI^{th} to the IX^{th} thoracic spinal nerves. Interestingly, there is a noticeable anatomical difference of intrahepatic nervous fibers distribution between rodents and humans: sympathetic fibers extend into hepatic lobes in primates and guinea pigs but not in mice or rats (**Figure 3**A). However, even if the density of innervation and adrenergic neurotransmitters content is remarkably different (the guinea pig liver has 6 times the noradrenaline content of the rodent liver), the primates produces similar vascular and metabolic responses to noradrenaline[12]. Also, in the human liver the direct contact was observed between catecholaminergic nerves and endothelial cells, Kupffer cells and stellate cells.

During development, the liver is poorly innervated, and the neural crest cells appear first in the portal tracts and in intra-lobular zones only toward term, which suggests that the fetal liver does not need extensive nervous system to exert the hematopoietic function, the first embryonic function of the liver. In the adult liver, hepatic nerves are derived from the vagal and splanchnic nerves that surround the portal vein, hepatic artery, and bile duct (**Figure 3**B). Although the liver is supplied by two main plexus, other nerve branches can reach the liver by other routes. All of the hepatic parasympathetic nerves pass along the hepatic anterior plexus, and the sympathetic nerves reach the liver via anterior (more marked) and posterior plexus.

The hepatic innervation has a well-known role on the regulation of liver functions, which are orchestrated, in synergy with the CNS, by the ANS. The afferent fibers deliver the information about nutrients levels and osmolality in the portal vein to the central nervous system (CNS). In contrast, the efferent fibers are crucial for regulation of metabolism, bloodstream and bile secretion. In addition, both fibers finely regulate the hepatic endocrine compartment, hepatic circadian rhythms and liver repair and regeneration[13,14]. In physiological conditions, the neural innervation in the liver is predominantly sympathetic rather than parasympathetic[15].
Interestingly, recent long-term follow-up studies showed the importance of hepatic innervation after transplantation, where the transplanted non-innervated liver is compromised to ensure a proper liver function, inducing dyslipidemia, postprandial hyperglycemia, insulin resistance, and intrahepatic microcirculation alteration[16].

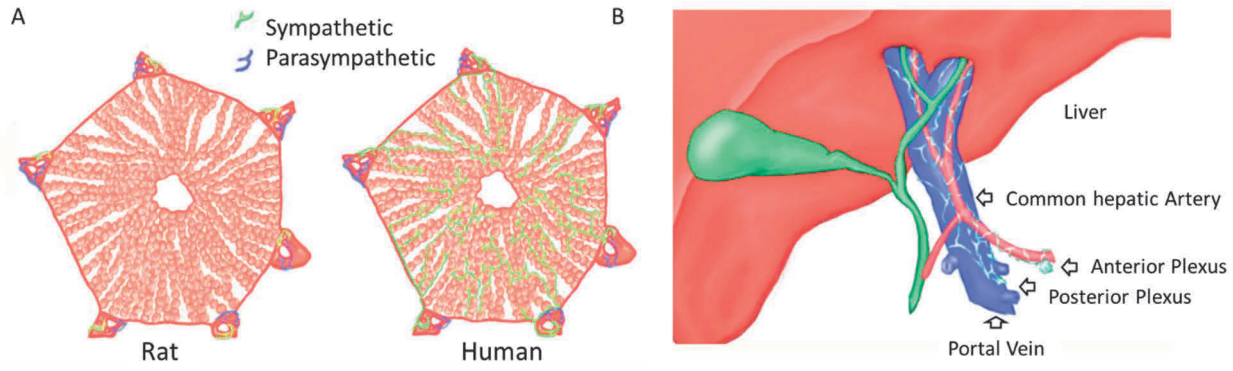

Figure 3. Hepatic nervous system

(A) Intrahepatic innervation in rats and in humans.
(B) Anatomy of hepatic nervous system.

Adapted from Jensen et al., 2013[17].

1.1.2. Chronic liver diseases

Chronic liver disease (CLD) is a progressive deterioration of liver functions for more than six months, which includes synthesis of clotting factors, detoxification of harmful metabolites and bile excretion. CLD is a continuous process marked by inflammation, fibrosis and disturbed hepatocytic regeneration. When present over a prolonged period of time these processes can lead to the development of cirrhosis, liver failure and hepatocellular carcinoma (HCC). The CLD can originate from a wide range of etiologies such as Non-Alcoholic Fatty Liver Disease/Non-Alcoholic SteatoHepatitis (NAFLD/NASH), viral hepatitis, autoimmune hepatitis, alcoholic liver disease (ALD), cholestatic diseases (primary biliary cirrhosis and primary sclerosis cholangitis), as well as genetic conditions (hemochromatosis, Wilson's disease and alpha1-antitrypsin deficiency) and drugs (e.g., nitrofurantoin, methotrexate, isoniazid). To date, CLDs are one of the ten leading causes of death worldwide[18].

Apoptosis

Apoptosis is crucial during various developmental processes (e.g., nervous system and immune system with initial overproduction of cells), in wound healing, as it is involved in removal of inflammatory cells and evolution of tissue into scar tissue, in follicular atresia of the postovulatory follicle or post-weaning mammary gland involution.

In the liver, cell death occurs mainly by apoptosis or necrosis, although other forms may occur (e.g., pyroptosis, ferroptosis, necroptosis). By counterbalancing mitosis, apoptosis regulates liver tissue homeostasis during normal cell turnover, and control liver regeneration and repair. The two main mechanisms of apoptosis are highly complex: (I) the extrinsic or death receptor pathway and (II) the intrinsic or mitochondrial pathway. Both pathways lead to the activation of the caspases 3 and 7, resulting in proteolysis, nuclear fragmentation, and apoptotic cell death[19].

Indeed, apoptosis in the liver is largely mediated by death receptors in disease states[20]. In addition, an endoplasmic reticulum (ER) stress is a recognized inducer of apoptosis in all main CLDs:

- The metabolism of alcohol plays a significant role in alcohol-induced ER and mitochondrial stress, resulting in apoptotic cell death. Alcohol and acetaldehyde are highly reactive and can cause increased reactive oxygen species (ROS) production and misfolded protein accumulation, triggering ER stress and CHOP-dependent apoptosis.

- There is a clear link between the unfolded protein response (UPR) sensors activating the ER stress response and insulin resistance, NASH, and lipotoxicity. The ER stress response leads to apoptotic cell death through JNK-mediated Bim activation and inhibition of the pro-survival Bcl2s.
- Viral infections such as hepatitis B virus (HBV) and hepatitis C virus (HCV) also have been shown to trigger the ER stress response. This can activate the intrinsic mitochondrial pathway and result in JNK and CHOP-mediated apoptosis[19].

Deregulation of the apoptosis is pathologically involved in virtually all acute and chronic liver diseases. The most dramatic liver disease - fulminant hepatic failure – is characterized by an uncontrolled massive hepatocytes' death[21]. Apoptosis mediates the mechanism of hepatic fibrosis and cirrhosis. Despite its strong regenerative abilities (liver can regenerate up to a 70% hepatectomy in 7-10 days by cell proliferation), regeneration may not be optimal in many CLDs where fibrotic scars gradually replace and displace functional hepatocytes.

Finally, apoptosis abnormalities are a significant component of liver cancer, where the normal mechanisms of cell death dysfunction (cell accumulation, tumor surveillance evasion by the immune system, multidrug resistance to cancer therapy)[22]. For example, p53 signals cell cycle arrest at a checkpoint to allow DNA repair or to trigger apoptosis if the damage is not repairable, and it is mutated in over 30% of cases of HCC[23]. Apoptosis can be inactivated by a number of genetic/epigenetic alterations (e.g., Bcl-2 activation , Bax inactivation)[24].

Inflammation

Long-lasting hepatic inflammation is an important component in progression of CLD and has already been defined as one of the hallmarks of cancer. Liver inflammation is regulated by cytokines (e.g., IL-6, IL-1b, Tumor Necrosis Factor-α (TNF-α), Interferon- β/γ (IFN-β/γ)) and chemokines (e.g., CCL2, CCL5, CXCL10), which regulate the migration and activities of hepatocytes and immune cells[25,26]. Kupffer cells play a central role in liver inflammation, which is regulated by the balance of pro-inflammatory M1 and anti-inflammatory M2 Kupffer cells, that are exposed to various stimuli such as nutrients, hepatotoxins or Pathogen-Associated Molecular Patterns (PAMPs). Recruited macrophages, neutrophils, DCs, Natural Killer cells (NK) and T lymphocytes are other immune cells playing central roles in both acute and chronic inflammation and in liver disease[27].

Inflammation-induced liver damage may be explained by two main mechanisms:

I) lipid accumulation (e.g., reduced secretion-oriented lipogenesis, accumulation of Free Fatty Acids (FFA) and/or oxidative stress and lipid peroxidation. In response to liver damage, the inflammatory cells and hepatocytes release cytokines (e.g., TNF-α) and ROS, triggering HSCs activation.

II) response to accumulation of infectious (PAMPs (e.g., dsDNA of HCV)) and non-infectious (DAMPs), material release, recognized by pattern-recognition receptors (PRRs) (e.g., Toll-like receptors (TLRs), NOD-like receptors (NLRs), C-type lectin receptors (CLRs))[28].

The histology-based simple and reproducible scoring system Metavir determines the necroinflammatory activity in the liver. As the portal inflammatory infiltrate (portal hepatitis) is sometimes present in normal liver or in case of acute hepatic injuries, the lobular inflammation may cause confluent necrosis and complete destruction of hepatocytes, is a feature associated with chronic injury. In case of chronic hepatitis lobular inflammatory activity may progress without any interface (portal) activity. Based on the assessment of piecemeal necrosis (interface

or portal hepatitis) and lobular or spotty necrosis (parenchymal injury) Metavir scoring allows to provide the grade of activity of chronic hepatitis (**Figure *4***A)[29].

In most CLDs chronic liver inflammation precedes liver fibrosis.

Fibrosis

The progressive accumulation of extracellular matrix is a hallmark of liver fibrosis, which destroys the hepatic physiological architecture. In advanced stages, the liver contains almost six times more extracellular matrix than normal. The crosstalk between injured hepatocytes, inflammatory cells and hepatic myofibroblasts leads to liver fibrosis :

- **Hepatocyte cell death**: dead hepatocytes releasing intracellular compounds called DAMPs (e.g., adenosine triphosphate, high-mobility group box-1) directly activate HSCs and Kupffer cells. Whereas lipotoxicity, fed through the high concentration of free cholesterol in hepatocytes and FFA accumulation in HSCs and Kupffer cells, accelerates fibrogenesis via enhanced immune response and inflammation.
- **Activation of HSCs**: main myofibroblast progenitor cells and key effectors of the fibrogenesis. Physiologically involved in tissue repair, myofibroblasts are cleared by inactivation or apoptosis. However, under chronic injury, their persistent activation triggers progressive liver fibrosis.
- **Liver macrophages**: Kupffer cells and monocyte-derived macrophages represent the largest population of non-parenchymal cells in the liver and play a central role in hepatic inflammation and fibrosis. While in the early phase of injury pro-inflammatory macrophages are dominant, they exhibit intermediate phenotypes during progression of injury and switch to an anti-inflammatory phenotype, and finally during end-stage injury they change into immunosuppressive phenotype, allowing immune evasion and tumor development.
- **Lymphocytes**: lymphocytes infiltration induced by production of pro-inflammatory mediators is also associated with liver fibrosis. Notably, IL-17- producing $CD4^+$ T cells and regulatory T cells (Tregs) are the major lymphocytes effectors of liver fibrogenesis[30].

Autophagy upregulation, micro-RNA secretion alteration (e.g., loss of miR-29, increase of miR-21), TGF-β and SMAD pathway activation are among other important pathogenic processes involved in liver fibrogenesis[31].

While hepatic fibrosis can be reversible, the transition time point to irreversible fibrosis is not completely understood. Histology-based scoring systems Metavir (**Figure *4***B) provides a semi-quantitative assessment of fibrosis[32].

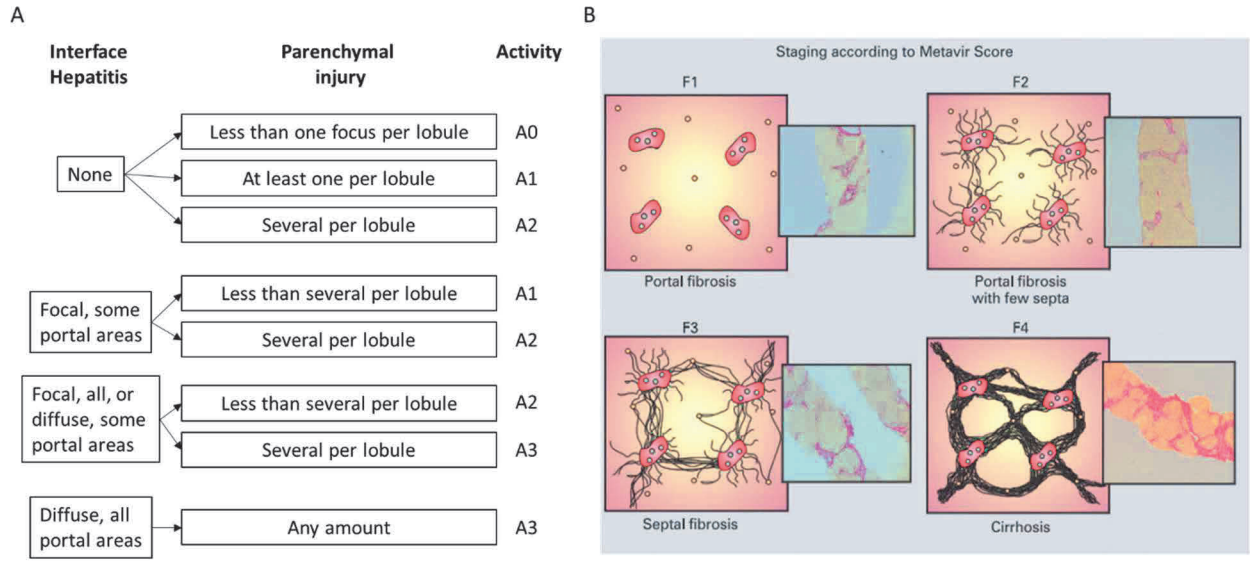

Figure 4. Metavir liver activity and fibrosis score system

(A) Algorithm for grading hepatitis activity according to the Metavir activity score of Bedossa et al[33], where chronic hepatitis is scored as A0 with no activity, as A1 with minimal or mild activity, as A2 with moderate activity, and as A3 with marked activity or bridging or multiacinar necrosis, according to the International Association for the Study of the Liver (IASL).
(B) Fibrosis is scored as F0 (absent), F1 (portal fibrosis), F2 (portal fibrosis with septa), F3 (septal fibrosis) and F4 (cirrhosis).

Adapted from Goodman et al., 2007[34] and Asselah et al., 2009[32].

Cirrhosis is a histological diagnosis and a final stage of CLD that results in disruption of liver architecture, formation of nodules, vascular reorganization, neo-angiogenesis, and deposition of extracellular matrix. The term "cirrhosis" is derived from Greek word *kirrhos,* meaning "tawny" and referring to the tan color of the liver. The three significant complications of cirrhosis are:

- portal hypertension (esophageal varices, ascites)
- hepatocellular insufficiency (encephalopathy, jaundice)
- HCC.

Also, due to the progressive haemodynamic alteration, nephrotoxicity and infections, patients with advanced cirrhosis often present renal function alteration or hepatorenal syndrome.

Cirrhosis is typically classified as compensated or decompensated, separating them into two distinct clinical states of disease. Patients with compensated cirrhosis compared to those with decompensated cirrhosis show longer survival and better quality of life. Patients with decompensated cirrhosis show progressive worsening of the liver function, accompanied by increased portal pressure and infections. The patients with compensated cirrhosis will decompensate at nearly 5% per year. The hallmarks of decompensation, ascites and encephalopathy, are associated with 50% and 20% mortality at 5 years, respectively. The latter ones together with bleeding and renal disfunction are associated with very poor survival. Decompensated cirrhosis is also a risk factor of HCC development[35].

Clinical features of cirrhosis constitute the basis of its scoring system, characterized by an unpredictable clinical progression, and have a prognostic classification value[36]:

- State 1. compensated cirrhosis without varices: very low mortality rate

- State 2. compensated cirrhosis with varices: 10% mortality at 5 years
- State 3. variceal bleeding: 18% mortality at 5 years before the development of other complication
- State 4. first non-bleeding decompensation (e.g., ascites): 25% mortality at 5 years before the development of other complication
- State 5. Further decompensation (complication combination): 88% mortality at 5 years
- State 6. Late advanced decompensation: 60-80% mortality at 1 year.

1.1.3. Hepatocellular carcinoma

HCC epidemiology

Liver cancer is the 7th most common cancer and the 3rd most common cancer in terms of mortality worldwide, responsible for 905,677 (4.7%) new cases and 830,180 (8.3%) deaths in 2020[37]. Like many other cancers, the vast majority of HCC cases develop progressively with the acquisition of precancerous features at first and frankly malignant lesions later (**Figure 5**).

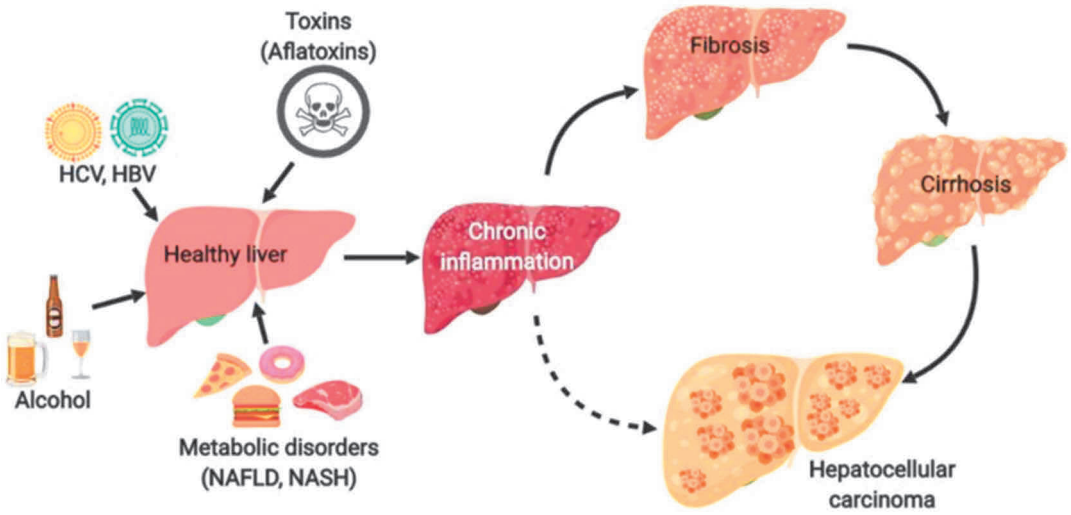

Figure 5. Risk factors and HCC progression

Adapted from Macek-Jilkova et al., 2019[38].

The contribution of the main different etiologies to HCC incidence varies between regions of the world (**Figure *6***). HCV and HBV remain the most global risk factors for HCC. HBV infection accounts for ~60% of HCC in Africa and Asia, HCV infection is the most common liver disease in Japan, Europe, North America and North Africa, while ALD globally accounts for ~15-30% of HCCs depending on the geographical region. Although nearly 25% of NASH-associated HCCs occur in the absence of cirrhosis, NASH became now the most common cause of cirrhosis almost in all parts of the world. Overall, NASH currently represents 15-20% of HCC cases in the occidental world[39]. The increasing prevalence of NAFLD and NASH may soon exceed overall viral factors as the major cause of HCC, as the latest epidemiological data forecast a continuous drop of HCV-related cancer cases and a linear increase of NASH-related cancer cases[40].

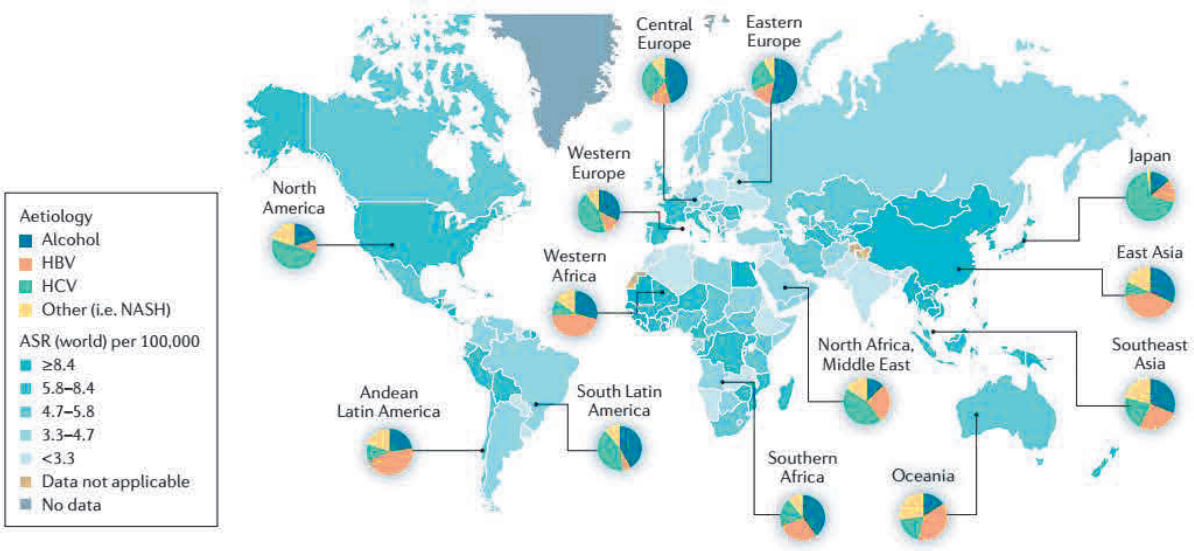

Figure 6. The incidence and major etiological factors of HCC

Adapted from Llovet et al., 2021[39].

Cellular and molecular events in HCC

The normal structure of the liver depends on a balance between cell death and regeneration. The liver is the only organ capable of natural regeneration. Small lesions caused by apoptosis or necrosis are immediately repaired without affecting liver function in a significant and/or prolonged manner. Hepatocyte loss induces re-proliferation of mature hepatocytes, allowing complete repair of the tissue loss.

HCC is an inflammation-associated cancer, with nearly 90% of HCC cases being associated with prolonged inflammation due to viral hepatitis, excessive alcohol intake, NAFLD or NASH. The liver harbors the largest number of immune cells in the body, of which are virtually all can have pro-tumor and anti-tumor roles. The major pro-tumorigenic mechanism through which immune cells promotes HCC is secretion of cytokines and growth factors which foster proliferation or counteract apoptosis of hepatocytes.[39] Also, during chronic inflammation, massive liver damage is caused by mechanisms of ER stress and oxidative stress, which lead to cycles of apoptosis, necrosis and regeneration of liver tissue. The proliferative capacity of the residual hepatocytes is impaired and another mechanism takes place: bipotent basophilic cells with oval nuclei, called "oval" cells, proliferate in the periportal region, migrate into the lobule and differentiate into hepatocytes or cholangiocytes[9]. The degree of liver regeneration often correlates with the degree of inflammatory activity. Following injury, but also surgery, hepatocytes begin to produce Hepatocyte Growth Factor (HGF), Epidermal Growth Factor (EGF) and TGF-α/β, and non-parenchymal cells (Kupffer cells, stellar cells) become activated and secrete IL-1, IL-6, and TNF-α. Overexpression of HGF induces overexpression of its receptor c-Met, Vascular Endothelial Growth Factor (VEGF) and many other transcription factors, remodeling molecules of the extracellular matrix. Overexpression of these molecules, involved in invasiveness and metastatic potentiation of HCC, promotes carcinogenesis[41].

HCC results from the accumulation of somatic genomic and epigenomic alterations over time. In average, between 40 and 60 somatic alterations are detected in protein-coding regions of the specimens genomes[42]. Integrative studies have shown that HCC is heterogeneous at the histological and molecular levels, with variable molecular features and clinical outcomes. They allowed to establish molecular classification (proliferation class and non-proliferation class) and

immune classification (immune-active, immune-intermediate, immune-exhausted and immune-excluded classes)[39]. High throughput next-generation sequencing enabled the identification of cancer driver genes (pro-oncogenes or tumor suppressor genes) that are recurrently altered in HCC (**Figure *7***):

- telomerase gene is overexpressed in 90% of HCC and its overexpression is related to Telomerase Reverse Transcriptase (*TERT)* promoter mutations (44-65% of patients) and to *TERT* gene amplification in 60% and 5% of cases, respectively. Two hotspots of mutations are located at nucleotide positions -124 and -146 upstream of ATG site, both creating a new binding site recognized by transcription factors[42].
- the Wnt/β-catenin pathway is activated through *CTNNB1* mutations that stabilize β-catenin, inactivating mutations in *AXIN1* or more rarely in *APC*, in 11-40%, 10% and 1-2% of HCC cases, respectively, and particularly in patients with well-differentiated tumors[43,44].
- mutations in *TP53,* coding for the major cell cycle regulator p53, occur in 21-31% of patients, with a specific hotspot of mutation (R249S) in patients with aflatoxin B1 exposure[43,44].
- chromatin remodeling complexes and epigenetic regulators are frequently impaired in HCC: mutations in BRG1- or HRBM-Associated factors (BAFs) and polybromo-associated BAF chromatin complex or in the histone methylation writer family KMT2-MLL in 4-28% or 10-32% of HCC cases, respectively.
- PI3K/AKT/mTOR and Ras/Raf/MAP kinase pathways are activated in 43% and 51% of HCC patients, respectively. This activation is caused by Fibroblast Growth Factor 3 (FGF3), FGF4 and FGF19 genes amplification in nearly 5% of tumors, and can be also related to inactivating mutations of Tuberous Sclerosis complex 1 (*TSC1*) and 2 (*TSC2,* 3-8% of cases) or in Phosphatase and TENsin homolog (*PTEN)* (1-3% of cases)[45].

While *TERT* promoter mutations are frequent at early stages, *CTNNB1* and *TP53* mutations increase with HCC progression. Few other signaling pathways are altered in many HCCs: hepatic differentiation (34%), oxidative stress (12%), IL-6/Jak/STAT (9%), and TGF-β (5%). Some risk factors were found associated to mutations in some genes: alcohol-related HCCs associate with *CTNNB1, TERT, CDKN2A* and *HGF*, while HBV-related HCCs relate to *TP53* alterations.

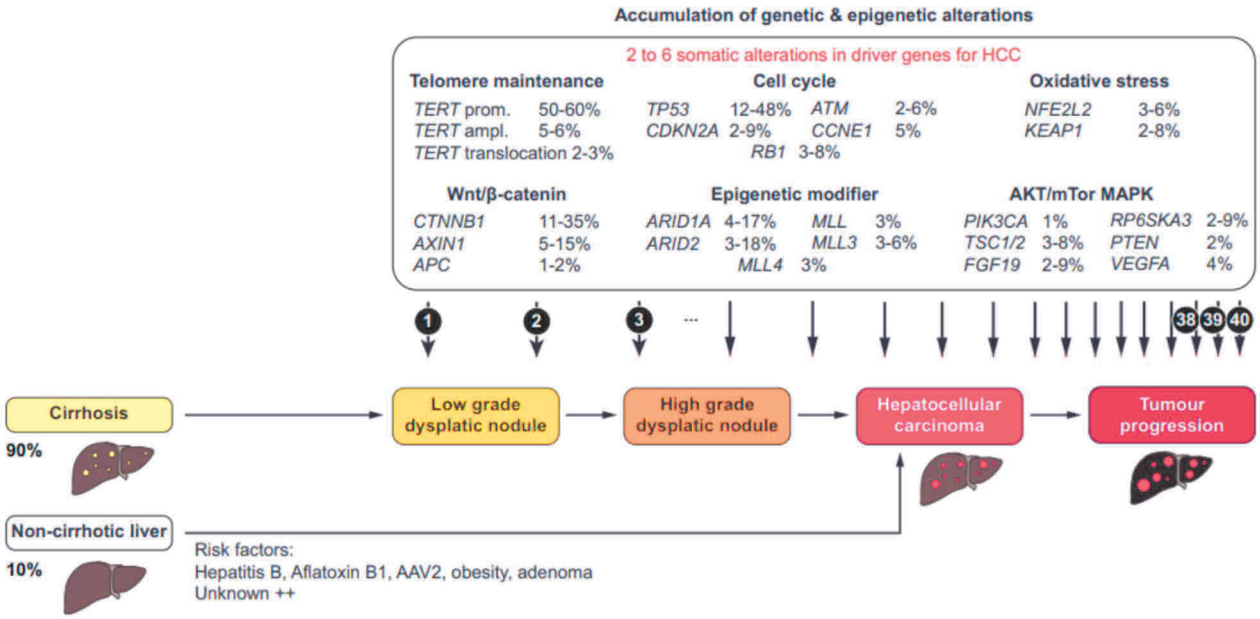

Figure 7. Genetic and epigenetic events in HCC

Adapted from Rebouissou et al., 2020[46].

Diagnosis and clinical forms

Although the diagnosis of HCC is often made during monitoring examinations for chronic liver disease, the disease may also be discovered accidently during a chest X-ray, following internal bleeding from a ruptured tumor, or on palpation of an abdominal mass. Patients with advanced HCC present with symptoms of advanced cirrhosis: pruritus, splenomegaly, cachexia, portal vein thrombosis leading to jaundice, esophageal varices, encephalopathy and ascites. Radiological examination alone or coupled with quantification of Alpha-FetoProtein (AFP), which is increased in more than half of the cases of HCC, and in the presence of risk factors for chronic liver disease (age >55 years, male sex, advanced cirrhosis) are sufficient to confirm the diagnosis[47]. After non-invasive examinations, histology remains then the reference for the diagnosis of HCC.

HCC is an aggressive tumor and is likely to rapidly invade the portal vein and hepatic vein, in 29-65% and 12-54% of cases respectively. It can also extend into the vena cava and even invade the atrium or ventricle. Numerous studies describe extrahepatic metastases in 30-50% of HCC, and especially for primary tumors larger than 5cm in advanced IVa stage of the disease. These are found predominantly in the lungs (18-60%), lymph nodes (27-42%) and bones (6-39%), and, less frequently, in the adrenal glands, peritoneum, diaphragm, connective tissues, brain, skin and oral cavity[48,49].

The differential diagnosis of HCC based on general imaging differential considerations includes: intrahepatic cholangiocarcinoma, hepatic adenoma, focal nodular hyperplasia, hepatic hemangioma, hepatoblastoma, primary hepatic lymphoma, hepatic tuberculoma but also hepatic metastases[50–52].

Prevention

The prevention of HCC is based on three levels[53]:

- Primary: avoid population exposure to risk factors (HBV vaccination, aflatoxin B1, overweight, alcohol consumption). Despite the vaccination programs initiated worldwide against HBV in children, which have significantly decreased the incidence of HBV infection, especially in high endemic countries, about 6% of the world population is a

carrier of HBV. Anti-HBV treatments do not eradicate the virus but prevent liver damage and decrease the risk of developing HCC[54].

- Secondary: protect patients with chronic liver disease (monitoring, diet and treatment). Regular monitoring and measurement of AFP in cirrhotic patients allows early diagnosis and surgical intervention in two-thirds of cases[55].
- Tertiary: avoid relapse of primary HCC by curative measures detailed below.

HCC classifications and treatments

Overall survival of patients with HCC varies across the world. Survival is poor, with overall 18% at 5 years. By stage, patients with localized disease have 32.6% survival at 5 years, patients with regional disease - 10.8% and patients with metastatic disease – only 2.4%[56]. The survival time depends on several factors, such as the extent of cirrhosis or portal vein thrombosis, which shortens it considerably. HCC induces complications that are often the cause of death in patients: liver failure, cachexia, esophageal varices hemorrhage and, more rarely, tumor rupture and peritoneal hemorrhage. The prognosis is very poor in the case of metastatic disease with 24.9% survival at 1 year and a median survival of 7 months[57].

At the time of diagnosis of HCC, only about one-third of patients are eligible for potentially curative therapies, such as resection, transplantation, or local ablation, with the average survival beyond 5 years. In patients with advanced disease, chemoembolization achieves an average survival of 26 months[58]. Surgical resection is an effective method in the treatment of early-detected HCC. Nevertheless, relapse and metastasis remain high (65% and 35%) and overall survival at 5 years is 50% after radical resection[59]. Surgery itself could cause relapse and metastasis, suggesting that liver regeneration could via micrometastases and residual or dormant cancer cells disseminate and induce relapse in this context[41].

Tumor classification is paramount for the understanding and management of HCC. At least 18 different classification systems have been proposed during the past four decades (**Figure *8***).

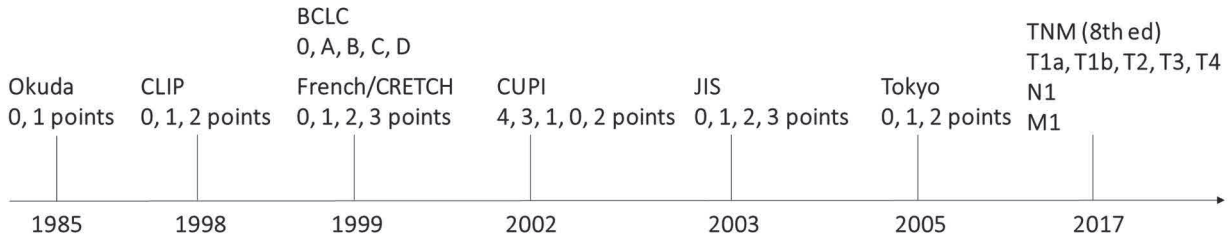

Figure 8. Frequently used HCC classifications

TNM, tumor-node-metastasis; CLIP, cancer of the liver Italian program; GRETCH, Groupe d'Etude et de Traitement du Carcinome Hépatocellulaire ; CUPI, Chinese University Prognostic Index ; JIS, Japan Staging Score.

Adapted from Couri et al., 2019[60].

Barcelona Clinic Liver Cancer (BCLC), which takes into account the state of liver function assessed with the Child-Pugh score (**Table *1***), the patient's general condition assessed with the Eastern Cooperative Oncology Group (ECOG) performance status scale, and tumor characterization. Thus, four grades are distinguished: 0 (very early), A (early), B (intermediate), C (advanced) and D (end stage)[60]. BCLC associates stage stratification with a treatment algorithm and is the reference staging system used in Europe and in North America.

Clinical/biological criteria	1	2	3
Encephalopathy	absent	slight to moderate (grade 1-2)	severe (grade 3-4)
Ascites	absent	slight	moderate
Bilirubin (mg/dL)	< 2.0	2-3	> 3
INR **Prothrombin time (%)**	< 1.7 > 50%	1.7-2.2 40-50%	> 2.2 < 40%
Albumin (g/dL)	> 3.5	2.8-3.5	< 2.8
Class A: 5-6 points, Class B: 7-9 points, Class C: 10-15 points			

Table 1. Score Child-Pugh

INR: International Normalized Ratio.

Adapted from Couri et al., 2019[60].

In developed countries nearly 40-50 % of patients with HCC are diagnosed at early stages (BCLC stage 0-A) (**Figure *10***) when potentially curative treatment, such as resection, liver transplantation, or local ablation, are possible, resulting in a median overall survival of 60 months. However up to 70 % of these patients relapse within 5 years, and there is no adjuvant therapy to prevent this complication. Patients with intermediate-stage disease (BCLC stage B) can benefit from TransArterial ChemoEmbolization (TACE) with an estimated median overall survival of 25-30 months. More than 50% of patients with HCC will receive systemic treatments, multiple Tyrosine Kinase Inhibitors (TKIs) (sorafenib, lenvatinib, cabozantinib and regorafenib), immune checkpoint inhibitors (pemrolizumab, atezoluzumab, nivolumab, ipilimumab), or VEGF inhibitor (ramucirumab)[42] (**Figure *10***), in a context that may not be yet fully adapted to their tumors' molecular and functional characteristics.

The TKI sorafenib has been the frontline therapy alone for several years, and since 2018 together with lenvatinib (judged as non-inferior), till the approval in 2020 of a bi-therapy based on atezolizumab (anti-Programmed Death-Ligand 1 (PD-L1) monoclonal antibody) in combination with bevacizumab (anti-VEGF monoclonal antibody). Sorafenib and lenvatinib block tyrosine kinase receptors presented on the cell surface, such as serine/threonine kinases c-RAF, mutant and wild-type BRAF in the RAF/MEK/ERK axis of the RAS cascade signaling, Vascular Endothelial Growth Factor Receptors 1-3 (VEGFR1-3), Platelet-Derived Growth Factor Receptor β and VEGFR1-3, PDFGR-α, Fibroblast Growth Factor Receptors 1-4 (FGFR1-4), and Rearrangement During Transfection (RET), respectively. According to the Phase III REFLECT clinical trial results, lenvatinib, having a more pleiotropic effect, should be preferred in patients with HBV etiology, whereas sorafenib should be preferred in patients with HCV background, preserved liver function and no extrahepatic spread. In addition, patients with baseline AFP concentration greater than 200 ng/ml achieved greater benefits with lenvatinib (**Figure *9***)[61,62].

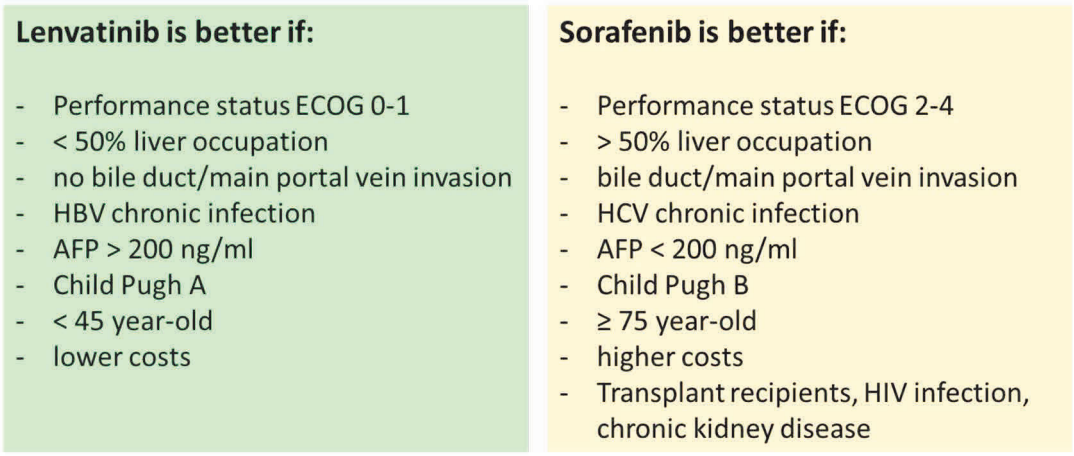

Figure 9. Proposed criteria to choose between sorafenib and lenvatinib

ECOG, Eastern Cooperative Oncology Group.

Adapted from Dipasquale et al., 2021[62].

TKIs improve patients' survival but are the source of important side effects due to their off-target effects. A considerable percentage of patients are insensitive to sorafenib. TKIs are subject to unpredictable drug-resistance and the number of patients who benefit from them is far from satisfactory. Although less than 30% of patients can benefit from sorafenib treatment, except for primary resistance, most patients treated with sorafenib develop resistance with 6 months. Epithelial-Mesenchymal Transition (EMT), hypoxia and autophagy are among the multiple processes of induced sorafenib resistance identified in the recent years. With significantly better overall response rates than in patients treated with sorafenib, lenvatinib was not a subject to resistance studies so far. Interestingly, a recent study has shown metabolic adaptation in patients who developed sorafenib resistance inducing extensive acetylation changes towards a more energetic metabolic phenotype *in vitro, in vivo* and in humans (PhosphoEnolPyruvate CarboxyCinase (PEPCK) C has been found to play a pivotal role in gluconeogenesis pathways) with shorter progression-free survival[63,64]. Indeed, sorafenib stimulates aerobic glycolysis known as "Warburg effect" preferentially used by cancer cells, and is highly toxic in glucose-decreased condition or in presence of glycolytic inhibitors[65].

Checkpoint blockade monotherapies benefit only to about 15-20% of patients. Whereas combining tyrosine kinase inhibitors or VEGF inhibitors with immune checkpoint inhibitors can modulate the immune microenvironment in a way that favors the development of more effective and durable responses to checkpoint inhibitors[39]. Notably, few Phase III clinical trials are being currently launched to evaluate the benefit of anti-HCC drug combinations, aiming to improve the clinical outcome of patients with advanced HCC (**Figure 10**). Whereas the foregoing Phase III clinical trials testing small molecules (e.g., erlotinib, sunitinib, linifanib, brivanib, everolimus, doxorubicin, tivatinib) showed insufficient antitumoral activity and higher toxicity compared to sorafenib[66].

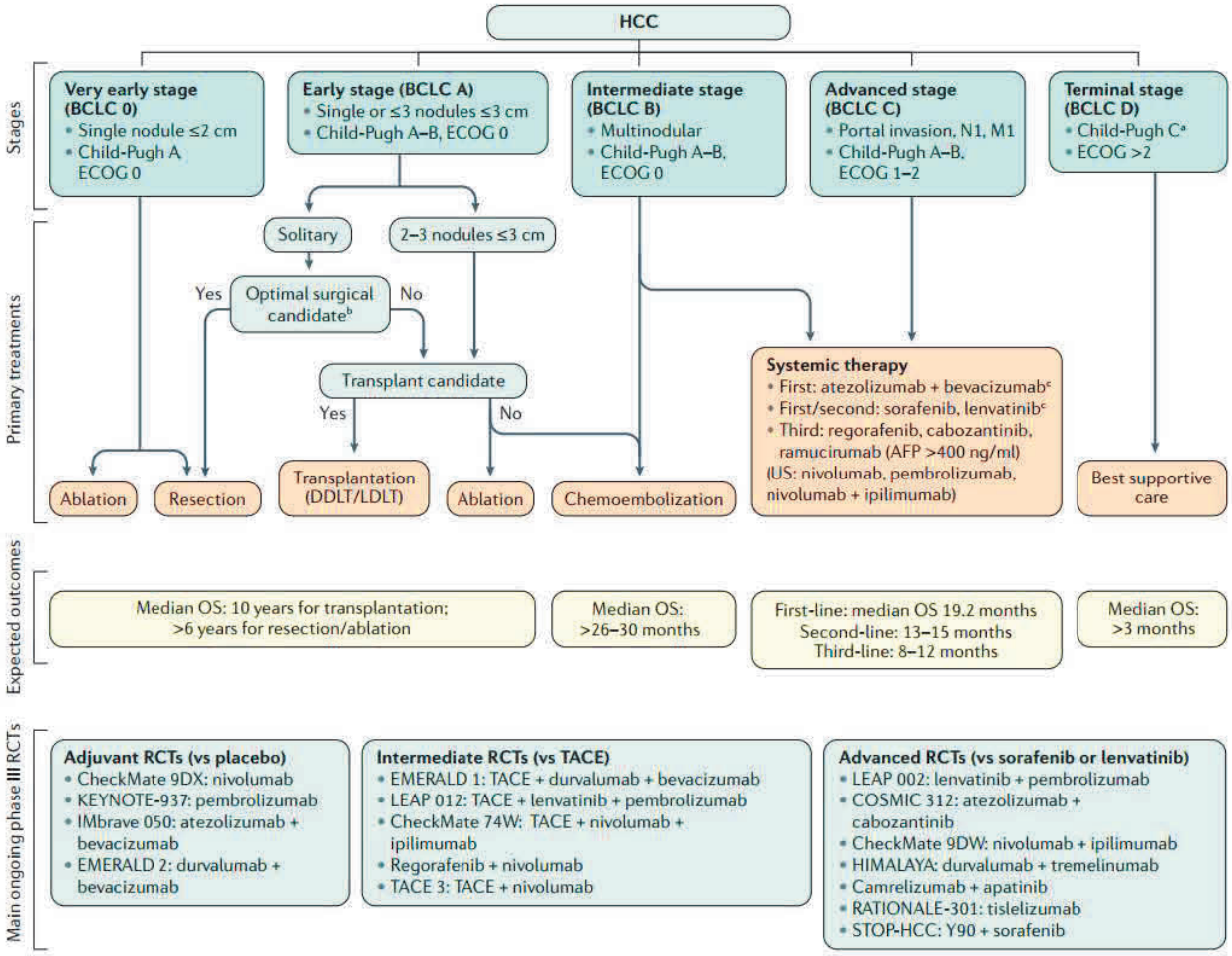

Figure 10. Treatment strategy in the management of HCC

Adapted from Lllovet et al., 2021[39].

1.2. The autonomic nervous system and the liver

1.2.1. Nerve dependence in tissue regeneration and cancer

Cancerous invasion of nerves has been documented in multiple solid tumors as a high-risk pathological marker, associated to a poorer survival in patients, and particularly in neurotrophic cancers (e.g., pancreatic and prostate cancers)[67].

The phenomenon of nerve dependence has been described in animal regeneration, where the axons outgrowth is necessary to reconstitute lost body parts and to remodel tissue in different species. Epimorphic (non-remodeled) regeneration shares some similarities with the tumor: epithelial-mesenchymal tissue crosstalk, stem cells involvement, neoangiogenesis and inflammation[68]. Nerve dependence has been shown in tissue growth and wound healing determining long-term pathological sensations close to the site of injury. The growth of nerve fibers in the blastema (stem/progenitor cells growth bud) begins early in its formation. Afferent nerves ablation prevents regeneration and induces fibrotic scar tissue formation, whereas nerves deviation to the blastema increases regeneration speed[69,70]. Growing nerve fibers originating from the stump progressively re-invade the microenvironment of the blastema and stimulate the regeneration process.

Even though the molecular mechanisms of nerve dependence remain a long-standing question, nerves may be critical to tumorigenesis as they are to tissue regeneration, particularly because

of the existence of multiple common pathophysiological processes shared by both regeneration and cancerogenesis. Neurotrophic growth factors and neurotransmitters are subject to research investigation to elucidate the mechanisms of nerve dependence in regeneration process and tumorigenesis (***Figure 11***). For instance, the secretion of growth factors such as Nerve Growth Factor (NGF) by immune cells (e.g., macrophages) was reported to contribute to nerve outgrowth in regenerating tissue, and secretion of multiple neurotrophic factors, such as cytokine oncostatin M, newt Anterior Gradient protein (nAG), Bone Morphogenetic Protein 2 (BMP-2) and FGFs, by Schwann cells - in tumorigenesis[71]. Interestingly, Schwann cells, sharing the same pluripotent neuronal cells precursors with parasympathetic neurons, have been identified in neoplastic sites prior to tumor formation in pancreatic and colon cancers[72,73].

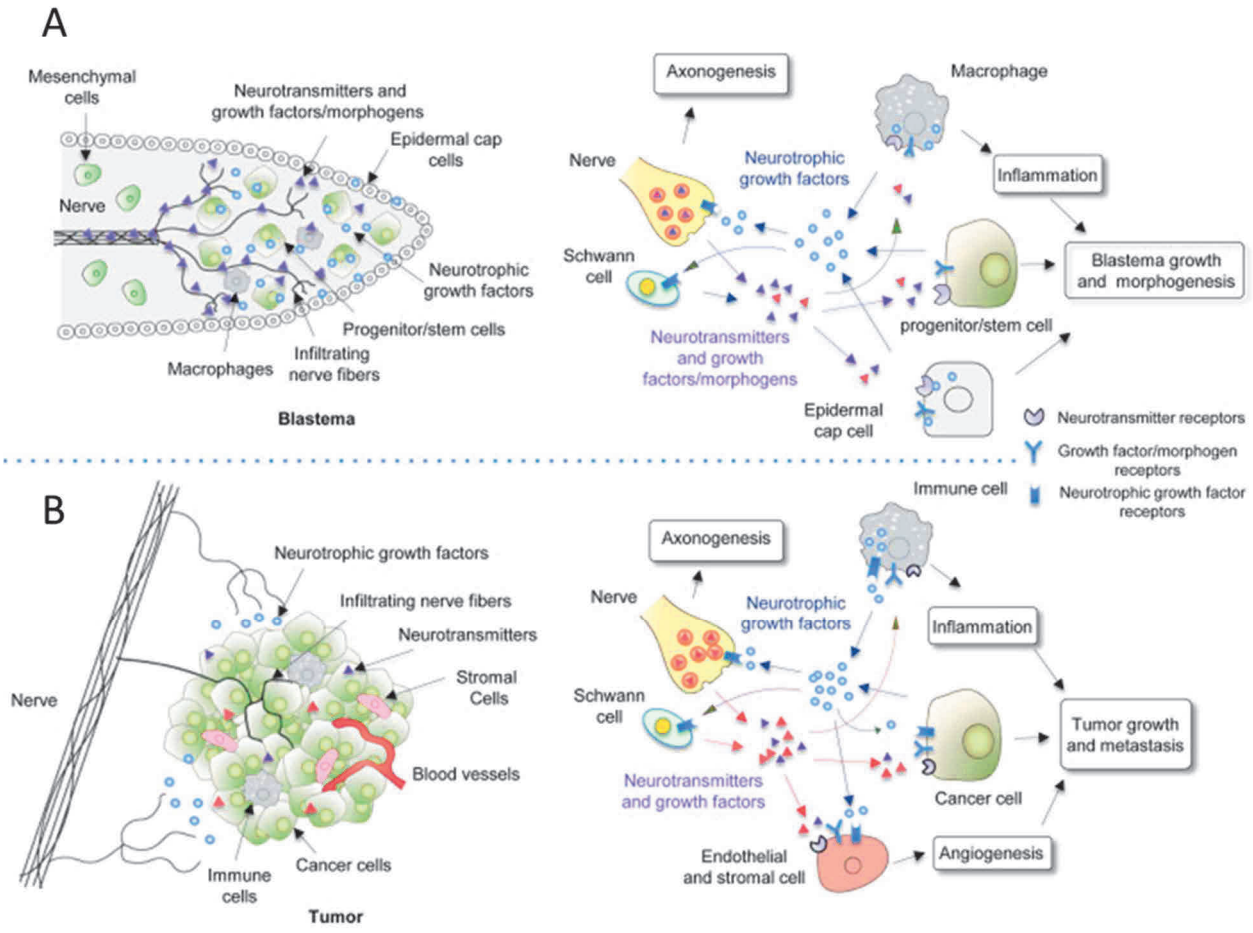

Figure 11. Molecular processes of nerve dependence in tissue regeneration and tumorigenesis

(A) In regeneration, axonogenesis is driven by neurotrophic molecules secreted by epidermal cells lining the bud and macrophages. The whole crosstalk allows the growth and morphogenesis.
(B) In the tumor, nerve growth is stimulated by neurotrophic factors secreted by cancer cells. Neurotransmitters, such as adrenaline, noradrenaline and acetylcholine, secreted by nerves, can activate stromal and cancer cells growth.

Adapted from Boilly et al., 2017[68].

1.2.2. ANS in cancer

Their important role in tissue formation and growth makes nerves an attractive target for interfering with cancer onset and progression. Nerves and neuronal cell markers were observed in many tumors, such as prostate, breast, pancreas, cervix, esophagus and stomach, with nearly doubling density of nerve fibers between preneoplastic and cancerous tissues. They were also

found to be associated with poor prognosis and overall survival and involved in angiogenesis and metastasis[74–76]. As mentioned in the section above, there is a crosstalk between nerves and cancer cells through the secretion of neurotrophic factors and neuroactive molecules. The very first phenomenon describing this interaction is Peri-Neural Invasion (PNI) of native nerves which, notably, leads to cancer-associated pain[77]. Nerves are also suggested to be the first route of cancer cells migration before even *bona fide* tumor establishment, and a possible route of metastasis[76]. Few recent studies have shown the evidence of ANS implication in cancer development and progression (**Table *2***).

Both arms of ANS innervate the tumor microenvironment. The sympathetic nerves, also related to stress-induced cancer behavior, are pro-tumorigenic in prostate and breast cancer, while parasympathetic nerves are pro-oncogenic in gastric, colorectal, prostate and lung cancers[76]. These pro-oncogenic effects may be mediated by changes in cancer cell behavior, angiogenesis and intra-tumoral immunity:

- In **gastric cancer**, vagal innervation plays a fundamental role at all stages of gastric cancerogenesis, as vagotomy or local injection of neurotoxic drug botulinum toxin type A in different mice models reduce tumor onset and progression, and this only in the denervated part of the stomach. In addition, muscarinic acetylcholine M3 receptor (CHRM3) inhibition by genetic knockout or inhibiting drugs (e.g., Botox, scopolamine) suppresses gastric cancerogenesis. Moreover, in patients, tumor progression stage correlates with dense nerve distribution and vagotomy reduces the incidence of gastric cancer[78]. Naturally more densely innervated by the para-sympathetic system than by its sympathetic counterpart, the gastric cells proliferation is under cholinergic nerve control. The activation of muscarinic receptors, found also in the liver, intestinal neoplasia and the brain, promotes Wnt signaling induction in gastric epithelium[78].
- In **ColoRectal Cancer (CRC),** CHRM3 inhibition (e.g., scopolamine, knock-out mice) decreases the incidence of adenocarcinoma, especially in mice with aberrant Wnt signaling, whereas cholinergic stimulation enhances tumorigenesis *in vivo*. Interestingly, the co-overexpression of CHRM3 and Epithelial Growth Factor Receptor (EGFR) is an important factor for CRC cells proliferation *in vitro* when stimulated with AcetylCholine (ACh) as compared to CRC cells overexpressing EGFR alone[79].
- In **breast cancer**, sympathetic nerves enhance cancer cell invasiveness and confer resistance to trastuzumab though ADRB2 inducing HER-2 overexpression and PI3K/AKT/mTOR pathway stimulation. A recent study has shown an anti-tumoral effect of cholinergic neurostimulation, through the inhibition of expression of immune checkpoint molecules in murine breast cancer models[76].
- In **Pancreatic Ductal AdenoCarcinoma (PDAC)**, sympathetic fibers are decreased and parasympathetic fibers' density remain unchanged as compared to non-tumoral tissue. *In vivo,* vagotomy enhances PDAC development, inhibiting Tumor-Associated Macrophages (TAMs) and TNF-α release, whereas muscarinic agonists inhibit tumorigenesis, notably through the CHRM1 receptor. Clinical samples analysis suggests a protective role of cholinergic fibers in patients with metastatic PDAC[80].
- In **prostate cancer**, surgical removal of autonomic nerves decreases tumor growth and dissemination. *In vivo*, the suppression of both, sympathetic or parasympathetic nerves, surgically by genetic deletion of *Adrb2* and *Adrb3,* or by 6-hydroxydopamine (6OHDA), suppresses tumorigenesis. Interestingly, adrenergic nerves stimulate the early stages of cancer development, whereas the cholinergic nerves induce tumor invasion and metastasis at later stages[68]. In patients, high thickness of cholinergic fibers (stained with

Vesicular ACh Transporter ($VAChT^+$)) largely restricted to the tumors and adrenergic fibers (stained with Tyrosine Hydroxylase (TH^+)) in normal prostate tissue surrounding the tumor was associated with poor clinical outcomes. Cholinergic fibers were also found to associate with extra-prostate tumor spread and with circulating pre-operative level of Prostate Specific Antigen (PSA)[81].

- In **lung cancer**, ACh expressed also by pulmonary epithelium and acting as autocrine and paracrine factor, confers higher potential of cell proliferation, adhesion, migration and invasion to cancer cells. Long-time exposure to nicotine leads to ACh induction and tumor development in Non-Small Cell Lung Cancer (NSCLC) *in vivo*, through the stimulation of CHRM3, followed by EGFR pathway activation, and the expression of cytokines IL-1, IL-6 and IL-8[82].

Cancer	Associated tumor nerves	Outcomes	Mechanism of Action
Gastric cancer	Vagus nerves	Promote gastric cancerogenesis Interferes with systemic chemotherapy	Wnt signaling activation through CHRM3 receptor, YAP function stimulation
CRC	Vagus nerves	Promote colorectal cell proliferation	Wnt signaling activation through CHRM3 receptor
PDAC	Vagus nerves	Inhibits tumor growth	TNF-α and TMA regulation
Breast cancer	Sympathetic nerves Parasympathetic nerves	Sympathetic nerves accelerate cancer growth and progression Parasympathetic nerves reduce cancer growth and progression Neuronal density is correlated with lymph node metastasis and clinical stage	PD-1, PDL-1 and Forkhead boX P3 (FOXP3) regulation
Prostate cancer	Sympathetic nerves Parasympathetic nerves	Promotes tumorigenesis, dissemination and poor clinical prognosis	Implicates ADRB2 and ADRB3 receptors as well as CHRM1 receptor
Lung cancer	Parasympathetic nerves	Promote tumorigenesis	Implicates CHRM3 receptor

Table 2. Roles of ANS in some solid tumors

Adapted from Xie et al., 2016[76] and Wang et al., 2021[79].

These data support the therapeutic potential of ANS modulation in some solid tumors, in monotherapy or in combination. Most of researchers are focusing on the genetic basis of cancer biology, which is highly heterogenous inter-individually and even intra-individually. Also, the interest in some common features of tumor microenvironment, such as autonomic nerves characteristics, is on the rise. Hence, few new therapeutic approaches are currently being investigated: β-blockers, vagotomy, electrical stimulation of vagal nerves and Adeno-Associated Virus (AAV) vector-based genetic local neuroengineering technology with intratumoral injections[83].

1.2.3. ANS implication in CLD and HCC

Yet in early 90s the clinicians and researchers have obtained first elements of evidence of ANS impairment in CLD and especially in cirrhosis (up to 70% of patients with cirrhosis[84]), which they called autonomic dysfunction. The autonomic dysfunction can be described as biological and clinical features resulting in vagal dysfunction (increased vasodilatation) or sympathetic dysfunction (vasoconstriction failure) as well as hyperdynamic circulation alteration (imbalance between sympathetic and parasympathetic functions with predominant vagal alteration)[84]. In a small retrospective study, about 75% of patients with cirrhosis, irrespective of etiology, show autonomic neuropathy, with 30% 4-year mortality rate compared to patients with normal ANS function[85].

The ANS is implicated in many normal liver functions[17] and in some pathological processes (e.g., post-injury liver regeneration)[86]. Thus, efferent hepatic nerve fibers regulate the hepatic blood supply with consequences on oxygenation and metabolism in the parenchyma. Few recent studies *in vivo* with conflicting results suggest the regenerative role of sympathetic (mediated by HGF induction and TGF-β1 reduction) or parasympathetic stimulation in rats. In addition, and importantly, activated myofibroblastic HSCs expressing adrenergic and nicotinic ACh[87] receptors, also producers of TGF-β1, are direct targets of ANS and express collagen in response to adrenergic (noradrenaline, peptide Y) or cholinergic neurotransmitters (ACh). The latter findings suggest the implication of both arms of the ANS in the maintenance of healthy liver architecture and in the remodeling of damaged liver[88]. One study has shown that the high thickness of sympathetic fibers and α1 adrenergic receptors expression in Kupffer cells are associated with poor prognosis in patients with HCC. In the same vein, sympathectomy or α1 adrenergic receptors inhibition decreased HCC incidence and attenuated IL-6 and TGF-β expression in DEN-induced rat model[89]. On the other hand, vagal stimulation, notably through the α7 nicotinic Acetylcholine Receptor (α7nAchR)[90], shows anti-inflammatory activity in animal models of NASH, a notion of crucial interest in fibrogenesis and, therefore in HCC development. In a somewhat preliminary study in patients that mobilized disputable approaches, high levels of both cholinergic ($VAChT^+$) and adrenergic (TH^+) fibers were detected in tumors, where VAChT and TH correlate with serum AFP, TNM clinical stage, vascular invasion and nodular spread[91]. Also, the expression of these two markers correlated with shorter survival time.

Overall, these scant data in the field of HCC 'neurology' suggest that the infiltration of autonomic nerves promotes the development of CLD and HCC. Despite these findings, sometimes conflicting, the exact role of sympathetic and parasympathetic nerves in chronic liver pathologies remain probably largely undocumented.

To date, ANS post-synaptic receptors, both adrenergic and cholinergic, have been shown to be favorably actionable in some experimental conditions in cancer[81,92]. In the same vein few families of neurotrophic factors promote a boom in interest in the clarification of pathological neuroregulation in cancer and in the search of new therapeutic targets.

1.3. Axon guidance molecules

Over the past decade, a large number of axon guidance ligands, including the semaphorins, slits, netrins and ephrins, and their receptors have been identified[93]. Although neurodevelopmental disorders, such as autism and schizophrenia, and neurodegenerative disorders, such as Alzheimer's or Parkinson's diseases, have all been linked to aberrant development or disintegration of neuronal circuits, respectively[94], there is an increasing evidence of implication of axon guidance molecules in cancer while their likely relevance in liver diseases merit consideration.

1.3.1. Molecules in axonal guidance during neurogenesis

During morphogenesis of the nervous system, neurons appear in specialized regions and then migrate to their final location. Each neuron develops dendrites and an axon that extends to reach its synaptic target. Axon guidance molecules are crucial for the development of neural circuits in 80 billion neurons of the human brain. They can be subdivided into attractive and repulsive cues navigating the axons through the pre-existing tissues to find their target cells. These signals can be soluble or bound to the extracellular matrix, operating over large or short distances, but are also restricted by interaction with the extracellular matrix or expressed through gradients[95] with likely diverse pharmacodynamics.

Semaphorins

Two receptor families exert repulsive signals elicited by 30 members (21 in mammals) of semaphorins (sema) ligand family: neuropilins – NP1 and NP2 – and plexins – plexA1-4, plexB1-3, plexC1 and plexD, requiring co-stimulation by NPs and plexins for signal transduction in sema3A-3F. Sympathetic, motor, cerebellar, hippocampal, olfactory and corticospinal neurons, among others, respond to semaphorins. A recent research describes the role of some semaphorins in cellular immunity and suppressive or stimulating inflammatory response[96]. Neuropilins are expressed by commissural neurons, important in the coordination of sensory information converging from the whole body, and are required for navigation of commissural axons across the midline of the CNS, where the semaphorins acts in coordination with another class of repellent proteins, the slits.

Slits

Large extracellular matrix proteins slit1-3 (SLIT1-SLIT3) act as chemorepellents at the midline of CNS but also induce commissural axon branching via roundabout 1-4 (ROBO1-ROBO4) receptors[97]. The co-expression of robo1-4 determines the medial-lateral position of axons within longitudinal tracts, whereas robo2 is also implicated in anterior-posterior axon guidance in the visual system[98].

Netrins

In contrast, a small family of proteins, named netrins ('the one who guides' in Sanskrit) attracts commissural axons via Deleted in Colorectal Cancer (DCC) family of receptors, including DCC and neogenin, but also repulse them with UNC5 family, including UNC5A, UNC5B, UNC5C and UNC5D receptors, in the absence of the major netrins receptor DCC[99,100]. Besides their role in axon guidance and nerve regeneration in the CNS and in the peripheral nervous system, netrins also have strong chemotropic function on cell migration, as well as activity on morphogenesis and angiogenesis[101].

Ephrins

Anchored to the plasma membrane, ephrinA1-A5 and ephrinsB1-B3 ligands act via ephA and ephB receptors, guiding the commissural axons across the midline and in the visual system. Through the contact between receptor-expressing cells and ligand-expressing cells, ephrins and ephs are capable of eliciting 'bidirectional triggering' where ephs mediate forward signaling and ephrins – reverse one. The ephrin-eph impact is not limited to the nervous system. EphA2, expressed in angiogenic vasculature, enhances neovascularization, and ephrin-A5, expressed in the pancreatic β cells, inhibits insulin secretion[102].

At the intracellular signaling level, guidance molecules' receptors implicate on the one hand Rho GTPases activation and, on the other hand, trigger clustering of several types of tyrosine kinase receptors or tyrosine phosphatases[103,104].

Development

In contrast to the CNS, the role of guidance ligands and receptors in the development of the peripheral and enteric nervous systems has not been fully investigated. Several studies *in vivo* show the expression of these factors. For instance, DCC receptor is present in the developing murine ANS in sensory ganglia and nerves associated with the glossopharyngeal (IX) ganglion and superior and inferior vagal (X) ganglia[105].

Adulthood

Several of these families' members continue to be expressed in the adult brain and spinal cord. Their expression seems to be involved in neuronal plasticity[106] and regulated upon nervous system injury in rodents and in neuropathology in humans. Importantly, the functions of axon guidance molecules are not limited to embryological axonal guidance. Indeed, semaphorins are important for heart and bone development; ephrins are crucial for vasculogenesis, somitogenesis and synaptic plasticity; slits play important role in cell migration, cell death and angiogenesis, and has a pivotal role during the development of other tissues such as the lung, kidney, liver and breast; and the expression of netrins and their receptors in non-neural tissues suggests a role in morphogenesis of branched organes[98,107,108].

Although their functions in the embryonic CNS have been extensively studied, the axonal guidance molecules seem to play important roles in the adult.

- Netrin-1 is also constitutively expressed in the adult mammalian nervous system. It is secreted by multiple types of neurons and by myelinating glia, such as oligodendrocytes in the CNS and Schwann cells in the ANS, where it is not fully soluble but mainly associated with membranes and extracellular matrix [109].
- Ephs and ephrins were shown to be involved in control of intestinal epithelium architecture (ephB2/3, in mammary gland development during pubertal and pregnancy phases and post-lactational gland involution (ephA2, ephB4), in permeability of tubule cells in the kidney (ephB2), in blood coagulation (ephA4, ephB1, ephrinB1), in insulin secretion (ephA5, ephrinA5)[110].
- Slit/robo signaling appears to have important functions in gonadal physiology, in pancreatic islets β-cells physiology and in peripheral nerve regeneration upon injury[111,112].
- Semaphorins are ubiquitously expressed almost in all tissues of the body[113]. They are known to affect vascular permeability (sema3A, sema3F, sema7A), to regulate immune cell migration and function, to control osteoclast activity in bone homeostasis (sema3A, sema3B, plexD1, sema4D/plexB1)[114].

Importantly, evidence suggests that semaphorin, slit, netrin and ephrin families signaling intersect between them to regulate different physiological functions, in organogenesis, but also in angiogenesis, cell proliferation and stem cells regulation[115].

1.3.2. Axonal guidance molecules in CLD

Hepatic neurogenesis is synchronous to hepatic organogenesis. It cannot therefore be excluded that those regenerative processes of the liver, which are reactivated during CLD and are functionally related to earlier developmental processes, could be again accompanied and regulated by neural events. Hepatic neural ablation highlighted the importance of autonomic innervation in both physiological and pathological contexts, including liver regeneration[17].

Both, sympathetic and parasympathetic systems influence nutrient metabolism, immune processes, hemodynamics, bloodstream and hormone homeostasis. Their implication in liver repair and regeneration in the context of CLD, such as cirrhosis and hepatocellular carcinoma, has been experimentally established[16,86].

Increased sympathetic neuropathy was observed in NAFLD patients, while sympathetic hyperstimulation induced progressively the metabolic syndrome, fatty liver disease and steatohepatitis in mice on normal diet, the latter being reversible by chemical sympathectomy[116]. In addition, increased activity of sympathetic fibers in the liver was reported in high-fat-diet obese mice, another model of NAFLD, and sympathetic disorganization of the sympathetic innervation was identified in steatotic mice fed on Western diet[16]. Instead, the blockage of such hepatic sympathetic overactivation improved the organ's metabolic phenotype. Interestingly, this sympathetic overactivity was reversible, which suggests the possibility of therapeutic intervention[15].

Fibrosis is an important process that occur during injury in the liver. The hepatic fibrogenesis is characterized by increased and altered deposition of EMC. Although several other cell types may also participate in liver fibrosis onset and development, HSC are now recognized as the primary cells responsible of extracellular matrix deposition. Multiple studies demonstrated the involvement of the four families to CLD physiopathology:

- Couples slit2-robo1 and slit2-robo2 were found overexpressed in patients with liver fibrosis. Robo2 was found in fibrotic septa of fibrotic liver and on the surface of HSCs in experimental models of fibrosis *in vivo,* whereas slit2 increases the expression of pro-fibrotic mediators, such as TGF-β1 and CTGF, as well as Col-1, a major fibrotic component *in vitro*[117]. Pharmacological targeting with neutralizing antibody anti-robo-1 inhibited the progression of fibrosis[118].
- Although mostly expressed during development, the ephrins-A/EphA system is reactivated in adulthood in pathological contexts. Ephrins and ephs regulate fundamental biological processes – cell migration, myofibroblast activation, angiogenesis and tissue remodeling – that are involved in fibrosis. Increased expression of ephrinB2 was observed in patients with cardiac, kidney, lung, skin and liver fibrosis. In liver, ephrinB2 has been shown to modulate HSC activation *in vitro* and enhance pathological sinusoidal remodeling and portal hypertension *in vivo* by stimulating VEGF production by HSCs[119].
- Sema3C, a new marker of HSC activation, was overexpressed in fibrotic patients' livers and exacerbates liver fibrosis *in vivo*. In addition, the inhibition of its receptor NRP2 reduced liver fibrosis *in vivo*[120]. Interestingly, serum concentration of sema3C and sema6D were associated with pathogenesis of viral hepatitis and progression of fibrosis in HCV-g1 and HCV-g3 infected patients, and were decreased after DAA and PegINFa treatment. Sema3C and sema5A, attenuating apoptosis and increasing angiogenesis, decrease were overexpressed in HCV cirrhotic liver and HCC tissues[96]. Instead, sema7A, another marker of HSC activation, was overexpressed in fibrotic patients and mice tissues, and was increased in the course of liver fibrosis[121]. Finally, sema3E showed to play a role in LSECs regeneration and in the progression of liver fibrosis in CCL4-treated mice[122].
- The pro-fibrotic role of netrin-1 was largely studied in pulmonary fibrosis and is systemic sclerosis[123], demonstrating fibroprotective effect of netrin-1 deficiency in mice, notably mediated through the decreased amount of fibrocytes in the EMC scaffold. Few studies document the controversial role of netrin-1 in the liver. One study showed the liver-protective and anti-inflammatory action of the neuroimmune netrin-1 through its receptor A2B[124], while another one demonstrated the association between overexpression of netrin-1 receptor UNC5B and apoptosis, inflammation and fibrosis in fibrotic rats. Interestingly, netrin-1 was expressed gradually between acinar zone III and I of the rat hepatic lobule[125]. In patients, netrin-1 was upregulated and its receptor UNC5A

was downregulated in HCV-positive hepatic lesions at all stages of fibrosis and in HCC[126,127].

1.3.3. Axonal guidance molecules in HCC

Given their implication in physiological and pathological conditions in various organs, neuronal guidance molecules are subject to extensive research in the field of cancer.

Some axon guidance cues may be implicated in intra-tumoral angiogenesis and in tumor immune infiltration:

- Netrin-1 was showed to inhibit leukocyte chemotaxis – migration of neutrophils, macrophages and lymphocytes – *in vitro* and *in vivo*[108]. Guo et al. showed that netrin-1 was also found expressed on the peritoneal macrophages in rats, while promoting neuroangiogenesis and facilitating nerve infiltration and sensitization through the MAPK pathways[128].
- Sema3B and sema3F from class 3 semaphorins are well described inhibitors of tumor angiogenesis, progression and metastasis, whereas sema3F inhibits tumor growth but promotes invasiveness and metastasis[129]. The expression of sema3A was also elevated in HCC patients. sema3A promotes HCC growth, invasion, and metastasis in vivo, by increasing CapG, galectin-3, enolase-2 and EpCAM *in vivo*[130]. Sema3A also binds to receptor complexes NRP-plexA on the TAMs, guiding them to hypoxic regions of tumor, where TAM promote angiogenesis and tumor growth. This phenomenon was reversed via *SEMA3A* RNA interference or macrophage-specific NRP inactivation *in vitro* and *in vivo* in lung cancer [131].
- *ROBO1* mRNA and protein are overexpressed in HCC patient samples compared to normal and adjacent peri-tumoral tissues, with a strong enrichment in poorly differentiated HCC compared with well-differentiated and moderately differentiated HCC[132]. Robo-1 promotes tumor angiogenesis and tumor growth in HCC *in vivo*[133]. Its targeting with a neutralizing monoclonal antibody showed anti-tumor activity in an HCC xenograft model. Slit2 was showed to inhibit leukocyte chemotaxis, whereas slit3 promotes monocyte migration[128].
- EphA1 and ephA2 were found overexpressed in HCC patient samples and closely associated with tumor nodules, absence of tumor capsule, portal vein invasion, differentiation grade[134], advanced TNM stage and poor prognosis of HCC[135]. Their inhibition *in vitro* attenuated neoangiogenesis and tumor growth in HCC *in vitro* and *in vivo*[136]. Some studies have demonstrated that the altered expression of ephrins is positively correlated with worse prognosis in patients with HCC[137].

Most axon guidance receptors associate with significantly unfavorable prognostic value at 5-year follow-up, whereas the ligands show both favorable or unfavorable prognostic value (**Figure *12***).

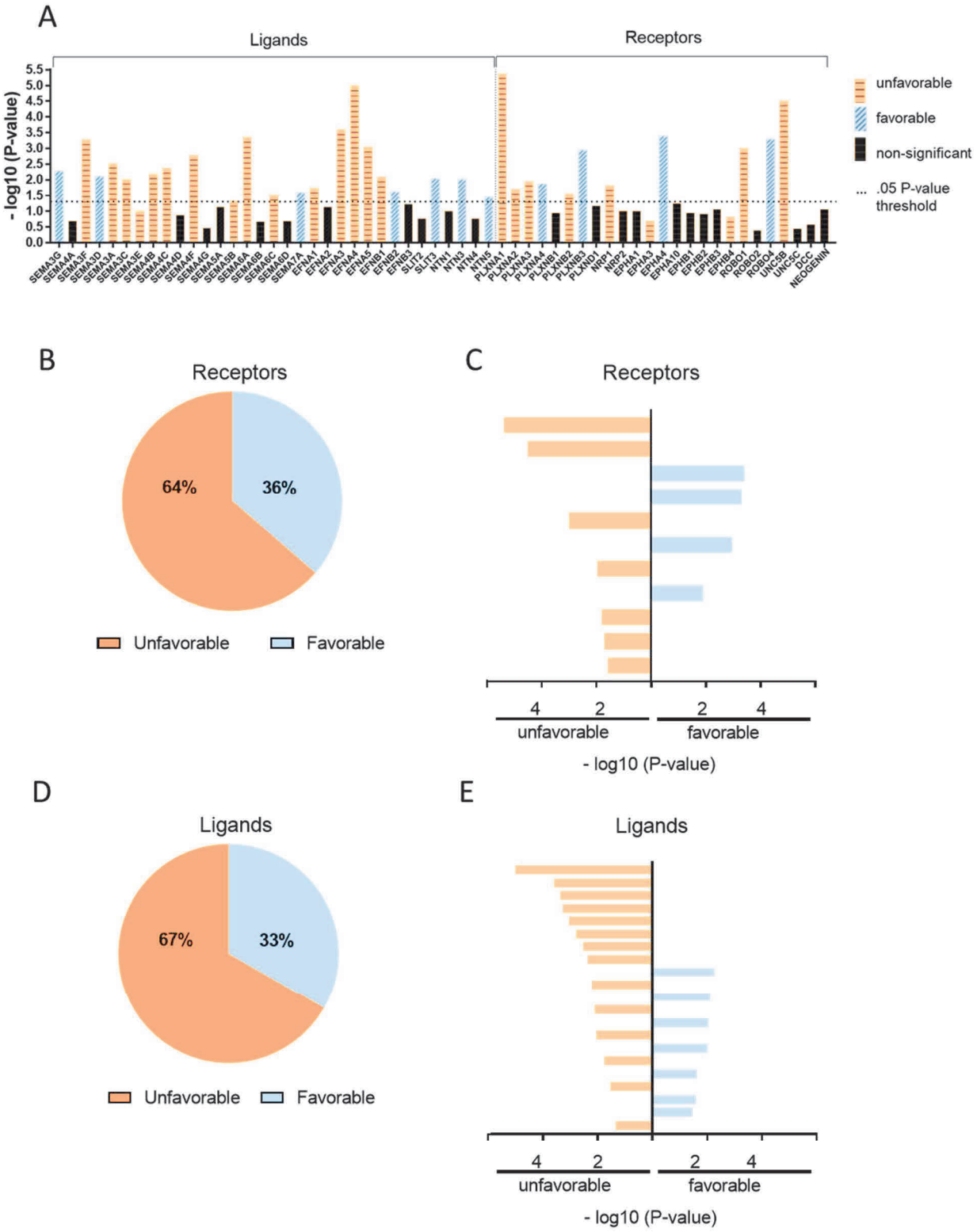

Figure 12. Most axon guidance ligands and receptors show prognostic value in HCC TCGA RNA samples

(A) Axon guidance's ligands and receptors prognostic values at 5-year mortality rate. Both ligands and receptors from all four axon guidance families show prognostic value in patients with HCC.

(B) , (D) Distribution of unfavorable and favorable prognostic markers. Data only included statistically significant markers among those available in public databases.

(C) , (E) Prevalence of unfavorable versus favorable prognostic markers with associated degree of certainty (p-value). Were included only statistically significant markers among those available in public databases.

Adapted from proteinatlas.org (accessed on May 16, 2022).

1.3.4. Axonal guidance molecules as new therapeutic targets in cancer treatment

Clinicians and researchers are hence looking for novel targetable HCC markers, by shedding light on unexplored features of cancers. In this respect, cellular/tissular structures linking the general pathophysiology of the patient with HCC may be of interest, as they are whole patient-specific and may allow novel ways of defining stratification criteria. In line with such notions, several recent studied have highlighted the relevance of studying cancer neurosciences of peripheral organs. In that context, pathological innervation and ANS involvement or dysregulation have been identified in colorectal, prostate, gastric, pancreatic and lung cancers[79–82], nurturing cancer cells and tumor microenvironment and conferring stronger tumorigenic properties:

- The concentration of secreted semaphorins in serum is currently been studied in a clinical trial aiming to evaluate it as a novel circulating biomarker in patients with NAFLD (NCT04573543). Whereas another clinical study evaluated transcript expression level of semaphorins in patients with NASH (NCT02820285).
- Small molecules, neutralizing antibodies and overexpression (or local or systemic administration) of a mutated, uncleavable form of protein, have been used to alter semaphorin signals: sema3A - *in vitro* and *in vivo* in the model of the impaired innervation [138], immunomodulator sema4D-plexB1 - in HER2+ breast and colon cancers *in vivo*[139], sema3E - in $HER2^{+}$ breast cancer *in vitro*.
- Given the role of slit2-robo1 couple in tumor progression, its inhibition could suppress metastasis. Moreover, both DCC and robos are inactivated by Disintegrin And Metalloproteinase 10 (ADAM10), a protease implicated in neurodegenerative diseases, dysfunction of the immune system and cancer[140]. ADAM10 inhibitors are being currently tested in the treatment of pediatric glioma (NCT0429575) and diabetic nephropathy (NCT00312780). However, despite its overexpression in CLD it is also a negative regulator of Liver Progenitor Cells (LPC). On one hand ADAM10 suppresses fibrosis and LPC proliferation by immune cell mediation, but induces bile acids accumulation and necrosis in ADAM10-deficient mice; while, on the other hand, which makes it difficult to target in the hepatic context[140,141].
- Netrin-1 targeting reduces vascular and nerve infiltration in endometriotic lesions in rats, notably through the CD146 receptor (melanoma adhesion cell molecule) and neogenin receptor[128]. It also appears as an attractive and promising anti-angiogenic target in diabetic retinopathy[142].

1.4. Netrin-1 and dependence receptors

1.4.1. Netrins and their receptors

In vertebrates, three secreted netrins, netrin-1, -3 and -4, and two membrane-anchored netrins, netrin G1 and G2, have been reported. As laminin-related proteins, netrins encode a N-terminal laminin VI domain, a central laminin V domain and C-terminal domain (**Figure *13***A). This C-domain is enriched in basic amino-acids and binds to heparin with high affinity, and may contribute to presenting secreted netrins on cell surface or retaining them in extracellular matrix through interaction with heparan sulphate proteoglycans[143]. Netrins engage a number of different receptors. Several of them belong to the immunoglobulin superfamily involved in signal

transduction and cell adhesion. In mammals, DCC family was first identified with DCC and neogenin proteins. Then, UNC5 family with UNC5A, -B, -C and -D, and Down's Syndrome Cell Adhesion Molecule (DSCAM). Several other non-canonical netrin receptors and ligands, such as draxin, RGM, FLRT, DSCAM or A2B have been discovered in the past decade (**Figure *13***B).

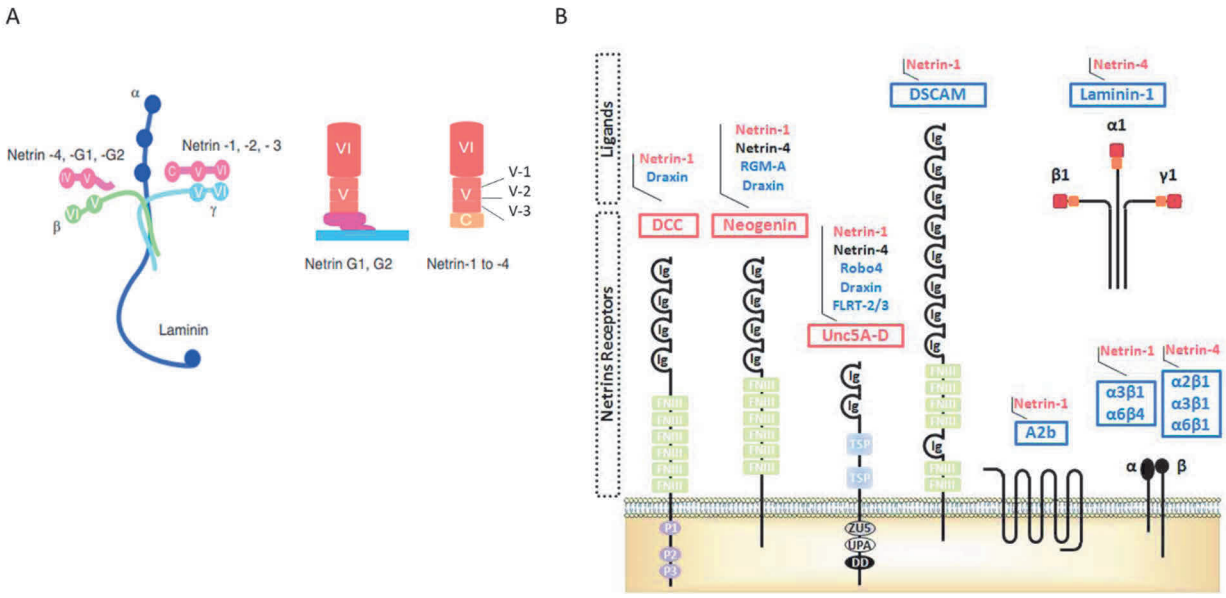

Figure 13. The netrin family of proteins and their receptors

(A) Netrins are members of the laminin superfamily. Netrin-1 is composed of three domains – VI, V and C-terminal, where domains V and VI are homologous to domains V and VI of laminins. V domain includes EGF-like domains V-1, -2 and- 3. B.

(B) Canonical (red) and non-canonical (blue) netrin receptors and typical (red) and atypical (blue) ligands are shown. DCC, Deleted in colorectal cancer; DSCAM, Down syndrome cell adhesion molecule; Draxin, Dorsal repulsive axon guidance protein; FLRT-2 and 3, Fibronectin and leucine-rich transmembrane protein-2 and 3; RGM-A, Repulsive Guidance Molecule-A; Robo4, Magic Roundabout. Ig, immunoglobulin domain; FNIII, fibronectin type III domain; P1-3, conserved region of the DCC cytoplasmic domain; TSP, thrombospondin type-1 domain; ZU-5, zona occludens 5; UPA, Unc5, PIDD and ankyrin domain; DD, death domain.

Adapted from Larrieu-Lahargue et al., 2012[144] & Xu et al., 2014[145].

1.4.2. Netrin-1

Netrin-1 is a secreted protein, a member of the netrin family involved in the development of the nervous system in the embryo through its direct activation of neuronal cell surface receptors. Discovered in 1994 by Marc Tessier-Lavigne, it is the first described chemoattractive molecule controlling the guidance of the commissural axons[146]. It is also the best characterized for its function and expression as a member of the netrin family. Netrin-1 is encoded by a gene situated on the chromosome 17p13-p12. Its transcription is directly initiated by NF-kB, ETS-1, ETS-1 and p53[147]. With 5954 bases, *NTN1* transcript includes 7 exons, but some cancer cells (e.g., neuroblastoma, pancreatic and colorectal cancers) also produce a truncated intranuclear form of netrin-1 ΔN-nertin-1, through an alternative promoter in intron 1[148].

During neuronal development, netrin-1 acts as a guidance factor as well as a survival factor. Indeed, several studies *in vivo* have shown that the presence of netrin-1 in the CNS along the pathway of migration may be important not only for axon attraction/repulsion but may as well be a key support survival of these neurons. Moreover, the neuronal crest cells in developing bowel and pancreas are also dependent on DCC/netrin-1 not only for migration but also for

survival[149]. Knockout mice of netrin-1 and its receptors UNC5 display aberrant phenotypes, indicating their critical roles in development, especially in neurogenesis[150] (**Table *3***).

Gene	Phenotype of knockout mice
***NTN1*$^{-/-}$**	embryonic lethality or postnatal early death, severe axon guidance defects
***UNC5A*$^{-/-}$**	decreased apoptosis, supernumerary neurons, abnormal spinal architecture
***UNC5B*$^{-/-}$**	aberrant extension in endothelial cells, excessive vessel branching and abnormal navigation
***UNC5C*$^{-/-}$**	long-range axon dorsal guidance defects, degeneration of neurons
***UNC5D*$^{-/-}$**	increase in dorsal root ganglia neurons, resistance to NGF depletion-induced apoptosis in sympathetic neurons

Table 3. Biological dysfunctions in development in netrin-1 or UNC5 knockout mice

Adapted from Zhu et al., 2021[150].

Although netrin-1's axonal impacts have been linked to DCC and UNC5 families, DCC and neogenin operate both chemoattraction and repulsion, and UNC5s mediate chemorepulsion in the absence or presence of DCC[151]. Alongside with signaling pathways of chemoattraction and chemorepulsion, mediated by activation of several kinases (e.g., Src-Family Kinase (SFKs), Fyn, Protein Tyrosine Kinase 2 (PTK2)) and Rho GTPases, PI3K, PhosphoLipase Cy (PLCy) and tyrosine phosphatase Sph2, netrin-1 acts through apoptotic dependance receptor signaling pathways. In the absence of netrin-1, DCC is a monomer with an accessible site for caspase-3 cleavage, crucial for DCC apoptotic activity. UNC5s are also cleaved by caspase-3 at the site located within the death domain of the UNC5s, and apoptosis is induced by the death domain interacting with Death-Associated Protein Kinase (DAPK), which in turn activates caspase-9, triggering enhanced caspase-3 activation. DCC -mediated apoptosis inhibition is induced by receptor dimerization upon netrin-1 binding, and therefore hiding of cleavage site from caspase-3 (**Figure *14***)[152].

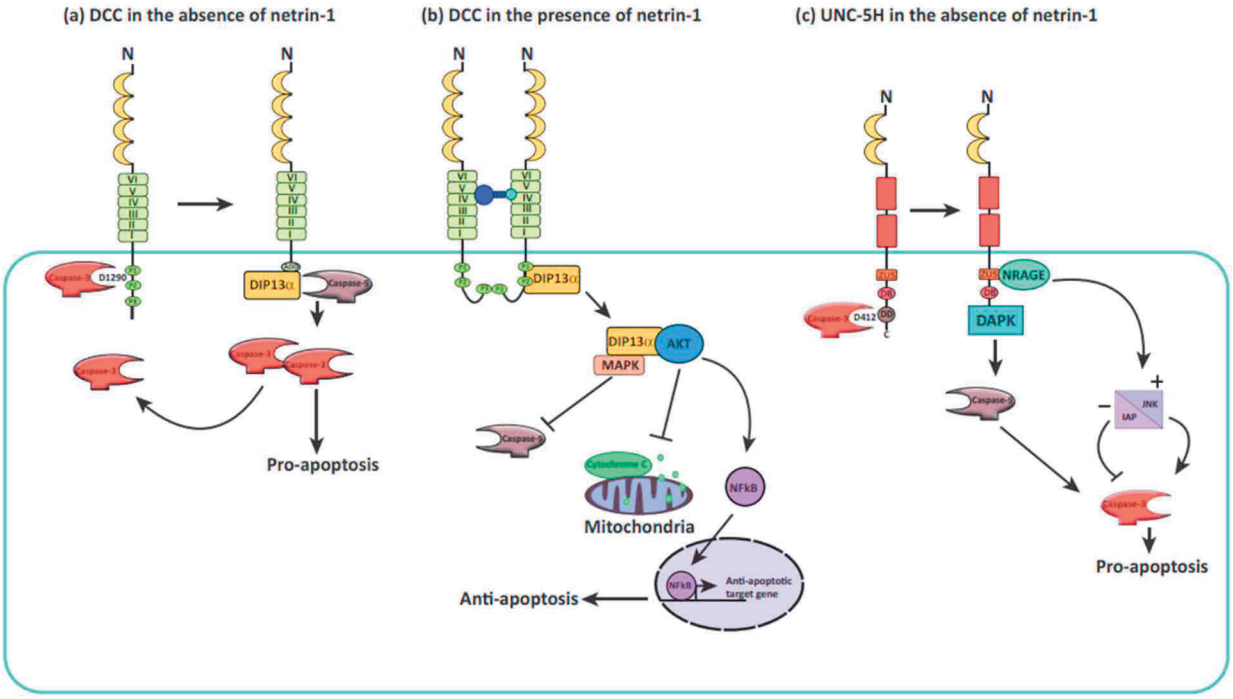

Figure 14. Netrin-1 death and anti-death dependence receptor signaling

Adapted from Ko et al., 2012[152].

The expression and function of netrin-1 in the developing CNS have been extensively studied. Interestingly, expression of netrin-1 receptor DCC was found in the developing enteric nervous system, the largest sub-division of the ANS, that is innervating the wall of gastrointestinal tract. Netri-1, expressed in the developing lung epithelium together with UN5CB, modulates the morphogenesis of the large airways in lung[153]. Several recent studies have suggested guidance roles for netrin-1, such as functioning as an instructional molecule for the building of complex non-neuronal structures in organs (e.g., inner ear and mammary gland)[154]. The expression of netrin-1 in many different human adult tissues (e.g., heart, kidney, liver, ovary, small intestine, mammary gland, lung, colon and prostate) suggests that netrin-1 may have a function (e.g., morphogenesis) outside the developing nervous system distinct from that in mediating axon outgrowth[155]. Thus, the interaction netrin-1/UNC5B is involved in the endothelial vessels' morphogenesis. In adults, the expression profile of netrin-1 and its receptors suggests its implication in local homeostatic control, particularly in tissue with intense cell renewal such as intestine or colon[156].

Interestingly, the netrin-1 receptor UNC5B also plays an important role in organ development, angiogenesis, immune response and stem cell regulation, and participates in survival and retention of macrophages, thus contributing to immune response to tumor cells[150].

1.4.3. Dependence receptors

Receptors are usually considered as inactive unless bound by their ligands. Recent studies have shown that some receptors, involved in both neurogenesis and tumorigenesis, exhibit the opposite behavior.

Cell survival is mediated by various receptors and sensors, such as trophic factors, hormones or cell-cell interaction. Although such stimuli are positive survival signals, a negative signal transduction in the absence of the required stimulus is mediated by specific "dependence receptors". Therefore, the expression of a dependency receptor creates a state of dependence on its ligand. In addition to their "positive" effects on cell survival, migration and differentiation when bound by their ligands, these receptors transduce signal of programmed cell death when unbound by a ligand. To date, twenty of such receptors have been identified (**Figure *15***): p75NTR, plexin D1, RET, TrkA and TrkC, MET, kremen-1, EPHA4, ALK, DCC and UNC5A-D, neogenin, the insulin receptor and its related receptor IGF-1R, some integrins, sonic hedgehog receptors Patched (Ptc) and CDON[157]. While not sharing much homology between them, most of these receptors trigger apoptosis upon a proteolytic cleavage of their intracellular domains.

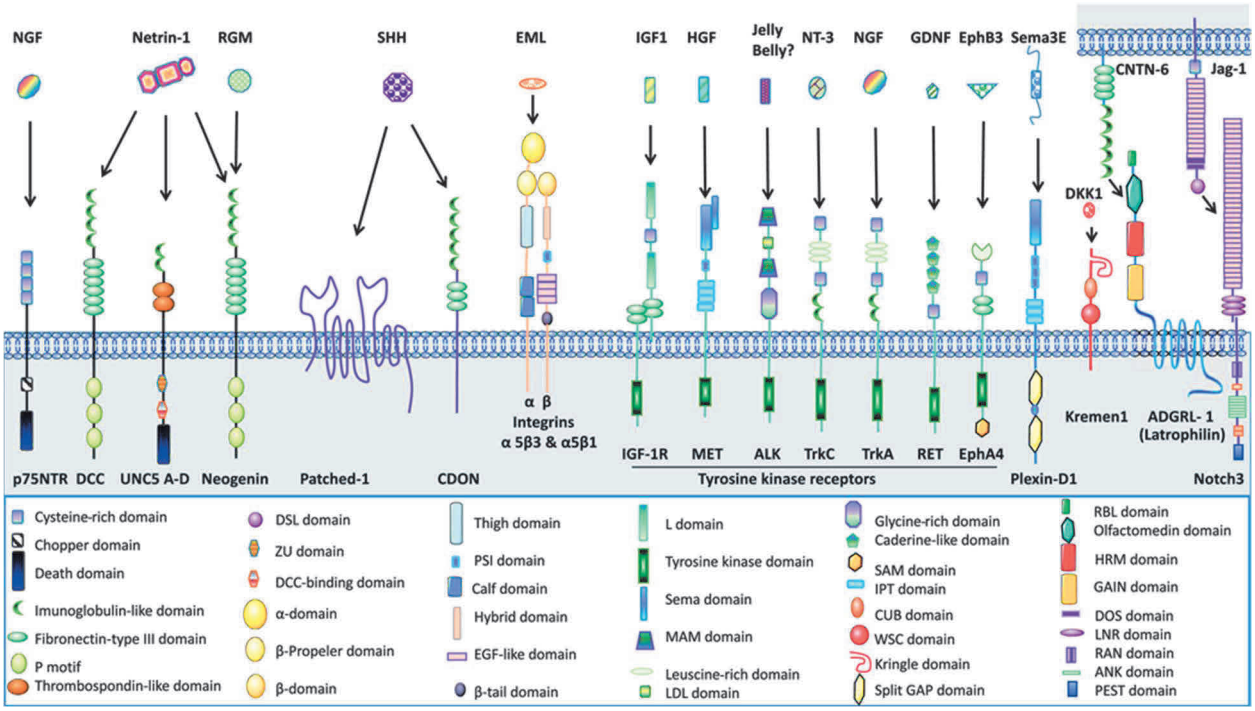

Figure 15. The family of dependance receptors

Adapted from Negulescu et al., 2018[158].

1.4.4. Netrin-1 and its dependence receptors in cancer

Studies of netrins' function in neural and non-neural tissues have revealed important contributions of netrins in regulating cell-cell adhesion and tissue organization. Leaving embryogenesis and entering the field of tissue repair, exciting findings have implicated netrin-1 in directing adult neural stem-cell migration, suggesting that netrin-1 may influence recovery following tissue injury.[143] Although netrin-1 dependence receptors play crucial roles in nervous system and morphogenesis, loss of these receptors and overexpression of netrin-1 have been observed in many cancers (31%-60% of metastatic breast cancer, 47% of lung cancer, 38 % of neuroblastoma, 7% of colorectal cancer)[156,157,159]. The mechanism of gain of function of netrin-1 appears to be due rather to a change in promoter activity, while it is also a direct transcriptional target of NF-kB, and both are upregulated in tumor cells. Netrin-1 expression is adversely linked with the time of relapse of patients with pancreatic cancer and is associated with poor prognosis[156]. Netrin-1 was also shown to be associated with metastasis in breast cancer[160].

The fact that the different dependence receptors trigger apoptosis in the absence of their ligands suggests that they all can regulate tumorigenesis. In contrast to classical tumor suppressors, dependence receptors may function as conditional tumor suppressors, as they acquire their suppressive activity only in the context of cell growth outside of high ligand availability, while potentially accelerating tumor development within the area of high ligand concentration.

If DCC and UNC5s play a role of safeguard mechanism preventing tumor proliferation in tissue with limited netrin-1 expression, an aggressive tumor cell should block this dependence receptors to survive:

Indeed, the *DCC* gene is deleted in 70% of CRC, and many other tumors. Also, *DCC*, initially reported as only rarely mutated, is finally the third most frequent mutated gene in sun-exposed melanoma[157]. Moreover, a whole series of studies show that *DCC/UNC5A/UNC5B/UNC5C* gene reintroduction suppresses tumorigenesis in cells[150,156]. UNC5s have been also shown to be

mutated in sporadic CRC - the expressions of *UNC5A, UNC5B* and *UNC5C* decrease in 48%, 27% and 74%-77% of CRC, respectively[150]. Because loss of DCC is observed with high frequency in late stage tumors and also because both DCC and UNC5s may be differentially important at these two periods, netrin-1 seems to have an effect at early (development of hyperplasia and adenoma) and later (adenocarcinoma development) stages of carcinogenesis[161]. In addition to CRC, *UNC5A*, *-B* and *-C* are downregulated in 88% of ovarian cancer, 49% of breast cancer, 48% of cervical cancer, 68% of gastric cancer, 74% of lung cancer and 81% of renal cancer[162] cases.

Several studies proposed have identified that the expression of UNC5s is regulated by genetic aberrations (loss of heterosygosity, point mutation, gene rearrangement), epigenetic regulation (promoter hypermethylation), transcriptional regulation (e.g., UNC5s are p53 dependent) and post-transcriptional (e.g., miR-129-5p downregulates UNC5B) and post-translational regulation (polyomavirus small T antigen stabilizes UNC5B) (**Figure *16***)[150].

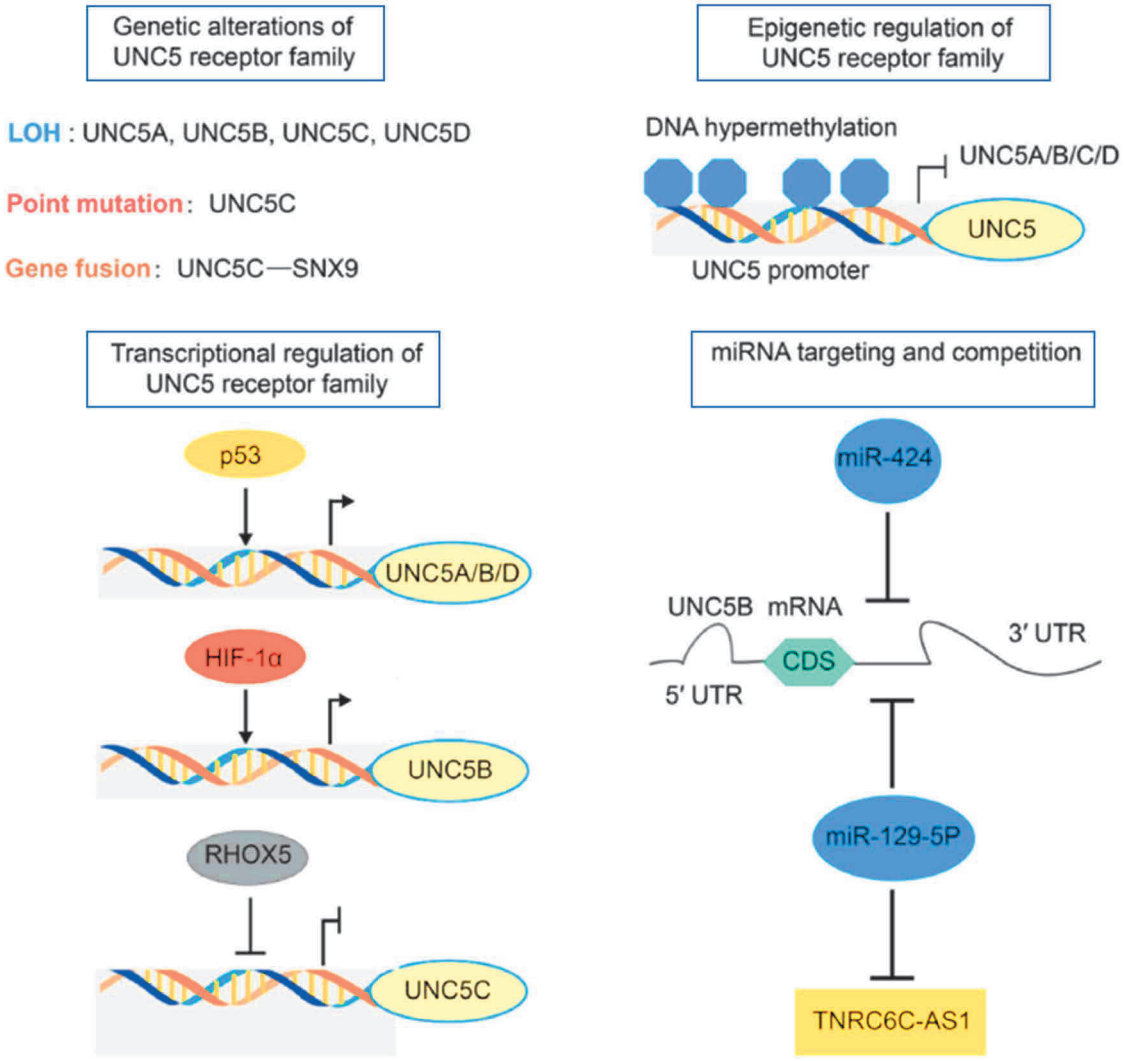

Figure 16. Molecular mechanisms of UNC5 receptor family regulation

LOH: Loss Of Heterozygosity.

Adapted from Zhu et al., 2021[150].

1.4.5. Netrin-1 and its dependance receptors in CLD and HCC

In addition to some solid tumors, netrin-1 is also overexpressed in some inflammatory diseases. Thus, irrespective of etiology, the laboratory has found that it is increased in cirrhotic liver and

shows a 10- to 30-fold increase upon HBV or HCV infection[127] . As mentioned above, ER stress is almost omnipresent in all CLDs irrespective of etiology, and clearly linked to the apoptosis and inflammation processes in the liver. To restore cell homeostasis, the response to ER stress is mediated by UPR, a process involving the activation of 3 main players: Protein Kinase R (PKR)-like Endoplasmic Reticulum Kinase (PERK), Activated Transcription Factor 6 (ATF6) and Inositol Requiring Enzyme 1α (IRE1α). The latter one was described to interact directly with netrin-1 in the axon guidance context[163]. In the context of well described UPR as a hallmark of HCC, a recent study of the laboratory has shed light on the relation between UPR and netrin-1. Indeed, netrin-1 provides hepatocytes the resistance to UPR-related cell death through its positive regulation upon ER stress and UPR-related global translational inhibition both *in vitro* and *in vivo*[164].

Moreover, and in consistence with these findings, a study of the netrin-1/UNC5A couple upon ER stress has shown the downregulation of the dependence receptor UNC5A *in vitro* and *in vivo*, suggesting that both netrin-1 and UNC5A work together to escape from UPR-induced apoptosis[165].

UNC5A receptor, downregulated in HCV-infected patients and essentially in those with advanced stages of fibrosis (F2-F4), reestablishes after anti-HCV treatment. This suggests that HCV strongly impacts the UNC5A biogenesis in patients, especially in preneoplastic liver. Reciprocally, my hosting team has shown that UNC5A is a negative regulator of HCV as it constrains HCV spread *in vitro*, notably through reducing viral replication. Anti-viral effect of UNC5A can be explain by its capacity of hindering autophagy, and this independently from its pro-apoptotic caspase-related action[127]. Of note, UNC5A is dramatically overexpressed in cirrhotic HCV-negative patients and collapses in patients with HCC (> 100-fold decrease), suggesting its possibly intensive implication in the preneoplastic liver and the possibly relevant timeframe to take a preventive action aiming netrin-1/UNC5A axis in HCV-positive patients at high risk to develop HCC.

In the same vein, another dependence receptor - UNC5C was found to collapse in HCC patients[127]. It was also found hypermethylated at early stage (TNM stage 1) of HCC.[166]

In contrast, netrin-1 shows pro-replicative effect through the augmentation of amount of viral RNA and mediates the viral assembly and morphogenesis of virions in HCV-infected hepatic cell lines through the UNC5A and in a non-death-related dependence receptor-conveyed manner, as caspase-3 activity remains unchanged in the process[127]. In turn, netrin-1 is increased in HCV-positive patients and drops after anti-HCV therapy. Plissonnier and al. propose a possible mechanism of netrin-1 augmentation where *NTN1* transcript links to RNA binding proteins LA-Related Protein 1 (LARP1) and NonStructural Protein 5 (NS5A) which favor its further translation upon HCV infection at translation-active sites of the ER.

In summary, the loss of UNC5A elevates HCV infectivity, while the latter induces netrin-1, which in turn enhances HCV infectivity. The direct pro-viral effect of netrin-1 comes together with its indirect effect on the persistence of the HCV cell surface co-receptor EGFR, also overexpressed in HCC patients, necessary for HCV receptors Claudin-1 and CD81 interaction[126]. More precisely, netrin-1 increases EGFR expression on the cell surface and its activation (through its phosphorylation) by jeopardizing its internalization. Thus, netrin-1-induced persisting EGFR empowers the viral entry into the target cell.

Of note, similar to HCV, netrin-1 was also overexpressed in HBV-positive patients.

These data support therapeutic potential of netrin-1/UNC5 targeting in chronic liver disease and HCC with viral etiology. Unpublished data suggests its implication in metabolic and alcohol-

related liver pathologies as well. However, more studies are needed to elucidate the role of netrin-1 in HCC development and its possible management via anti-netrin-1 therapy (**Figure *17***).

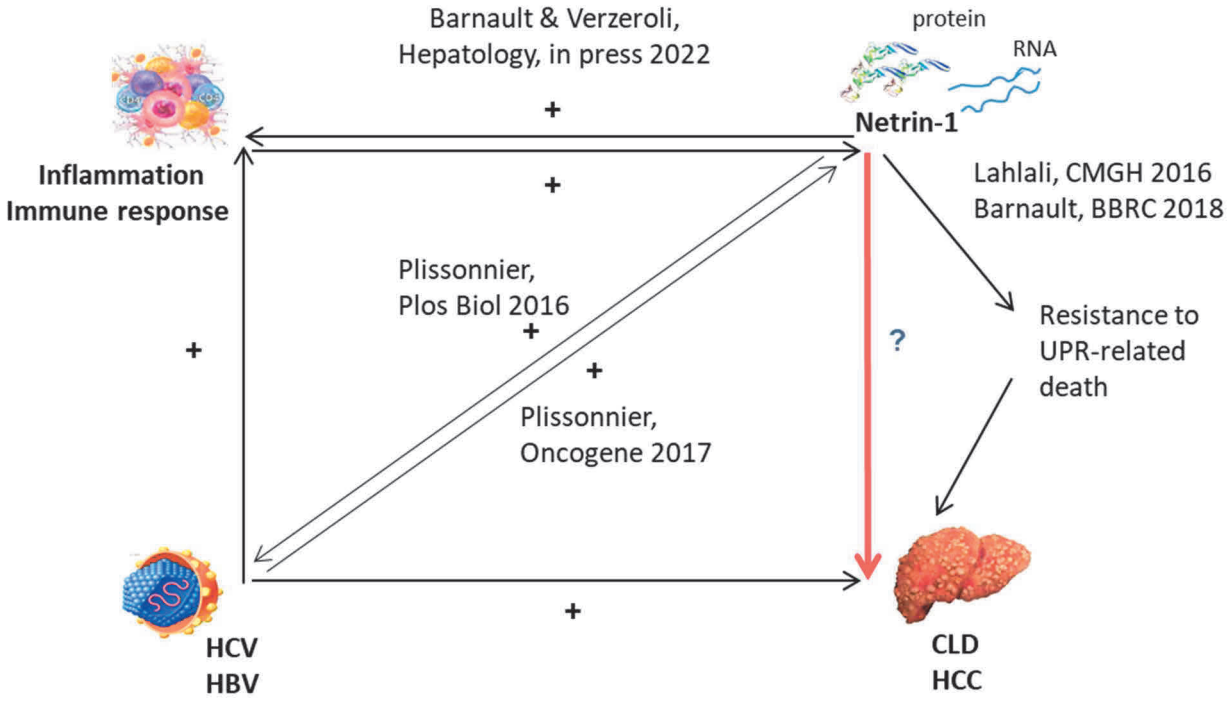

Figure 17. Schematic overview of netrin-1 implication in liver pathologies

1.4.6. Potential clinical application of netrin-1 in cancer treatment

As UNC5s and DCC have apoptosis-inducing function, it makes them attractive for development of anti-tumor therapy, but the core issue surrounding clinical application is to activate their apoptotic function specifically in tumors. There are two options: to restore dependence receptor expression in order to titrate the netrin-1 function as a ligand, or to block the binding of netrin-1 to its receptors.

Several studies report that in some patients UNC5s are highly expressed along with netrin-1, suggesting that blocking ligand-receptor binding may be beneficial for these patients[167]. The findings from multiple *in vivo* studies reveal a potential clinical applicability for netrin-1 targeting. In particular, a Phase I clinical trial assessing a humanized monoclonal antibody targeting netrin-1 (NP137) has shown anti-tumor activity in patients with advanced solid tumors. A Phase Ib/II clinical trial GYNET is ongoing to investigate the clinical and biological activity of NP137 in combination with carboplatin plus paclitaxel and/or anti-PD-1 monoclonal antibody pembrolizumab in patients with locally advanced/metastatic endometrial carcinoma or cervix carcinoma (NCT04652076).

Of note, the epitope recognized by NP137 in netrin-1 shares 90% of homology with netrin-3, upregulated almost exclusively in neuroblastoma and Small Cell Lung Cancer (SCLC). While their expressions are mutually exclusive in tumors, their affinity for the dependence receptors is similar, suggesting that NP137 would be a promising candidate for NB and SCLC treatment as well[150].

Inducing UNC5s expression while blocking netrin-1 binding is another interesting scheme. Indeed, a recent study has shown the inducibility of netrin-1 and DCC, UNC5A, -B and -C by conventional anti-cancer treatment such as doxorubicin, paclitaxel, cisplatin and 5-fluorouracil

in 15 human cancer cell lines[168]. In addition, the similar upregulation of netrin-1 and its receptors was observed in patients with ovarian cancer treated with carboplatin and taxol[150].

This introduction provides an overview of the common features of chronic liver diseases as the precursor to liver cancer, nerves in cancer and HCC in particular, and the axon guidance neurotrophic factor netrin-1, overexpressed in multiple cancers.

Chapter 2: Research project

2.1. Thesis objectives

This project is dedicated to the study of the role of the ANS and the neural ligand netrin-1 in pathological liver conditions such as fibrosis, cirrhosis and hepatocellular carcinoma and to propose a new therapeutic approach in their management. The latter, being a major health problem worldwide, still benefits from a weak therapeutic arsenal and constitutes a real unmet medical need worldwide. With very few published data on ANS implication in CLDs and HCC, my project proposes a renewed look on the liver as a consequence of neuronal-hepatic relation along hepatic pathology development.

Together with efferent ANS fibers, pathological liver is also enriched in neurotropic factors such as netrin-1, an axon guidance molecule normally expressed in pre-existing trophic neuronal tissue in the embryo. We aimed to investigate in our study whether there is an established relation between hepatic neuropathy and netrin-1 in CLD and HCC context.

Since netrin-1 is involved in several cancer types and clinical outcomes, also accumulating in inflammatory gastrointestinal tract-related cancers, we hypothesize that netrin-1 may:

- speed up cirrhosis-to-HCC evolution as a cirrhosis-accumulating[164] anti-apoptotic factor
- participate in treatment failure.

Since active p53 is an *UNC5* inducer and *NTN1* is a direct gene target of p53[169–172], netrin-1 impact may be conditioned by the *TP53* gene mutational status (and its functional phenotype) of the tumor, which could modify the death transduction level related to netrin-1 capture because of its transcriptional implication on UNC5s expression. Netrin-1 targeting may ameliorate transduction of hepatocytic cell death-inducing signal conveyed by UNC5 receptors and may be a promising anti-HCC target, more likely in combination with other drugs. Given the last findings describing netrin-1 as a pathology-associated factor in HCV/HBV-related CLD and HCC (**Figure *17***), it is worth to go deeper in our understanding of its role in HCC onset and progression in viral and non-viral contexts and to study its targetability in fibrosis/cirrhosis and HCC.

Using clinical samples and animal models, the objectives of my PhD projects are:

1. To evaluate the expression of ANS pre-synaptic and post-synaptic actors in CLD/HCC and identify their possible association with CLD/HCC clinical and biological parameters, clinical complications and outcomes
2. To identify the biological role of the neurotropic factor netrin-1 and UNC5s in CLD/HCC and identify their possible association with CLD/HCC clinical and biological parameters, clinical complications and outcomes
3. To test the pertinence of targeting the netrin-1/UNC5 axis in HCC prevention and treatment.

2.2. Working models

2.2.1. *In vitro*

First, pharmacological studies assessing netrin-1 modulation and its effect on the cell viability were carried out in human hepatocyte-like cells (HCC cell lines Hep3B, CLP13, Huh7, Huh7.5, HepG2 and proliferative bipotent progenitor cell line HepaRG isolated from the cirrhotic patient) and Primary Human Hepatocytes (PHHs, isolated from patients' livers resections, quiescent and functionally differentiated). Netrin-1 expression status was integrated into experimental designs

(**Figure 22**A). In addition, pharmacological tests including TKIs were performed in the rat HCC HR-4 cell line.

2.2.2. *In vivo*

In rodents, the liver has a similar architecture, functions and similar cells types than in human liver. However, the macroscopic structure differs as the number and disposition of hepatic lobes is different between murine and human livers. Rodent models of hepatic diseases constitute today a convenient tool of study of human pathologies and of pharmacological assessment of new drug candidates and drug combinations.

Rat model: DEN-induced HCC to test anti-netrin-1 immune therapy

Here, we used a DiEthylNitrosamine (DEN)-induced cirrhotic rat model with HCC to test safety and efficacy of NP137, a clinically used and well tolerated neutralizing anti-netrin-1 monoclonal antibody (NCT04652076), as well as to establish connection between netrin-1/UNC5 axis and ANS orientation (sympathetic or parasympathetic) in a model of the chronic liver disease and HCC.

The advantage of this model, previously described by Schiffer et al.[173,174] and allowing to obtain a fully developed HCC on a cirrhotic liver after 14 weeks, is its close physiopathology to human disease, as the majority of HCC cases develop and progress in cirrhotic context. 6-week-old Fischer 344 male rats were treated weekly with intra-peritoneal (IP) injections of 50 mg/kg DEN diluted in pure olive oil. Then, rats were randomized in two groups and were treated during six weeks by i) Phosphate-Buffered Saline (PBS), or ii) NP137 (10 mg/kg) **(Figure 23B).** Of note, the epitope of netrin-1 protein (ARRCRFNMELYKLSGRKSGGVC, 347- 368 aminoacids[175]) recognized by NP137 is the same in mice.

Mouse model: transgenic mice overexpressing netrin-1

To study the biological role of netrin-1 in HCC development and its relationship with ANS in HCC, 7-week-old transgenic mice were treated with a single injection of DEN (25mg/kg) diluted in pure olive oil at 7 days of life and then with tamoxifen (10mg/kg) at 15 days of life only in mice expressing (Cre^+) to induce HCC at 8 months of life with no associated fibrosis or cirrhosis (**Figure *25***B). The tumor incidence is expected to reach 100% in male mice and about 20% in female mice[176].

This model was also used to study the modulation of the immune and inflammatory responses in netrin-1 overexpressing mice by Flow Cytometry or Fluorescence-Activated Cell Sorting (FACS). Of note, despites few differences in immunity profiles, mice are frequently used to study the immunity response. Rich in granulocytes and monocytes, human blood is poorer in lymphocytes T and B than murine blood, which suggests that human liver has faster and/or stronger inflammatory response. Overall, the mediators of immune response in mice and in humans are much the same, reconciling most murine models with the human ones[177].

2.2.3. Clinical samples

- To assess a connection between the expression of netrin-1 and the stage of hepatic fibrosis and HCC, we measured the level of *NTN1* mRNA in a cohort of 418 patient liver biopsies previously described[126], taken either from virus-free patients (n=165), from HCV-infected patients (n=223), or from HBV-infected patients (n=30).
- To assess netrin-1's potential as a prognostic of factor of cirrhosis – to – HCC progression, we analyzed *NTN1* transcripts in the hepatic biopsies of cirrhotic 101 patients followed in Hospices Civils de Lyon.

- To investigate the role of netrin-1 and UNC5s and their correlation with clinico-biological features in fibrotic and tumoral liver we assessed netrin-1 and UNC5s mRNA expression in 166 patient samples (paired tumoral and peri-tumoral cirrhotic (F4) tissues from the French National HCC Biobank (under IRB agreement of Inserm Ethics Committee (CEEI, #1862)). This cohort was also used to assess ANS pre-synaptic and post-synaptic markers and to establish connection between the netrin-1/UNC5 axis and the liver ANS orientation (sympathetic or parasympathetic).
- To assess netrin-1 protein expression, we analyzed five commercially available patients' Tumor MicroArrays (TMAs).
- To study ANS polarity we performed biostatistical analysis using the HCC-LIHC cohort (Cancer Genome Atlas Research Network, 2017) database from the TCGA Research Network (https://www.cancer.gov/tcga). Data were then crossed with previously reported metadata to obtain a cohort of 193 patients.

2.3. Results

2.3.1. Netrin-1/UNC5 axis in CLD and HCC

Netrin-1 is upregulated in acute hepatic inflammation *in vitro* and *in vivo* and its modulation mediates the inflammatory response

To date, the relationship between inflammation and HCC development, as a model of predominantly inflammation-associated cancer, is not fully understood and is mainly described by pathological activation of the NF-kB/STAT3/IL-6 pathway[178]. Netrin-1 induces NF-κB p65ser536 phosphorylation and c-Myc expression in a UNC5A-dependent manner. In turn, *NTN1* is a direct transcriptional target of NF-kB and its NF-kB-mediated overexpression confers a selective advantage for Dextran Sodium Sulfate-induced colorectal tumor development in mice[147].

Chronic inflammation triggers acellular extracellular matrix –enriched tissue remodeling. Given its common structural features with extracellular matrix -constituting proteins laminins[144,145] and its expression in pre-existing trophic non-neuronal tissue during neurogenesis[146], netrin-1 could participate in extracellular matrix growth. Indeed, macrophage-secreted netrin-1 was already described as a fibrosis promoter in lung fibrosis[179].

Migration of inflammatory cells is a hallmark of the inception of immune responses. Several studies have shown that netrin-1 is highly expressed by the vascular endothelium in the lung and jejunum, and particularly in postcapillary venules, whereas UNC5B is expressed in leukocytes $CD45^{+}$[154]. Netrin-1 was previously reported as a regulator of migration of leukocytes (lymphocytes, monocytes, and granulocytes) during the inflammation outside of CNS, and its receptor UNC5B blocking abolishes the chemotactic effect of netrin-1 on cell migration[154]. Augmented level of netrin-1 and its receptor UNC5B in macrophages have been reported to inhibit macrophage emigration through chemokine CCL2 and CCL19 in a dose dependent manner and maintain inflammation in the peripheral circulation, thus assigning to the netrin-1/UNC5B complex a role of positive regulators of leukocyte migration[180]. The exact cell types expressing netrin-1 in the liver remain unstudied.

In the liver, netrin-1 was identified as a hepatic inflammation-inducible factor *in vitro* and in a model of acute inflammation *in vivo*. Moreover, netrin-1 trapping by the anti-netrin-1 antibody NP137 displayed a clear anti-inflammatory effect (Barnault & Verzeroli et al., 2022). As a laminin-related protein, netrin-1 may be secreted or attached to the extracellular surface of the cell

plasma membrane or extracellular matrix through its heparin-binding C-terminal NeTRin-like (NTR) module. This structural module is implicated in netrin-1 association with cell surface or matrix Heparan Sulfate Proteoglycans (HSPG) and with heparin[181]. Under acute inflammation conditions *in vitro* in HepaRG cells and PHHs, netrin-1 upregulation seems to originate both from enhanced translation and from the release from the pool of hepatocytic cell membrane-bound netrin-1. Interestingly, this upregulation was cell death-unrelated with no impact on cell viability, which underlines the importance of netrin-1 receptors' expression and the significance of the balance ligand/receptor.

Netrin-1 trapping by NP137 reduced the amount of intrahepatic macrophages ($CD45^+/CD11b^+/F4/80^+/Ly6C^+$), known as negative regulators of inflammation (notably through IL-1β and TNF-α) and stimulators of HSCs[182], but also significantly reduced the level of transcripts encoding soluble pro-inflammatory factors IL-1β, CCL2 and CCXL10 *in vivo (***Figure *18****B, D).* Moreover, a transcriptional analysis of 248 inflammation-related transcripts showed the reversion of 15 (cytokines *Ccl2, Ccl3, Ccl5, Ccl8*, ISGs *Stat1, Oas1a, Oasl1, Ifi44* and cyclooxygenase *Ptgs2* and its product prostaglandin I2 (*Ptgir*)) out 81 inflammation-related transcripts upregulated in induced acute inflammation (**Figure *18***C) (Barnault & Verzeroli et al., 2022). However, few tests on human primary monocytes experimentally differentiated in macrophages M1 or M2 showed some conflicting results, where the supplementation with recombinant netrin-1 induced the release of anti-inflammatory IL-10 and reduction of pro-inflammatory IL-1β, IL-6 and TNF-α in M1 macrophages (not shown). These data will be discussed in oral presentation.

In patients, we have observed the upregulation of netrin-1 expression in chronic active and chronic persistent hepatitis compared to normal liver tissue (Barnault & Verzeroli et al., 2022).

On the whole, these data identify netrin-1 as a pro-inflammatory factor in the context of acute and chronic hepatic inflammatory response, in accordance with the findings in other organs, as well as in chronic cancer-associated inflammatory diseases of the gastrointestinal tract such as colitis and Crohn's disease[180,183,184].

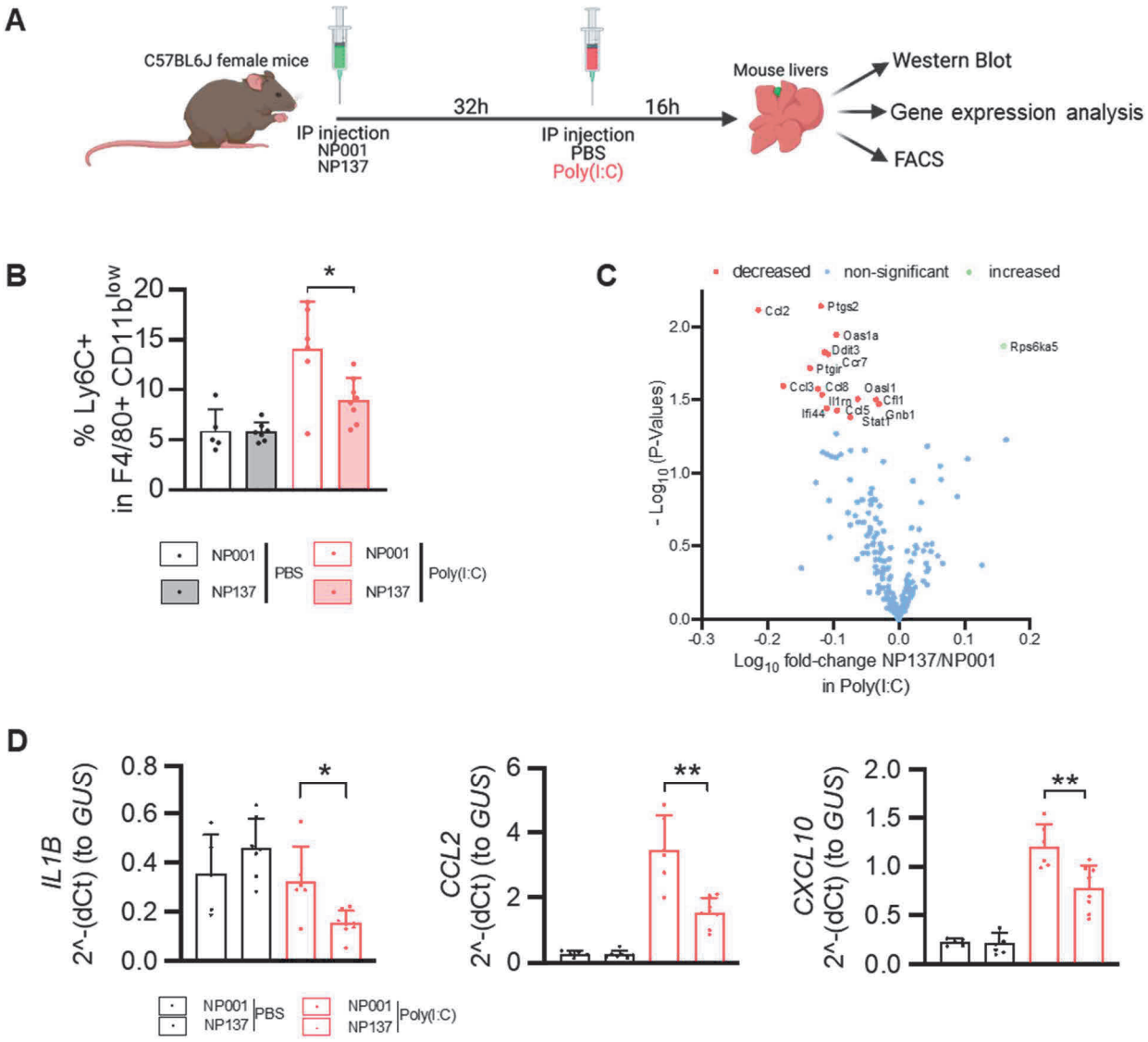

Figure 18. Netrin-1 trapping attenuates hepatic inflammation in mice

(A) Study protocol. Induction of acute inflammation in mice.
(B) Percentage of $CD45^+/CD11b^+/F4/80/Ly6C^+$ cells in different experimental conditions.
(C) Identification of 17 inflammation-related transcripts modulated by netrin-1 capture.
(D) IL-1b, CCL2 and CXCL10 mRNA was quantified RT-qPCR. Mann-Whitney *U* test, *p < 0.05, **p<0.01, ***p<0.001.

Netrin-1/UNC5 axis variations associate with cirrhosis-to-HCC transition

To assess a connection between the expression of netrin-1 and UNC5s and stage of hepatic fibrosis of HCC, we measured the level of *NTN1* and *UNC5*s mRNA in 418 patients with fibrosis or HCC. The findings show a massive induction of *NTN1* in cirrhotic and HCC patients, irrespective of etiology. *UNC5B* and *UNC5C* receptors are also significantly upregulated in cirrhosis and HCC, whereas *UNC5A* expression first drastically augments in cirrhosis and then collapses in HCC patients (**Figure *19***A). The same trend was observed separating the four main etiologies of CLD and HCC (HCV and HBV infections, ALD and NASH). We then analyzed the ratios *NTN1/UNC5,* which reflect the balance of pro-survival ligand to death receptor abundance. Interestingly, the ratio of *NTN1* over *UNC5A* was significantly increased throughout fibrosis progression and in HCC, but collapsed in cirrhotic liver, in accordance with previously published findings[126]. In the same vein, *NTN1/UNC5B* and *NTN1/UNC5C* ratios were upregulated at all fibrosis stages and in HCC as

well when compared to non-fibrotic tissues, respectively. Importantly, in addition to its pro-survival role, mediated by UNC5s, it should be kept in mind the second, and initially primary, chemotactic role of netrin-1, which, we hypothesize, are put at stake to mediate liver disease progression.

Although the causal status of netrin-1 in CLDs and hepatocarcinogenesis remains to be established, a retrospective study of 101 HCV-infected cirrhotic patients attributed a prognostic value for *NTN1* levels. Indeed, patients with high expression of *NTN1* display shorter cancer-free survival (probability of HCC onset is 85% vs. 65%) and have 2.9 times higher risk to develop HCC at 4-year follow-up post cirrhosis diagnosis (**Figure *19***B).

Importantly, in the absence of correlation between transcript and protein expressions observed in previously published and unpublished data, we sought to characterize netrin-1 protein variations in CLDs and HCC. We have analysed netrin-1 in commercially available TMAs containing 624 analysable patient samples, including normal tissue, chronic hepatitis, cirrhosis and HCC samples, with a specific staining anti-netrin-1 antibody validated in previously published multiple studies. We observed an overexpression of netrin-1 in HCC samples compared to normal tissue but also compared to cirrhotic tissue (**Figure *19***C). The etiology data were not available for these TMAs. Indeed, as all patients are from Asian origin (China and Japan), where the predominant etiologies of liver disease are HBV, HCV and ALD[185], it remains to be confirmed whether one is witnessing viral infection-restricted netrin-1 upregulation or a general CLD effect irrespective of etiology. The expression of netrin-1 did not show any correlation with clinical features of HCC (e.g., TNM staging, differentiation grade, sex, and age) in these commercial samples.

Given these data, we can therefore hypothesize that the evolution of fibrotic patients towards HCC may involve the reshaping of netrin-1/UNC5 axis functions during the evolution of the disease.

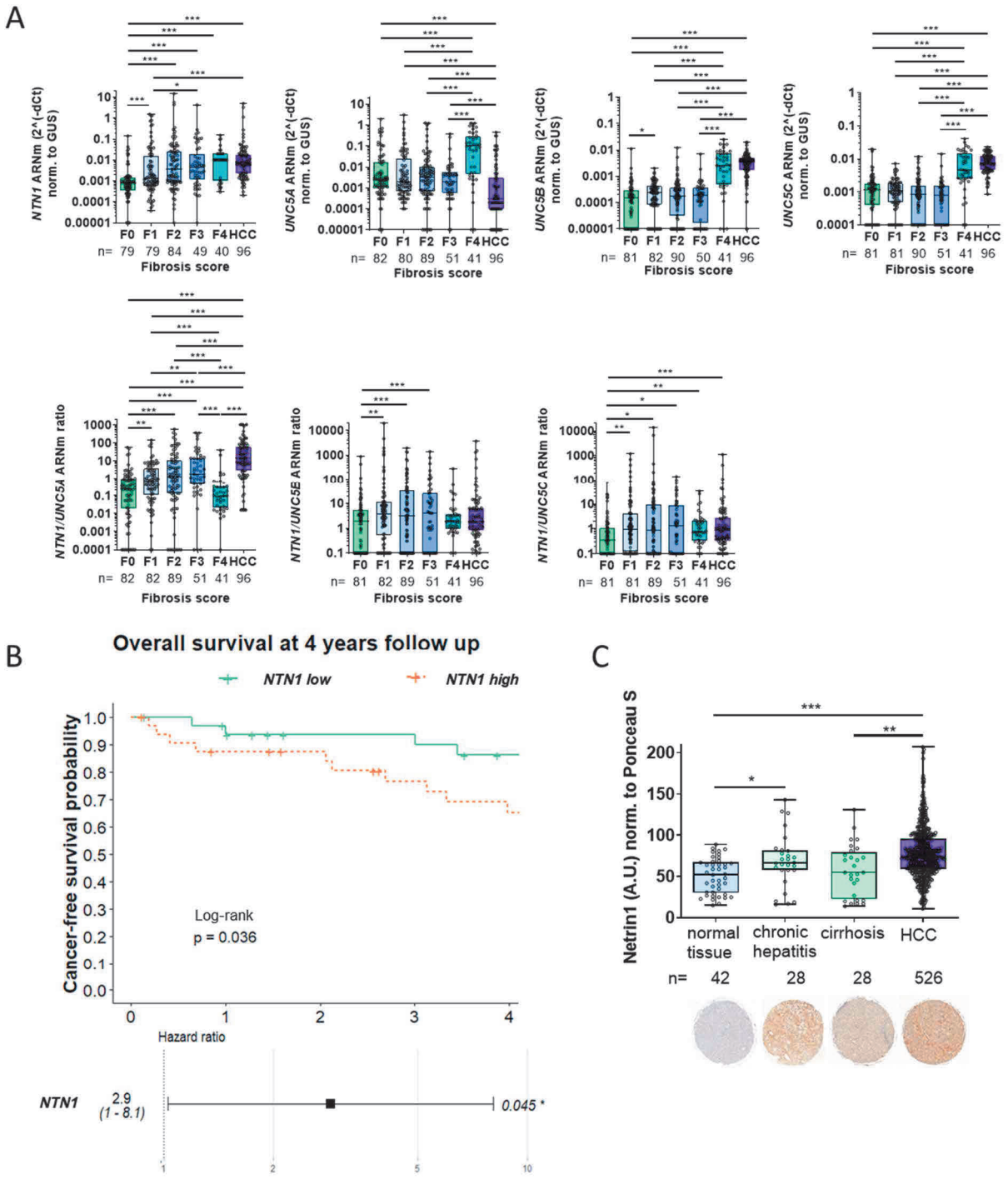

Figure 19. Netrin-1/UNC5 regulation in CLD progression towards HCC

(A) *NTN1, UNC5B* and *UNC5C* transcripts are massively induced in cirrhosis and HCC, whereas *UNC5A* transcript collapses in cirrhosis and HCC. Intrahepatic mRNA levels were quantified by RT-qPCR. Fibrosis scores were determined by histopathology and using the Fibroscan method. Kruskal-Wallis and Mann-Whitney *U* tests, $p < 0.05$, **p<0.01, ***p<0.001.

(B) Netrin-1 rates predict HCC-free evolution in a Lyon cohort of HCV-infected cirrhotic patients (n=101). Threshold was defined as the median of *NTN1* expression levels across the cohort. Increase in HCC onset rates amongst high *NTN1* expressers (>median) was 2.9-fold (Confidence Interval (CI) = 1-8.1. Kaplan-Meier test and Cox model implementing Log-rank test, *p <0.05.

(C) Netrin-1 augments in HCC patients as compared to normal liver or cirrhotic liver. Immunohistochemistry staining of netrin-1 in tumor microarray liver samples. Mann-Whitney *U* test, *p < 0.05, **p<0.01, ***p<0.001.

Netrin-1/UNC5 axis is reshuffled in HCC

To gain deeper insight on netrin-1 and UNC5 modulation during hepatocarcinogenesis, we initially evaluated the *NTN1* and *UNC5* transcription levels in a cohort of HCC patients from the French National HCC Biobank. This cohort is constituted of patient samples of different etiologies: NASH (27%), ALD (21%), HCV (24%) and HBV (28%), different levels of tumor differentiation and Child-Pugh score, in particular (**Table 6**). Analysis of 166 HCC and paired peri-tumoral cirrhotic (F4) tissues revealed that mRNA expression of *UNC5A, UNC5B* and *UNC5C* was significantly lower in HCC tissues than in adjacent cirrhotic tissues (**Figure 20**A). *NTN1* mRNA level showed tiny downregulation in HCC samples. However, the ratios *NTN1/UNC5A* and *NTN1/UNC5C* were significantly upregulated in HCC, indicating likely higher pro-survival signals in HCC compared to cirrhotic tissue. We then wanted to assess the expression of netrin-1 protein and its receptors in these samples with help of a semi-quantitative quantification (Western blotting using an internal range of recombinant netrin-1). The interindividual variation of netrin-1 protein was limited and non-significant (**Figure 20**A). The same trend was observed for *NTN1/UNC5* mRNA levels and their ligand/receptor ratios and netrin-1 protein level when analyzed separately for four main etiologies. Also, due to the limitation of technical tools, - only anti-UNC5B specific antibody is currently available, we unsuccessfully tried to evaluate UCN5B protein level as the signal was too weak to quantify. Although *UNC5B* mRNA was easily quantified by RT-qPCR, the low expression of UNC5B protein can be explained by a weak translation or loss of expression in cirrhosis and HCC.

To investigate the prognostic value of netrin-1 (mRNA and protein) and its receptors as well as their implication as a risk factor, we used Kaplan-Meier survival curves (function of survival) and Cox regression model (Hazard Ratio (HR), function of risk) methods, respectively. The patients were separated into two groups according to the median value of transcript expression or in three groups according to the three quartiles (<Q1, Q1-Q2, >Q3) values of transcript expression. While the analysis based on the median threshold neither showed any significant variation of survival nor of HR in any group (under and above the median value), the quartile-based group distinction allowed to identify the patients with the highest (Q3) *NTN1/UNC5A* and *NTN1/UNC5C* ratios as patients with shorter survival, and high *NTN1/UNC5C* ratio as a risk factor of mortality (HR=2.33, p<0.05) at 4-year follow-up (**Table 4**). Interestingly, these findings were even more evident (higher HR) in patients who underwent tumor resection compared to transplanted patients. Also, the transcripts were analyzed by Cox regression model as continuous variables. Higher *NTN1/UNC5A* ratio in HCC samples increases the risk of mortality by 1.032 (p<0.0001) (**Table 4**). Still this HR is marginal in terms of medical interest, it is consistent with the pathological feature of *NTN1/UNC5A* ratio in HCC, mentioned above, and should be considered for its future consideration in HCC studies. The same trend was observed in analyses based on the etiology or tumor differentiation grade stratifications. Then we assessed the impact of the ligand and transcripts on the cirrhosis-to-HCC progression at 4-year follow up. Indeed, the patients with high *UNC5B* expression in tumoral tissue have 2.24-fold higher risk (p<0.05) to develop HCC at 4-year follow up and the patients with high *UNC5C* have this risk reduced by 56% (p<0.01) (**Table *5***).

These data suggest that the impaired balance *NTN1/UNC5* may be associated with poor survival in HCC patients. To confirm this finding, we will continue to follow the cohort and update the analysis. The limiting factor being the lacking data of mortality for an important percentage of patients so far in our cohort, the analysis should be continued periodically till the mortality data is complete for the whole cohort.

Then, Spearman correlation test was used to explore the correlation between transcript and protein expression levels. The *NTN1* versus *UNC5* rates correlate at the cirrhotic level but not at the HCC level, suggesting that the loss of coregulation of *NTN1* vs. *UNC5* levels are beneficial for a switch to the malignant phenotype at the cirrhotic level (**Figure 20**C). The correlation between *NTN1* and *UNC5B* expression was observed in NASH and HCV-related cirrhotic tissues, and between *NTN1* and *UNC5C* expression – in HCV-related samples. The correlation between *NTN1* and *UNC5A* was observed in cirrhotic tissues of all studied etiologies (ALD, NASH, HCV, HBV). Globally, the most abundant transcript, both in cirrhotic and tumoral tissues, was *UNC5B,* followed by *UNC5A* and *UNC5C* (**Figure 20**D). Such data prompt for definitive identification of each expressing cell type for each of these receptors so proper interpretation of such data can be made.

To explore the association between netrin-1 and UNC5s and clinico-biological parameters of patients in cirrhosis and HCC, we performed multiple comparisons tests. The top 5 most significant parameters associated to high *NTN1/UNC5B* and *NTN1/UNC5C* (**Figure 20**E) ratios in cirrhotic and tumoral tissues (and *NTN1/UNC5A* only in HCC) were related to liver function (absence of oesophageal varices, jaundice, ascites, low bilirubin level and higher prothrombin time) suggesting their protective role for liver function. Although these clinical and biological features were not all significantly correlated after Bonferroni correction required for the multiple comparison analysis, it is worth to take them into consideration as the trend was observed for all three studied *NTN1/UNC5* ratios. In addition, high *NTN1* transcript level was associated to the presence of portal hypertension and hepatic insufficiency complications ascites and jaundice, but also only before the Bonferroni correction.

Further Principal Component Analysis (PCA) of netrin-1 (mRNA and protein) and *UNC5*s transcripts did not allow to distinguish the main contributors to the phenotype of the analyzed groups of patients (all patients were analyzed as high (above the median value) or low (under the median value) with respect to transcripts' abundance) (**Figure *20***F). To further explore the connection between the *NTN1/UNC5* axis we implemented multivariable analysis such as multiple correspondence analysis, discriminant factorial analysis, ANOVA or ANCOVA and hierarchical clustering, allowing to mix quantitative (biological parameters) and qualitative (categorical features) data. However, this exploratory analysis did not allow to identify the discriminant clinical or biological parameter enabling to choose the patient category that would benefit most from netrin-1 capture in the clinic.

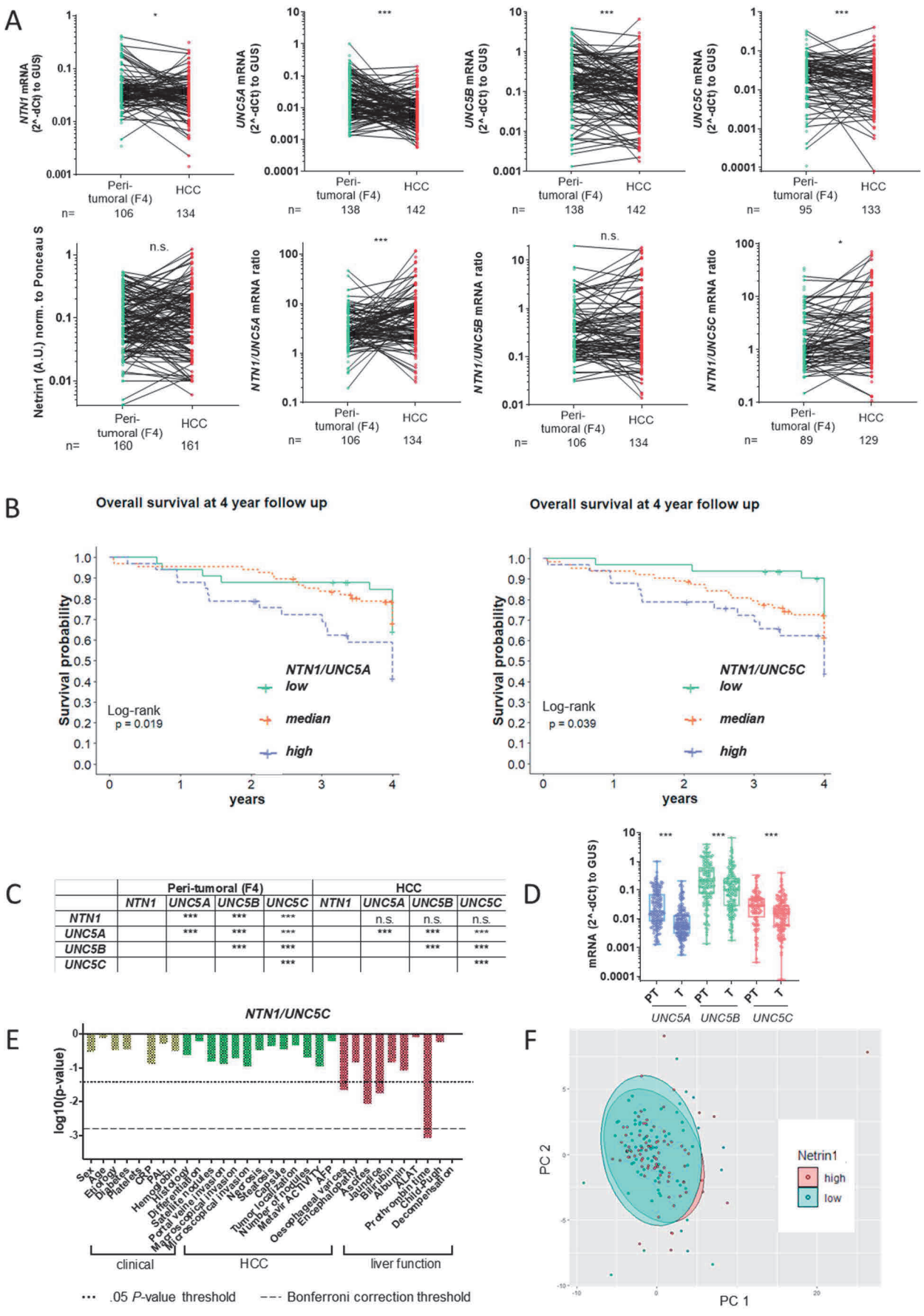

Figure 20. Netrin-1 and UNC5 markers are reshuffled during cirrhosis to HCC transition

(A) *UNC5A, UNC5B* and *UNC5C* transcripts collapse in HCC, whereas *NTN1* transcript shows tiny downregulation in HCC compared to peri-tumoral tissue (F4). *NTN1/UNC5A* and *NTN1/UNC5C* ratios are increased in HCC. Intrahepatic mRNA levels were quantified by RT-qPCR. Statistical significance was determined using the Kruskal-Wallis and Wilcoxon tests, *p<0.05, **p<0.01, ***p<0.001.

(B) *NTN1/UNC5A* and *NTN1/UNC5C* rates predict HCC-related mortality. Three groups (high, median and low) were defined as the quartiles of *NTN1* expression levels across the cohort. Increase in HCC-related mortality amongst high *NTN1/UNC5C* expressers (>3rd quartile) was 2.3-fold. Kaplan-Meier test and Cox model implementing Log-rank test, *p<0.05.

(C) *NTN1/UNC5* rates correlate at the cirrhotic level but not at the HCC level, suggesting that tightly regulated *NTN1* vs. *UNC5* levels are beneficial for switch to the malignant phenotype at the cirrhotic level. Spearman correlation coefficient, *p<0.05, **p<0.01, ***p<0.001.

(D) *UNC5* receptor abundance and expression in peritumoral tissue (F4) and HCC. 166 pairs of liver tissues were analyzed. Wilcoxon test, * p < 0.05, ** p<0.01, *** p <0.001.

(E) Liver function parameters associate with *NTN1/UNC5A, -B* and *-C* ratios. Multiple comparison analysis with Bonferroni correction. Mann-Whitney U test and Spearman correlation coefficient.

(F) Principal Component Analysis of netrin-1 protein expression. Two different colors represent different groups of the samples: high (pink) for netrin-1 above the median value and low (turquoise) for netrin-1 under the median value.

		HCC		Peri-tumoral (F4)	
Covariate		HR (95% CI)	*P*-value	HR (95% CI)	*P*-value
Continuous variable	*NTN1/UNC5A*	**1,032 (0,88-1,15)**	**0,00004**	1,01 (0,78-1,12)	0,70
	NTN1/UNC5B	0,9 (0,78-1,13)	0,08	0,88 (0,81-1,03)	0,50
	NTN1/UNC5C	1 (0,97-1,01)	0,70	0,99 (0,88-1,10)	0,80
	Netrin-1	0,81 (070- 1,05)	0,60	0,8 (0,71-1,19)	0,50
Low/median/high	*NTN1/UNC5A*	1,26 (0,75-2,1)	0,40	0,79 (0,61-1,23)	0,50
	NTN1/UNC5B	0,59 (0,3-1,2)	0,13	1,01 (0,91-1,20)	0,90
	NTN1/UNC5C	**2,33 (1,07-5,1)**	**0,033**	1,2 (1,01-1,53)	0,60

Table 4. Hazard Ratio comparing risk of HCC-related death at 4-year follow up in patients depending on the *NTN1* and *UNC5s* expression

Time-dependent HR (continuous variable) and time-independent HR (3 categories). Cox regression multivariate analysis implementing Log-rank test.

		HCC	
Covariate		HR (95% CI)	*P*-value
Low/median/high	*NTN1*	1 (0,98-1,03)	0,90
	UNC5A	0,99 (0,91-1,26)	0,90
	UNC5B	**2,27 (1,11-3,43)**	**0,024**
	UNC5C	**0,44 (0,34-1,05)**	**0,009**

Table 5. Hazard Ratio comparing risk of HCC onset at 4-year follow up in cirrhotic patients depending on the *NTN1* and *UNC5s* expression

Time-independent HR (3 categories). Cox regression multivariate analysis implementing Log-rank test.

Variable	Available data (Total: 166)	Values
Age, *y* ± SD	166	69 ± 10
Gender (male/female)	166	140 (84%)/26 (16%)
Etiology (%)	166	
Alcoholic liver disease		36 (21%)
Hepatitis B virus		46 (28%)
Hepatitis C virus		39 (24%)
Non-alcoholic steato-hepatitis		45 (27%)
Serum alpha-fetoprotein, >100 ng/mL	111	17 (16%)
Child-Pugh score (A/B/C) (%)	87	72 (83%)/9 (11%)/6 (6%)
Prothrombin, % ± SD	146	81 ± 22
Bilirubin, µMol/L ± SD	137	14 ± 75
Albumin, g/L ± SD	100	36 ± 7
Platelet count, G/L ± SD	149	131 ± 102
Encephalopathy (%)	164	18 (11%)
Ascites (%)	164	37 (3%)
Jaundice (%)	162	22 (14%)
Esophageal varices (%)	156	62 (40%)
Histological and gross features of the tumors		
Tumor size, *mm* ± SD	165	34 ± 31
Tumor localization (left liver/right liver/double)	165	47 (29%)/112 (68%)/6 (4%)
Intact tumor capsule (%)	143	91 (64%)
Satellite nodules (%)	165	34 (21%)
Macrovascular invasion, Microvascular invasion (%)	151	22 (15%), 81 (52%)
Differentiation grade (poor/moderately/well) (%)	165	15 (9%)/74 (45%)/76 (46%)
Architectural pattern (%)	136	
Trabecular		104 (76%)
Pseudoglandular		10 (7%)
Compact		5 (4%)
Clear cells		4 (3%)
Others		13 (9%)
Tumoral steatosis (%)	165	108 (66%)
Tumoral necrosis (%)	150	84 (56%)
Liver fibrosis score METAVIR (F4) (%)	166	166 (100%)
Inflammation activity score (%)	137	
METAVIR 0		51 (37%)
METAVIR 1		55 (40%)
METAVIR 2		23 (17%)
METAVIR 3		8 (6%)

Table 6. Characteristics of paired peri-tumoral (F4)/HCC patient samples (French National HCC Biobank cohort) used in the study

Median ± standard deviation (SD) is shown for all qualitative data.

Associations between molecular alterations and netrin-1/UNC5 in HCC

Liver is a rare target of classical genetic cancer predisposition syndromes, with few exceptions such as *HFE1* gene in hemochromatosis, *ATP7B* gene in Wilson disease, *SERPINA1* gene in α1 antitrypsin deficiency or *FAH* gene in tyrosinemia type 1, that can trigger HCC, mainly via development of cirrhosis. Also, many polymorphisms impair signaling pathways involved in hepatocarcinogenesis (e.g., *IL1B, TGFB, TNFA, MDM2, TP53* and *EGF*)[186]. Alongside with mendelian diseases and polymorphisms the connection was established between the multiple environmental and viral factors and genetic/epigenetic alterations in the liver. The mechanisms of malignant transformation in HCC starting as early as at the cirrhotic stage include notably the mutations in *TERT* promoter and chromosomal instability. Later mutational events in cirrhotic context and early events in non-cirrhotic context include the mutations in *TP53*, (e.g., R249S in aflatoxin B1 exposure context), *CTNNB1, ARID1A* and *AXIN1.* With nearly 35-80 mutations per tumor, a small number mutations occurs in cancer driver genes. Belonging to the key signaling pathways involved in hepatocarcinogenesis, telomere maintenance, Wnt/β-catenin pathways and p53 cell cycle pathways constitute the triad of top HCC driver genes.

Few recent studies have identified a close relationship between UNC5s and tumor suppressor p53. *UNC5A* and *UNC5B* have been proved to be direct downstream target genes of p53, suggesting that UNC5s may play a role in p53-dependent apoptosis, and therefore a role in tumor suppression[169–171,187]. UNC5 receptors induces apoptosis only when p53 protein is normally expressed and functional, but fails in the context of p53 loss and p53 mutation[150]. Taking into account these findings indicating the tight regulatory relationship of p53-UNC5, we wanted to know whether p53 could be a possible biomarker for further choice of patient that could benefit from anti-netrin-1 therapy. The connection between netrin-1/UNC5 and *CTNNB1* and *TERT* activities remain unstudied, if any.

A systematic Sanger sequencing was performed in a subset of 332 samples (166 of peri-tumoral and 166 HCC samples) on *CTNNB1* gene and *TERT* promoter region, and the Next Generation Sequencing (NGS) was performed to explore the mutations in *TP53* gene. Sequencing of the corresponding adjacent tissue also allowed to verify the somatic origin of the mutation found in tumoral tissue. Taking account of the existing molecular classification of HCC, we investigated the connection between the mutational status and netrin-1/UNC5s.

43%, 16% and 26% of patients bore at least one mutation in *TERT* promoter region, *CTNNB1* and *TP53* genes respectively, with the highest mutation incidence in HCV patients (**Figure *21***A, B).

In accordance with the literature, all mutations C>T localized to the -124pb (95%) and -146bp (5%) positions (**Figure *21***C) from ATG start site of the *TERT* gene creating CCGGAA/T consensus sites for Erythroblast Transformation Specific (ETS) transcription factors. The binding of the ETS transcription factors triggers epigenetic transformations and recruitment of RNA polymerase II leading to mono-allelic *TERT* expression. We did not observe any association between mutational status in *TERT* promoter region and netrin-1/UNC5s reshaping, irrespectively of the etiology or tumor differentiation grade. However, we showed that *TERT* promoter mutations in non-mutated HCC patients were associated with an increased transcription (3.3-fold) of telomerase, compared to cirrhotic tissue. Globally, cirrhotic samples were poor *TERT* expressers, with only 30% of positive samples and low median expression level. Surprisingly, the *TERT* mRNA was 3.7-

fold higher in *TERT* non-mutated patients compared to HCC samples harboring *TERT* mutations (not shown), phenomenon already observed in other studies[188]. The level of *TERT* mRNA positively correlated with *NTN1*, *UNC5A, UNC5B and UNC5C* mRNA levels in cirrhotic tissues and tumoral tissue with no *TERT* mutation, whereas *NTN1* did not correlate with *TERT* mRNA in mutated HCC. *TERT* mRNA negatively correlated with *NTN1/UNC5* ratios in cirrhotic but not in tumoral tissues (**Figure *21***D). These data suggest that other mechanisms could activate *TERT* transcription (e.g., *TERT* gene amplification, translocation, HBV insertion) in non-mutated tumors. Of note, one mutation C>T localized to the -124pb was identified in peri-tumoral tissues while absent in the paired tumoral tissues.

The mutations spotted in *CTNNB1* gene were hotspot mutations, representing previously defined three levels of β-catenin activation[189]: weak (S45), moderate (T41) and, predominantly, highly active mutations leading to amino acid substitutions within the β-TRCP binding site (D32-S37), therefore conferring to b-catenin an enhanced stability from the degradation by the proteasome. To validate the functionality of β-catenin activation we evaluated the transcription of its two target genes coding for glutamine synthetase (*GLUL*) and Leucine-rich repeat-containing G-protein coupled Receptor 5 (*LGR5*). Tumors with highly active mutations demonstrated strong/homogeneous *GLUL* and *LGRP5* expression and correlation with mutational status (**Figure *21***E, F). *UNC5A, UNC5B* and *UNC5C* receptors were significantly downregulated in *CTNNB1* mutated tumors, but neither *NTN1*, nor *NTN1/UNC5* ratios nor netrin-1 protein (**Figure *21***G), suggesting a relationship between the receptor-dependent pathway and the canonical Wnt signaling pathway, as recent findings demonstrated that netrin-1 regulates the Wnt/β-catenin signaling pathway through indirect stabilization of β-catenin[190,191].

NGS covering exons 2-11 of *TP53* gene allowed to map the mutations in the coding sequence of the gene. Predominantly missense mutations identified in HCCs (**Figure *21***H), present all over the coding sequence (transactivation region, DNA binding domain, negative regulation region), lead to the abnormal activity of the p53 protein. Except for the R249S mutation related to aflatoxin B1 exposure, no other recurrent *TP53* mutation hotspot has been identified. We did not observe any association of the *TP53* mutational status with netrin-1/UNC5s evolution, irrespectively of the etiology or tumor differentiation grade. Then we looked at the correlation between p53 functionality status and netrin-1/UNC5 expression profiles as well as ligand/receptor ratios using the available p53 functionality classifications Sorts Intolerant From Tolerant substitutions (SIFT)[192], Align – Grantham Variation – Grantham Variation (AVGDG)[193], Transactivation[194], Phenotypic Selection Model[195], and unpublished Cluster classification in collaboration with P. Hainaut's group (IAB, Grenoble). Essentially, these classifications allow to classify p53 protein sequences depending on their mutations into non-functional, partially functional, functional, neutral or supertrans protein, and consequently score p53. The analysis did not show any significant difference between p53 functionality and netrin-1/UNC5 expression.

Multivariable analysis did not allow to discriminate a group of patients susceptible to associate the netrin-1/UNC5 expression levels and mutational status of *TERT, CTNNB1* or *TP53* (**Figure *21***I).

Although these data may be not exhaustive due to intratumor heterogeneity, these findings suggest that the netrin-1/UNC5 axis remains insensitive to the functions of the main markers of HCC genetics.

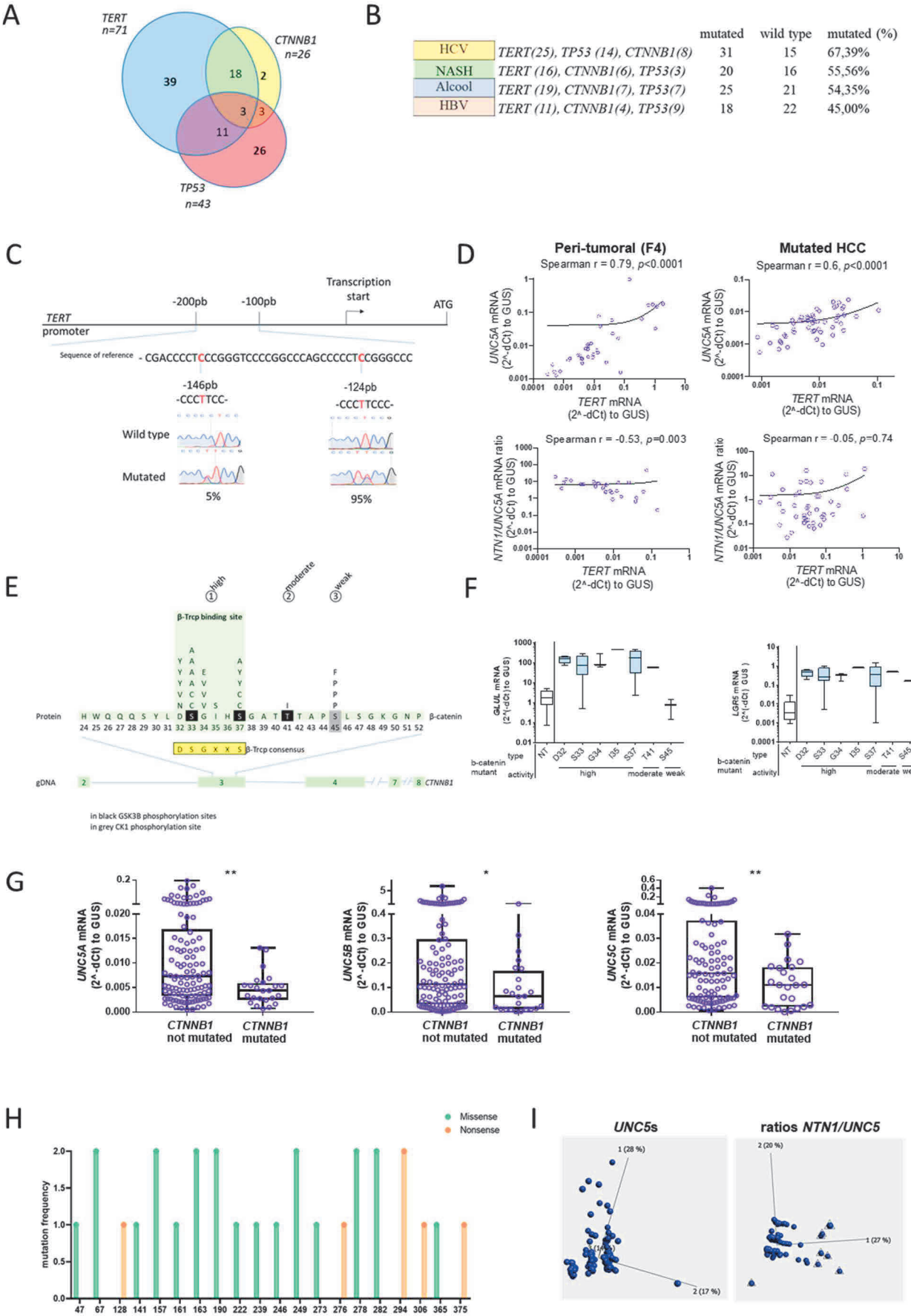

Figure 21. Molecular events affecting the three top liver cancer-related genes do not correlate with NTN1/*UNC5* levels in HCC

(A) Venn diagram showing number of mutations in *TERT* promoter region, *CTNNB1* and *TP53*, and their co-occurrence in tumors.
(B) Percentage of mutational events in patients with specific etiology.
(C) Two hotspot mutations in the *TERT* promoter region and their incidence in tumors.
(D) *UNC5A* mRNA level positively correlates with *TERT* mRNA expression level in peri-tumoral tissue (F4) and *NTN1/UNC5A* ratio negatively correlate with *TERT* mRNA expression level in cirrhosis. Spearman correlation coefficient.
(E) *CTNNB1* mutations in HCC samples. Amino acid substitutions are shown above the β-catenin protein sequence. Amino acid residues are numbered according to P35222 reference β-catenin sequence. The three groups of b-catenin activity are mentioned on the top. gDNA, genomic DNA.
(F) Box plot graphs showing *GLUL* and *LGR5* mRNA expression in HCC samples compared to peri-tumoral tissue (NT) according to b-catenin mutation type.
(G) Box plot graphs showing the downregulation of UNC5 in CTNNB1 mutated tumors. Mann-Whitney *U* test, * $p < 0.05$, ** $p < 0.01$.
(H) Mutation frequency and distribution in *TP53* gene.
(I) Mixed PCA of *UNC5* (left panel) and PCA of *NTN1/UNC5* ratios (right panel). Qlucore Omics Explorer 3.7 software.

In search of a candidate for combination therapy with netrin-1 capture

Despite many potential therapeutic targets, many drugs have failed to exceed the efficacy of the currently available compounds sorafenib in phase III trials, indicating for further identification of future HCC targets. Such targets may not be obligatorily related to kinases or growth factors functions.

Translational characterization of patient samples suggests the involvement of the netrin-1/UNC5 system as a pathological feature of the transition from cirrhosis to HCC. We wanted to take our investigation a step further and assess the targetability of netrin-1/UNC5 in the liver pathological context.

First, we have screened several HCC cell lines with regards to the expression of *NTN1*/*UNC5s* at the mRNA level, but also, with respect to protein expression of netrin-1 and its receptor UNC5B, for which antibodies were in-house validated (**Figure *22***A). We then have performed drug testing in six liver cell lines (Hep3B, HepG2, Huh7, Huh7.5, CLP13 and progenitor cell line HepaRG) in order to evaluate their sensitivity to 20 compounds showing anti-cancer activity, including drugs in clinical use, in clinical development for HCC or other cancers and targeting key pathways of liver tumorigenesis (**Figure *22***D). We used two main approaches to assess the sensibility of cancerous cells to netrin-1 modulation: (1) loss-of-function, by either genetic deletion of the *NTN1* gene via the CRISPR/Cas9 approach in netrin-1-positive cells or netrin-1 trapping by the NP137 antibody; (2) gain-of-function, by the supplementation of netrin-1-negative cells with recombinant netrin-1. Colorimetric cell viability tests MTT, SulfoRhodamine B assay (SRB) and Neutral Red Assay (NRA) showed comparable results, and NRA was selected as a readout for all tests. **Figure *22***B (upper panel) details the protocol used for cell treatment.

Overall, when treated in monotherapy, netrin-1-positive hepatic cell lines were resistant to netrin-1 capture and netrin-1-negative hepatic cell lines were insensitive to supplementation by recombinant netrin-1, with the half maximal Inhibitory Concentration 50 (IC50) greater than the maximum screening concentration. Then we tested the sensitivity of cells in such conditions to anti-HCC TKIs used in the clinic (sorafenib, lenvatinib, regorafenib and cabozantinib), assessing

IC50s or Combination Indexes (CI)[196]. NP137 did not show neither synergy nor potentiation of any TKI. Of note, no compensation was observed by overexpression of other ligands of repression of dependence receptors (e.g., *NTN3*, *NTN4, Neogenin, A2B*) in the *NTN1* CRISPR/Cas9 clones (not shown).

We then wanted to investigate the sensitization potential to cell death of netrin-1 trapping by counteracting several of the main pathological processes involved in hepatocarcinogenesis (e.g., inflammation, UPR) by ad hoc drugs and compounds. **Figure *22***B (lower panel) details the protocol used for cell treatment. However, the concomitant or sequential treatment of cells pretreated with a low dose (1/4 IC50) of drugs having anti-cancer activity with NP137 in combination with one or two pharmaceutical agents did not allow to identify a potentially efficient combination therapy.

Of note, NP137 treatment neither affected PHHs viability nor showed a synergy with TKIs, PHHs being globally much less sensitive to TKI treatment than HCC cells. NP137 treatment in rat HCC cell line HR-4 was consistent with findings in human cells (not shown).

These data suggest that 2D tissue culture system may be insufficient, notably because of the lack of liver specific microenvironment, and that more complex system (three-dimensional liver tissue culture systems such as HCC organoids or spheroids) may be better suited to study the potential of netrin-1 trapping *in vitro.* Also, the expression of netrin-1 and UNC5B in tested cell lines may be insufficient to impact cell viability through netrin-1 capture. In addition, as the protein expression of UNC5A and UNC5C is unknown due to our repeated inability to in-house validate ad hoc antibodies, it is difficult to judge through what UNC5 receptor netrin-1 may exert its effects in HCC.

A

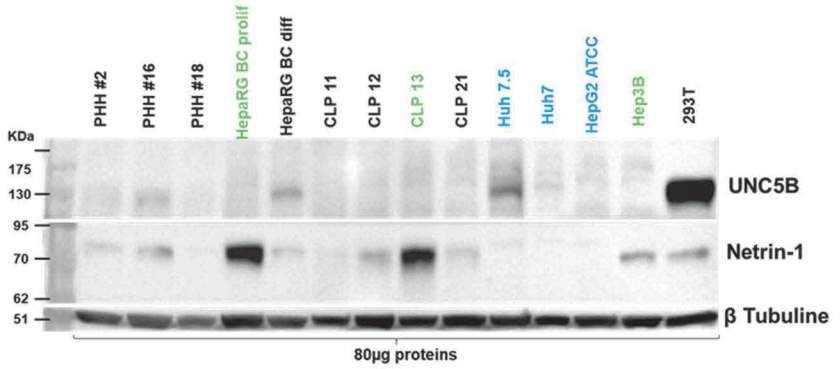

Netrin-1- positive cell lines:
Hep3B
HepaRG proliferative
CLP13

Netrin-1- negative cell lines:
Huh7
Huh7.5
HepG2

B

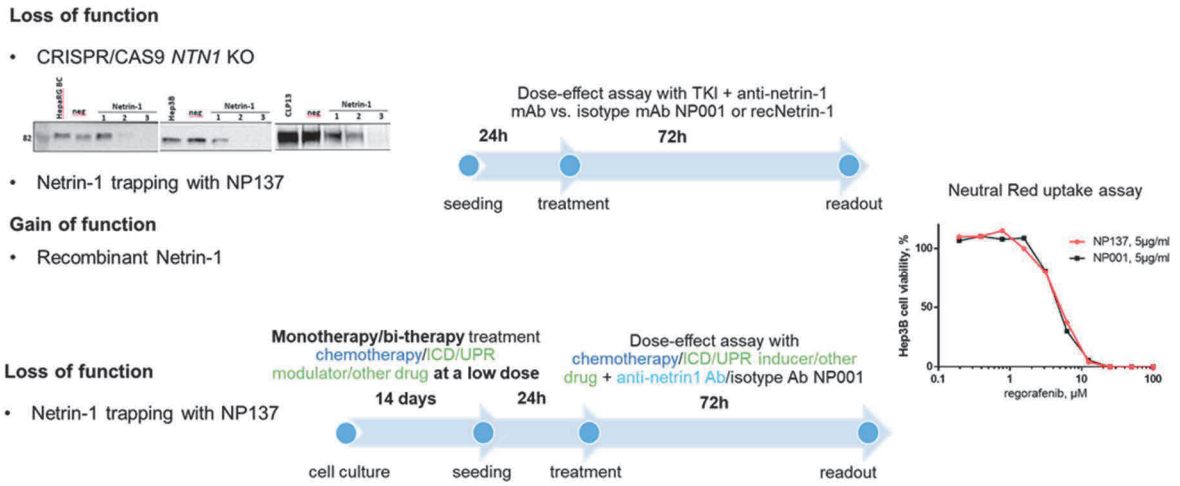

C

Compound	Mechanism of action	IC50 (µM)		IC50 (µg/mL)	
		Hep3B WT	Hep3B *NTN1* KO	Hep3B + NP001	Hep3B + NP137
Sorafenib	c-RAF, RAS, VEGFR 1-3, PDGFR-b,	3,49	3,39	3,87	3,96
Regorafenib	VEGFR 1-3, TIE2, PDGFR-b, FGFR, c-KIT, RET, RAF	1,87	1,83	4,61	3,98
Lenvatinib	VEGFR 1-3, PDGFR-a, FGFR 1-4, RET	5,75	4,74	10,47	10,3
Cabosantinib	c-MET, RET, AXL, VEGFR-2, FLT3, c-KIT	3,89	4,08	4,89	6,46
Doxorubicin, control	type II topoisomerase inhibitor	0,29	0,27	0,38	0,44

D

Process/Pathway	Mechanism of action	Compound	IC50 in Hep3B
UPR	*p300 HAT i, HDACi, Nrf2/NF-kbi*	curcumin	12,06µM
	non-competitive inhibitor of the sarco/ER Ca ATPase (SERCA)	thapsigargin	3,1nM
	COX2 inhibitor	celecoxib	47,93µM
	IRE1 Inhibitor I	STF083010	33,69µM
	COX1/2 inhibitor (low dose COX1)	aspirin	-
	protease inhibitor	bortezomib	2,9nM
differentiation	pro-differentiation	ATRA	75,58µM
integrin/ECM	integrin αvβ5 &αvβ3 inhibitor	cilengitide	7,74µM
	integrin α1β1 inhibitor	obtustatin	-
inflammation	corticosteroid	dexamethasone	29µM
	gp130 inhibitor, IL6R inhibitor	SC144	12,06µM
ICD	alkylant	oxaliplatin	3,89µM
	type II topoisomerase inhibitor	mitoxantrone	0,21µM
	antimetabolite	gemcitabine	24,14µM
	type II topoisomerase inhibitor	doxorubicin	184 nM
	PKM2 inhibitor	shikonin	0,55µM
	type II topoisomerase inhibitor	idarubicin	18uM
others	HDACi	panobinostat	63,85nM
	PIK3CA inhibitor	taselisib	1,89µM
	ERK1/2 inhibitor	ulixertinib	0,45µM

Figure 22. Drug screening for identification of the candidate for combination therapy

(A) Netrin-1 and UNC5B protein expression in different hepatocyte-like cell lines and PHHs.
(B) Treatment protocol of cancerous cells for classical cell viability assay (upper panel) in six cell lines and with pre-treatment (lower panel) in Hep3B.

(C) Sensitivity of TKIs when used in co-treatment with NP137. Representative data for one CRISPR/CAS9 clone (n=3) and for netrin-1 trapping in one of the netrin-1-positive cell lines Hep3B.
(D) Summary of the different compounds used in the drug screening, the associated pathway and IC50 data generated for the Hep3B cell line.

Netrin-1 targeting in the DEN-induced HCC rat model

Most of animal models, such as chemically induced, genetically engineered, syngeneic, humanized and xenograft models including patient-derived xenografts, allow development of HCC with no associated cirrhosis. Hence, we aimed to probe the effects of anti-netrin-1 therapy in histological setting that would allow us to obtain results meaningful for clinical translation. A rat model of genotoxic carcinogenesis using DEN was identified. When injected into an animal, DEN is metabolized by centrolobular hepatocytes, inducing DNA damage (DEN interacts directly with DNA and forms covalent bonds, which result in DNA adducts), but also inflammation and fibrosis when injected chronically. A rat model of DEN-induced HCC recapitulates the evolution of human cirrhosis-based HCC. In addition, the gene expression profile of this gender-dependent model is very similar to the gene expression profile of human HCCs with poorer survival, and particularly close to human alcohol-induced HCC[38].

First, we wanted to evaluate netrin-1/UNC5 expression in this context and hence assess the possibility to use this model to target the netrin-1/UNC5 axis. We observed a significant upregulation of the *NTN1* and *UNC5B* transcripts, and a collapse of *UNC5C* expression in tumoral samples (**Figure *23***A). Netrin-1 and UNC5B antigens were unchanged between the groups. Given the presence of netrin-1 and UNC5s, we have designed a study based on NP137 treatment vs. PBS injected in rats once the animals reached the cirrhotic stage (**Figure *23***B).

The macroscopic analysis revealed no difference in terms of tumor number and median tumor size between both groups of treatment. Apoptosis (cleaved caspase-3), fibrosis (Sirius red), vascularization (CD34), cell proliferation (Ki-67, CyclinD1) and inflammation (ALAT, CRP) markers were not significantly different (**Figure 23**C). Importantly, the NP137 group showed higher mortality (n=3) compared to PBS group (n=1). The analysis of other features involved in HCC development was addressed using extracted mRNA and proteins. *NTN1* and *UNC5* transcripts were downregulated and UNC5B protein was upregulated. Necroptosis, angiogenesis, EMT, inflammation and de-differentiation markers were globally upregulated in NP137-treated tumors (

Table *7*) reflecting rather pro-tumoral, yet marginal, shift. The latter may be explained as a first assumption, as resistance mechanism to treatment.

We also hypothesize that the model may be too aggressive and should be used for testing a combination treatment or that NP137 should be administered earlier during liver disease progression as a prevention therapy. Also, Magnetic Resonance Imaging (MRI) analysis, lacking in this study would help to gain deeper insight of HCC progression in addition to the final outcome as result in addition to the ability it provides to reshuffle both groups of animals to attribute similar tumoral burdens prior to treatment, avoiding biases at baseline. Finally, one can hypothesize that the nature of NP137 is implicated in the observed treatment failure. Indeed, NP137 is a humanized monoclonal antibody of type IgG1, and the analysis of rat serum samples showed the presence of circulating anti-human IgG1 antibodies in one animal. These data are

worth to be elucidated to explain possible attenuation of NP137's activity by the murine immune system if this model is to be reused for future studies implicating NP137.

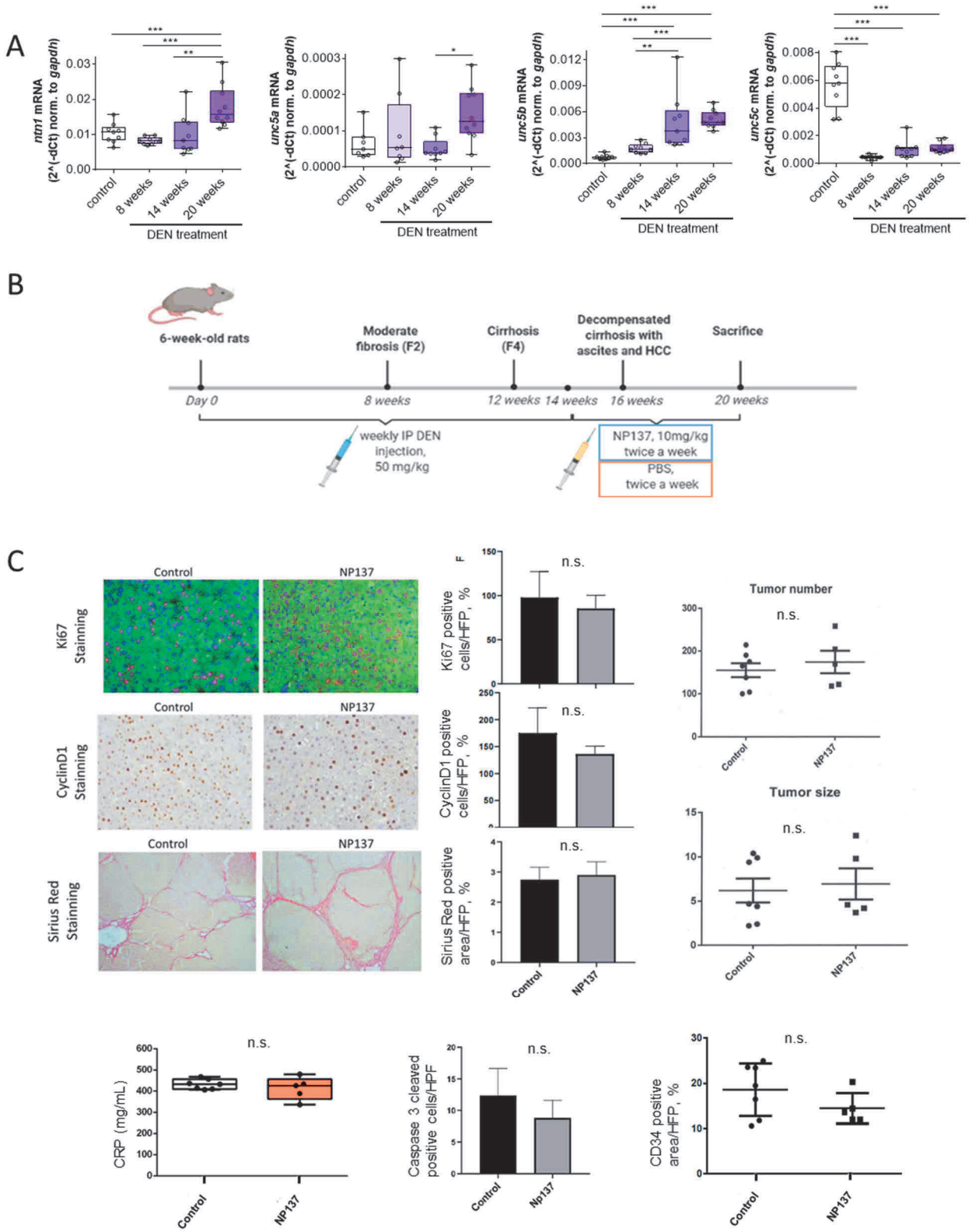

Figure 23. Netrin-1 trapping in DEN-induced HCC in rats showed limited results

(A) *NTN1* and *UNC5B* mRNA are upregulated and *UNC5C* is downregulated in DEN-induced HCC in rats.

(B) Study design of anti-netrin-1 therapy as a single agent comparing to PBS.

(C) The proliferation was assessed with anti-Ki67 and anti-cyclin D1 antibodies. The fibrosis was detected with Sirius red staining solution. The apoptosis was analyzed using anti-caspase 3 cleaved antibody. The vascularization was estimated with anti-CD34 antibody. Macroscopical analysis showing no difference in terms of tumor number or median tumor size. Inflammation was analyzed using ELISA kit for CRP.

NP137 vs. PBS	mRNA	Proteins	Final effect	Consequence on HCC
target	*UNC5A, UNC5B, UNC5C, NTN1*↘ Unchanged *NTN1/UNC* ratios	Netrin-1, UNC5B↗	decreased RNA, increased proteins	-
Apoptosis		Cleaved caspase-3 unchanged	unaltered	-
Necroptosis		Cleaved RIP1↗, RIP3↘	impaired	Pro-tumoral
Proliferation		CyclinD1, p-Yap↗, p-ERK ↗	increased	Pro-tumoral
inflammation	IL-6 unchanged	ALAT, CRP unchanged	unaltered	-
Angiogenesis	*VEGFR2* ↗	CD34 unchanged	pro-angiogenic	Pro-tumoral
Immune cells	*CD4*↗, *PD1/L1, CTLA4, FoxP3* unchanged		unaltered	Pro-tumoral
EMT	*αSMA, CDH1*↘, *Zeb1, Slug* ↗	p-ERK↗	increased	Pro-tumoral
Differentiation	*AFP* ↗, *TGF-β*↘	EpCAM ↗	dedifferentiation	Pro-tumoral

Table 7. Biological effects of the NP137 treatment in DEN-induced HCC in rats compared to PBS

2.3.2. ANS orientation is modulated by anti-netrin-1 treatment *in vivo*

As netrin-1 is known to be involved in the nervous system development and is expressed in adult, in nerve regeneration context or in non-neuronal tissues, and given its overexpression in multiple cancers, it was intuitive to hypothesize the existence of the link between ANS orientation (sympathetic or parasympathetic) and netrin-1 expression.

Using the model of DEN-induced HCC in rats described above we analyzed how netrin-1 capture may possibly modulate the ANS orientation in the HCC context. For this we evaluated the expression of thirteen adrenergic or cholinergic receptors (*Adra1A, Adra1B, Adra1D, Adra2B, Adrb1, Adrb2, Adrb3, Chrna2, Chrna4, Chrna5, Chrna7, Chrnb1, Chrm3)* in tumoral and peri-tumoral tissues of rats treated with PBS or NP137. The most abundant transcripts were *Adra2B,*

Adra1B, Adra1A, Adra1D among the adrenergic receptors and *Chrnb1, Chrm3, Chrna7 and Chrna4* among cholinergic receptors. *Adra1A* was higher in tumors compared to peri-tumoral cirrhotic tissue in PBS-treated rats, while *Adrb1* was lower in tumors compared to peri-tumoral cirrhotic tissue in NP137-treated rats, and *Chrna5* was decreased in tumors of NP137 treated rats compared to PBS treated rats (**Figure *24***A).

In order to address the ANS orientation in both experimental groups, we analyzed the global level of adrenergic or cholinergic signals, calculating the sum of the four most plentiful transcripts. We observed a global prominence of adrenergic signal in tumoral and peri-tumoral tissues, irrespective of treatment group. Also, adrenergic/cholinergic ratio was similar in peri-tumoral and tumoral tissues in both groups. Interestingly, adrenergic/cholinergic ratio was lower, still non-significantly, in the tumoral tissues compared to peri-tumoral tissues of PBS-treated rats (p=0.07). Interestingly, the adrenergic/cholinergic ratio was downregulated in the tumors of NP137 treated group (p=0.02). (**Figure *24***B, C), suggesting that netrin-1 fosters adrenergic orientation of the ANS in the diseased rat liver.

Even though the abundance of transcripts may not translate into proteins to the same extent, and despite the small number of studied animals in each group, we can, however, hypothesize at this stage that netrin-1 capture in this animal model of cirrhotic HCC reorients the ANS, in particular in the cirrhotic tissue.

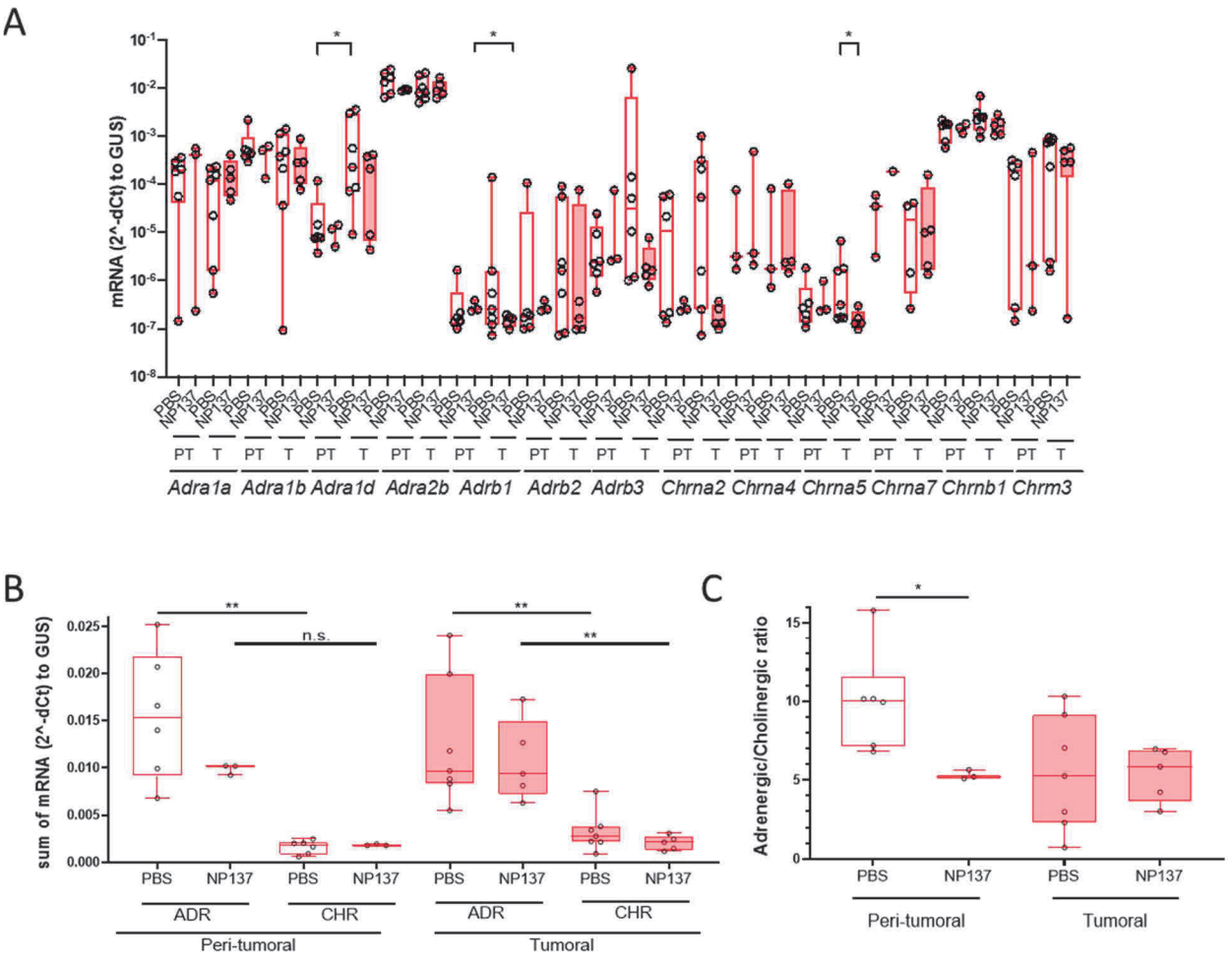

Figure 24. ANS orientation is modulated by anti-netrin-1 treatment *in vivo*

(A) Box plot graph showing the expression of adrenergic and cholinergic receptors at the mRNA level in both experimental groups. Mann-Whitney *U* test, * $p < 0.05$, ** $p < 0.01$.

(B) Abundance of adrenergic (ADR) and cholinergic (CHR) transcripts in DEN-treated rats treated with PBS or NP137. Each point corresponds to the sum of the 4 most abundant transcripts (*Adra1a+Adra2b+Adra1b+Adra1d* for ADR and *Chrna4+Chrna7+Chrm3+Chrnb1* for CHR).

(C) Adrenergic/Cholinergic ratio was calculated for each patient as follows: (*Adra1A+Adra2b+Adra1b+Adra1d) / (Chrna4+Chrna7+Chrm3+Chrnb1*), where the latter ones are the most expressed receptors in patient samples. Mann-Whitney U test, * $p < 0.05$, ** $p < 0.01$.

To confirm the implication of netrin-1 in ANS remodeling in cirrhotic/HCC context and to establish the connection between netrin-1 and the ANS using another approach, we designed a study in an animal model overexpressing the netrin-1. **Figure *25***A, B details the experimental protocol. The mice were a subject to a single injection of DEN to induce inflammation and liver lesions and then separated into groups with or without induction of netrin-1. So far, the preliminary results show no impact of netrin-1 induction in DEN- treated mice (**Figure *25***C), which may be explained by small sample number in some groups.

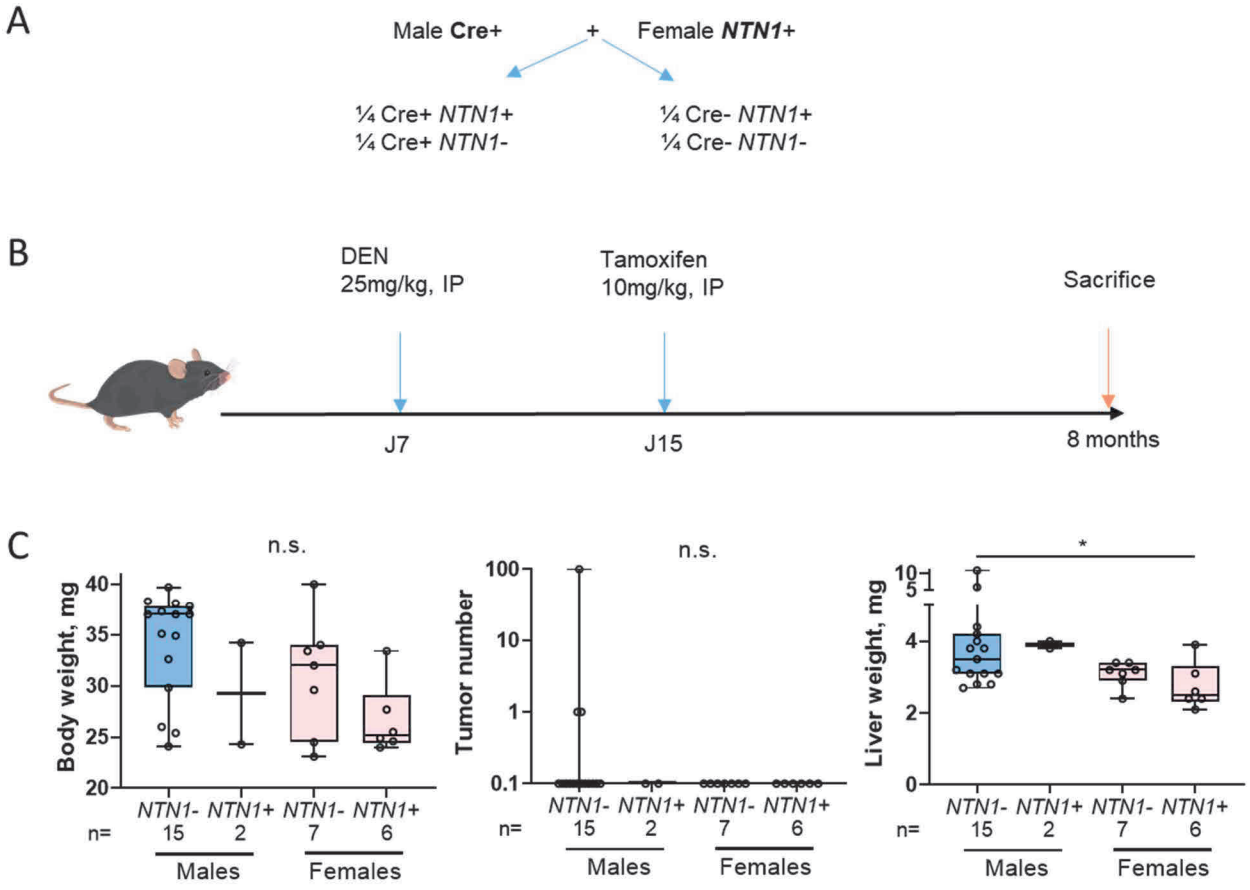

Figure 25. Preliminary results in DEN-treated mice overexpressing netrin-1

(A) Offspring generation outline from male *Cre*$^{+}$ and female *NTN1*$^{+}$mice.

(B) Treatment protocol. All mice were injected with DEN. Mice with *Cre*$^{+}$ genotype were then injected with tamoxifen to induce netrin-1 expression.

(C) Preliminary results. Macroscopic analysis of mouse body weight, tumor number and liver weight. Mann-Whitney *U* test, * $p < 0.05$, ** $p < 0.01$.

2.3.3. ANS in CLD and HCC

Characterization of hepatic innervation in cirrhosis and HCC

Data from the rat model of cirrhosis and HCC showed the potential link between ANS orientation and netrin-1. Inherently, we addressed the issue of sympathetic/parasympathetic orientation in patient samples.

To characterize the liver innervation of patient samples from the French National HCC Biobank cohort we assessed the protein expression of the following neuronal markers: Neuronal Nuclear protein (NeuN) as a mature neuron marker, Doublecortin (DCX) and Alpha-InterNexin (INA) as immature neuron markers, Tyrosin Hydroxylase (TH) and Vesicular AcetlyCholine Transporter (VAChT) as specific ANS neuron markers for adrenergic and cholinergic signals, respectively. Immunoblotting highlighted the presence of immature (DCX/INA^+) and parasympathetic ($VAChT^+$) neurons in HCC samples compared to normal liver, whereas normal liver expressed TH but not the other markers cited hereabove. The analysis revealed no significant difference between cirrhotic and HCC samples (**Figure *26***A). However, the immature and mature markers were differently expressed in tumors depending on the etiology: well differentiated tumors of HBV or ALD patients showed lower immature markers, NeuN and INA and well differentiated tumors NASH tumors expressed lower cholinergic marker VAChT.

Given that the transduction of neural signals in the diseased tissue implicate postsynaptic ANS receptors, we compared the expression of several transcripts encoding ANS receptors (*ADRA1A, ADRA1B, ADRA1D, ADRB1, ADRB2, ADRB3, CHRNA4, CHRNA7, CHRM3)* in paired cirrhosis and HCC samples. Transcript abundance is shown for both groups in the **Figure *26***B. Although the physiology of liver innervation is not completely the same between rodents and humans, similar to rat samples described above, patient sample showed the prevalent abundance of adrenergic transcripts, and especially *ADRA1A, ADRA1B, ADRA1D,* and, unlike rat samples, high expression of *ADRB2* and *CHRNA4*. Within the adrenergic group, *ADRA1A* and *ADRB1* displayed a down-regulation in HCC of more than 2-fold, whereas *ADRA1D* and *ADRB2* were up-regulated by 3.2-fold and 2-fold compared to cirrhotic tissues, respectively. The nicotinic receptor *CHRNA4* was profoundly depleted (> 10-fold) (**Figure *26***B) in HCC compared to cirrhotic tissue. One can hypothesize that the reshaping of ANS receptors expression between cirrhotic and tumoral tissues highly likely participate in ANS-regulated phenotypes concomitant to the cirrhosis-to-HCC transition. Multiple comparisons tests exploring the association between clinico-biological parameters and adrenergic/cholinergic transcripts abundance did not allow to identify any significant correlation.

We then wanted to know whether the cholinergic or adrenergic polarity is connected to the genetic abnormalities in *TERT*, *TP53* and *CTNNB1* liver cancer driver genes. The analysis showed a correlation between cholinergic orientation and *TP53* mutations ($p<0.05$), and correlation between adrenergic polarity and *CTNNB1* mutations ($p<0.001$) in clinical samples of the French National HCC Biobank cohort. Further study in 193 HCC samples from the TCGA database showed that cholinergic tumors, correlated with *TP53* mutations ($p<0.05$), shorter progression-free interval (PFI) and overall survival (OS), displayed more pathogenic molecular traits (e.g., AFP-rich, proliferative tumors, higher mitotic functions including DNA repair, EMT, Ras, and Akt/mTOR pathways), aggressive HCC signatures and B cell accumulation, whereas adrenergic tumors, predominant in patients with mutated *CTNNB1*, were correlated with better OS and PFI ($p<0.05$), and numerous immune pathways.

To establish the connection between netrin-1/UNC5 and ANS postsynaptic receptors in patient samples we analyzed the expression association between them in cirrhotic and tumoral samples. We observed that the adrenergic receptors mostly negatively correlated with *NTN1, UNC5A* and *UNC5B* in cirrhosis and acquire more positive correlation with cholinergic transcripts in HCC. Interestingly, patients with resected tumors showed more prominent netrin-1/UNC5 association with cholinergic orientation compared to transplanted patients (**Figure *26***C, D). In addition, *CHRNA4*, highly expressed but drastically decreased in HCC compared to cirrhosis, was positively correlated with *UNC5A, UNC5B* and *UNC5C*, and negatively correlated with ligand/receptor ratios *NTN1/UNC5A, NTN1/UNC5B* and *NTN1/UNC5C* in HCC samples ($p<0.001$). Meaning that still highly expressed but massively downregulated in HCC, *CHRNA4* may be a key player in relationship between netrin-1 and ANS orientation, altering the adrenergic/cholinergic balance towards adrenergic predominance in HCC.

We then analyzed the correlation between *NTN1/UNC5s* and ANS receptors in 81 HCC patient samples with different stages of fibrosis (F0-F4) from the publicly available RNAseq dataset (GEO: GSE62232) published by Schulze et al[197]. This dataset includes patients with different fibrosis stage but also different etiology and tumor differentiation grade. Tumoral samples in patients with fibrosis stages F2-F3 showed the most relevant positive association of *NTN1/UNC5* axis with cholinergic orientation compared to F0-F1 and F4 stages (**Figure *26***E). Analysis of French National HCC Biobank cohort showed a negative correlation of the *NTN1/UNC5* axis with the adrenergic orientation in cirrhotic samples, and a positive correlation of the *NTN1/UNC5* with cholinergic orientation in tumoral samples (**Figure *26***C). Analysis of ANS receptors' transcripts showed a progressive increase of number of significantly upregulated cholinergic receptors in tumoral tissue compared to healthy liver (F0-F1 HCC: 9 transcripts, F2-F3 HCC: 11 transcripts and F4 HCC: 13 transcripts), whereas the adrenergic dynamics remained unchanged (**Figure *26***F), irrespective of HCC etiology.

To sum up, the relationship *NTN1/UNC5* – ANS is reshuffled during hepatocarcinogenesis and one cannot exclude that the extracellular matrix remodeling plays a role in this relationship, netrin-1 being indeed a laminin-like protein. In addition, the single sample Gene Set Enrichment Analysis (ssGSEA) in 81 HCC patient samples showed the induction of metabolism-related pathways and inhibition of pathways relative to extracellular matrix remodeling (and particularly Rho-GTPase pathways, key regulators of cell morphology, cell-matrix adhesion and cytoskeletal reorganization) in samples with high *NTN1* expression (**Figure *27***). As the enhanced anabolism of the liver is rather associated with parasympathetic (cholinergic) activity, aiming to store the nutrients and to augment liver volume, we could hypothesize that the switch to a more parasympathetic innervation may be important for hepatic malignant transformation. Indeed, the ssGSEA analysis of 193 HCC samples showed that 97% of energetic pathways, representing functions fostering general proliferation, were correlated to cholinergic tumors (not shown).

Currently, no published data is available describing the neuroregulation in HCC *in vivo.* We evaluated the ability of the DEN-induced HCC rat model (**Figure *23***B) to recapitulate the ANS processes by monitoring the same neural markers as those used for clinical samples. The analysis revealed that NeuN signals increased throughout disease progression. Interestingly, signals related to the DCX progenitor marker increased transiently, in samples bearing early HCCs. In the case of ANS-specific markers, though levels of the adrenergic TH marker remained unchanged across disease progression, an increase in the cholinergic VAChT marker was observed in rats suffering from early HCC. We then analyzed the quantitative evolution of neural markers during CLD and HCC progression, which confirmed neo-neurogenesis and the parasympathetic neural

features of HCC in the rat (**Figure *28***B-F). Altogether, such data led to the identification of a cirrhosis-bearing HCC animal model with adequate features for HCC neurological research.

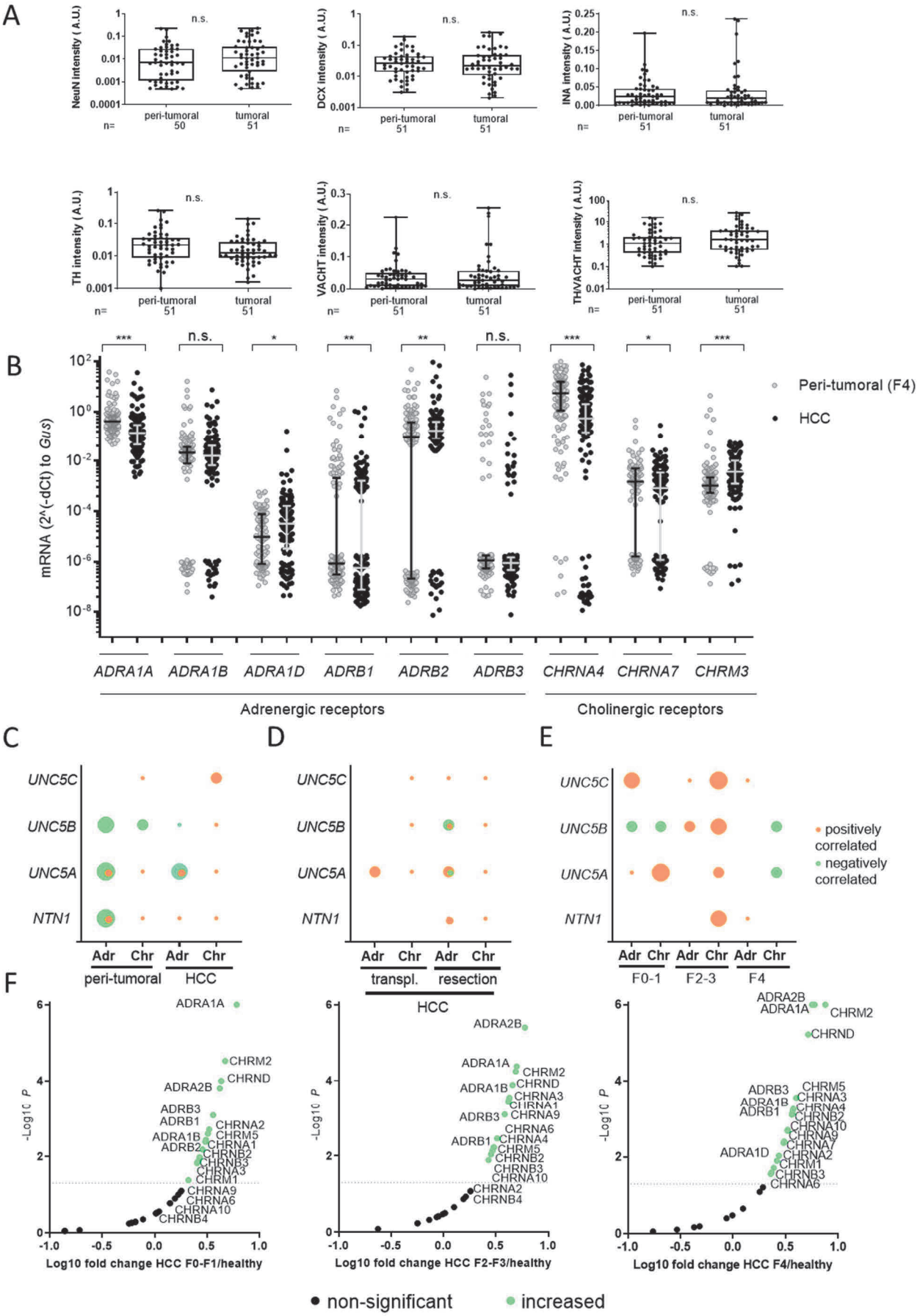

Figure 26. Expression of neuronal markers and ANS post-synaptic markers in peri-tumoral and tumoral tissue of patient samples

(A) Expression of mature and progenitor neural markers in human HCC by immunoblotting. HBV (n = 14), HCV (n = 9), ALD (n = 14) and NASH (n = 14), total of 51 patients. Mann-Whitney *U* test, * $p < 0.05$, ** $p < 0.01$.

(B) Adrenergic and cholinergic receptor expression in peritumoral tissue (F4) and HCC. Mann-Whitney *U* test, * $p < 0.05$, ** $p < 0.01$.

(C) , (D) Correlation between *NTN1* and UNC5s vs. adrenergic (Adr) and cholinergic (Chr) receptors' expression in tumoral and paired peri-tumoral tissues (C), in tumoral tissues (D). Spearman test.

(E) Correlation between *NTN1* and *UNC5s* and adrenergic and cholinergic receptors' expression in HCC samples of 81 patients (RNA data from Schulze et al, Nat Genet. 2015[197]). The magnitude of the dots is proportional to the number of receptors positively (orange) or negatively (green) significantly correlated.

(F) Volcano plot showing the modulation of ANS receptors' expression in tumors (n=81) compared to healthy tissue (n=10). Overall cholinergic orientation increases throughout fibrosis stages, while adrenergic one remains stable (RNAseq data from Schulze et al,[197]).

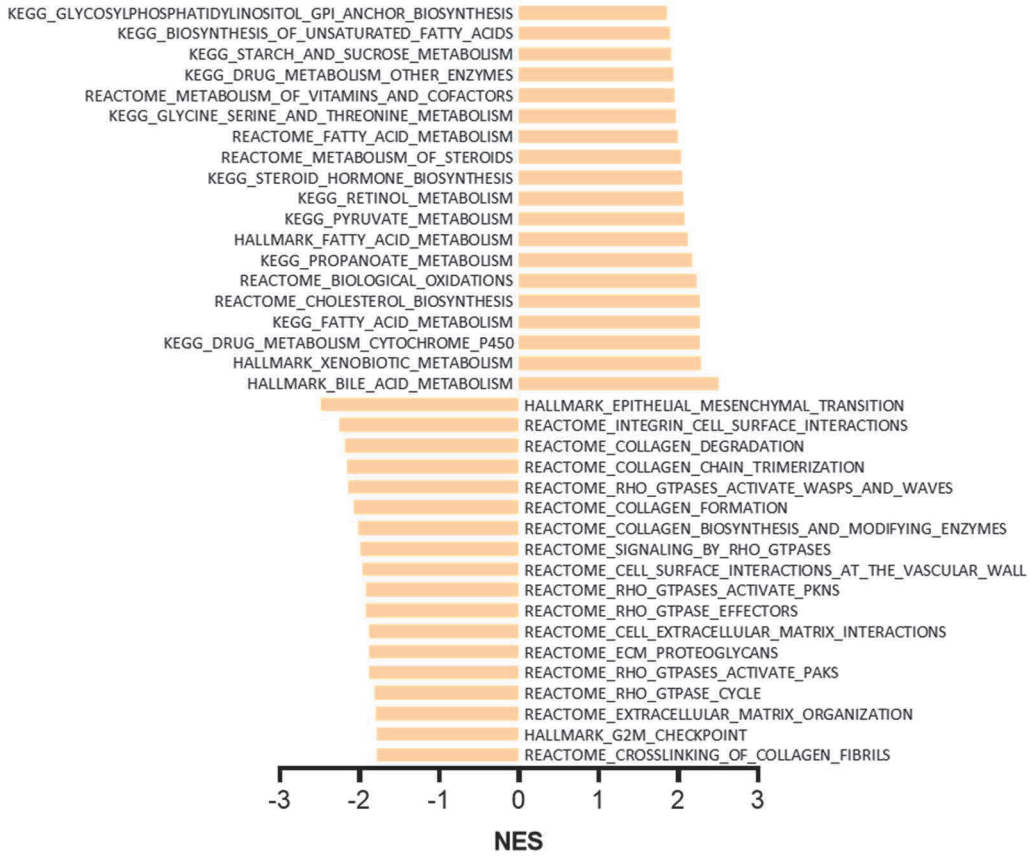

Figure 27. ssGSEA of two categories of gene sets enriched in HCC patient samples

193 pathways were downregulated and 83 pathways upregulated in *NTN1*-high HCC samples (n=81) compared to healthy liver (n=10). False Discovery Rate < 0.01; Normalized Enrichment Score (NES) > 1.78 (1.78 min; 2.49 max).

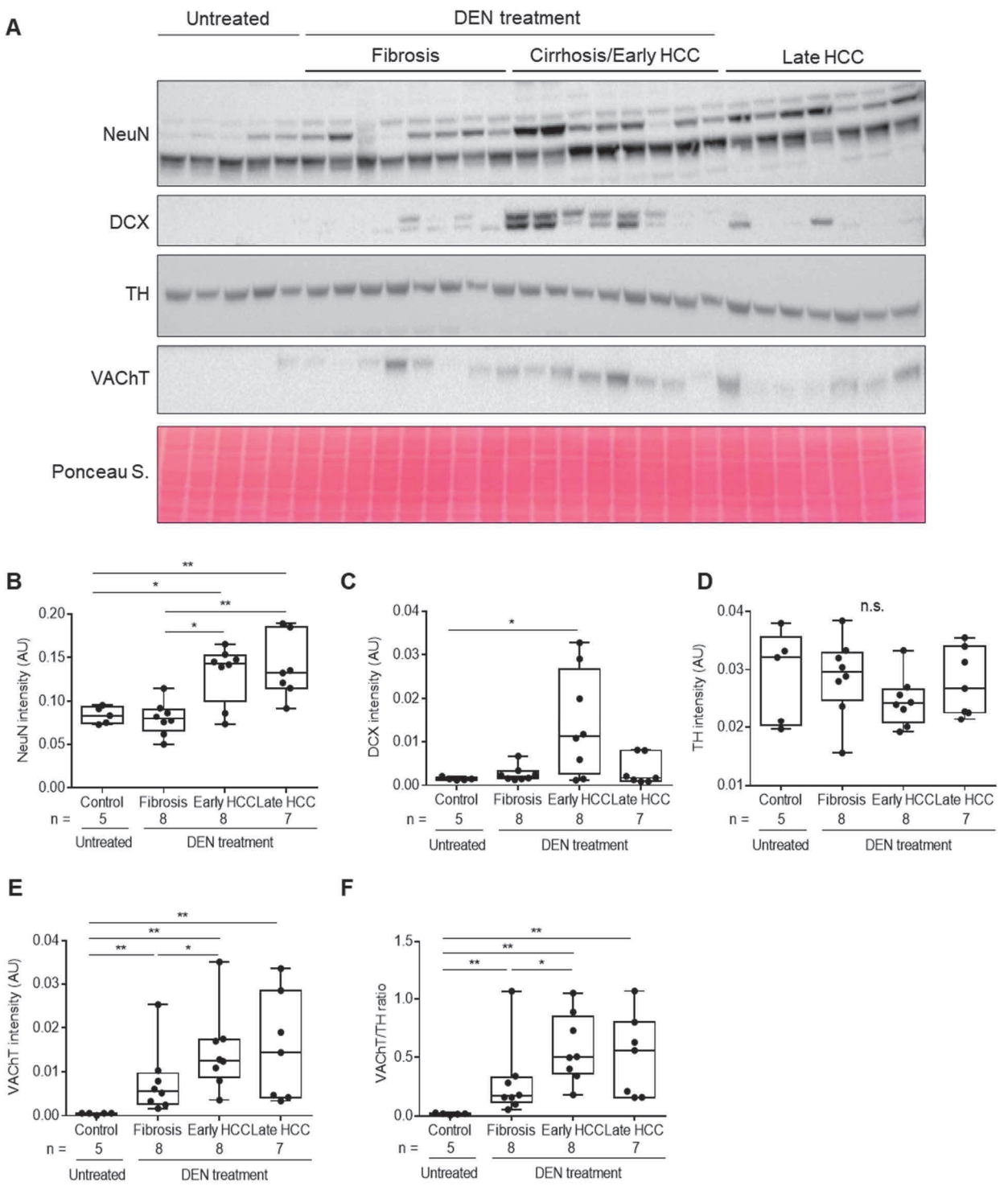

Figure 28. Pathological hepatic remodeling is correlated with induction of immature neuronal marker DCX and parasympathetic features in the HCC-bearing cirrhotic rat

(A) Western blotting of NeuN (mature neuronal marker), DCX (immature neuronal marker), TH (adrenergic marker) and VAChT (cholinergic marker).

(B) , (C), (D), (E), (F) Box plot graphs showing overall cholinergic orientation in liver disease progression towards HCC. Protein quantification, using whole lane Ponceau S fluorescence for normalization. Mann-Whitney *U* test, * $p < 0.05$, ** $p < 0.01$.

Correlation between ANS and immunity in HCC

To gain insight into the ANS orientation in the hepatic immune response we analyzed the number of immune pathways linked to pro-adrenergic or pro-cholinergic tumors (classification established depending on the ANS receptors' transcript predominance, Hernandez et al., unpublished data). The analysis revealed that the number of immune pathways linked to adrenergic tumors was higher than those linked to cholinergic tumors. Moreover, naïve $CD4^+$ cells, γδ T cells, B cells (total, naïve and memory) and myeloid dendritic cells were significantly enriched in cholinergic tumors, whereas hematopoietic stem cells, NK cells and macrophages (total and M2) were enriched in adrenergic tumors (**Figure *29***). The data suggest that a $CD4^+$/B cell orientation, known to foster immunotolerance, may be favored by the cholinergic polarity of the tumor. Indeed, vagal/cholinergic signaling relays anti-inflammatory signaling systemically and in the gastrointestinal tract[198–200]. This could provide an explanation for higher aggressiveness of cholinergic tumors (Hernandez et al., unpublished data), through the notion that cholinergic/vagal mitigation of local immunity could indeed oppose proper mounting of anti-tumoral response.

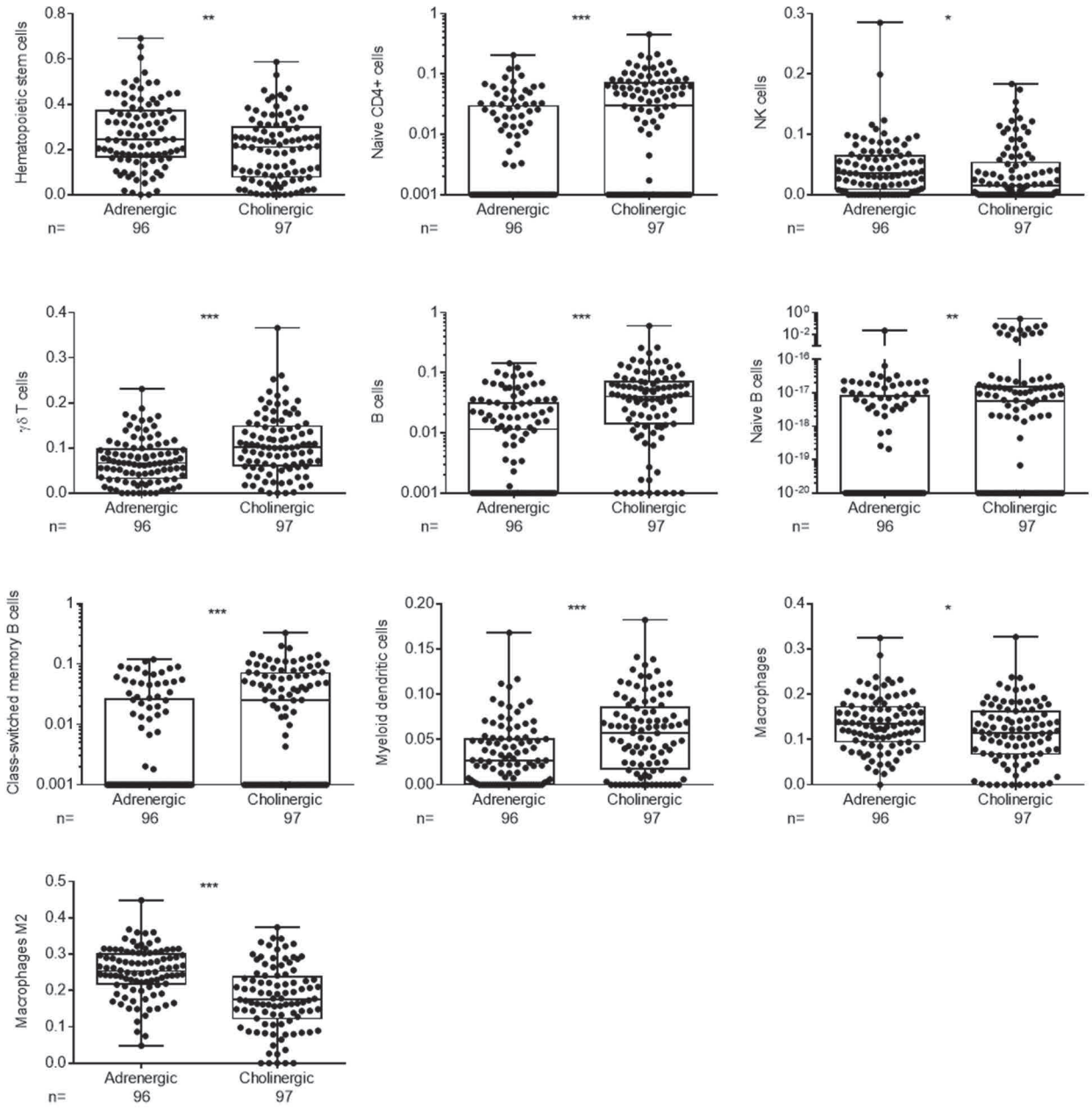

Figure 29. Immune cell population enrichment in pro-adrenergic and pro-cholinergic tumors

2.4. Discussion and perspectives

2.4.1. Netrin-1/UNC5 system is involved in cirrhosis-to-HCC progression

Our research group has been studying the role of netrin-1 and its receptors in liver pathologies and in the context of HCV infection. It has shown that netrin-1 is overexpressed in cirrhotic liver and it protects cancer cells from UPR-induced cell death[164]. Its receptor UNC5A is downregulated upon ER stress, overexpressed in fibrotic liver but collapses in HCC patients, more so in HCV-infected patients and essentially in those with advanced stages of fibrosis (F2-F4), suggesting that HCV strongly impacts UNC5A biogenesis in patients, especially in preneoplastic liver[127]. Thus, the pro-survival signal of netrin-1/UNC5s system may foster malignant transformation of cirrhotic liver towards hepatocellular carcinoma.

UNC5 dependence receptors may transduce two opposite signals: when unbound by the ligand they induce apoptotic signal, and when unbound by the ligand they induce cell survival, migration

and differentiation. Importantly, unlike UNC5 dependence receptors, secreted netrin-1 protein may act as an autocrine or paracrine factor. The exact cell types expressing netrin-1 or/and UNC5s, other than hepatocytes, in the liver are not identified. Also, netrin-1 is a diffusible factor. Unravelling the main actors sensitive to netrin-1/UNC5 regulation would help to understand the dynamics of tissue transformation.

In the present study, we demonstrated that netrin-1 receptors UNC5s are downregulated at the mRNA level and the ratios *NTN1/UNC5A* and *NTN1/UNC5C* were upregulated in the tumors compared to cirrhotic liver, irrespective of etiology and viral infection status in general. The UPR[164] and acute inflammation (Barnault & Verzeroli et al., 2022) seem to positively regulate netrin-1 expression at the translational but not at the transcriptional level. Therefore, we can hypothesize that the chronic inflammation and/or fibrosis also foster nontranscriptional changes that fall under the radar in transcriptomic studies. Also, overexpression of netrin-1 in chronic liver pathology was shown to confer an advantage to HCV infection, fostering virus infectivity, our study showed that the pathological role of netrin-1 is extended to non-viral contexts favorable to HCC development.

Moreover, we found that the netrin-1/UNC5 axis shows prognostic value for HCC onset in the cirrhotic context. Netrin-1 is a risk factor for cirrhosis-to-HCC progression, as patients with high *NTN1* mRNA level have 2.9-fold higher risk of HCC development. High *NTN1/UNC5A* and *NTN1/UNC5C* ratios were associated with shorter survival, while high *NTN1/UNC5C* ratio represented a risk factor for higher mortality (HR=2.33, $p<0.05$) in patients at 4-year follow-up, irrespective of etiological factors of HCC.

2.4.2. Netrin-1/UNC5 system and main liver cancer driver genes

HCC is an inflammation-driven condition in which chronicity matters. Indeed, nearly 90% of HCCs develop in the context of chronic liver inflammation, which induced fibrosis and/or subsequent cirrhosis[45]. Alongside the cellular stress, epigenetic modifications and mitochondrial alteration, the chronic necroinflammation triggers proliferation-associated DNA damage and genetic instability involved in CLD progression to HCC. So far, molecular characterization of HCC did not allow to identify biomarkers or stratify patients for the best therapeutic choice. In addition, studies in mice show that the transcriptome of the liver tumors driven by the same oncogenes varies and depends on the level of inflammation and the tumor microenvironment. Recent whole-exome studies describe a mean of 40 somatic alterations in coding regions in each tumor.

Mutations in the promoter region of *TERT* are the most common genetic alterations in HCC (all etiological risk factors mixed), followed by those in tumor suppressor *TP53* gene (associated with HBV-induced cirrhosis and advanced stages of disease) and gene coding for β-catenin (associated with ALD-induced cirrhosis)[201]. Approximately 11-41% of primary liver tumors bear *CTNNB1*-activating mutations, 13-48% harbor *TP53* inactivating mutations and 60-90% harbor *TERT* promoter activating mutations[202]. The latter one is of the earliest genomic alterations and is considered as a tumor gatekeeper. The p53 regulated multiple biological processes (e.g., angiogenesis through the regulation of VEGF-A expression). Recent studies showed that *NTN1, UNC5A* and *UNC5B* expression is regulated by p53 activity, demonstrating that netrin-1 binding to its receptors inhibits p53-dependent apoptosis[150,169–171,187]. We addressed the association between the functionality of p53 and netrin-1/UNC5 expression in cirrhosis and HCC. The analysis did not show any association between mutational status of *TP53* gene or functionality of p53 protein and netrin-1/UNC5 expression in cirrhosis or HCC at the total mRNA level.

However, we found an association between *NTN1* and *UNC5s* and *TERT* expression. Telomerase activation triggers the stabilization of the telomere length of the cancer cells, thus providing them with unlimited proliferation potential[203]. *NTN1, UNC5A, UNC5B* and *UNC5C* are associated with *TERT* induction in HCC, suggesting that pro-survival signal handled by netrin-1 overexpression may work together with this of telomerase. On the other hand, *NTN1/UNC5* ratios appear to be negatively correlated with *TERT* expression in cirrhosis and show no correlation in HCCs. These findings point out the differential dynamics of tissue remodeling and transformation in cirrhosis and tumors. Also, there was no significant modulation of netrin-1/UNC5 with regards to mutational status of patients (wild type vs. mutated). We can hypothesize that, as *TERT* expression does not associate with mutational status in the HCCs studied here, other mechanisms of telomerase induction may be involved, such as c-Myc, TGF-β/Smad pathway, Wnt/β-catenin pathway, HIFs or ER stress induction, that are known to be the regulators of *TERT* expression, but also some viral proteins (e.g., HBV-X transactivator protein HBX, HCV-Core protein[204]).

Recent findings demonstrated that netrin-1 regulates classical Wnt signaling by indirect stabilization of b-catenin, notably by its receptor UNC5B[190,191]. Moreover, secreted frizzled related proteins, which are regulators of classical Wnt signaling, present a structural homology with netrin-1 as they contain a carboxy-terminal netrin-related motif NTR. Of note, NTR domains are found in a wide range of other proteins (e.g., tissue inhibitors of metallo-proteinases (TIMPs), complement proteins and type I procollagen C-proteinase enhancer proteins (PCOLCEs)) playing different biological roles[205]. Still our study did not show any correlation between netrin-1 expression (mRNA or protein) and *CTNNB1* mutational status in HCC patients, we found a negative correlation between *UNC5A/UNC5B*/*UNC5C* expression and *CTNNB1* mutations. In addition, one study addressing Wnt-UNC5 interaction suggests that non-canonical Wnt receptor Frizzled receptor MOM-5 negatively regulates the UNC-5 in C. elegans[206]. We can hypothesize that β-catenin stabilization in the canonical Wnt signaling or stimulation by an unidentified factor in the non-canonical Wnt signaling may exert suppressive action on the UNC5s in the HCC context. However, although netrin-1 receptors were downregulated in *CTNNB1* mutated patients, the ratios ligand/receptor remained unchanged, indicating that Wnt activation may modulate *UNC5* dependence receptors expression but the overall apoptotic signal is compensated by *NTN1* expression.

2.4.3. Connection between netrin-1 and the ANS warrants further investigation

The role of the ANS in cancer is of increasing interest to researchers. My project proposed the implication of the ANS in cirrhosis and HCC in patient samples and in an experimental model of cirrhotic HCC in rats.

We observed that in DEN-treated rats netrin-1-capture induces the downregulation of overall adrenergic signal in cirrhotic tissue, but does not affect adrenergic/cholinergic balance in tumors at the transcripts level. Overall adrenergic/cholinergic ratio was lower in cirrhotic tissue of NP137 treated rats compared to PBS group, in accordance with the observed phenomenon of a negative correlation of adrenergic regulation with *NTN1/UNC5* expression in patient samples, suggesting a differential regulation of the ANS in cirrhosis compared to HCC. As our study showed no correlation between ligand and its receptors expression in tumors, but the existence of such positive correlation in cirrhosis, we can hypothesize that the relationship ANS-netrin-1/UNC5 may also feature different dynamics in cirrhosis and in tumors, a notion that emphasizes a potential specific role for neurons in HCC.

The parasympathetic orientation, observed in our study in HCC in the clinical samples and in cirrhotic rats through the increase of cholinergic cues or through downregulation of adrenergic cues and associated immune system modulation, suggests the relevance of a possible therapeutic strategy based on ANS modulation. The liver is innervated by the parasympathetic craniosacral nervous system through the vagus nerve X and the celiac plexus. These nerve branches innervate guts, hearts, lung, bladder and sexual organs in the abdominal cavity, and other cholinergic branches innervate head. To date, several classical anti-parasympathetic molecules with strong anti-cholinergic effects are used in the treatment of gastrointestinal conditions (e.g., anticholinergic hyoscine or scopolamine, methylscopolamine, while others are more respiratory system-oriented (e.g., tiotropium, ipratropium) or clearly psychotropic (e.g., rivastigmine, procyclidine). Of note, globally nearly 100 drugs used in the clinic today show low, moderate or severe anti-cholinergic effects (e.g., antipsychotic or anxiolytic drugs), suggesting that cholinergic signaling unofficially participates to a variety of effects in many pathological settings.

Although the role of the vagus nerve depends on the organ and the pathology (e.g., vagotomy reduces the risk of gastric cancer[207]), the modulation of the hepatic innervation in the CLD and HCC may gain increasing interest, and testing anticholinergic drugs in preclinical models may also become an interesting approach. With almost no evidence of a clear effect of vagotomy (surgical or pharmacological) in the hepatic context, only few studies showed a suppression of liver regeneration in rats after hepatic branch vagotomy[17,208] as well as steatosis in vagotomized cirrhotic mice[209]. Testing anti-cholinergic agents, many of which are clinically safe and well characterized, in monotherapy and in combination with anti-HCC drugs, will help to evaluate the usefulness of pharmacological modulation of the cholinergic nervous system in the prevention and treatment of HCC.

Finally, following our observations on the ANS and netrin-1 connections at the mRNA level, we wish to elucidate their relationship at the protein level as well. We have selected 80 patient samples of HCC with different etiologies in order to perform multiplex immunostaining exploring the expression of netrin-1, UNC5B, proliferation marker Ki67, hepatocyte marker Hep-Par, cytotoxic T cell marker CD8, immune checkpoint marker on the immune cells PD1 and on non-immune cells PDL1, adrenergic marker TH and cholinergic marker VAChT. Expected results will allow to determine the cell population expressing the ligand netrin-1 and its receptor UNC5B, to evaluate its proximity with effector immune cells, and to correlate the expression of netrin-1/UNC5B with intrinsic immune blockade mechanisms, as well as with sympathetic/parasympathetic nerves presence.

2.4.4. How sympathetic and parasympathetic nervous systems regulate liver inflammation in CLD and HCC?

The ANS controls the immune system through two opposing mechanisms: the anti-inflammatory reflex of the cholinergic system and the immune stimulating pro-inflammatory effects of the adrenergic system[210]. The release of substance P and corticotrophin-releasing hormone mediated by the peripheral nerves ensures the local regulation of the immune system, as all immune cells have receptors for hormones, neuropeptides and neurotransmitters. Vagus nerve regulates inflammation in the gastrointestinal tract and is known to suppress hepatic inflammation and mitigate the metabolic alterations in the context of acute liver injury, obesity, NASH and hemorrhagic shock. Little is known about the ANS actors in the regulation of the hepatic inflammatory process. It is known that α7nAChR (*CHRNA7*) expressed in Kupffer cells, dendritic cells and macrophages constitutes a major factor for cholinergic regulation of hepatic inflammation, notably through the inhibition of NF-kB nuclear translocation[211]. ACh inhibits the

hepatic production of TNF-α, IL-1, IL-6 and IL-18 by human macrophages at the post-transcriptional stage, with no impact on anti-inflammatory factors such as IL-10 in a model of acute hepatic inflammation *in vivo*[212], suggesting that vagotomy may be responsible of enhanced pro-inflammatory response in this condition. In addition, sympathetic factors, such as noradrenaline, are also known to induce the HSCs activation and the release of pro-inflammatory TNF-α and IL-6 from macrophages. Interestingly, these data are in accordance with findings in our study, showing an association between an anti-inflammatory signal and parasympathetic ANS in the chronic inflammation-based condition HCC in patients. Our bioinformatic analysis revealed that the number of immune pathways linked to adrenergic tumors was higher than those linked to cholinergic tumors. Moreover, naïve $CD4^+$ cells, γδ T cells, B cells and myeloid dendritic cells were significantly enriched in cholinergic tumors, whereas hematopoietic stem cells, NK cells and macrophages (total and M2) were enriched in adrenergic tumors, suggesting that adrenergic signaling is correlated with immune processes that may better interfere pathology progression.

In the cirrhotic liver, innervation is significantly decreased compared with that of liver with chronic hepatitis and healthy liver[13]. Depending on the cohort and study, up to 80% of cirrhotic patients have autonomic dysfunction, vagal or sympathetic, associated with unfavorable prognosis and cirrhosis complications, notably variceal bleeding[213]. Few animal studies showed the involvement of adrenergic arm in hepatic fibrogenesis: pharmacological sympathectomy reduced liver fibrosis in hypertensive rats with overactive sympathetic activation, a model developing severe hepatic fibrogenesis, whereas the CCL4-treated rats developing fibrosis showed significant decrease of fibrosis (83%) in rats treated with prazosin, as an antagonist of alpha1-adrenergic receptor [214].

2.4.5. Targeting netrin-1/UNC5 axis in the CLD and HCC

Although netrin-1 is normally expressed at low levels in peripheral nerves, with a major source in Schwann cells[215] in adults, this axon navigation cue overexpressed in colorectal[216], breast[160] and pancreatic[217] cancers was proposed to play a crucial role during tumorigenesis by regulating apoptosis.

We studied for the first time the effects of netrin-1 targeting by a clinical grade antibody in the context of CLD and hepatocarcinogenesis. Netrin-1-capture was unable to increase cell death in *vitro* in cancer cells lines expressing netrin-1 and UNC5B at different levels, and supplementing cancer cells negative for netrin-1 expression with recombinant netrin-1 had no effect on cell viability *in vitro* neither. Aware of possible discrepancies and unpredictability between *in vitro* and *in vivo* studies we investigated the effects of the anti-netrin-1 in monotherapy. Our study in DEN-treated rats revealed no significant impact of netrin-1 capture in the cirrhotic HCC. However, this study presented few limitations and we defined a new protocol proposing anti-netrin-1 as a preventive treatment of HCC in the cirrhotic context. Unfortunately, this study was not finalized due to project-independent concerns also due to the viral pandemic.

As an alternative model, our study of netrin-1 induction in mice treated with DEN will help to further delineate the biological role of netrin-1 in liver cancer onset and progression. Preliminary results showed a low incidence of tumor, irrespective of the genotype, which is conflicting with published studies in wild type mice. While 100% of tumor incidence is expected in DEN-treated males and nearly 20% in females[176], we observe much lower HCC incidence rates in males and females in our study. It is not surprising that the results may differ from mice (genetic background is not 100% identical in all mice of the same strain worldwide) and the final analysis may follow the documented tumor incidence and gender proportion. The expected results will also help to

understand the immune component modulation through FACS analysis, and ANS – netrin-1 and UNC5s relationship through immunostaining in tumors and peri-tumoral tissue.

With the recent approval of bi-therapy of atezolizumab in combination with bevacizumab in the frontline of anti-HCC treatment, that became a golden standard of HCC systemic treatment, we studied the effects of anti-netrin-1 antibody in combination with atezolizumab in chicken embryos bearing human HCC cancer cells. Study using SNU-182 HCC cell line positive for netrin-1 and UNC5B expression for such combination assay did not show any significant difference in tumor growth (not shown). This study presents few limitations, as cancer cells proliferation was weak and tumor volume was small, resulting in nonsignificant statistical difference, and the protein expression levels of other UNC5 receptors was unknown in this cell line. We then searched for the murine HCC cell line positive for netrin-1 and UNC5B to perform immunotherapy assays in the syngeneic model in immunocompetent mice. So far, no such cell line was identified. Hepa1-6 cell line is only UNC5B-positive but netrin-1 negative, and in perspective it may be a subject to genetic modifications to induce netrin-1 expression and such pharmacological tests.

A Phase I clinical trial assessing a humanized monoclonal antibody targeting netrin-1 (NP137) has shown anti-tumor activity in patients with advanced solid tumors. A Phase Ib/II clinical trial GYNET is ongoing to investigate the clinical and biological activity of NP137 in combination with carboplatin plus paclitaxel and/or anti-PD-1 monoclonal antibody pembrolizumab in patients with locally advanced/metastatic endometrial carcinoma or cervix carcinoma (NCT04652076). NP137 presents a safe tolerance profile with almost no side effect.

However, as to date only ~20% of patients respond to immunotherapy, it is worth to continue to investigate alternative approaches. Two TKIs, sorafenib and lenvatinib, stand in the first/second line in systemic treatment of advanced HCC in Europe. While Phase III clinical trial REFLECT showed no inferiority of lenvatinib to sorafenib (overall survival 13.6 months with lenvatinib vs. 12.3 months with sorafenib), lenvatinib has more pleiotropic effect, and particularly marked tumor stroma-regulating effect. We decided to address the combination of NP137 and lenvatinib in immunodeficient mice bearing a tumor after the intrahepatic injection of HCC cells SNU-182. This study is currently ongoing and includes graft assay, lenvatinib dose-escalation and combination assays. Expected results would help to evaluate the potentiation or synergy effect of anti-netrin-1 antibody.

Netrin -1 as a novel target in the pathological hepatic stroma?

The progression of CLD is characterized by a continuous liver injury, leading to necrosis and apoptosis of the hepatocytes, therefore leading to the formation of liver fibrosis which may culminate in cirrhosis. In addition to inflammation, hepatic fibrogenesis is characterized by hepatic stellate cell activation, leading to tissue remodeling and repair with increased accumulation of extracellular matrix (e.g., fibrillar collagens I and III). Late stage of fibrosis (cirrhosis), is linked to poor survival and increased risk of developing HCC[218]. To date, liver transplantation is the only curative treatment for patients with cirrhosis and its clinical complications. Finding an alternative and a better treatment to counteract or reverse liver fibrosis is one of the greatest challenges in the field of liver pathologies and has promoted a boom in interest in the search of a new efficient therapeutic agent.

The extracellular matrix interacts with cells to adjust diverse functions (e.g., proliferation, migration and differentiation). Indeed, extracellular matrix remodeling is one of the processes constituting a common denominator driving the development and progression of tissue fibrosis towards cancer. Deregulation of extracellular matrix composition, structure, stiffness and abundance contributes to CLD and HCC. Netrin-1 is a member of the laminin superfamily and is

a secreted protein associated with the extracellular matrix. To date, the study of extracellular matrix composition is a somewhat overlooked area of drug discovery, and addressing this gap by dissecting how netrin-1 regulates liver structure and function and how netrin-1 may affect extracellular matrix remodeling may open fruitful avenues for future research.

Netrin-1 may be secreted or attached to the extracellular matrix through its heparin-binding C-terminal netrin-like module. So far, our study showed that under the acute inflammation condition *in vitro* in HepaRG cells and PHHs, netrin-1 upregulation also stems from the release of cell membrane-bound netrin-1 of hepatocytes. Moreover, as this upregulation was cell death-unrelated with no impact on cell viability, one can hypothesize that netrin-1 may convey a rapid response to acute inflammation through its chemotactic et/or scaffolding of extracellular matrix properties. The impact of netrin-1 on the extracellular matrix stiffness modulation and its consequences in the condition of induced acute or chronic inflammation was not studied in this project, but may be an interesting approach to gain deeper insight in netrin-1 function in the liver.

Netrin-1/UNC5 axis in the angiogenesis regulation

Not less complex than nerves, blood vessels are complex branched networks that require guidance to ensure their proper positioning in the body. Few recent studies have identified the endothelial cells resembling axonal growth cones present at the tips of new growing capillaries. These cells on the capillaries in formation grow out in response to gradients of some well-known pro-angiogenetic factors present in extracellular matrix (e.g., VEGF), but also in response to some axon guidance molecules that regulate axon terminal arborization (semaphorins, slits and netrins)[219]. In addition to its role in axon guidance, netrin-1 and its receptors has been implicated in angiogenesis the most likely through their ability to regulate pro-survival signals. Netrin-1 may also act as bifunctional cue during angiogenesis. It enhances capillary density and smooth muscle cells to form vessels *in vitro* and *in vivo*. Wilson et al. have shown promitogenic and promigratory effects of netrin-1 *in vitro* and proangiogenic effects of netrin-1 in post-ischemic revascularization, through unidentified receptors[220]. While the repulsive actions of netrin-1 via UNC5B were already observed in developmental angiogenesis[221], the study of pathological angiogenesis showed that activation of UNC5B as an agonist inhibits angiogenic sprouting and neovascularization, thus identifying UNC5B as a potential anti-angiogenic target[222].

Even though our study of patient cohort did not reveal any significant association between macrovascular/microvascular invasion of tumors in patients and netrin-1/UNC5s, a study in DEN-treated rats showed an increased bleeding-related mortality in animals receiving anti-netrin-1 treatment. This interesting finding relates to the increased cholinergic orientation of the treated group, parasympathetic signaling fostering vasodilatation. Although at the microscopic level ($CD34^+$ staining) the neovascularization was similar, irrespective of treatment, bleedings occurred in animals suggest increased vessel fragility/permeability or hemodynamics alteration (portal hypertension). The final cause of this event is however difficult to determine since other factors, such as sympathetic nervous system, known to be responsible of hemodynamics alterations, may compete with netrin-1/UNC5 axis modulation in the pathological liver.

2.4.6. Identification of a cirrhotic and neurally-relevant animal model for HCC studies

Only through trial-and-practice can researchers find new molecules that are both safe and effective. High attrition rate makes that about 12% of the drugs that enter clinical development are ultimately approved for the use in the clinic[223]. Due to the gap between pre-clinical results and efficacy in man and to the lack of efficacy when finally tested in man in late-stage trials, experimental science remains inherently unpredictable. One of the major limitations of failure is

thought to be current *in vitro* and *in vivo* models used in research, limiting the efficient pre-clinical-to-clinical translation. To our knowledge, ANS regulation (neuropathy and neurogenesis) in HCC has never been investigated *in vivo.* In a context where HCC occurs in a cirrhotic background in 90% of cases[38], we showed that the animal model of chronically DEN-treated rats recapitulating the human physiopathology[174] of HCC may constitute an adequate tool for studying neuroregulation in HCC.

The hepatic innervation displays an important, yet much subtle, role in the overall regulation of the organism, notably in terms of metabolism and altering disease processes. Since 1967, when the first liver transplantation was performed by Thomas Starzl in United States, more than 80 000 procedures were performed to date. Cirrhosis (67%) and cancer (15%) are the leading causes of liver transplantation, followed by cholestatic disease (10%), acute hepatic failure (8%), metabolic diseases (6%) and Budd-Chiarri syndrome (4%)[224]. The innervation of the transplanted liver has not been extensively studied yet. However, following liver transplantation, liver allograft is completely isolated from the neuronal control of CNS of the host. Although there is no obvious deficiency in metabolic liver function and bile production the liver transplantation has an important impact on the microcirculation, glycemia (insulin resistance), cholangiocytes (increased proliferation) and oval cells (decreased proliferation) according to the recent *in vivo* studies. Selective hepatic vagotomy in rats with hepatitis decreased hepatic progenitor cells, whereas the stimulation of hepatic vagal nerves stimulated progenitor cells proliferation, notably through CHRM3 receptor[225]. Similar observations were documented in humans. Very few studies show the effect of transplantation in animal models, associated with complete sympathectomy[226]. Transplanted patients have persistent abnormal hemodynamics, attributed to the loss of normal vasomotor tone. It appears from few old studies[227] that the transplanted liver can be regarded as disconnected rather than denervated. Indeed, many small nerves appear in the portal tracts and the parenchyma forming an intrinsic plexus but more peripheral tissue showed no nerves. Importantly, this innervation was not constant in time, and there is no evidence for functional hepatic sympathetic reinnervation with 5 years post transplantation. DEN-induced HCC in rats may represent an interesting tool of studying the role of ANS denervation (surgical or pharmacological sympathectomy or vagotomy) in HCC in the cirrhotic context. Since tumor recurrence occurs in 15-20% patients transplanted patients it would be interesting to address the question of the role of hepatic innervation in the relapse incidence in patients[228] and also to define the origin of these nerves with respect to donor or the recipient. To start with, a study of hepatic denervation at cirrhotic stage and early HCC would provide the insight of such approach.

2.4.7. Conclusion notes

Despite extensive efforts, liver cancer research to date has not even achieved a single effective drug for liver cancer therapy, as sorafenib was originally developed for renal carcinoma and immune checkpoint inhibitors were first tested effective in other solid tumors (e.g., Avastin (bevacizumab) in metastatic colorectal cancer in 2004), Tecentriq (atezolizumab) in urothelial carcinoma in 2016). This disappointing situation can be changed by shedding the light and handling special immune cell compositions, extracellular matrix remodeling, intrahepatic innervation, dynamics and functions in the liver to achieve a breakthrough in developing alternative and more efficient therapeutic options. My project proposes to offer its contribution to such integrative approaches.

An article in preparation

Translational characterization and therapeutic targeting of netrin-1 in hepatocellular carcinoma

Ievgeniia Chicherova[1], Claire Verzeroli[1], Carole Fournier[2], Mathieu Richaud[1], Florence Le Calvez-Kelm[3], Amelie Chabrier[3], Catherine Voegele[3], Matthieu Foll[3], Emilie Montellier[4], David Neves, Benjamin Gibert[1], Benjamin Ducarouge[1], Patrick Mehlen[1], Thomas Decaens[2], Pierre Hainaut[4], Fabien Zoulim[1], Romain Parent[1]

[1] – INSERM 1052/CNRS 5286, Cancer Research Lyon Center Lyon, University of Lyon, Lyon 69000, France,

[2] – INSERM 1209/CNRS 5309, Institute for Advanced Biosciences, University Grenoble Alpes, La Tronche 38700, France

[3] – International Agency for Research on Cancer, 69372 Lyon, France

[4] – INSERM U823, Institut Albert Bonniot, University Grenoble Alpes, La Tronche 38700, France

Introduction

Hepatocellular carcinoma (HCC) is one of the most common malignant tumors in the world, and its incidence rate is rising. According to the latest global cancer survey by the World Health Organization, there were 905,677 newly diagnosed liver cancer cases and more than 830,000 liver cancer-related deaths in 2020, with liver cancer being the third leading cause of cancer-related death worldwide[1,2]. A recent study predicts the continuous rise of HCC incidence until 2030, where metabolic disorders such as nonalcoholic fatty disease (NAFLD) is a predominant risk factor. The presence of cirrhosis, estimated between 85% and 95%, is a key factor of the development of HCC[2,3], sharing with the other chronic liver diseases (CLDs) the main etiological conditions for cancer onset. Despite the existence of the potentially curative treatment options, such as surgery or liver transplantation, the majority of patients are not eligible to undergo them. With the advanced precision medicine, treatment tailored to each patient will be the future of HCC care.

Although in adults, netrin-1 is normally expressed at low levels in peripheral nerves, with a major source in Schwann cells[4], this axon navigation cue overexpressed in colorectal[5], breast[6] and pancreatic[7] cancers was proposed to play a crucial role during tumorigenesis by regulating apoptosis. Netrin-1 is operating through binding to “dependence receptors”, such as DCC and UNC5A-D. The expression of one of these receptors at the surface of a cancer cell renders this cell dependent on ligand availability for its survival. Hence, the loss of dependence receptor activity confers a selective advantage for tumor cells.[6] We have previously demonstrated that netrin-1, a well described cancer mediator in epithelial and neuronal contexts[8], endows hepatocytes with increased resistance to apoptosis during the unfolded protein response (UPR)[9], one of the hallmarks of chronic liver conditions[10–12]. In the context of Hepatitis C virus (HCV) infections, netrin-1 was also showed to foster entry of virus into hepatocyte, which in turn induces netrin-1 expression. Interestingly, the phenotype was reversed in HBV patients treated with anti-viral therapy.

In possession of the available data on the implication of netrin-1 in the progression of chronic liver disease and HCC onset, its pro-inflammatory and anti-apoptotic input and lacking data in

terms of its potential therapeutic targetability in patients with liver cancer, we have extensively characterized the netrin-1/UNC5 axis in clinical samples, attempting to determine the population of potential responders to anti-netrin-1 therapy.

Through a series of experiments on HCC cell lines positive or negative for netrin-1/UNC5 expression, including loss of function (CRISPR/Cas9 knock-out and neutralizing monoclonal antibody treatment) and gain of function (recovery with recombinant netrin-1 protein) approaches, and using a DEN-induced HCC rat model, we also aimed at the identification of potential candidates to be combined with anti-netrin-1 therapy.

Materials and methods

Human Tissue Samples

A total of 332 fresh-frozen tissues samples, including 166 tumoral tissues and 166 paired peri-tumoral tissues, in this study were included were from the French National HCC Biobank (under IRB agreement of Inserm Ethics Committee (CEEI, #1862)). Tumoral and para-tumoral tissues have been obtained in accordance with French law and the National Ethics Committee.

Animal housing, treatment and harvest

All animals received humane care in accordance with the Guidelines on the Humane Treatment of Laboratory Animals (Directive 2010/63/EU), and experiments were approved by the animal Ethics Committee: GIN Ethics Committee n°004.

Rats

6-week-old Fischer 344 male rats (Charles River, Wilmington, MA, USA) were housed in the Plateforme de Haute Technologie Animale animal facility (Jean Roget, University of Grenoble-Alpes, France). All rats were treated weekly with intra-peritoneal injections of 50 mg/kg of diethylnitrosamine (DEN) (Sigma-Aldrich, France), which were diluted in olive oil to obtain a cirrhotic liver with hepatocellular carcinoma after 14 weeks[13]. At 20 weeks of life animals were anesthetized with isoflurane and euthanized. Hepatic tissues were immediately snap frozen in liquid nitrogen and subsequently thawed on ice prior to homogenization using a Dounce apparatus previously refrigerated, followed by the addition of RIPA or Trizol (see below, Protein extraction and western blotting and Quantitive RT-qPCR). Circulating levels were determined in serum of rats by following Elisa kits: Rat CRP/C-Reactive Protein ELISA Kit; Sigma-Aldrich (RAB0097), Human IgG ELISA Kit; Sigma-Aldrich (RAB0001).

Mice

Mice were maintained in a specific pathogen-free animal facility (Anican, Lyon - France) and stored in sterilized filter-topped cages. Mice were handled in agreement with the institutional recommendations and procedures approved by the animal care committee (#CECCAP 2019112210118207). Independent transgenic (Tg) mouse lines were established from transgenic founders using seven-week-old (20–22 g body weight) female and male C57BL/6 mice (Janvier Labs, Indianapolis, Saint Berthevin - France). The offspring animals were housed in standard cages (five animals/cage) with litter and food. Enrichment was achieved by adding cotton for nesting. The mice were injected intraperiotoneally with 25 mg/kg of diethylnitrosamine (DEN, Sigma-Aldrich, France) at day 7, with 10mg/kg of tamoxifen (producteur, pays) at day 15 of life and sacrificed at 8 months prior to liver harvest. Hepatic lobe samples were immediately snap frozen in liquid nitrogen and subsequently thawed on ice prior to homogenization using a Dounce apparatus previously refrigerated, followed by the addition of RIPA or Trizol. Blood was collected

by intracardiac route and centrifuged at 2000g for 10min, then serum was transfered to liquid nitrogen for storage.

Tissue microarrays and immunohistochemistry

The following tissue microarrays were purchased from US Biomax, Inc: LV2084, LV2081, LV8011a, LV2085, LV2086. For histological examination of fresh tissue, samples were fixed in 10% buffered formalin and embedded in paraffin. 4-µm-thick tissue sections of formalin-fixed, paraffin-embedded tissue were prepared according to conventional procedures. Sections were then stained with hematoxylin and eosin and examined with a light microscope. Immunohistochemistry was performed on an automated immunostainer (Ventana Discovery XT, Roche, Meylan, France) using Omnimap DAB Kit according to the manufacturer's instructions. Sections were incubated with a rabbit anti Netrin 1 (1/300; Abcam, Ab126729). An anti-rabbit - HRP was applied on sections. Staining was visualized with DAB solution with 3,3'-diaminobenzidine as a chromogenic substrate. Finally, the sections were counterstained with Gill's hematoxylin. Then, sections were scanned with panoramic scan II (3D Histech, Budapest, Hungary) at 20X.

Cell culture

Cells were grown in a 5% CO_2 humidified atmosphere at 37°C. All reagents were purchased from ThermoFischer Scientific (Les Ulis, France) unless otherwise indicated. HepaRG and CLP13 cells were seeded at a density of $4.10^4/cm^2$ in William's E medium containing insulin 5 mg/mL, penicillin 100 IU/mL, streptomycin 100 mg/mL, Glutamax 100mg/l, 10% fetal bovine serum (Hyclone, Illkirch, France) and hydrocortisone hemisuccinate 5.10^{-5} mol/L (Pharmacia Upjohn, Guyancourt, France). Hep3B, Huh7, Huh7.5 and HepG2 cells were seeded at a density of $2.10^4/cm^2$ in DMEM medium containing penicillin 100 IU/mL, streptomycin 100 mg/mL, Glutamax 100mg/l, and 10% fetal bovine serum (Hyclone, Illkirch, France). Medium was renewed twice a week. Primary human hepatocytes (PHHs) were isolated from surgical liver resections, after informed consent of patients (IRB agreements #DC-2008-99 and DC-2008-101) as previously described[14] and cultured in complete William's medium supplemented with 1.8% DMSO (Sigma, St Quentin, France). All PHH-related data were obtained from at least three distinct patients.

Cell viability assay

The Neutral Red (NR) assay was conducted as previously described[15]. Briefly, the NR stock solution (40 mg NR dye in 10 mL PBS) was diluted in culture medium to a final concentration of 4 mg/mL and then centrifuged at 600*g* for 10 min to remove any precipitated dye crystals. Cells were then incubated with 100 µL of NR medium for 2 h. NR medium was removed and the cells washed twice with PBS. Plates were incubated for 10 min under shaking with 150 µL/well of NR destain solution (50% ethanol 96%, 49% deionized water, 1% glacial acetic acid) to extract NR from the cells. OD was measured at 540 nm. The 50% inhibitory concentration (IC50) for each cell line was estimated after 72 h of incubation with an active substance.

Effects of active substances on the viability of HCC cell lines in vitro

The cells ($4\text{-}5\times10^4$ cells per well) were seeded in 96-well plates (Thermo Fisher Science, Roskilde, Denmark), cultured for 24 h, and the culture medium was changed to a new medium with or without pharmacologic agent. After culturing for 72 h, the number of viable cells was examined using the NRA cell growth assay.

Protein extraction and western blotting

Whole-cell lysates were obtained with 40 to 80µg of the lysis buffer RIPA (50mM Tris-HCl pH8.0, 150mM NaCl, 1% NP-40, 0.5% sodium deoxycholate, 0.1% SDS, 1x Protease inhibitor cocktail (Roche), 50mM Orthovanadate, 10mM NaF)-processed cell lysates. Lysates were centrifuged at 10,000 g for 5 min at 4 °C. 40 to 65 µg of protein extract were resolved on a 8% SDS-PAGE and transferred on a nitrocellulose membranes (Amersham Biosciences). Membranes were blocked in 5% low fat dried milk in PBS for 1 hr at room temperature, then incubated overnight at 4°C with specific primary antibodies: Netrin1 (1/2000; Abcam, Ab126729), UNC5B (1/1000; Cell signaling, 13851S). After three washes in PBS-Tween 0.1%, membranes were incubated for 1hr at room temperature with secondary antibodies coupled to HRP (1/5000, Sigma-Aldrich, St-Quentin, France) prior to chemiluminescence-based revelation using the Clarity Western ECL substrate (Bio-Rad, Versailles, France).

Quantitive RT-qPCR

Total RNA was extracted using Trizol (Invitrogen). One µg of RNA was DNAse I-digested (Promega, Charbonnières, France) and then reverse transcribed using MMLV reverse transcriptase (ThermoFischer) according to the manufacturer's instructions. Quantitative real-time PCR was performed on 1/10th diluted samples on a LightCycler 96 device (Roche, Meylan, France) using the low Rox qPCR mix (Bioline, Paris, France). PCR primers sequences (5'-3') and qPCR conditions are listed in the ad hoc section. Specificity of all primers (see **Supplementary table *1***) was assessed by melting curve analyses and agarose gel electrophoresis.

Next-generation sequencing

Primer Design and Amplification of Targets

Twenty-one amplicons of 150 bp in size were designed (Eurofins Genomics Ebersberg, Germany) to cover exons 2 to 10 of TP53. The GeneRead DNAseq Panel PCR Kit V2 (Qiagen) was used for target enrichment. A validated in-house protocol was used to set up multiplex PCRs in 10 µL reaction volume, containing 20 ng cfDNA, 60 nM of primer pool and 0.73 µL of HotStarTaq enzyme (6U/ul). The experiments were carried out in two physically isolated laboratory spaces: one for sample preparation and another one for post-amplification steps. Amplification was carried out in a 96-well format plates DNA engine Tetrad 2 Peltier Thermal Cycler (BIORAD) as follows: 15 min at 95 °C and 30 cycles of 15 s at 95 °C and 2 min at 60 °C and 10 min at 72 °C.

Library construction and deep sequencing

As quality control of amplification, approximately 5% of the PCR products were quantified by QubitTM dsDNA HS Assay Kit and (Invitrogen) and Qubit® 2.0 fluorometer. PCR products from the samples were purified with NucleoMag NGS Clean-up Size Select (Macherey-Nagel) at a ratio of 1.8X of beads to PCR products and quantified again by QubitTM dsDNA HS Assay Kit and (Invitrogen) and Qubit® 2.0 fluorometer. Library preparation was done using the NEB Next® Fast DNA Library Prep Set for Ion Torrent™ kit (New England Biolabs) with some modifications, where each volume of reagents was reduced by a factor 4. Briefly, 12µl of the 20µl purified products were end-repaired in 15µl, and added to 8.6µl of ligation reaction mix, 0.7µl of the Ion P1 Adapter and 0.7 µl of each Ion Barcode for the ligation step. The barcoded products were purified using NucleoMag NGS Clean-up Size Select (Macherey-Nagel) at final concentration of 1.8X, amplified with a final step of 8 PCR cycles in 25µl and quantified using Qubit quantification system and pooled in a equimolar way into a single tube . Cleanup and size selection of pooled libraries (180-220 bp) was performed in a 2% agarose gel and MinElute Gel Extraction Kit (Qiagen). The pool of purified barcoded libraries was quantified using the Qubit quantification system and the assessment of the library quality (molarity and size analysis) was done using the Agilent® High

Sensitivity DNA Kit and the Agilent Technologies 2100 BioanalyzerTM (Agilent Technologies). Emulsion amplification was performed on the Ion OneTouch 2 system (Thermoscience Fisher, Waltham, MA) using 8 µL of 100 pM library and the Ion PI Hi-Q OT2 200 Kit (Thermoscience Fisher), according to the manufacturer's protocol. Quality control of Ion PI Ion Sphere Particles was performed using the Qubit 2.0 fluorometer, as described in the protocol. The sequencing reaction was performed on an Ion Proton System (Thermoscience Fisher) using Life Technologies' Ion PI™ Chip Kit v3 and Ion PGM™ Hi-Q™ Sequencing Kit (Thermoscience Fisher), according to the manufacturer's instructions. Library preparation and sequencing conditions were adapted from previous protocols[16–18].

Bioinformatics analyses

Sequencing reads were mapped to the human genome hg19 by the mapper from the Torrent SuiteTM Software v5.8 mapper (TMAP) using default parameters. Resulting bam files were realigned using abra2 v3.0 (https://github.com/IARCbioinfo/abra-nf). The new bam files were checked for coverage and quality using bedtools and QC3. All samples had on-target median depth above 3700.

We then called variants in *TP53* screened regions with Needlestack, our in-house developed variant caller algorithm suitable for the detection of low-abundance mutations[19] (https://github.com/IARCbioinfo/needlestack version 1.1). The approach is based on the inclusion of sequencing data of a sufficient number of samples to robustly estimate the sequencing error rates at each position considered and for each possible base change. For the calling we used only reads with a base quality above 13 at *TP53* screened positions Sequencing error was modeled using a negative binomial regression to avoid bias in parameters estimation due to the potential presence of genetic variants detected as being outliers from this error model. We calculated for each sample a p-value for being a variant (outlier from the regression) that we further transformed into q-values to account for multiple testing. q-values are reported in Phred scale Q=-10 log10(q-value), and we used a threshold of Q>50 to call variants. One sample (barcode IonXpress-018) who had too many variants (169 vs less than 61 for all other samples with an average of 15.2 variants per sample) was removed before re-calling. The variants found were then annotated using Annovar databases and were finally filtered to keep variants with RVSB (relative strand bias) < 0.85 and AF (allelic fraction) > 10%.

Flow cytometry analysis

Pieces of liver were minced and digested in RPMI-1640 supplemented with mouse tumor dissociation enzymes (Miltenyi Biotec, Bergisch Gladbach, Germany) for 40 min at 37°C. Digested samples were filtered through a 70 µm nylon mesh to obtain uniform single-cell suspensions. Cells were washed with complete RPMI medium containing 10% decomplemented foetal bovine serum (FBS), 1% NEAA, 1% Sodium Pyruvate and 1% Penicillin-Streptomycin (GibcoTM) and resuspended in 500 µL of Flow Cytometry Staining Buffer (FCSB) (eBioscienceTM). 100 µL of cell suspension was used for staining in U-shaped 96-well plates. After PBS 1X washing, cells were stained with LIVE/DEAD™ Fixable Red Dead Cell Stain Kit for 30 min protected from light at room temperature. Fc receptors were blocked with anti-CD16/CD32 (TruStain FcX™; Biolegend) and cells were stained for cell surface antigens (see **Supplementary table *2***). For intracellular staining, cells were fixed and permeabilized using the Foxp3 / Transcription Factor Staining Buffer Set (eBioscienceTM). Events were acquired on a BD-LSRII flow cytometer (BD Biosciences, Le Pont-De-Claix, France), collected with the BD FACSDiva 6.3.1 software and analysed using the Flowlogic software.

Statistical analyses

All statistical analysis were performed using R software (version 4.0.4) or GraphPad Prism (version 7.05). For continuous variables, a Mann-Whitney *U* test, and for categorical variants, Wilcoxon test, a Kruskal-Wallis test with Bonferroni correction were used due to deviation from normality. Normality was tested using the Shapiro-Wilk test. Survival curves were calculated using the Kaplan-Meier method, and the log-rank test was used to compare the survivals. Univariate and multivariate Cox regression analyses were implemented to identify independent predictor of survival. The proportional hazard assumption was evaluated through correlation tests between the weighted Schoenfeld residuals and event times. A *P*- value <0.05 was considered significant as follows: * *p*-value <0.05, ** *p*-value <0.01, *** *p*-value <0.001.

Results

Clinical relevance of netrin-1 targeting in HCC patients

To assess a connection between the expression of netrin-1/UNC5s and stage of hepatic fibrosis and HCC, we measured the level of *NTN1* and *UNC5*s mRNA in 418 patients with fibrosis or HCC. The findings show massive induction of *NTN1* in cirrhotic and HCC patients, irrespective of etiology. *UNC5B* and *UNC5C* receptors are also significantly upregulated in cirrhosis and HCC, whereas *UNC5A* expression first drastically augmented in cirrhosis and then collapsed in HCC patients (**Figure *1***A). The same trend was observed separating the four main etiologies of CLD and HCC (HCV and HBV infections, ALD and NASH) (not shown). We then analyzed the *NTN1/UNC5s* ratios, which reflect the balance of pro-survival ligand to death receptor. Interestingly, the *NTN1/UNC5A* ratio was significantly increased throughout fibrosis progression and in HCC, but collapsed in cirrhotic liver, in accordance with previously published findings[20]. In the same vein, *NTN1/UNC5B* increased in fibrosis compared to normal tissue and *NTN1/UNC5C* increased in fibrosis, cirrhosis and HCC. Importantly, in addition to its pro-survival role it should be kept in mind the second, and initially primary, chemotactic role of netrin-1, which, we hypothesize, is also put at stake to mediate liver disease.

Although the causal role of netrin-1 in CLD and hepatocarcinogenesis remains to be established, a retrospective study of 101 HCV-infected cirrhotic patients attributed a prognostic value for *NTN1* levels. Indeed, patients with high expression of *NTN1* display shorter cancer-free survival (probability of HCC onset is 65% vs. 85%) and have 2.9 times higher risk to develop HCC at 4-year follow-up post cirrhosis diagnosis (**Figure *1***B).

Importantly, in the absence of correlation between transcript and protein expressions observed in previously published and unpublished data on netrin-1, we sought to document netrin-1 protein variation in CLDs and HCC. We have analysed netrin-1 in commercially available TMAs containing 624 analysable patient samples, including normal tissue, chronic hepatitis, cirrhosis and HCC samples, with a staining using an anti-netrin-1 antibody validated in previously published study (Barnault & Verzeroli et al., 2022). We observed an overexpression of netrin-1 in HCC samples compared to normal tissue but also compared to cirrhotic tissue (**Figure *1***C). The etiology data was not available for these TMAs, however, as all patients have Asian origin (China and Japan), where the predominant etiologies of liver disease are HBV, HCV and ALD[21], it remains to be confirmed whether viral infection-specific netrin-1 upregulation occurs or if a general effect

unfolds, irrespective of etiology. The expression of netrin-1 did not show any correlation with clinical features of HCC (e.g., TNM staging, differentiation grade, sex, and age) in these samples.

Because of these data, we can therefore speculate that the evolution of fibrotic patients towards HCC may involve the reshaping of netrin-1/UNC5s axis functions across the evolution of the disease.

Netrin-1/UNC5 axis is reshuffled in HCC

To gain deeper insight on a putative impact of netrin-1 and UNC5 on hepatocarcinogenesis we initially evaluated the *NTN1* and *UNC5* transcription levels in a cohort of HCC patients from the French National HCC Biobank. We analyzed the expression of netrin-1 and its receptors UNC5A, UNC5B and UNC5C in the HCC clinical samples of 166 patients from the French National HCC Biobank (**Table 1**). There was a strong male predominance (84%), with main risk factors being alcoholic liver disease (ALD, 21%), non-alcoholic steatohepatitis (NASH, 27%), HBV infection (28%) and HCV infection (24%). Different liver function stages were included with class A (83%), class B (11%) and class C (6%), as well different stages of tumor differentiation: poor (9%), moderately (45%) and well differentiated (46%). High alpha-fetoprotein (AFP) levels (>100ng/ml) were detected in 16% of patients. All patients had METAVIR fibrosis score F4 (cirrhotic liver).

The expression of *NTN1* and *UNC5*s was measured by RT-qPCR, and western blotting was used to quantify netrin-1 and UNC5B protein expression. The analysis of 166 HCC and paired peri-tumoral cirrhotic (F4) tissue revealed that mRNA expression of *UNC5A, UNC5B* and *UNC5C* was significantly lower in HCC tissues than in adjacent cirrhotic tissues (**Figure *2***A). *NTN1* mRNA level showed a limited downregulation in HCC samples. However, the ratios *NTN1/UNC5A* and *NTN1/UNC5C* were significantly upregulated in HCC, indicating higher pro-survival signals at mRNA level in HCC compared to cirrhotic tissues. We then wanted to assess the expression of netrin-1 protein and its receptors in these samples with the help of a semi-quantitative quantification (Western blotting using an internal range of recombinant netrin-1). The interindividual variation of netrin-1 protein was tiny and non-significant (**Figure *2***A). The same trend was observed for *NTN1/UNC5* mRNA levels and their ligand/receptor ratios and netrin-1 protein level when analyzed separately for four main etiologies. Also, due to the limitation of technical tools, - only an anti-UNC5B specific antibody is currently robustly validated in our hands, UNC5 protein analyses were limited to UNC5B. We unsuccessfully tried to evaluate UCN5B protein levels in these samples as signals were too weak to quantify.

To investigate the prognostic value of netrin-1 (mRNA and protein) and its receptors as well as their risk factor status, we used Kaplan-Meier survival curves (function of survival) and Cox regression model (Hazard Ratio (HR), function of risk) methods respectively. The patients were separated into two groups according to the median value of transcript expression or in three groups according to the three quartiles (<Q1, Q1-Q2, >Q3) values of transcript expression. While the analysis based on the median threshold showed neither any significant variation of survival nor of HR in either group (under or above the median value), the quartile-based group distinction allowed to identify the patients with the highest (Q3) *NTN1/UNC5A* and *NTN1/UNC5C* ratios as patients with shorter survival, and high *NTN1/UNC5C* ratio as a risk factor of mortality (HR=2.33, $p<0.05$) at 4-year follow-up (**Table 2**). Interestingly, these findings were even more evident (higher HR) in patients who underwent tumor resection compared to transplanted patients. Also, the transcripts were analyzed by Cox regression model as continuous variables. Higher *NTN1/UNC5A* ratios in HCC samples correlate with increased risk of mortality by 1.032 ($p<0.0001$)

(**Table 2**). The same trend was observed in analyses based on the etiology or tumor differentiation grade stratifications (not shown). Then we assessed the involvement of the ligand and receptors' transcripts on cirrhosis-to-HCC progression in a 4-year follow up. Indeed, patients with high *UNC5B* expression in tumoral tissue have 2.24-fold higher risk ($p<0.05$) to develop HCC within a 4-year follow up while patients with high *UNC5C* have this risk reduced by 56% ($p<0.01$) (**Table 3**).

These data suggest that the impaired *NTN1/UNC5* balance may be associated with poor survival in HCC patients. To confirm these findings, we will continue to follow the cohort and update the analysis. The limiting factor being the lacking data of mortality for the important percentage of patients, the analysis should be continued till mortality data are deemed complete for the whole cohort.

Then, Spearman correlation test was used to explore the correlation between transcripts and protein expressions. The *NTN1/UNC5* rates correlate at the cirrhotic level but not at the HCC level, suggesting that co-regulated *NTN1* vs. *UNC5* levels are beneficial for switch to the malignant phenotype at the cirrhotic level, or conversely, limit this progression (**Figure *2***C). The correlation between *NTN1* and *UNC5B* expression was observed in patients with NASH and HCV etiologies, between *NTN1* and *UNC5C* expression – in HCV-infected patients. The correlation between *NTN1* and *UNC5A* was observed in cirrhotic tissues of all studied etiologies (ALD, NASH, HCV, HBV). Globally, the most abundant transcript, both on cirrhotic and tumoral tissues, was *UNC5B,* followed by *UNC5A* and *UNC5C* (**Figure *2***D).

To explore the association between netrin-1, UNC5s and clinico-biological parameters of patients in cirrhosis and HCC, we performed multiple comparisons tests. The top 5 most significant parameters associated to high *NTN1/UNC5B* and *NTN1/UNC5C* (**Figure *2***E) ratios in cirrhotic and tumoral tissues (and *NTN1/UNC5A* only in HCC) were related to liver function (absence of oesophageal varices, jaundice, ascites, low bilirubin level and higher prothrombin time) suggesting their protective role for liver function. Although these clinical and biological features were not all significantly correlated after Bonferroni correction required for the multiple comparison analysis, it is worth to take these into consideration as the same trend was observed for all three studied *NTN1/UNC5* ratios. In addition, high *NTN1* transcript levels were associated to the presence of portal hypertension and hepatic insufficiency complications, such as ascites and jaundice, but only before Bonferroni correction.

Further Principal Component Analysis (PCA) of netrin-1 (mRNA and protein) and *UNC5*s transcripts did not allow to distinguish the main contributors to the phenotype of the analyzed groups of patients (all patients were analyzed as high (above the median value) or low (under the median value) with respect to transcripts' abundance) (**Figure *2***F). To further explore the connection between the *NTN1/UNC5* axis we implemented multivariable analysis such as multiple correspondence analysis, discriminant factorial analysis, ANOVA or ANCOVA and hierarchical clustering, allowing to mix quantitative (biological parameters) and qualitative (categorical features) data. However, this exploratory analysis did not allow to identify discriminant clinical or biological parameters enabling to choose patient categories that would benefit the most from netrin-1 capture in the clinic.

Associations between molecular alterations and netrin-1/UNC5 in HCC

We first searched for associations between alterations of major oncogenes and tumor suppressor genes versus netrin-1/UNC5 levels. A systematic Sanger sequencing was performed in a subset of 332 paired samples (166 patients) on *CTNNB1* gene and *TERT* promoter region. Next Generation Sequencing (NGS) was performed to explore the mutations in *TP53* gene. Sequencing of the corresponding adjacent tissue also allowed to verify the somatic origin of the mutation found in tumoral tissue. Taking into account the existing molecular classification of HCC, we investigated the connection between samples mutational status and netrin-1/UNC5s. We identified mutations in *TERT* promoter (43%, n=71/166), *CTNNB1* (26%, n=43/166) and *TP53* (16%, n=26/166) (**Table 1**), with the highest mutational burden in HCV patients (**Figure *3***A, B).

In accordance with the literature, all mutations C>T localized to the -124pb (95%) and -146bp (5%) positions (**Figure *3***C) from ATG start site of the *TERT* gene creating CCGGAA/T consensus sites for Erythroblast Transformation Specific (ETS) transcription factors. The binding of the ETS transcription factors triggers epigenetic transformations and recruitment of RNA polymerase II leading to mono-allelic *TERT* expression. We did not observe any association between mutational status in the *TERT* promoter region and netrin-1/UNC5s altered levels, irrespective of the etiology or tumor differentiation grade. However, we showed that *TERT* promoter mutations in non-mutated HCC patients were associated with an increased level (3.3-fold) of telomerase, compared to cirrhotic tissue. Globally, cirrhotic samples were poor expressers of *TERT* expression, with only 30% of positive samples and low median expression level. Surprisingly, *TERT* mRNA was 3.7-fold higher in *TERT* non-mutated patients compared to HCC samples harboring *TERT* mutations, a phenomenon of importance, that was already observed in other studies[22]. The levels of *TERT* mRNA positively correlated with *NTN1*, *UNC5A, UNC5B and UNC5C* mRNA levels in cirrhotic tissues and tumoral tissue with no *TERT* mutation, whereas *NTN1* did not correlate with *TERT* mRNA in mutated HCC. *TERT* mRNA negatively correlated with *NTN1/UNC5* ratios in the cirrhotic but not in the tumoral tissues (**Figure *3***D). These data suggest that other mechanisms could activate *TERT* mRNA levels (e.g., *TERT* gene amplification, translocation, HBV insertion) in non-mutated tumors. Of note, one mutation C>T localized to the -124pb was identified in peri-tumoral tissues while absent in paired tumoral tissues.

The mutations spotted in *CTNNB1* gene were hotspot mutations, representing previously defined three levels of β-catenin activation[23]: weak (S45), moderate (T41) and, predominantly, highly active mutations leading to amino acid substitutions within the b-TRCP binding site (D32-S37), therefore conferring to β-catenin an enhanced stability from the degradation by the proteasome. To validate the functionality of β-catenin activation we evaluated the levels of encoded transcripts of its two target genes glutamine synthetase (*GLUL*) and Leucine-rich repeat-containing G-protein coupled Receptor 5 (*LGR5*). Tumors with highly active mutations demonstrated strong/homogeneous *GLUL* and *LGRP5* expression and correlation with mutational status (**Figure *3***E, F). *UNC5A, UNC5B* and *UNC5C* receptors were significantly downregulated in *CTNNB1* mutated tumors, but neither *NTN1*, nor *NTN1/UNC5* ratios nor netrin-1 protein were (**Figure *3***G).

NGS covering exons 2-11 of *TP53* gene allowed to map the mutations in the coding sequence of the gene. Predominantly missense (**Figure *3***H) present all over the coding sequence (transactivation region, DNA binding domain, negative regulation region) were the found mutations, leading to the abnormal activity of the p53 protein. Except for the R249S mutation related to aflatoxin B1 exposure, no other recurrent *TP53* mutation hotspot has been identified. We did not observe any association of *TP53* mutational status with netrin-1/UNC5s levels, irrespective of the etiology or tumor differentiation grade. Then, we considered correlations between p53 functionality status, netrin-1/UNC5 expression profiles and ligand/receptor ratios

using the available p53 functionality classifications Sorts Intolerant From Tolerant substitutions (SIFT)[24], Align - Grantham Variation - Grantham Variation (AVGDG)[25], Transactivation[26], Phenotypic Selection Model, and unpublished Cluster classification in collaboration with P. Hainaut's (IAB, Grenoble) group. Essentially, these classifications allow to categorize p53 protein sequences depending on their mutations into non-functional, partially functional, functional, neutral or supertrans protein, consequently scoring p53 activity. The analysis did not show any significant association between p53 functionality and netrin-1/UNC5 expression. Multivariable analysis did not allow to discriminate a group of patients susceptible to integrate the netrin-1/UNC5 expression levels and mutational status of *TERT, CTNNB1* or *TP53* (**Figure *3***I). Although these data may be not exhaustive due to intratumor heterogeneity, these findings suggest that the netrin-1/UNC5 axis remains insensitive to the functions of the main markers of HCC genetics.

In search of a candidate for HCC therapy in combination with netrin-1 capture

Despite many potential therapeutic targets, many drugs have failed to exceed the efficacy of the currently available compounds sorafenib in phase III trials, indicating for further identification of future HCC targets. Such targets may not be obligatorily related to kinases or growth factors functions.

First, we have screened several HCC cell lines with regards to the expression of *NTN1*/*UNC5s* at the mRNA level, but also, with respect to protein expression of netrin-1 and its receptor UNC5B, for which antibodies were in-house validated. We then have performed drug testing in six liver cell lines (Hep3B, HepG2, Huh7, Huh7.5, CLP13 and progenitor cell line HepaRG) in order to evaluate their sensitivity to 20 compounds showing anti-cancer activity, including drugs in clinical use, or in clinical development for HCC or other cancers and targeting key pathways of liver tumorigenesis. We used two main approaches to assess the sensibility of cancerous cells to netrin-1 modulation: (1) loss-of-function, by either genetic deletion of the *NTN1* gene via the CRISPR/Cas9 approach in netrin-1-positive cells or netrin-1 trapping by NP137 antibody; (2) gain-of-function, by the supplementation of netrin-1-negative cells with recombinant netrin-1. Colorimetric cell viability tests MTT, SulfoRhodamine B assay (SRB) and Neutral Red Assay (NRA) showed comparable results (not shown), and NRA was selected as a readout for all tests.

Overall, when treated in monotherapy, netrin-1-positive hepatic cell lines were resistant to netrin-1 capture and netrin-1-negative hepatic cell lines were insensitive to supplementation by recombinant netrin-1, with the half maximal Inhibitory Concentration 50 (IC50) greater than the maximum screening concentration. Then we tested the sensitivity of cells to anti-HCC TKIs used in the clinic (sorafenib, lenvatinib, regorafenib and cabozantinib), assessing IC50s or Combination Indexes (CI)[27]. NP137 did not show neither synergy nor potentiation of any TKI (data not shown). Of note, no compensation was observed by overexpression of other ligands of dependance receptors (e.g., *NTN3*, *NTN4, NEOGENIN, A2B*) in the *NTN1* CRISPR/Cas9 clones (not shown). We then wanted to investigate the sensitization potential to cell death of netrin-1 trapping by counteracting the main pathological processes involved in hepatocarcinogenesis (e.g., inflammation, UPR) by ad hoc drugs and compounds. However, the concomitant or sequential treatment of cells pretreated with a low dose (1/4 IC50) of drugs having anti-cancer activity with NP137 in combination with one or two pharmaceutical agents (e.g., an UPR inhibitors celecoxib and thapsigargin, a corticosteroid dexamethasone), did not allow to identify any potential efficient combination therapy. Of note, NP137 treatment neither affected PHH viability alone

nor showed a synergy with TKIs. NP137 treatment in the rat HCC cell line HR-4 was consistent with finding in human cells (not shown). These data suggest that 2D tissue culture system may be insufficient, notably because of the lack of liver specific microenvironment, and that more complex system (tress-dimensional liver tissue culture systems such as HCC organoids or spheroids) would be better suited to study the potential of netrin-1 trapping *in vitro.* Also, the expression of netrin-1 and UNC5B may be insufficient to impact cell viability during netrin-1 capture. Indeed, as the protein expression of UNC5A and UNC5C is unknown, it is difficult to judge through what UNC5 receptor netrin-1 exerts its effect in HCC.

A rat model that allows HCC growth on genuine cirrhosis exists[28]. First, we wanted to evaluate netrin-1/UNC5 expression in this context and hence assess the possibility to use this model to target the netrin-1/UNC5 axis. We observed a significant upregulation of *NTN1* and *UNC5B* transcripts, paralleled by a collapse of *UNC5C* expression in tumoral samples (**Figure *4***A). Netrin-1 and UNC5B were unchanged between the groups. Given the presence of netrin-1 and UNC5s, we have designed a study based on NP137 treatment vs. PBS injected in rats that have reached the cirrhotic stage prior to HCC onset (**Figure *4***B).

Macroscopic analysis of the samples revealed no difference in terms of tumor number and median tumor size between both groups of treatment. Apoptosis (cleaved caspase-3), fibrosis (Sirius red), vascularization (CD34), cell proliferation (Ki-67, CyclinD1) and inflammation (ALAT, CRP) markers were not significantly different. Importantly, the NP137 group showed higher mortality (n=3) compared to PBS group (n=1). The analysis of other features pertinent to HCC development was addressed using extracted mRNA and proteins. *NTN1* and *UNC5* transcripts were downregulated and UNC5B protein was upregulated in NP137 treated rats compared to PBS treated group. Necroptosis, angiogenesis, EMT, inflammation and de-differentiation markers were globally upregulated in tumors of NP137-treated rats (**Table 4**) reflecting a rather pro-tumoral shift. The latter one can be explained as a resistance mechanism to treatment.

To independently document the implication of netrin-1 in the cirrhotic/HCC context, we designed a study in an animal model overexpressing netrin-1 by genetic means. **Figure *5***A, B details the experimental outline. Mice were injected with DEN to induce evolving liver disease and then separated into groups with or without induction of netrin-1. So far, preliminary results showed no carcinogenic impact of netrin-1 induction in DEN-treated mice (**Figure *5***C), which may be explained by small sample number in some groups.

Discussion

HCC is an inflammation-driven condition in which chronicity matters. Indeed, nearly 90% of HCCs develop in the context of chronic liver inflammation, which induced fibrosis and/or subsequent cirrhosis[29]. Although netrin-1 is normally expressed at low levels in peripheral nerves, with a major source in Schwann cells[30] in adults, this axon navigation cue overexpressed in colorectal[31], breast[6] and pancreatic[32] cancers was proposed to play a crucial role during tumorigenesis by regulating apoptosis.

Our research group has been studying the role of netrin-1 and its receptors in liver pathologies and in the context of HCV infection. It has shown that netrin-1 is overexpressed in cirrhotic liver and it protects cancer cells from UPR-induced cell death[12]. Its receptor UNC5A is downregulated upon ER stress, overexpressed in fibrotic liver but collapses in HCC patients, more so in HCV-

infected patients and essentially in those with advanced stages of fibrosis (F2-F4), suggesting that HCV strongly impacts UNC5A biogenesis in patients, especially in preneoplastic liver[33]. Thus, the pro-survival signal of netrin-1/UNC5s system may foster malignant transformation of cirrhotic liver towards hepatocellular carcinoma. UNC5 dependence receptors may transduce two opposite signals: when unbound by the ligand they induce apoptotic signal, and when unbound by the ligand they induce cell survival, migration and differentiation. Importantly, unlike UNC5 dependence receptors, secreted netrin-1 protein may act as an autocrine or paracrine factor. The exact cell types expressing netrin-1 or/and UNC5s, other than hepatocytes, in the liver are not identified. Also, netrin-1 is a diffusible factor. Unravelling the main actors sensitive to netrin-1/UNC5 regulation would help to understand the dynamics of tissue transformation.

In the present study, we demonstrated that netrin-1 receptors UNC5s are downregulated at the mRNA level and the ratios *NTN1/UNC5A* and *NTN1/UNC5C* were upregulated in the tumors compared to cirrhotic liver, irrespective of etiology and viral infection status in general. As UPR[12] and acute inflammation (Barnault & Verzeroli et al., 2022) seem to positively regulate netrin-1 expression at the translational but not at the transcriptional level. Therefore, we can hypothesize that the chronic inflammation and/or fibrosis also foster non-transcriptional changes that fall under the radar in transcriptomic studies. Also, overexpression of netrin-1 in chronic liver pathology was shown to confer an advantage to HCV infection, fostering virus infectivity, our study showed that the pathological role of netrin-1 is extended to non-viral contexts favorable to HCC development. Moreover, we found that the netrin-1/UNC5 axis shows prognostic value for HCC onset in the cirrhotic context. Netrin-1 is a risk factor for cirrhosis-to-HCC progression, as patients with high *NTN1* mRNA level have 3-fold higher risk of HCC development. High *NTN1/UNC5A* and *NTN1/UNC5C* ratios were associated with shorter survival, while high *NTN1/UNC5C* ratio represented a risk factor for higher mortality (HR=2.33, $p<0.05$) in patients at 4-year follow-up, irrespective of etiological factors of HCC.

Targeting netrin-1/UNC5 axis in the CLD and HCC

We studied for the first time the effects of netrin-1 targeting by a clinical grade antibody in the context of CLD and hepatocarcinogenesis. Netrin-1-capture was unable to increase cell death in *vitro* in cancer cells lines expressing netrin-1 and UNCB5 at different levels, and supplementing cancer cells negative for netrin-1 expression with recombinant netrin-1 had no effect on cell viability *in vitro* neither. Aware of possible discrepancies and unpredictability between *in vitro* and *in vivo* studies we investigated the effects of the anti-netrin-1 in monotherapy.

While the most of animal models, such as chemically induce, genetically engineered, syngeneic, humanized and xenograft models including patient-derived xenograft, allow to obtain HCC with no associated development of cirrhosis we aimed to test anti-netrin-1 therapy in model that would allow us to obtain results meaningful for clinical translation. A model of genotoxic carcinogenesis using DEN particularly gained our attention. When injected into an animal, DEN is metabolized in the centrilobular hepatocytes inducing DNA damage (DEN interacts directly with DNA and form covalent bonds, which result in DNA adducts), but also inflammation and fibrosis when injected chronically. A rat model of DEN-induced HCC recapitulates the evolution of human cirrhosis-based HCC. In addition, the gene expression profile of this gender-dependent model is very similar to the gene expression profile of human HCCs with poorer survival, and particularly close to human alcohol-induced HCC[34]. Our study in DEN-treated rats revealed no significant impact of netrin-1 capture in the cirrhotic HCC. However, this study presented few limitations

and we defined a new protocol proposing anti-netrin-1 as a preventive treatment of HCC in the cirrhotic context. Unfortunately, this study was not finalized due to the project-independent concerns also due to the viral pandemic.

As an alternative model, our study of netrin-1 induction in mice treated with DEN will help to further delineate the biological role of netrin-1 in liver cancer onset and progression. Preliminary results showed a low incidence of tumor, irrespective of the genotype, which is conflicting with published studies in wild type mice. While 100% of tumor incidence is expected in DEN-treated males and nearly 20% in females[35], we observe much lower HCC incidence rates in males and females in our study. It is not surprising that the results may differ from mice (genetic background is not 100% identical in all mice of the same strain worldwide) and the final analysis may follow the documented tumor incidence and gender proportion. The expected results will also help to understand the immune component modulation through FACS analysis, and ANS – netrin-1/UNC5 relationship through immunostaining in tumors and peri-tumoral tissue.

With the recent approval of bi-therapy of atezolizumab in combination with bevacizumab in the frontline of anti-HCC treatment, that became a golden standard of HCC systemic treatment, we studied the effects of anti-netrin-1 antibody in combination with atezolizumab in chicken embryos bearing human HCC cancer cells. Study using SNU-182 HCC cell line positive for netrin-1 and UNC5B expression for such combination assay did not show any significant difference in tumor growth (not shown). This study presents few limitations, as cancer cells proliferation was weak and tumor volume was small, resulting in non-significant statistical difference, and the protein expression levels of other UNC5 receptors was unknown in this cell line.

A Phase I clinical trial assessing a humanized monoclonal antibody targeting netrin-1 (NP137) has shown anti-tumor activity in patients with advanced solid tumors. A Phase Ib/II clinical trial GYNET is ongoing to investigate the clinical and biological activity of NP137 in combination with carboplatin plus paclitaxel and/or anti-PD-1 monoclonal antibody pembrolizumab in patients with locally advanced/metastatic endometrial carcinoma or cervix carcinoma (NCT04652076). NP137 present a safe tolerance profile with almost no side effect.

However, as to date only 20% of patients respond to immunotherapy, it is worth to continue to investigate alternative approaches. Two TKIs, sorafenib and lenvatinib, share the first/second line in systemic treatment of advanced HCC in Europe. While Phase III clinical trial REFLECT showed no inferiority of lenvatinib to sorafenib (overall survival 13.6 months with lenvatinib vs. 12.3 months with sorafenib), lenvatinib has more pleiotropic effect, and particularly marked tumor stroma-regulating effect. We decided to address the combination of NP137 and lenvatinib in immunodeficient mice bearing a tumor after the intrahepatic injection of HCC cells SNU-182. This study is currently ongoing and includes graft assay, lenvatinib dose-escalation and combination assays. Expected results would help to evaluate the potentiation or synergy effect of anti-netrin-1 antibody.

Netrin-1/UNC5 system and main liver cancer driver genes

So far, molecular characterization of HCC did not allow to identify biomarkers or stratify patients for the best therapeutic choice. The mechanisms of malignant transformation in HCC starting as early as the cirrhotic stage include notably the mutations in *TERT* promoter and chromosomal instability. Later mutational events in cirrhotic context and early events in non-cirrhotic context include the mutations in *TP53*, (e.g., R249S in aflatoxin B1 exposure context), *CTNNB1, ARID1A* and *AXIN1.* With nearly 35-80 mutations per tumor, a small number mutation occurs in cancer driver genes. Belonging to the key signaling pathways involved in hepatocarcinogenesis,

telomere maintenance, Wnt/β-catenin pathways and p53 cell cycle pathways constitute the triad of top HCC driver genes. Few recent studies have identified a close relationship between UNC5s and tumor suppressor p53. UNC5A and UNC5B have been proved to be direct downstream target genes of p53, suggesting that UNC5s may play a role in p53-dependent apoptosis, and therefore a role in tumor suppression[36–39]. UNC5 receptors induces apoptosis only when p53 protein is normally expressed and functional, but fails in the context of p53 loss and p53 mutation[40]. We addressed the association between the functionality of p53 and netrin-1/UNC5 expression in cirrhosis and HCC. The analysis did not show any association between mutational status of *TP53* gene or functionality of p53 protein and netrin-1/UNC5 expression in cirrhosis or HCC at the transcriptional level. However, we found an association between *NTN1/UNC5* and *TERT* expression. Telomerase activation triggers the stabilization of the telomere length of the cancer cells, thus providing them with unlimited proliferation potential[41]. *NTN1, UNC5A, UNC5B* and *UNC5C* are associated with *TERT* induction in HCC, suggesting that pro-survival signal handled by netrin-1 overexpression may work together with this of telomerase. On the other hand, *NTN1/UNC5* ratios appear to be negatively correlated with *TERT* expression in cirrhosis and show no correlation in HCCs. These findings point out the differential dynamics of tissue remodeling and transformation in cirrhosis and tumors. Also, there was no significant modulation of netrin-1/UNC5 with regards to mutational status of patients (wild type vs. mutated). We can hypothesize that, as *TERT* expression does not associate with mutational status in the HCCs studied here, other mechanisms of telomerase induction may be involved, such as c-Myc, TGF-β/Smad pathway, Wnt/β-catenin pathway, HIFs or ER stress induction, that are known to be the regulators of *TERT* expression, but also some viral proteins (e.g., HBV-X transactivator protein HBX, HCV-Core protein[42]). Recent findings demonstrated that netrin-1 regulates classical Wnt signaling by indirect stabilization of β-catenin, notably by its receptor UNC5B.[43,44] Moreover, secreted frizzled related proteins, which are regulators of classical Wnt signaling, present a structural homology with netrin-1 as they contain a carboxy-terminal netrin-related motif NTR. Of note, NTR domains are found in a wide range of other proteins (e.g., tissue inhibitors of metallo-proteinases (TIMPs), complement proteins and type I procollagen C-proteinase enhancer proteins (PCOLCEs)) playing different biological roles[45]. Still, our study did not show any correlation between netrin-1 expression (mRNA or protein) and *CTNNB1* mutational status in HCC patients we found a negative association of *UNC5A, UNC5B* and *UNC5C* with *CTNNB1* mutations. In addition, one study addressing Wnt-UNC5 interaction suggests that non-canonical Wnt receptor Frizzled receptor MOM-5 negatively regulates the UNC-5 in C. elegans[46]. We can hypothesize that β-catenin stabilization in the canonical Wnt signaling or stimulation by an unidentified factor in the non-canonical Wnt signaling may exert suppressive action on the UNC5s in the HCC context. However, although netrin-1 receptors were downregulated in the *CTNNB1* mutated patients, the ratios ligand/receptor remained unchanged indicating that Wnt activation may modulate *UNC5* dependence receptors expression but the overall apoptotic signal is compensated by *NTN1* expression.

Conclusion remarks

Despite extensive efforts, liver cancer research to date has not even achieved a single effective drug for liver cancer therapy, as sorafenib was originally developed for renal carcinoma and immune checkpoint inhibitors were first tested effective in other solid tumors. This disappointing situation can be changed by shedding the light and handling special immune cell compositions, extracellular matrix remodeling, intrahepatic innervation, dynamics and functions in the liver to achieve a breakthrough in developing alternative and more efficient therapeutic options. Netrin-1 is proposed such an unprecedented factor.

Table *1*. Characteristics of paired peri-tumoral (F4)/HCC patient samples (French National HCC Biobank cohort) used in the study. Median ± standard deviation (SD) is shown for all qualitative data.

Variable	Available data (Total: 166)	Values
Age, *y* ± SD	166	69 ± 10
Gender (male/female)	166	140 (84%)/26 (16%)
Etiology (%)	166	
Alcoholic liver disease		36 (21%)
Hepatitis B virus		46 (28%)
Hepatitis C virus		39 (24%)
Non-alcoholic steato-hepatitis		45 (27%)
Serum alpha-fetoprotein, >100 ng/mL	111	17 (16%)
Child-Pugh score (A/B/C) (%)	87	72 (83%)/9 (11%)/6 (6%)
Prothrombin, % ± SD	146	81 ± 22
Bilirubin, µMol/L ± SD	137	14 ± 75
Albumin, g/L ± SD	100	36 ± 7
Platelet count, G/L ± SD	149	131 ± 102
Encephalopathy (%)	164	18 (11%)
Ascites (%)	164	37 (3%)
Jaundice (%)	162	22 (14%)
Esophageal varices (%)	156	62 (40%)
Histological and gross features of the tumors		
Tumor size, *mm* ± SD	165	34 ± 31
Tumor localization (left liver/right liver/double)	165	47 (29%)/112 (68%)/6 (4%)
Intact tumor capsule (%)	143	91 (64%)
Satellite nodules (%)	165	34 (21%)
Macrovascular invasion, Microvascular invasion (%)	151	22 (15%), 81 (52%)
Differentiation grade (poor/moderately/well) (%)	165	15 (9%)/74 (45%)/76 (46%)
Architectural pattern (%)	136	
Trabecular		104 (76%)
Pseudoglandular		10 (7%)
Compact		5 (4%)
Clear cells		4 (3%)
Others		13 (9%)
Tumoral steatosis (%)	165	108 (66%)
Tumoral necrosis (%)	150	84 (56%)
Liver fibrosis score METAVIR (F4) (%)	166	166 (100%)
Inflammation activity score (%)	137	
METAVIR 0		51 (37%)
METAVIR 1		55 (40%)
METAVIR 2		23 (17%)

METAVIR 3	4 (6%)
Gene alterations (%)	
TERT promoter	71 (43%)
TP53	43 (26%)
CTNNB1	26 (16%)

Figure 1. Netrin-1/UNC5 regulation in CLD progression towards HCC. **(A)** NTN1, UNC5B and UNC5C transcripts are massively induced in cirrhosis and HCC, whereas UNC5A transcript collapses in cirrhosis and HCC. Intrahepatic mRNA levels were quantified by RT-qPCR. Fibrosis scores were determined by histopathology and using the Fibroscan method. Kruskal-Wallis and Mann-Whitney U tests, $p < 0.05$, **p<0.01, ***p<0.001. **(B)** Netrin-1 rates predict HCC-free evolution in a Lyon cohort of HCV-infected cirrhotic patients (n=101). Threshold was defined as the median of NTN1 expression levels across the cohort. Increase in HCC onset rates amongst high NTN1 expressers (>median) was 2.9-fold (Confidence Interval (CI) = 1-8.1. Kaplan-Meier test and Cox model implementing Log-rank test, *p < 0.05. **(C)** Netrin-1 augments in HCC patients as compared to normal liver or cirrhotic liver. Immunohistochemistry staining of netrin-1 in tumor microarray liver samples. Mann-Whitney U test, *p < 0.05, **p<0.01, ***p<0.001.

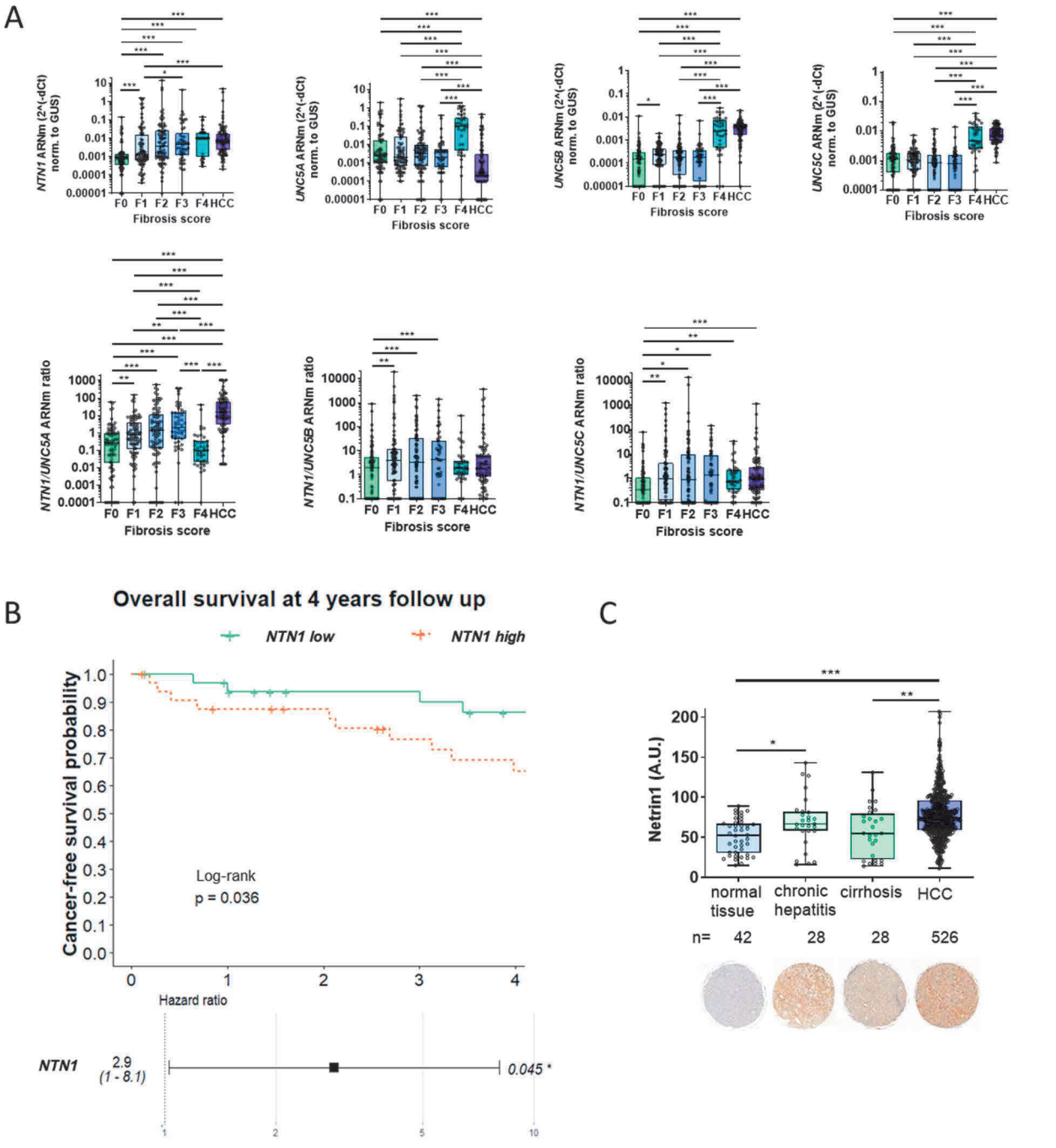

Figure 2. Netrin-1/UNC5 markers are reshuffled during cirrhosis-to-HCC transition. **(A)** *UNC5A, UNC5B* and *UNC5C* transcripts collapse in HCC, whereas *NTN1* transcript shows tiny downregulation in HCC compared to peri-tumoral tissue (F4). *NTN1/UNC5A* and *NTN1/UNC5C* ratios are increased in HCC. Intrahepatic mRNA levels were quantified by RT-qPCR. Statistical significance was determined using the Kruskal-Wallis and Wilcoxon tests, *p<0.05, **p<0.01, ***p<0.001. **(B)** *NTN1/UNC5A* and *NTN1/UNC5C* rates predict HCC-related mortality. Three groups (high, median and low) were defined as the quartiles of *NTN1* expression levels across the cohort. Increase in HCC-related mortality amongst high *NTN1/UNC5C* expressers (>3rd quartile) was 2.3-fold. Kaplan-Meier test and Cox model implementing Log-rank test, *p < 0.05. **(C)** *NTN1/UNC5* rates correlate at the cirrhotic level but not at the HCC level, suggesting that tightly regulated *NTN1* vs. *UNC5* levels are beneficial for switch to the malignant phenotype at the cirrhotic level. Spearman correlation coefficient, *p<0.05, **p<0.01, ***p<0.001. **(D)** UNC5 receptor abundance and expression in peritumoral tissue (F4) and HCC. 166 pairs of liver tissues were analyzed. Wilcoxon test, * p < 0.05, ** p < 0.01, *** p <0.001. **(E)** Liver function parameters associate with *NTN1/UNC5A*, *-B* and *-C* ratios. Multiple comparison analysis with Bonferroni correction. Mann-Whitney *U* test and Spearman correlation coefficient. **(F)** Principal Component Analysis of netrin-1 protein expression. Two different colors represent different groups of the samples: high (pink) for netrin-1 above the median *value and low (turquoise) for netrin-1 under*

the median value.

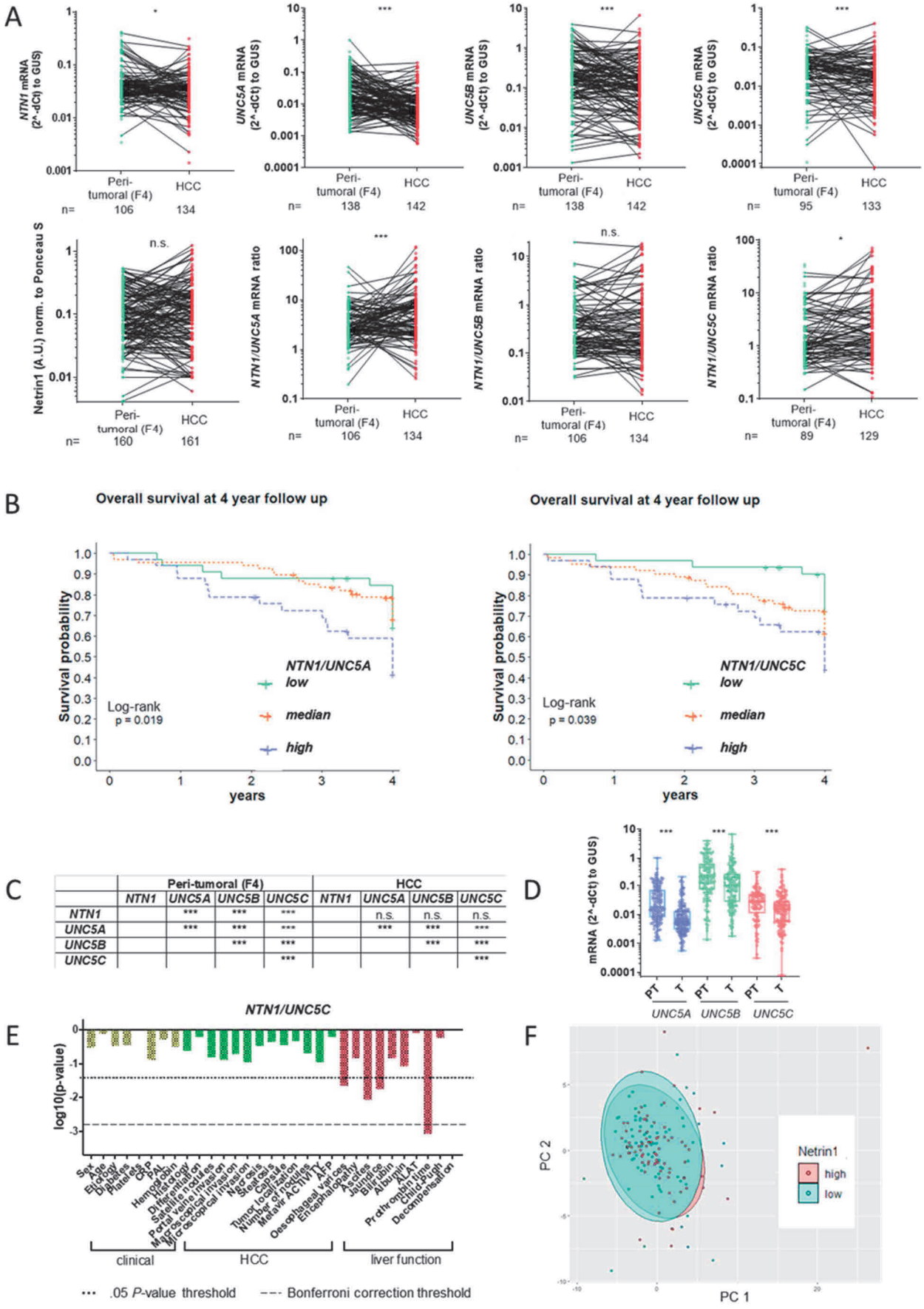

Table 2. Hazard Ratio comparing risk of HCC-related death at 4-year follow up in patients depending on the NTN1 and UNC5s expression. Time-dependent HR (continuous variable) and time-independent HR (3 categories). Cox regression multivariate analysis implementing Log-rank test.

		HCC		Peri-tumoral (F4)	
Covariate		HR (95% CI)	*P*-value	HR (95% CI)	*P*-value
Continuous variable	*NTN1/UNC5A*	**1,032 (0,88-1,15)**	**0,00004**	1,01 (0,78-1,12)	0,70
	NTN1/UNC5B	0,9 (0,78-1,13)	0,08	0,88 (0,81-1,03)	0,50
	NTN1/UNC5C	1 (0,97-1,01)	0,70	0,99 (0,88-1,10)	0,80
	Netrin-1	0,81 (070- 1,05)	0,60	0,8 (0,71-1,19)	0,50
Low/median/high	*NTN1/UNC5A*	1,26 (0,75-2,1)	0,40	0,79 (0,61-1,23)	0,50
	NTN1/UNC5B	0,59 (0,3-1,2)	0,13	1,01 (0,91-1,20)	0,90
	NTN1/UNC5C	**2,33 (1,07-5,1)**	**0,033**	1,2 (1,01-1,53)	0,60

Table 3. Hazard Ratio comparing risk of HCC onset at 4-year follow up in cirrhotic patients depending on the NTN1 and UNC5s expression. Time-independent HR (3 categories). Cox regression multivariate analysis implementing Log-rank test.

		HCC	
Covariate		HR (95% CI)	*P*-value
Low/median/high	*NTN1*	1 (0,98-1,03)	0,90
	UNC5A	0,99 (0,91-1,26)	0,90
	UNC5B	**2,27 (1,11-3,43)**	**0,024**
	UNC5C	**0,44 (0,34-1,05)**	**0,009**

Figure 3. Molecular events affecting the three top liver cancer-related genes do not correlate with *NTN1*/*UNC5* levels in HCC. **(A)** Venn diagram showing number of mutations in *TERT* promoter region, *CTNNB1* and *TP53*, and their co-occurrence in tumors. **(B)** Percentage of mutational events in patients with specific etiology. **(C)** Two hotspot mutation in the *TERT* promoter region and their incidence in tumors. **(D)** *UNC5A* mRNA level positively correlates with *TERT* mRNA expression level in peri-tumoral tissue (F4) and *NTN1/UNC5A* ratio negatively correlate with *TERT* mRNA expression level in cirrhosis. Spearman correlation coefficient. **(E)** CTNNB1 mutations in HCC samples. Amino acid substitutions are shown above the β-catenin protein sequence. Amino acid residues are numbered according to P35222 reference β-catenin sequence. The three groups of β-catenin activity are mentioned on the top. gDNA, genomic DNA. **(F)** Box plot graphs showing *GLUL* and *LGR5* mRNA expression in HCC samples compared to peri-tumoral tissue (NT) according to β-catenin mutation type. **(G)** Box plot graphs showing the downregulation of *UNC5* in *CTNNB1* mutated tumors. Mann-Whitney *U* test, * $p < 0.05$, ** $p < 0.01$. (H) Mutation frequency and distribution in TP53 gene. (I) Mixed PCA of UNC5 (left panel) and PCA of NTN1/UNC5 ratios (right panel). Qlucore Omics Explorer 3.7 software.

A

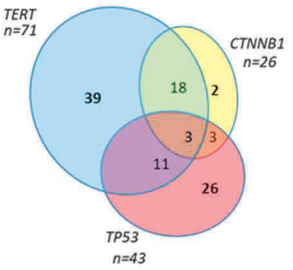

B

		mutated	wild type	mutated (%)
HCV	*TERT(25), TP53 (14), CTNNB1(8)*	31	15	67,39%
NASH	*TERT (16), CTNNB1(6), TP53(3)*	20	16	55,56%
Alcool	*TERT (19), CTNNB1(7), TP53(7)*	25	21	54,35%
HBV	*TERT (11), CTNNB1(4), TP53(9)*	18	22	45,00%

C

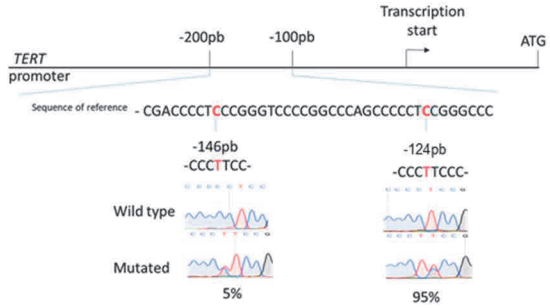

D

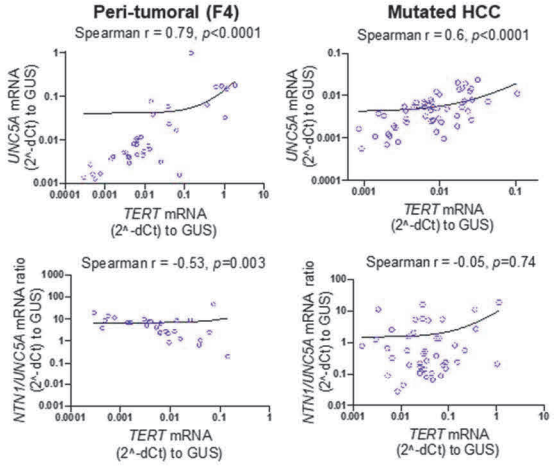

E

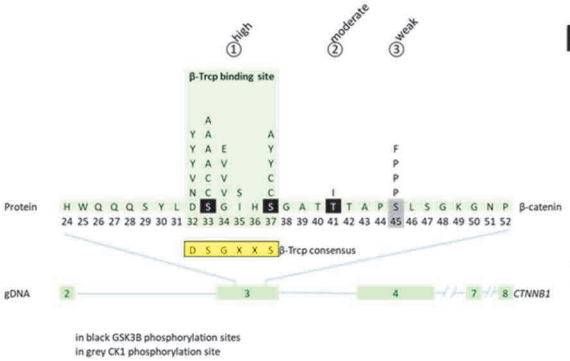

F

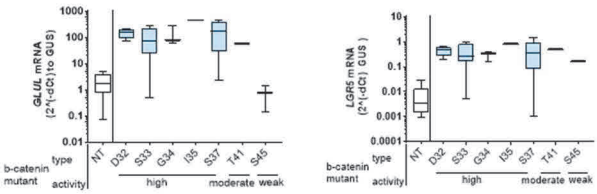

G

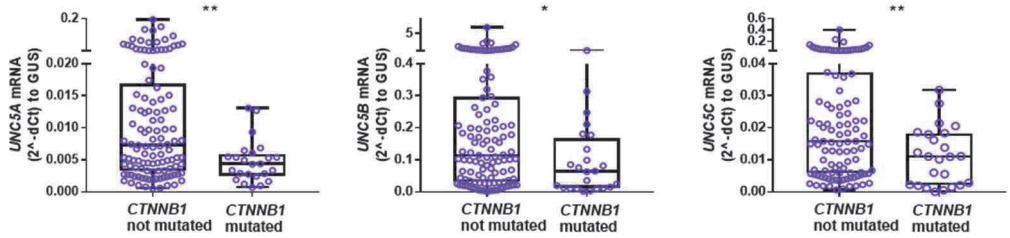

H

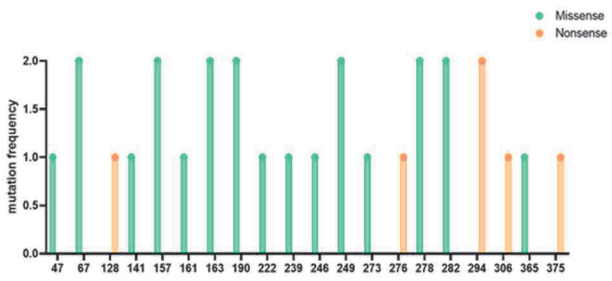

I

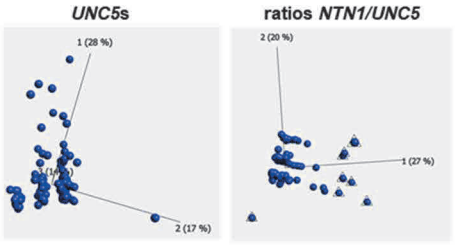

Figure 4. Netrin-1 trapping in DEN-induced HCC in rats showed limited results. **(A)** *NTN1* and *UNC5B* mRNA are upregulated and *UNC5C* is downregulated in DEN-induced HCC in rats. **(B)** Study design of anti-netrin-1 therapy as a single agent comparing to PBS. **(C)**The proliferation was assessed with anti-Ki67 and anti-Cyclin D1 antibodies. The fibrosis was detected with Sirius red staining solution. The apoptosis was analyzed using anti-caspase 3 cleaved antibody. The vascularization was estimated with anti-CD34 antibody. Macroscopical analysis showing no difference in terms of tumor number or median tumor size. Inflammation was analyzed using ELISA kit for CRP.

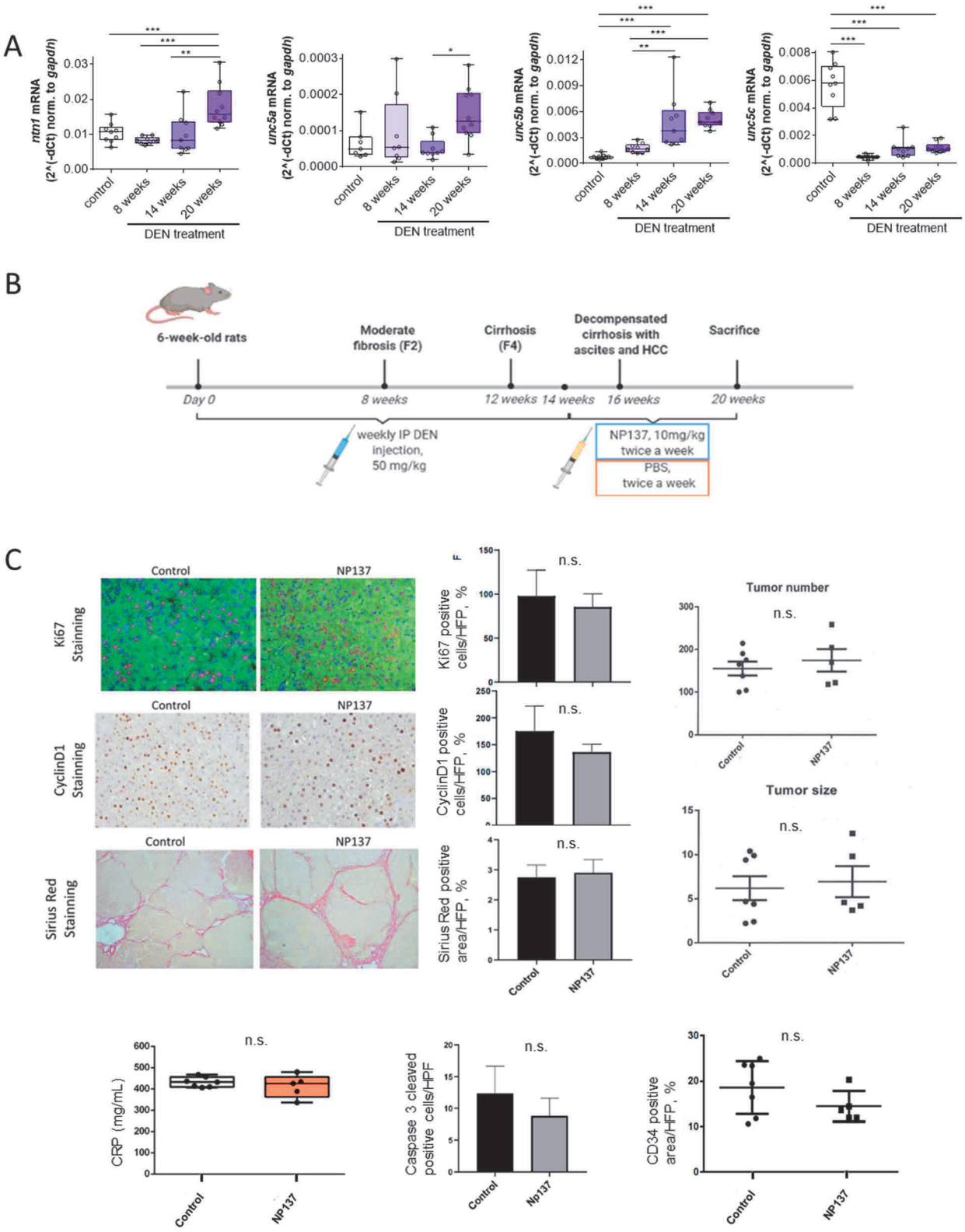
A
ntn1 mRNA (2^(-dCt) norm. to gapdh)
unc5a mRNA (2^(-dCt) norm. to gapdh)
unc5b mRNA (2^(-dCt) norm. to gapdh)
unc5c mRNA (2^(-dCt) norm. to gapdh)
control
8 weeks
14 weeks
20 weeks
DEN treatment
B
6-week-old rats
Moderate fibrosis (F2)
Cirrhosis (F4)
Decompensated cirrhosis with ascites and HCC
Sacrifice
Day 0
8 weeks
12 weeks
14 weeks
16 weeks
20 weeks
weekly IP DEN injection, 50 mg/kg
NP137, 10mg/kg twice a week
PBS, twice a week
C
Control
NP137
Ki67 Stainning
CyclinD1 Stainning
Sirius Red Stainning
Ki67 positive cells/HFP, %
CyclinD1 positive cells/HFP, %
Sirius Red positive area/HFP, %
n.s.
Tumor number
Tumor size
CRP (mg/mL)
Caspase 3 cleaved positive cells/HPF
CD34 positive area/HFP, %
Np137

Table 4. Biological effects of NP137 treatment in DEN-induced HCC in rats compared to PBS.

NP137 vs. PBS	mRNA	Proteins	Final effect	Consequence on HCC
target	*UNC5A, UNC5B, UNC5C, NTN1*↘ Unchanged *NTN1/UNC* ratios	Netrin-1, UNC5B↗	decreased RNA, increased proteins	-
Apoptosis		Cleaved caspase 3 unchanged	unaltered	-
Necroptosis		Cleaved RIP1↗, RIP3↘	impaired	Pro-tumoral
Proliferation		CyclinD1, p-Yap↗, p-ERK ↗	increased	Pro-tumoral
inflammation	IL-6	ALAT, CRP unchanged	unaltered	-
Angiogenesis	*VEGFR2* ↗	CD34 unchanged	pro-angiogenic	Pro-tumoral
Immune cells	*CD4*↗, *PD1/L1, CTLA4, FoxP3* unchanged		unaltered	Pro-tumoral
EMT	*αSMA, CDH1*↘, *Zeb1, Slug* ↗	p-ERK↗	increased	Pro-tumoral
Differentiation	*AFP* ↗, *TGF-β*↘	EpCAM ↗	dedifferentiation	Pro-tumoral

Figure 5. Preliminary results in DEN-treated mice overexpressing netrin-1. **(A)** Offspring's generation outline from male Cre$^+$ and female NTN1$^+$ mice. **(B)** Treatment protocol. All mice were injected with DEN. Mice with Cre$^+$ genotype were then injected with tamoxifen to induce netrin-1 expression. **(C)** Preliminary results. Macroscopic analysis of mouse body weight, tumor number and liver weight. Mann-Whitney U test, * $p < 0.05$, ** $p < 0.01$.

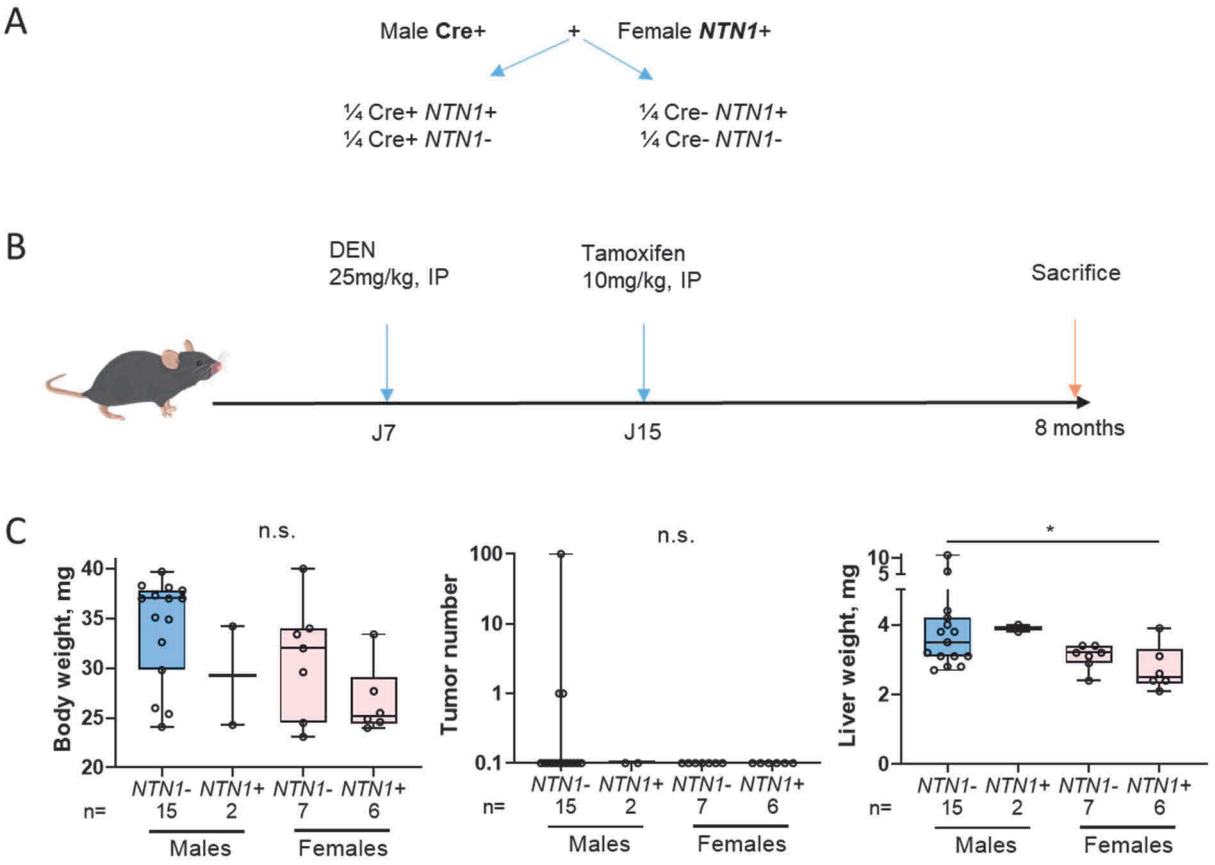

Supplementary table 1. Human and murine qPCR primers.

Gene symbol	Genbank acc. #	Primer sequences (5'-3', F/R)	PCR conditions	Amplicon length, bp
NTN1 (human)	NM_004822.3	CTTCTGCGGCAGGCGGACAGAT ACGCGTTGCAGAGGTGGCACGA	Denaturation, 95°C; annealing, 65°C, 3-step, 10% DMSO	385
UNC5A (human)	NM_170747.4	CATCACCAAGGACACAAGGTTTGC GGCTGGAAATTATCTTCTGCCGAA	Denaturation, 95°C; annealing, 60°C	125
UNC5B (human)	NM_170744.4	GGGCTGGAGGATTACTGG TGCAGGAGAACCTCATGGTC	Denaturation, 95°C; annealing, 60°C	155
UNC5C (human)	NM_003728.3	GCAAATTGCTGGCTAAATATCAGGAA GCTCCACTGTGTTCAGGCTAAATCTT	Denaturation, 95°C; annealing, 60°C	114
GUS (human)	NM_001293105	CGTGGTTGGAGAGCTCATTTGGAA TTCCCCAGCACTCTCGTCGGT	Denaturation, 95°C; annealing, 55°C	72
Ntn1 (rat)	NM_008744.2	CCTGTCACCTCTGCAACTCT TGTGCGGGTTATTGAGGTCG	Denaturation, 95°C; annealing, 55°C	78
Unc5a (rat)	NM_022206.1	GGGCAGAATGTCCAGAAAAC CAGGCTGACCACTTACTCCAC	Denaturation, 95°C; annealing, 60°C	83
Unc5b (rat)	NM_022207.1	GGTCTACTGTCTGGAGGACACTC CCAAGTAGCCACCCAGAGTC	Denaturation, 95°C; annealing, 60°C	77
Unc5c (rat)	NM_199407.1	GAAAATAGCATGCACCACGTT ACCATTTGCTCCACGAAGTC	Denaturation, 95°C; annealing, 60°C	62
Gus (rat)	NM_010368.1	GTGGTATGAACGGGAAGCAAT AACTGCATAATAATGGGCACTGT	Denaturation, 95°C; annealing, 55°C	97

Supplementary table 2. Antibodies.

Antigen	Ig Species	Cat. Number & supplier	Antibody registry (RRID) #
Netrin-1	Rabbit monoclonal	Ab126729, Abcam	AB_11131145
Netrin-1	Mouse monoclonal (humanized)	NP137, Netris Pharma	AB_2811180
UNC5B	Rabbit monoclonal	13851, Cell signaling	D9M7Z
CyclinD1	Rabbit monoclonal	55506T, Cell signaling	D27E11
CD34	Goat monoclonal	AF4117, R&D systems	ND
Ki67	Rabbit monoclonal	MA5-14520, Invitrogen	AB_10979488
PDI (P4HB)	Mouse monoclonal	sc-74551, Santa Cruz	AB_2156462
Caspase-3	Rabbit polyclonal	9662, Cell Signaling	AB_331439
PD1 (P4HB)	Rabbit monoclonal	Ab2792, Abcam	AB_303304
Giantin	Rabbit polyclonal	Ab80864, Abcam	AB_10670397
GM130	Mouse monoclonal	610823, BD Biosciences	AB_398142
CD11b	Rat IgG2b, κ	10705, Stem Cells Technologies	AB_215609
CD68	Rat IgG2a	BLE137029	ND
F4/80	Rat IgG2a, κ	BLE123135	ND
Ly6C	Rat IgG2c, κ	BLE128017	ND
Ly6G	Rat IgGa, κ	25-5932-82, ThermoFischer	AB_2573503
CD38	Rat IgG2a, κ	12-0381-82, ThermoFischer	AB_10128557
Rabbitt isotype control	Rabbit IgG	Ab172730, Abcam	AB_2687931

Human isotype control	Mouse IgG1 (humanized)	NP001, Netris Pharma	ND
Anti-mouse-HRP	Goat polyclonal	A4416, Sigma	AB_258167
Anti-Rabbit-HRP	Goat polyclonal	A6154, Sigma	AB_258284
Anti-mouse 594	Goat monoclonal	A11032, Invitrogen	AB_2534091

References

1. Sung, H. *et al.* Global Cancer Statistics 2020: GLOBOCAN Estimates of Incidence and Mortality Worldwide for 36 Cancers in 185 Countries. *CA: A Cancer Journal for Clinicians* **71**, 209–249 (2021).
2. Heimbach, J. K. *et al.* AASLD guidelines for the treatment of hepatocellular carcinoma. *Hepatology* **67**, 358–380 (2018).
3. Couri, T. & Pillai, A. Goals and targets for personalized therapy for HCC. *Hepatol Int* **13**, 125–137 (2019).
4. Madison, R. D., Zomorodi, A. & Robinson, G. A. Netrin-1 and Peripheral Nerve Regeneration in the Adult Rat. *Experimental Neurology* **161**, 563–570 (2000).
5. Mazelin, L. *et al.* Netrin-1 controls colorectal tumorigenesis by regulating apoptosis. *Nature* **431**, 80–84 (2004).
6. Fitamant, J. *et al.* Netrin-1 expression confers a selective advantage for tumor cell survival in metastatic breast cancer. *Proc Natl Acad Sci U S A* **105**, 4850–4855 (2008).
7. Dumartin, L. *et al.* Netrin-1 mediates early events in pancreatic adenocarcinoma progression, acting on tumor and endothelial cells. *Gastroenterology* **138**, 1595–1606, 1606.e1–8 (2010).
8. Plissonnier, M.-L., Lahlali, T., Mehlen, P. & Parent, R. [Hepatitis C, EGFR, cirrhosis and netrin-1: potential implications for HCC onset]. *Med Sci (Paris)* **32**, 566–568 (2016).
9. Barnault, R. *et al.* Hepatocellular carcinoma-associated depletion of the netrin-1 receptor Uncoordinated Phenotype-5A (UNC5A) skews the hepatic unfolded protein response towards prosurvival outcomes. *Biochem Biophys Res Commun* **495**, 2425–2431 (2018).
10. Paridaens, A. *et al.* Modulation of the Unfolded Protein Response by Tauroursodeoxycholic Acid Counteracts Apoptotic Cell Death and Fibrosis in a Mouse Model for Secondary Biliary Liver Fibrosis. *Int J Mol Sci* **18**, E214 (2017).
11. Heindryckx, F. *et al.* Endoplasmic reticulum stress enhances fibrosis through IRE1α-mediated degradation of miR-150 and XBP-1 splicing. *EMBO Mol Med* **8**, 729–744 (2016).
12. Lahlali, T. *et al.* Netrin-1 Protects Hepatocytes Against Cell Death Through Sustained Translation During the Unfolded Protein Response. *Cellular and Molecular Gastroenterology and Hepatology* **2**, 281-301.e9 (2016).
13. Jilkova, Z. M. *et al.* Combination of AKT inhibitor ARQ 092 and sorafenib potentiates inhibition of tumor progression in cirrhotic rat model of hepatocellular carcinoma. *Oncotarget* **9**, 11145–11158 (2018).
14. Lecluyse, E. L. & Alexandre, E. Isolation and culture of primary hepatocytes from resected human liver tissue. *Methods Mol Biol* **640**, 57–82 (2010).
15. Repetto, G., del Peso, A. & Zurita, J. L. Neutral red uptake assay for the estimation of cell viability/cytotoxicity. *Nat Protoc* **3**, 1125–1131 (2008).
16. Fernandez-Cuesta, L. *et al.* Identification of Circulating Tumor DNA for the Early Detection of Small-cell Lung Cancer. *EBioMedicine* **10**, 117–123 (2016).
17. Perdomo, S. *et al.* Circulating tumor DNA detection in head and neck cancer: evaluation of two different detection approaches. *Oncotarget* **8**, 72621–72632 (2017).

18. Le Calvez-Kelm, F. *et al.* KRAS mutations in blood circulating cell-free DNA: a pancreatic cancer case-control. *Oncotarget* **7**, 78827–78840 (2016).
19. Delhomme, T. M. *et al.* Needlestack: an ultra-sensitive variant caller for multi-sample next generation sequencing data. *NAR Genom Bioinform* **2**, lqaa021 (2020).
20. Plissonnier, M.-L. *et al.* Epidermal Growth Factor Receptor-Dependent Mutual Amplification between Netrin-1 and the Hepatitis C Virus. *PLoS Biol* **14**, e1002421 (2016).
21. Wong, M. *et al.* The changing epidemiology of liver diseases in the Asia–Pacific region. *Nature Reviews Gastroenterology & Hepatology* (2018) doi:10.1038/s41575-018-0055-0.
22. Nault, J. C. *et al.* High frequency of telomerase reverse-transcriptase promoter somatic mutations in hepatocellular carcinoma and preneoplastic lesions. *Nat Commun* **4**, 2218 (2013).
23. Rebouissou, S. *et al.* Genotype-phenotype correlation of CTNNB1 mutations reveals different ß-catenin activity associated with liver tumor progression. *Hepatology* (2016) doi:10.1002/hep.28638.
24. Ng, P. C. & Henikoff, S. Predicting Deleterious Amino Acid Substitutions. *Genome Res.* **11**, 863–874 (2001).
25. Mathe, E. *et al.* Computational approaches for predicting the biological effect of p53 missense mutations: a comparison of three sequence analysis based methods. *Nucleic Acids Research* **34**, 1317–1325 (2006).
26. Kato, S. *et al.* Understanding the function–structure and function–mutation relationships of p53 tumor suppressor protein by high-resolution missense mutation analysis. *PNAS* **100**, 8424–8429 (2003).
27. Chou, T.-C. Drug combination studies and their synergy quantification using the Chou-Talalay method. *Cancer Res* **70**, 440–446 (2010).
28. Roth, G. S. *et al.* Efficacy of AKT Inhibitor ARQ 092 Compared with Sorafenib in a Cirrhotic Rat Model with Hepatocellular Carcinoma. *Mol Cancer Ther* **16**, 2157–2165 (2017).
29. Llovet, J. M. *et al.* Hepatocellular carcinoma. *Nat Rev Dis Primers* **2**, 16018 (2016).
30. Madison, R. D., Zomorodi, A. & Robinson, G. A. Netrin-1 and peripheral nerve regeneration in the adult rat. *Exp Neurol* **161**, 563–570 (2000).
31. Mazelin, L. *et al.* Netrin-1 controls colorectal tumorigenesis by regulating apoptosis. *Nature* **431**, 80–84 (2004).
32. Dumartin, L. *et al.* Netrin-1 mediates early events in pancreatic adenocarcinoma progression, acting on tumor and endothelial cells. *Gastroenterology* **138**, 1595–1606, 1606.e1–8 (2010).
33. Plissonnier, M.-L. *et al.* Reciprocal antagonism between the netrin-1 receptor uncoordinated-phenotype-5A (UNC5A) and the hepatitis C virus. *Oncogene* **36**, 6712–6724 (2017).
34. Macek Jilkova, Z., Kurma, K. & Decaens, T. Animal Models of Hepatocellular Carcinoma: The Role of Immune System and Tumor Microenvironment. *Cancers* **11**, 1487 (2019).
35. Naugler, W. E. *et al.* Gender disparity in liver cancer due to sex differences in MyD88-dependent IL-6 production. *Science* **317**, 121–124 (2007).
36. Arakawa, H. Netrin-1 and its receptors in tumorigenesis. *Nat Rev Cancer* **4**, 978–987 (2004).
37. Miyamoto, Y. *et al.* Identification of UNC5A as a novel transcriptional target of tumor suppressor p53 and a regulator of apoptosis. *Int J Oncol* **36**, 1253–1260 (2010).
38. Tanikawa, C., Matsuda, K., Fukuda, S., Nakamura, Y. & Arakawa, H. p53RDL1 regulates p53-dependent apoptosis. *Nat Cell Biol* **5**, 216–223 (2003).
39. Aziz, A. ur R. *et al.* Doxorubicin-induced toxicity to 3D-cultured rat ovarian follicles on a microfluidic chip. *Toxicology in Vitro* **62**, 104677 (2020).
40. Zhu, Y., Li, Y. & Nakagawara, A. UNC5 dependence receptor family in human cancer: A controllable double-edged sword. *Cancer Lett* **516**, 28–35 (2021).
41. Yuan, X., Larsson, C. & Xu, D. Mechanisms underlying the activation of TERT transcription and telomerase activity in human cancer: old actors and new players. *Oncogene* **38**, 6172–6183 (2019).
42. Bellon, M. & Nicot, C. Regulation of telomerase and telomeres: human tumor viruses take control. *J Natl Cancer Inst* **100**, 98–108 (2008).
43. Huyghe, A. *et al.* Netrin-1 promotes naive pluripotency through Neo1 and Unc5b co-regulation of Wnt and MAPK signalling. *Nat Cell Biol* **22**, 389–400 (2020).

44. Gao, K., Niu, J. & Dang, X. Neuroprotection of netrin-1 on neurological recovery via Wnt/β-catenin signaling pathway after spinal cord injury. *Neuroreport* **31**, 537–543 (2020).
45. Bányai, L. & Patthy, L. The NTR module: domains of netrins, secreted frizzled related proteins, and type I procollagen C-proteinase enhancer protein are homologous with tissue inhibitors of metalloproteases. *Protein Sci* **8**, 1636–1642 (1999).
46. Levy-Strumpf, N., Krizus, M., Zheng, H., Brown, L. & Culotti, J. G. The Wnt Frizzled Receptor MOM-5 Regulates the UNC-5 Netrin Receptor through Small GTPase-Dependent Signaling to Determine the Polarity of Migrating Cells. *PLoS Genet* **11**, e1005446 (2015).

References

1. Malarkey, D. E., Johnson, K., Ryan, L., Boorman, G. & Maronpot, R. R. New insights into functional aspects of liver morphology. *Toxicol Pathol* **33**, 27–34 (2005).
2. Nelsen, C. J. *et al.* Induction of hepatocyte proliferation and liver hyperplasia by the targeted expression of cyclin E and skp2. *Oncogene* **20**, 1825–1831 (2001).
3. Tabibian, J. H., Masyuk, A. I., Masyuk, T. V., O'Hara, S. P. & LaRusso, N. F. Physiology of Cholangiocytes. *Compr Physiol* **3**, 10.1002/cphy.c120019 (2013).
4. Higashi, T., Friedman, S. L. & Hoshida, Y. Hepatic stellate cells as key target in liver fibrosis. *Adv Drug Deliv Rev* **121**, 27–42 (2017).
5. Hosseini, V. *et al.* Current progress in hepatic tissue regeneration by tissue engineering. *Journal of Translational Medicine* **17**, 383 (2019).
6. Lee, J. S. *et al.* Liver extracellular matrix providing dual functions of two-dimensional substrate coating and three-dimensional injectable hydrogel platform for liver tissue engineering. *Biomacromolecules* **15**, 206–218 (2014).
7. Arriazu, E. *et al.* Extracellular Matrix and Liver Disease. *Antioxid Redox Signal* **21**, 1078–1097 (2014).
8. Matsumoto, T. & Kawakami, M. The unit-concept of hepatic parenchyma--a re-examination based on angioarchitectural studies. *Acta Pathol Jpn* **32 Suppl 2**, 285–314 (1982).
9. Laperche, Y. Le cellules ovales et la régénération du foie. **19**, 3 (2003).
10. Jenne, C. N. & Kubes, P. Immune surveillance by the liver. *Nat Immunol* **14**, 996–1006 (2013).
11. Huang, L.-R. *et al.* Intrahepatic myeloid-cell aggregates enable local proliferation of CD8(+) T cells and successful immunotherapy against chronic viral liver infection. *Nat Immunol* **14**, 574–583 (2013).
12. Lautt, W. W. *Hepatic Nerves*. *Hepatic Circulation: Physiology and Pathophysiology* (Morgan & Claypool Life Sciences, 2009).
13. Kandilis, A. N., Papadopoulou, I. P., Koskinas, J., Sotiropoulos, G. & Tiniakos, D. G. Liver innervation and hepatic function: new insights. *Journal of Surgical Research* **194**, 511–519 (2015).
14. Mizuno, K. & Ueno, Y. Autonomic Nervous System and the Liver. *Hepatol Res* **47**, 160–165 (2017).
15. Liu, K. *et al.* Metabolic stress drives sympathetic neuropathy within the liver. *Cell Metab* **33**, 666-675.e4 (2021).
16. Adori, C. *et al.* Disorganization and degeneration of liver sympathetic innervations in nonalcoholic fatty liver disease revealed by 3D imaging. *Sci Adv* **7**, eabg5733 (2021).
17. Jensen, K. J., Alpini, G. & Glaser, S. Hepatic Nervous System and Neurobiology of the Liver. *Compr Physiol* **3**, 655–665 (2013).
18. An, K. *et al.* Integrative Review of Co-Occurring Symptoms Across Etiologies of Chronic Liver Disease and Implications for Symptom Management Research and Practice. *J Nurs Scholarsh* **47**, 310–317 (2015).
19. Shojaie, L., Iorga, A. & Dara, L. Cell Death in Liver Diseases: A Review. *Int J Mol Sci* **21**, E9682 (2020).
20. Guicciardi, M. E., Malhi, H., Mott, J. L. & Gores, G. J. Apoptosis and Necrosis in the Liver. *Compr Physiol* **3**, 10.1002/cphy.c120020 (2013).
21. Schulze-Bergkamen, H., Schuchmann, M., Fleischer, B. & Galle, P. R. The role of apoptosis versus oncotic necrosis in liver injury: Facts or faith? *Journal of Hepatology* **44**, 984–993 (2006).
22. Wang, K. & Lin, B. Pathophysiological Significance of Hepatic Apoptosis. *ISRN Hepatology* **2013**, e740149 (2012).
23. Lee, J.-S. The mutational landscape of hepatocellular carcinoma. *Clin Mol Hepatol* **21**, 220–229 (2015).
24. Elmore, S. Apoptosis: A Review of Programmed Cell Death. *Toxicol Pathol* **35**, 495–516 (2007).
25. Sun, B. & Karin, M. Inflammation and liver tumorigenesis. *Front Med* **7**, 242–254 (2013).
26. Marra, F. & Tacke, F. Roles for chemokines in liver disease. *Gastroenterology* **147**, 577-594.e1 (2014).
27. Koyama, Y. & Brenner, D. A. Liver inflammation and fibrosis. *J Clin Invest* **127**, 55–64.
28. Del Campo, J. A., Gallego, P. & Grande, L. Role of inflammatory response in liver diseases: Therapeutic strategies. *World J Hepatol* **10**, 1–7 (2018).

29. Shiha, G. & Zalata, K. *Ishak versus METAVIR: Terminology, Convertibility and Correlation with Laboratory Changes in Chronic Hepatitis C*. *Liver Biopsy* (IntechOpen, 2011). doi:10.5772/20110.
30. Roehlen, N., Crouchet, E. & Baumert, T. F. Liver Fibrosis: Mechanistic Concepts and Therapeutic Perspectives. *Cells* **9**, 875 (2020).
31. Jung, Y. K. & Yim, H. J. Reversal of liver cirrhosis: current evidence and expectations. *Korean J Intern Med* **32**, 213–228 (2017).
32. Asselah, T. *et al.* Gene expression and hepatitis C virus infection. *Gut* **58**, 846–858 (2009).
33. Bedossa, P. & Poynard, T. An algorithm for the grading of activity in chronic hepatitis C. The METAVIR Cooperative Study Group. *Hepatology* **24**, 289–293 (1996).
34. Goodman, Z. D. Grading and staging systems for inflammation and fibrosis in chronic liver diseases. *Journal of Hepatology* **47**, 598–607 (2007).
35. Alavi, M. *et al.* Time to decompensated cirrhosis and hepatocellular carcinoma after an HBV or HCV notification: A population-based study. *Journal of Hepatology* **65**, 879–887 (2016).
36. D'Amico, G. *et al.* Clinical states of cirrhosis and competing risks. *Journal of Hepatology* **68**, 563–576 (2018).
37. Sung, H. *et al.* Global Cancer Statistics 2020: GLOBOCAN Estimates of Incidence and Mortality Worldwide for 36 Cancers in 185 Countries. *CA: A Cancer Journal for Clinicians* **71**, 209–249 (2021).
38. Macek Jilkova, Z., Kurma, K. & Decaens, T. Animal Models of Hepatocellular Carcinoma: The Role of Immune System and Tumor Microenvironment. *Cancers* **11**, 1487 (2019).
39. Llovet, J. M. *et al.* Hepatocellular carcinoma. *Nat Rev Dis Primers* **7**, 1–28 (2021).
40. February 27, P. date: & 2018. NASH rapidly overtaking hepatitis C as cause of liver cancer. https://www.mdedge.com/hcvhub/article/159549/hepatitis/nash-rapidly-overtaking-hepatitis-c-cause-liver-cancer/page/0/1.
41. Li, H.-M. & Ye, Z.-H. Microenvironment of liver regeneration in liver cancer. *Chin J Integr Med* **23**, 555–560 (2017).
42. Llovet, J. M., Montal, R., Sia, D. & Finn, R. S. Molecular therapies and precision medicine for hepatocellular carcinoma. *Nat Rev Clin Oncol* **15**, 599–616 (2018).
43. Calderaro, J. *et al.* Histological subtypes of hepatocellular carcinoma are related to gene mutations and molecular tumour classification. *Journal of Hepatology* **67**, 727–738 (2017).
44. Wheeler, D. A. & Roberts, L. R. Comprehensive and Integrative Genomic Characterization of Hepatocellular Carcinoma. *Cell* **169**, 1327-1341.e23 (2017).
45. Llovet, J. M. *et al.* Hepatocellular carcinoma. *Nat Rev Dis Primers* **2**, 16018 (2016).
46. Rebouissou, S. & Nault, J.-C. Advances in molecular classification and precision oncology in hepatocellular carcinoma. *Journal of Hepatology* **72**, 215–229 (2020).
47. Diagnostic du Carcinome Hepatocellulaire. *Centre Hépato-Biliaire Paul Brousse* https://www.centre-hepato-biliaire.org/maladies-foie/cancers-foie/carcinome-hepatocellulaire/diagnostic-chc.html (2014).
48. Becker, A. K., Tso, D. K., Harris, A. C., Malfair, D. & Chang, S. D. Extrahepatic Metastases of Hepatocellular Carcinoma: A Spectrum of Imaging Findings. *Canadian Association of Radiologists Journal* **65**, 60–66 (2014).
49. Sneag, D. B. *et al.* Extrahepatic spread of hepatocellular carcinoma: spectrum of imaging findings. *AJR Am J Roentgenol* **197**, W658-664 (2011).
50. Bohlok, A. *et al.* Primary Hepatic Lymphoma Mimicking a Hepatocellular Carcinoma in a Cirrhotic Patient: Case Report and Systematic Review of the Literature. *Case Reports in Surgery* **2018**, e9183717 (2018).
51. Katyal, S. *et al.* Extrahepatic metastases of hepatocellular carcinoma. *Radiology* **216**, 698–703 (2000).
52. Zorbas, K., Koutoulidis, V., Foukas, P. & Arkadopoulos, N. Hepatic tuberculoma mimicking hepatocellular carcinoma in an immunocompetent host. *BMJ Case Rep* **2013**, bcr2013008775 (2013).
53. Erstad, D. J., Razavi, A. A., Li, S., Tanabe, K. K. & Fuchs, B. C. Prevention Strategies for Hepatocellular Carcinoma. in *Hepatocellular Carcinoma: Translational Precision Medicine Approaches* (ed. Hoshida, Y.) (Humana Press, 2019).

54. Ott, J. J., Stevens, G. A., Groeger, J. & Wiersma, S. T. Global epidemiology of hepatitis B virus infection: new estimates of age-specific HBsAg seroprevalence and endemicity. *Vaccine* **30**, 2212–2219 (2012).
55. Buendia, M.-A. & Neuveut, C. Hepatocellular Carcinoma. *Cold Spring Harb Perspect Med* **5**, a021444 (2015).
56. Yang, J. D. *et al.* A global view of hepatocellular carcinoma: trends, risk, prevention and management. *Nat Rev Gastroenterol Hepatol* **16**, 589–604 (2019).
57. Llovet, J. M., Fuster, J. & Bruix, J. Prognosis of hepatocellular carcinoma. *Hepatogastroenterology* **49**, 7–11 (2002).
58. Lee, S. J. & Lim, H. Y. Hepatocellular carcinoma treatment: a comparative review of emerging growth factor receptor antagonists. *Expert Opin Emerg Drugs* **22**, 191–200 (2017).
59. Suh, S.-W. *et al.* Prediction of aggressiveness in early-stage hepatocellular carcinoma for selection of surgical resection. *Journal of Hepatology* **60**, 1219–1224 (2014).
60. Couri, T. & Pillai, A. Goals and targets for personalized therapy for HCC. *Hepatol Int* **13**, 125–137 (2019).
61. Zhao, Y., Zhang, Y.-N., Wang, K.-T. & Chen, L. Lenvatinib for hepatocellular carcinoma: From preclinical mechanisms to anti-cancer therapy. *Biochimica et Biophysica Acta (BBA) - Reviews on Cancer* **1874**, 188391 (2020).
62. Dipasquale, A., Marinello, A. & Santoro, A. A Comparison of Lenvatinib versus Sorafenib in the First-Line Treatment of Unresectable Hepatocellular Carcinoma: Selection Criteria to Guide Physician's Choice in a New Therapeutic Scenario. *J Hepatocell Carcinoma* **8**, 241–251 (2021).
63. Jing, Z. *et al.* Acetylation-induced PCK isoenzyme transition promotes metabolic adaption of liver cancer to systemic therapy. *Cancer Letters* **519**, 46–62 (2021).
64. Castello, A. *et al.* Metabolic Switch in Hepatocellular Carcinoma Patients Treated with Sorafenib: a Proof-of-Concept Trial. *Mol Imaging Biol* **22**, 1446–1454 (2020).
65. Tesori, V. *et al.* The multikinase inhibitor Sorafenib enhances glycolysis and synergizes with glycolysis blockade for cancer cell killing. *Sci Rep* **5**, 9149 (2015).
66. Villanueva, A. Hepatocellular Carcinoma. *N Engl J Med* **380**, 1450–1462 (2019).
67. Zhang, L., Yang, L., Jiang, S. & Yu, M. Nerve Dependence in Colorectal Cancer. *Frontiers in Cell and Developmental Biology* **10**, (2022).
68. Boilly, B., Faulkner, S., Jobling, P. & Hondermarck, H. Nerve Dependence: From Regeneration to Cancer. *Cancer Cell* **31**, 342–354 (2017).
69. Singer, M. The nervous system and regeneration of the forelimb of adult triturus. VII. The relation between number of nerve fibers and surface area of amputation. *Journal of Experimental Zoology* **104**, 251–265 (1947).
70. Clarke, P. G. H. & Clarke, S. Nineteenth century research on naturally occurring cell death and related phenomena. *Anat Embryol* **193**, 81–99 (1996).
71. Rosenberg, A. F., Wolman, M. A., Franzini-Armstrong, C. & Granato, M. In vivo nerve-macrophage interactions following peripheral nerve injury. *J Neurosci* **32**, 3898–3909 (2012).
72. Demir, I. E. *et al.* Investigation of Schwann cells at neoplastic cell sites before the onset of cancer invasion. *J Natl Cancer Inst* **106**, dju184 (2014).
73. Espinosa-Medina, I. *et al.* Parasympathetic ganglia derive from Schwann cell precursors. *Science* (2014) doi:10.1126/science.1253286.
74. Zahalka, A. H. & Frenette, P. S. Nerves in cancer. *Nat Rev Cancer* **20**, 143–157 (2020).
75. Zahalka, A. H. *et al.* Adrenergic nerves activate an angio-metabolic switch in prostate cancer. *Science* **358**, 321–326 (2017).
76. Wang, H. *et al.* Role of the nervous system in cancers: a review. *Cell Death Discov.* **7**, 1–12 (2021).
77. Bapat, A. A., Hostetter, G., Von Hoff, D. D. & Han, H. Perineural invasion and associated pain in pancreatic cancer. *Nat Rev Cancer* **11**, 695–707 (2011).
78. Zhao, C.-M. *et al.* Denervation suppresses gastric tumorigenesis. *Sci Transl Med* **6**, 250ra115 (2014).
79. Xie, G. & Raufman, J.-P. Muscarinic receptor signaling and colon cancer progression. *Journal of Cancer Metastasis and Treatment* **2**, 195–200 (2016).

80. Gasparini, G. *et al.* Nerves and Pancreatic Cancer: New Insights into A Dangerous Relationship. *Cancers (Basel)* **11**, 893 (2019).
81. Magnon, C. *et al.* Autonomic nerve development contributes to prostate cancer progression. *Science* **341**, 1236361 (2013).
82. Friedman, J. R. *et al.* Acetylcholine Signaling System in progression of Lung Cancers. *Pharmacol Ther* **194**, 222–254 (2019).
83. Kamiya, A., Hiyama, T., Fujimura, A. & Yoshikawa, S. Sympathetic and parasympathetic innervation in cancer: therapeutic implications. *Clin Auton Res* **31**, 165–178 (2021).
84. Di Stefano, C., Milazzo, V., Milan, A., Veglio, F. & Maule, S. The role of autonomic dysfunction in cirrhotic patients before and after liver transplantation. Review of the literature. *Liver International* **36**, 1081–1089 (2016).
85. Hendrickse, M. T., Thuluvath, P. J. & Triger, D. R. Natural history of autonomic neuropathy in chronic liver disease. *Lancet* **339**, 1462–1464 (1992).
86. Parent, R., Gidron, Y., Lebossé, F., Decaens, T. & Zoulim, F. The Potential Implication of the Autonomic Nervous System in Hepatocellular Carcinoma. *Cell Mol Gastroenterol Hepatol* **8**, 145–148 (2019).
87. Oben, J. A., Yang, S., Lin, H., Ono, M. & Diehl, A. M. Acetylcholine promotes the proliferation and collagen gene expression of myofibroblastic hepatic stellate cells. *Biochemical and Biophysical Research Communications* **300**, 172–177 (2003).
88. Oben, J. A. *et al.* Hepatic fibrogenesis requires sympathetic neurotransmitters. *Gut* **53**, 438–445 (2004).
89. Huan, H. *et al.* Sympathetic nervous system promotes hepatocarcinogenesis by modulating inflammation through activation of alpha1-adrenergic receptors of Kupffer cells. *Brain, Behavior, and Immunity* **59**, 118–134 (2017).
90. Kimura, K. *et al.* Nicotinic alpha-7 acetylcholine receptor deficiency exacerbates hepatic inflammation and fibrosis in a mouse model of non-alcoholic steatohepatitis. *J Diabetes Investig* **10**, 659–666 (2019).
91. Zhang, L. *et al.* Sympathetic and parasympathetic innervation in hepatocellular carcinoma. *neo* **64**, 840–846 (2017).
92. Renz, B. W. *et al.* Cholinergic Signaling via Muscarinic Receptors Directly and Indirectly Suppresses Pancreatic Tumorigenesis and Cancer Stemness. *Cancer Discov* **8**, 1458–1473 (2018).
93. Dickson, B. J. Molecular Mechanisms of Axon Guidance. *Science* **298**, 1959–1964 (2002).
94. Stoeckli, E. T. Understanding axon guidance: are we nearly there yet? *Development* **145**, dev151415 (2018).
95. Barallobre, M. J., Pascual, M., Del Río, J. A. & Soriano, E. The Netrin family of guidance factors: emphasis on Netrin-1 signalling. *Brain Res Brain Res Rev* **49**, 22–47 (2005).
96. Papic, N. *et al.* The association of semaphorins 3C, 5A and 6D with liver fibrosis stage in chronic hepatitis C. *PLoS One* **13**, e0209481 (2018).
97. Guthrie, S. Axon guidance: starting and stopping with slit. *Curr Biol* **9**, R432-435 (1999).
98. Grunwald, I. C. & Klein, R. Axon guidance: receptor complexes and signaling mechanisms. *Curr Opin Neurobiol* **12**, 250–259 (2002).
99. Seeger, M. A. & Beattie, C. E. Attraction versus repulsion: modular receptors make the difference in axon guidance. *Cell* **97**, 821–824 (1999).
100. Friocourt, F. & Chédotal, A. The Robo3 receptor, a key player in the development, evolution, and function of commissural systems. *Dev Neurobiol* **77**, 876–890 (2017).
101. Dun, X.-P. & Parkinson, D. B. Role of Netrin-1 Signaling in Nerve Regeneration. *Int J Mol Sci* **18**, E491 (2017).
102. Baudet, S., Bécret, J. & Nicol, X. Approaches to Manipulate Ephrin-A:EphA Forward Signaling Pathway. *Pharmaceuticals (Basel)* **13**, 140 (2020).
103. Huot, J. Ephrin signaling in axon guidance. *Prog Neuropsychopharmacol Biol Psychiatry* **28**, 813–818 (2004).
104. Brückner, K. & Klein, R. Signaling by Eph receptors and their ephrin ligands. *Curr Opin Neurobiol* **8**, 375–382 (1998).

105. Seaman, C., Anderson, R., Emery, B. & Cooper, H. M. Localization of the netrin guidance receptor, DCC, in the developing peripheral and enteric nervous systems. *Mechanisms of Development* **103**, 173–175 (2001).
106. de Wit, J. & Verhaagen, J. Role of semaphorins in the adult nervous system. *Progress in Neurobiology* **71**, 249–267 (2003).
107. Dickinson, R. E. & Duncan, W. C. The SLIT-ROBO pathway: a regulator of cell function with implications for the reproductive system. *Reproduction* **139**, 697–704 (2010).
108. Mehlen, P., Delloye-Bourgeois, C. & Chédotal, A. Novel roles for Slits and netrins: axon guidance cues as anticancer targets? *Nat Rev Cancer* **11**, 188–197 (2011).
109. Moon, C. *et al.* Enhanced expression of netrin-1 protein in the sciatic nerves of Lewis rats with experimental autoimmune neuritis: Possible role of the netrin-1/DCC binding pathway in an autoimmune PNS disorder. *Journal of Neuroimmunology* **172**, 66–72 (2006).
110. Merlos-Suárez, A. & Batlle, E. Eph-ephrin signalling in adult tissues and cancer. *Curr Opin Cell Biol* **20**, 194–200 (2008).
111. Martinot, E. & Boerboom, D. Slit/Robo signaling regulates Leydig cell steroidogenesis. *Cell Communication and Signaling* **19**, 8 (2021).
112. Yang, Y. H. C., Manning Fox, J. E., Zhang, K. L., MacDonald, P. E. & Johnson, J. D. Intraislet SLIT-ROBO signaling is required for beta-cell survival and potentiates insulin secretion. *Proceedings of the National Academy of Sciences* **110**, 16480–16485 (2013).
113. Yazdani, U. & Terman, J. R. The semaphorins. *Genome Biol* **7**, 211 (2006).
114. Alto, L. T. & Terman, J. R. Semaphorins and their Signaling Mechanisms. *Methods Mol Biol* **1493**, 1–25 (2017).
115. Blockus, H. & Chédotal, A. Slit-Robo signaling. *Development* **143**, 3037–3044 (2016).
116. Menacho-Márquez, M. *et al.* Chronic sympathoexcitation through loss of Vav3, a Rac1 activator, results in divergent effects on metabolic syndrome and obesity depending on diet. *Cell Metab* **18**, 199–211 (2013).
117. Zeng, Z. *et al.* Slit2-Robo2 signaling modulates the fibrogenic activity and migration of hepatic stellate cells. *Life Sci* **203**, 39–47 (2018).
118. Chang, J. *et al.* Activation of Slit2-Robo1 signaling promotes liver fibrosis. *J Hepatol* **63**, 1413–1420 (2015).
119. Wu, B., Rockel, J. S., Lagares, D. & Kapoor, M. Ephrins and Eph Receptor Signaling in Tissue Repair and Fibrosis. *Curr Rheumatol Rep* **21**, 23 (2019).
120. Rigotti, F. D. A. *et al. Semaphorin 3C exacerbates liver fibrosis*. 2021.07.29.454292 https://www.biorxiv.org/content/10.1101/2021.07.29.454292v1 (2021) doi:10.1101/2021.07.29.454292.
121. De Minicis, S. *et al.* Semaphorin 7A contributes to TGF-β-mediated liver fibrogenesis. *Am J Pathol* **183**, 820–830 (2013).
122. Yagai, T., Miyajima, A. & Tanaka, M. Semaphorin 3E Secreted by Damaged Hepatocytes Regulates the Sinusoidal Regeneration and Liver Fibrosis during Liver Regeneration. *The American Journal of Pathology* **184**, 2250–2259 (2014).
123. Sun, H. *et al.* Netrin-1 Regulates Fibrocyte Accumulation in the Decellularized Fibrotic Sclerodermatous Lung Microenvironment and in Bleomycin-Induced Pulmonary Fibrosis. *Arthritis Rheumatol* **68**, 1251–1261 (2016).
124. Schlegel, M. *et al.* The neuroimmune guidance cue netrin-1 controls resolution programs and promotes liver regeneration. *Hepatology* **63**, 1689–1705 (2016).
125. Lopez, D. *et al.* The neuronal guidance cue and survival factor, Netrin-1, in liver fibrogenesis. *Z Gastroenterol* **47**, P1_30 (2009).
126. Plissonnier, M.-L. *et al.* Epidermal Growth Factor Receptor-Dependent Mutual Amplification between Netrin-1 and the Hepatitis C Virus. *PLoS Biol* **14**, e1002421 (2016).
127. Plissonnier, M.-L. *et al.* Reciprocal antagonism between the netrin-1 receptor uncoordinated-phenotype-5A (UNC5A) and the hepatitis C virus. *Oncogene* **36**, 6712–6724 (2017).
128. Guo, X. *et al.* Macrophage-derived netrin-1 is critical for neuroangiogenesis in endometriosis. *International Journal of Biological Macromolecules* **148**, 226–237 (2020).

129. Klagsbrun, M. & Shimizu, A. Semaphorin 3E, an exception to the rule. *J Clin Invest* **120**, 2658–2660 (2010).
130. Li, X. *et al.* Novel role of semaphorin 3A in the growth and progression of hepatocellular carcinoma. *Oncology Reports* **37**, 3313–3320 (2017).
131. Worzfeld, T. & Offermanns, S. Semaphorins and plexins as therapeutic targets. *Nat Rev Drug Discov* **13**, 603–621 (2014).
132. Ito, H. *et al.* Identification of ROBO1 as a Novel Hepatocellular Carcinoma Antigen and a Potential Therapeutic and Diagnostic Target. *Clin Cancer Res* **12**, 3257–3264 (2006).
133. Ao, J.-Y. *et al.* Robo1 promotes angiogenesis in hepatocellular carcinoma through the Rho family of guanosine triphosphatases' signaling pathway. *Tumor Biol.* **36**, 8413–8424 (2015).
134. Cui, X.-D. *et al.* EFNA1 ligand and its receptor EphA2: potential biomarkers for hepatocellular carcinoma. *International Journal of Cancer* **126**, 940–949 (2010).
135. Fan, M. *et al.* Increased expression of EphA2 and E-N cadherin switch in primary hepatocellular carcinoma. *Tumori* **99**, 689–696 (2013).
136. Wang, Y. *et al.* EphA1 activation promotes the homing of endothelial progenitor cells to hepatocellular carcinoma for tumor neovascularization through the SDF-1/CXCR4 signaling pathway. *J Exp Clin Cancer Res* **35**, 65 (2016).
137. Ieguchi, K. & Maru, Y. Roles of EphA1/A2 and ephrin-A1 in cancer. *Cancer Sci* **110**, 841–848 (2019).
138. Kumagai, K. *et al.* Nerve Regeneration in the Central Nervous System by a Semaphorin Inhibitor. 8 (2005).
139. Evans, E. E. *et al.* Antibody Blockade of Semaphorin 4D Promotes Immune Infiltration into Tumor and Enhances Response to Other Immunomodulatory Therapies. *Cancer Immunol Res* **3**, 689–701 (2015).
140. Wetzel, S., Seipold, L. & Saftig, P. The metalloproteinase ADAM10: A useful therapeutic target? *Biochimica et Biophysica Acta (BBA) - Molecular Cell Research* **1864**, 2071–2081 (2017).
141. Müller, M. *et al.* A disintegrin and metalloprotease 10 (ADAM10) is a central regulator of murine liver tissue homeostasis. *Oncotarget* **7**, 17431–17441 (2016).
142. Wu, W., Lei, H., Shen, J. & Tang, L. The role of netrin-1 in angiogenesis and diabetic retinopathy: a promising therapeutic strategy. *Discov Med* **23**, 315–323 (2017).
143. Rajasekharan, S. & Kennedy, T. E. The netrin protein family. *Genome Biol* **10**, 239 (2009).
144. Xu, K. *et al.* Neural migration. Structures of netrin-1 bound to two receptors provide insight into its axon guidance mechanism. *Science* **344**, 1275–1279 (2014).
145. Larrieu-Lahargue, F., Thomas, K. R. & Li, D. Y. Netrin ligands and receptors: lessons from neurons to the endothelium. *Trends Cardiovasc Med* **22**, 44–47 (2012).
146. Kennedy, T. E., Serafini, T., Torre, J. de la & Tessier-Lavigne, M. Netrins are diffusible chemotropic factors for commissural axons in the embryonic spinal cord. *Cell* **78**, 425–435 (1994).
147. Paradisi, A. *et al.* NF-kappaB regulates netrin-1 expression and affects the conditional tumor suppressive activity of the netrin-1 receptors. *Gastroenterology* **135**, 1248–1257 (2008).
148. Delloye-Bourgeois, C. *et al.* Nucleolar localization of a netrin-1 isoform enhances tumor cell proliferation. *Sci Signal* **5**, ra57 (2012).
149. Mehlen, P. & Thibert, C. Dependence receptors: between life and death. *Cell. Mol. Life Sci.* **61**, 1854–1866 (2004).
150. Zhu, Y., Li, Y. & Nakagawara, A. UNC5 dependence receptor family in human cancer: A controllable double-edged sword. *Cancer Lett* **516**, 28–35 (2021).
151. Cirulli, V. & Yebra, M. Netrins: beyond the brain. *Nat Rev Mol Cell Biol* **8**, 296–306 (2007).
152. Ko, S. Y., Dass, C. R. & Nurgali, K. Netrin-1 in the developing enteric nervous system and colorectal cancer. *Trends in Molecular Medicine* **18**, 544–554 (2012).
153. Nasarre, P., Potiron, V., Drabkin, H. & Roche, J. Guidance molecules in lung cancer. *Cell Adh Migr* **4**, 130–145 (2010).
154. Ly, N. P. *et al.* Netrin-1 inhibits leukocyte migration in vitro and in vivo. *Proc Natl Acad Sci U S A* **102**, 14729–14734 (2005).
155. Meyerhardt, J. A. *et al.* Netrin-1: interaction with deleted in colorectal cancer (DCC) and alterations in brain tumors and neuroblastomas. *Cell Growth Differ* **10**, 35–42 (1999).

156. Mehlen, P. & Guenebeaud, C. Netrin-1 and its dependence receptors as original targets for cancer therapy. *Current Opinion in Oncology* **22**, 46–54 (2010).
157. Gibert, B. & Mehlen, P. Dependence Receptors and Cancer: Addiction to Trophic Ligands. *Cancer Res* **75**, 5171–5175 (2015).
158. Negulescu, A.-M. & Mehlen, P. Dependence receptors – the dark side awakens. *The FEBS Journal* **285**, 3909–3924 (2018).
159. Padua, M. B. *et al.* Dependence receptor UNC5A restricts luminal to basal breast cancer plasticity and metastasis. *Breast Cancer Res* **20**, 35 (2018).
160. Fitamant, J. *et al.* Netrin-1 expression confers a selective advantage for tumor cell survival in metastatic breast cancer. *Proc Natl Acad Sci U S A* **105**, 4850–4855 (2008).
161. Mazelin, L. *et al.* Netrin-1 controls colorectal tumorigenesis by regulating apoptosis. *Nature* **431**, 80–84 (2004).
162. Thiebault, K. *et al.* The netrin-1 receptors UNC5H are putative tumor suppressors controlling cell death commitment. *Proc Natl Acad Sci U S A* **100**, 4173–4178 (2003).
163. Asakura, T., Ogura, K. & Goshima, Y. IRE-1/XBP-1 pathway of the unfolded protein response is required for properly localizing neuronal UNC-6/Netrin for axon guidance in C. elegans. *Genes Cells* **20**, 153–159 (2015).
164. Lahlali, T. *et al.* Netrin-1 Protects Hepatocytes Against Cell Death Through Sustained Translation During the Unfolded Protein Response. *Cellular and Molecular Gastroenterology and Hepatology* **2**, 281-301.e9 (2016).
165. Barnault, R. *et al.* Hepatocellular carcinoma-associated depletion of the netrin-1 receptor Uncoordinated Phenotype-5A (UNC5A) skews the hepatic unfolded protein response towards prosurvival outcomes. *Biochem Biophys Res Commun* **495**, 2425–2431 (2018).
166. Hibi, K. *et al.* Methylation of the UNC5C gene is frequently detected in hepatocellular carcinoma. *Hepatogastroenterology* **59**, 2573–2575 (2012).
167. Bernet, A. *et al.* Inactivation of the UNC5C netrin-1 receptor is associated with tumor progression in colorectal malignancies. *Gastroenterology* **133**, 1840–1848 (2007).
168. A, P. *et al.* Combining chemotherapeutic agents and netrin-1 interference potentiates cancer cell death. *EMBO molecular medicine* **5**, (2013).
169. Miyamoto, Y. *et al.* Identification of UNC5A as a novel transcriptional target of tumor suppressor p53 and a regulator of apoptosis. *Int J Oncol* **36**, 1253–1260 (2010).
170. Tanikawa, C., Matsuda, K., Fukuda, S., Nakamura, Y. & Arakawa, H. p53RDL1 regulates p53-dependent apoptosis. *Nat Cell Biol* **5**, 216–223 (2003).
171. Arakawa, H. Netrin-1 and its receptors in tumorigenesis. *Nat Rev Cancer* **4**, 978–987 (2004).
172. Arakawa, H. p53, apoptosis and axon-guidance molecules. *Cell Death Differ* **12**, 1057–1065 (2005).
173. Schiffer, E. *et al.* Gefitinib, an EGFR inhibitor, prevents hepatocellular carcinoma development in the rat liver with cirrhosis. *Hepatology* **41**, 307–314 (2005).
174. Roth, G. S. *et al.* Efficacy of AKT Inhibitor ARQ 092 Compared with Sorafenib in a Cirrhotic Rat Model with Hepatocellular Carcinoma. *Mol Cancer Ther* **16**, 2157–2165 (2017).
175. Grandin, M. *et al.* Structural Decoding of the Netrin-1/UNC5 Interaction and its Therapeutical Implications in Cancers. *Cancer Cell* **29**, 173–185 (2016).
176. Naugler, W. E. *et al.* Gender disparity in liver cancer due to sex differences in MyD88-dependent IL-6 production. *Science* **317**, 121–124 (2007).
177. Rongvaux, A. *et al.* Human Hemato-Lymphoid System Mice: Current Use and Future Potential for Medicine. *Annu Rev Immunol* **31**, 635–674 (2013).
178. He, G. & Karin, M. NF-κB and STAT3 – key players in liver inflammation and cancer. *Cell Res* **21**, 159–168 (2011).
179. Gao, R. *et al.* Macrophage-derived netrin-1 drives adrenergic nerve–associated lung fibrosis. *J Clin Invest* **131**, e136542.
180. van Gils, J. M. *et al.* The neuroimmune guidance cue netrin-1 promotes atherosclerosis by inhibiting the emigration of macrophages from plaques. *Nat Immunol* **13**, 136–143 (2012).
181. Kappler, J. *et al.* Glycosaminoglycan-binding properties and secondary structure of the C-terminus of netrin-1. *Biochem Biophys Res Commun* **271**, 287–291 (2000).

182. Dong, X., Liu, J., Xu, Y. & Cao, H. Role of macrophages in experimental liver injury and repair in mice. *Exp Ther Med* **17**, 3835–3847 (2019).
183. Paradisi, A. *et al.* Netrin-1 up-regulation in inflammatory bowel diseases is required for colorectal cancer progression. *Proc Natl Acad Sci U S A* **106**, 17146–17151 (2009).
184. Coissieux, M.-M. *et al.* Variants in the Netrin-1 Receptor UNC5C Prevent Apoptosis and Increase Risk for Familial Colorectal Cancer. *Gastroenterology* **141**, 2039–2046 (2011).
185. Wong, M. *et al.* The changing epidemiology of liver diseases in the Asia–Pacific region. *Nature Reviews Gastroenterology & Hepatology* (2018) doi:10.1038/s41575-018-0055-0.
186. Zucman-Rossi, J., Villanueva, A., Nault, J.-C. & Llovet, J. M. Genetic Landscape and Biomarkers of Hepatocellular Carcinoma. *Gastroenterology* **149**, 1226-1239.e4 (2015).
187. Aziz, A. ur R. *et al.* Doxorubicin-induced toxicity to 3D-cultured rat ovarian follicles on a microfluidic chip. *Toxicology in Vitro* **62**, 104677 (2020).
188. Nault, J. C. *et al.* High frequency of telomerase reverse-transcriptase promoter somatic mutations in hepatocellular carcinoma and preneoplastic lesions. *Nat Commun* **4**, 2218 (2013).
189. Rebouissou, S. *et al.* Genotype-phenotype correlation of CTNNB1 mutations reveals different ß-catenin activity associated with liver tumor progression. *Hepatology* (2016) doi:10.1002/hep.28638.
190. Huyghe, A. *et al.* Netrin-1 promotes naive pluripotency through Neo1 and Unc5b co-regulation of Wnt and MAPK signalling. *Nat Cell Biol* **22**, 389–400 (2020).
191. Gao, K., Niu, J. & Dang, X. Neuroprotection of netrin-1 on neurological recovery via Wnt/β-catenin signaling pathway after spinal cord injury. *Neuroreport* **31**, 537–543 (2020).
192. Ng, P. C. & Henikoff, S. Predicting Deleterious Amino Acid Substitutions. *Genome Res.* **11**, 863–874 (2001).
193. Mathe, E. *et al.* Computational approaches for predicting the biological effect of p53 missense mutations: a comparison of three sequence analysis based methods. *Nucleic Acids Research* **34**, 1317–1325 (2006).
194. Kato, S. *et al.* Understanding the function–structure and function–mutation relationships of p53 tumor suppressor protein by high-resolution missense mutation analysis. *PNAS* **100**, 8424–8429 (2003).
195. Giacomelli, A. O. *et al.* Mutational processes shape the landscape of TP53 mutations in human cancer. *Nat Genet* **50**, 1381–1387 (2018).
196. Chou, T.-C. Drug combination studies and their synergy quantification using the Chou-Talalay method. *Cancer Res* **70**, 440–446 (2010).
197. Schulze, K. *et al.* Exome sequencing of hepatocellular carcinomas identifies new mutational signatures and potential therapeutic targets. *Nat Genet* **47**, 505–511 (2015).
198. Borovikova, L. V. *et al.* Vagus nerve stimulation attenuates the systemic inflammatory response to endotoxin. *Nature* **405**, 458–462 (2000).
199. Bonaz, B., Sinniger, V. & Pellissier, S. Vagus Nerve Stimulation at the Interface of Brain-Gut Interactions. *Cold Spring Harb Perspect Med* **9**, a034199 (2019).
200. Bonaz, B. L. & Bernstein, C. N. Brain-gut interactions in inflammatory bowel disease. *Gastroenterology* **144**, 36–49 (2013).
201. Ringelhan, M., Pfister, D., O'Connor, T., Pikarsky, E. & Heikenwalder, M. The immunology of hepatocellular carcinoma. *Nat Immunol* **19**, 222–232 (2018).
202. Khemlina, G., Ikeda, S. & Kurzrock, R. The biology of Hepatocellular carcinoma: implications for genomic and immune therapies. *Mol Cancer* **16**, 149 (2017).
203. Yuan, X., Larsson, C. & Xu, D. Mechanisms underlying the activation of TERT transcription and telomerase activity in human cancer: old actors and new players. *Oncogene* **38**, 6172–6183 (2019).
204. Bellon, M. & Nicot, C. Regulation of telomerase and telomeres: human tumor viruses take control. *J Natl Cancer Inst* **100**, 98–108 (2008).
205. Bányai, L. & Patthy, L. The NTR module: domains of netrins, secreted frizzled related proteins, and type I procollagen C-proteinase enhancer protein are homologous with tissue inhibitors of metalloproteases. *Protein Sci* **8**, 1636–1642 (1999).

206. Levy-Strumpf, N., Krizus, M., Zheng, H., Brown, L. & Culotti, J. G. The Wnt Frizzled Receptor MOM-5 Regulates the UNC-5 Netrin Receptor through Small GTPase-Dependent Signaling to Determine the Polarity of Migrating Cells. *PLoS Genet* **11**, e1005446 (2015).
207. Rabben, H.-L., Zhao, C.-M., Hayakawa, Y., Wang, T. C. & Chen, D. Vagotomy and Gastric Tumorigenesis. *Curr Neuropharmacol* **14**, 967–972 (2016).
208. Ohtake, M., Sakaguchi, T., Yoshida, K. & Muto, T. Hepatic branch vagotomy can suppress liver regeneration in partially hepatectomized rats. *HPB Surg* **6**, 277–286 (1993).
209. Zhang, Y. *et al.* Hepatic Branch Vagotomy Modulates the Gut-Liver-Brain Axis in Murine Cirrhosis. *Front Physiol* **12**, 702646 (2021).
210. Eskandari, F., Webster, J. I. & Sternberg, E. M. Neural immune pathways and their connection to inflammatory diseases. *Arthritis Res Ther* **5**, 251–265 (2003).
211. Metz, C. N. & Pavlov, V. A. Vagus nerve cholinergic circuitry to the liver and the gastrointestinal tract in the neuroimmune communicatome. *Am J Physiol Gastrointest Liver Physiol* **315**, G651–G658 (2018).
212. Muñoz-Ortega, M. *et al.* Modulation of amoebic hepatic abscess by the parasympathetic system: Amoebiasis and parasympathetic system. *Parasite Immunology* **33**, 65–72 (2011).
213. Varghese S, J. *et al.* Does autonomic dysfunction in cirrhosis liver influence variceal bleed? *Annals of Hepatology* **6**, 104–107 (2007).
214. Dubuisson, L. *et al.* Inhibition of rat liver fibrogenesis through noradrenergic antagonism. *Hepatology* **35**, 325–331 (2002).
215. Madison, R. D., Zomorodi, A. & Robinson, G. A. Netrin-1 and peripheral nerve regeneration in the adult rat. *Exp Neurol* **161**, 563–570 (2000).
216. Mazelin, L. *et al.* Netrin-1 controls colorectal tumorigenesis by regulating apoptosis. *Nature* **431**, 80–84 (2004).
217. Dumartin, L. *et al.* Netrin-1 mediates early events in pancreatic adenocarcinoma progression, acting on tumor and endothelial cells. *Gastroenterology* **138**, 1595–1606, 1606.e1–8 (2010).
218. Simón Serrano, S. *et al.* Evaluation of NV556, a Novel Cyclophilin Inhibitor, as a Potential Antifibrotic Compound for Liver Fibrosis. *Cells* **8**, 1409 (2019).
219. Carmeliet, P. & Tessier-Lavigne, M. Common mechanisms of nerve and blood vessel wiring. *Nature* **436**, 193–200 (2005).
220. Wilson, B. D. *et al.* Netrins Promote Developmental and Therapeutic Angiogenesis. *Science* **313**, 640–644 (2006).
221. Lu, X. *et al.* The netrin receptor UNC5B mediates guidance events controlling morphogenesis of the vascular system. *Nature* **432**, 179–186 (2004).
222. Larrivée, B. *et al.* Activation of the UNC5B receptor by Netrin-1 inhibits sprouting angiogenesis. *Genes Dev.* **21**, 2433–2447 (2007).
223. Fleming, S. Drug Prices And Innovation. *Forbes* https://www.forbes.com/sites/stanfleming/2019/06/20/the-relationship-between-drug-prices-and-innovation/.
224. EASL Clinical Practice Guidelines: Liver transplantation. *Journal of Hepatology* **64**, 433–485 (2016).
225. Colle, I., Van Vlierberghe, H., Troisi, R. & De Hemptinne, B. Transplanted liver: consequences of denervation for liver functions. *Anat Rec A Discov Mol Cell Evol Biol* **280**, 924–931 (2004).
226. Wheatley, A. M. *et al.* Effect of orthotopic liver transplantation and chemical denervation of the liver on the activities of hepatic monoamine oxidase and catechol-O-methyltransferase. *Transplantation* **56**, 202–207 (1993).
227. Dhillon, A. P. *et al.* Immunohistochemical studies on the innervation of human transplanted liver. *J Pathol* **167**, 211–216 (1992).
228. Filgueira, N. A. Hepatocellular carcinoma recurrence after liver transplantation: Risk factors, screening and clinical presentation. *World J Hepatol* **11**, 261–272 (2019).

Cancer Cell

Neural features of hepatocellular carcinoma define targetable neuroclasses with distinct pathogenic and prognostic statuses

--Manuscript Draft--

Manuscript Number:	
Full Title:	Neural features of hepatocellular carcinoma define targetable neuroclasses with distinct pathogenic and prognostic statuses
Article Type:	Research Article
Keywords:	Hepatocellular carcinoma; autonomic nervous system; adrenergic; cholinergic; neuroclass; classification; bioinformatics
Corresponding Author:	Romain Parent Lyon, FRANCE
First Author:	Charlotte Hernandez
Order of Authors:	Charlotte Hernandez
	Claire Verzeroli
	Ievgeniia Chicherova
	Abud-Jose Farca-Luna
	Laurie Tonon
	Pascale Bellaud
	Bruno Turlin
	Alain Fautrel
	Zuzana Macek-Jilkova
	Thomas Decaens
	Sandra Rebouissou
	Alain Viari
	Fabien Zoulim
	Romain Parent
Abstract:	The unexplained interpatient variation of hepatocellular carcinoma (HCC) onset and clinical outcome remains a major challenge for clinicians. Here, we focused on the under-explored association between the disease and the hepatic autonomic nervous system (ANS), which links the central nervous system (CNS) to the liver. We characterized the innervation of HCC samples in tumor capsules, fibrotic areas, and in tumor bulk and highlight the predominant parasympathetic polarity of these nerves. We also demonstrated that a cirrhotic rat model of HCC hosts liver neurogenesis with cholinergic features synchronous to cancer onset. Using the TCGA HCC dataset (n = 193), we then defined an HCC neural signature, derived from adrenergic and cholinergic receptor levels, that allowed patient stratification into two groups of neuroclasses. On the one hand, cholinergic tumors, correlated with TP53 mutations (p 0.05), shorter progression-free interval (PFI) and overall survival (OS), displayed more pathogenic molecular traits (e.g. , AFP-rich, proliferative tumors, higher mitotic functions including DNA repair, EMT, Ras, and Akt/mTOR pathways), aggressive HCC signatures and B cell accumulation. On the other hand, adrenergic tumors, predominant in patients aged >60 and with mutated CTNNB1 , were correlated with better OS and PFI (p < 0.05), and numerous immune pathways. Hence, our results enrich existing patient classification. Altogether, we show that the parasympathetic branch of the ANS is implicated in the pathobiology of HCC, and advocate for the use of ANS-targeting drugs in HCC studies, many of which are clinically safe and well characterized.

Suggested Reviewers:	Michelle Monje Stanford University mmonje@stanford.edu Expertise in cancer neuroscience
	Josep M Llovet Universitat de Barcelona jmllovet@clinic.cat Expertise in liver cancer
Opposed Reviewers:	
Additional Information:	
Question	**Response**
Original Code Does this manuscript report original code?	No
Standardized datasets A list of datatypes considered standardized under Cell Press policy is available here. Does this manuscript report new standardized datasets?	No

Neural features of hepatocellular carcinoma define targetable neuroclasses with distinct pathogenic and prognostic statuses

Charlotte Hernandez[+1], Claire Verzeroli[+1], Ievgeniia Chicherova[1], Abud-José Farca-Luna[2], Laurie Tonon[2], Pascale Bellaud[3], Bruno Turlin[3], Alain Fautrel[3], Zuzana Macek-Jilkova[4,5], Thomas Decaens[4,5], Sandra Rebouissou[6], Alain Viari[2], Fabien Zoulim[1,7], Romain Parent*[1]

[1] Pathogenesis of Chronic Hepatitis B and C laboratory - LabEx DEVweCAN, Inserm U1052, Cancer Research Centre of Lyon, F-69003 Lyon, France, University of Lyon, F-69003 Lyon, University of Lyon 1, ISPB, Lyon, F-69622, France, CNRS UMR5286, F-69083 Lyon, France, Centre Léon Bérard, F-69008 Lyon, France

[2] Fondation Synergie Lyon Cancer, Plateforme de bioinformatique Gilles Thomas, Centre Léon Bérard, F-69008 Lyon, France

[3] H2P2 platform, University of Rennes, Rennes, France

[4] Institute for Advanced Biosciences, Inserm U1209, University of Grenoble-Alpes, F-38700 La Tronche, France

[5] Service d'hépato-Gastroentérologie, Pôle Digidune, CHU Grenoble-Alpes, 38700 La Tronche, France

[6] Centre de Recherche des Cordeliers, Inserm, Sorbonne Université, USPC, Université Paris Descartes, Université Paris Diderot, Paris, France

[7] Hospices Civils de Lyon, Service of Hepato-Gastroenterology, F-69001 Lyon, France

[+] Equal contributions

Abstract

The unexplained interpatient variation of hepatocellular carcinoma (HCC) onset and clinical outcome remains a major challenge for clinicians. Here, we focused on the under-explored association between the disease and the hepatic autonomic nervous system (ANS), which links the central nervous system (CNS) to the liver. We characterized the innervation of HCC samples in tumor capsules, fibrotic areas, and in tumor bulk and highlight the predominant parasympathetic polarity of these nerves. We also demonstrated that a cirrhotic rat model of HCC hosts liver neurogenesis with cholinergic features synchronous to cancer onset. Using the TCGA HCC dataset (n = 193), we then defined an HCC neural signature, derived from adrenergic and cholinergic receptor levels, that allowed patient stratification into two groups of neuroclasses. On the one hand, cholinergic tumors, correlated with *TP53* mutations ($p \leq 0.05$), shorter progression-free interval (PFI) and overall survival (OS), displayed more pathogenic molecular traits (*e.g.*, AFP-rich, proliferative tumors, higher mitotic functions including DNA repair, EMT, Ras, and Akt/mTOR pathways), aggressive HCC signatures and B cell accumulation. On the other hand, adrenergic tumors, predominant in patients aged >60 and with mutated *CTNNB1*, were correlated with better OS and PFI ($p < 0.05$), and numerous immune pathways. Hence, our results enrich existing patient classification. Altogether, we show that the parasympathetic branch of the ANS is implicated in the pathobiology of HCC, and advocate for the use of ANS-targeting drugs in HCC studies, many of which are clinically safe and well characterized.

Introduction

Primary liver cancer casualties are ranked 3rd worldwide (Sung et al., 2021) and are still on the rise despite the recent advent of adequate hepatitis B and C (HBV and HCV) therapies. Genetic diseases of the liver and hepatic comorbidities, such as alcoholic liver disease (ALD) and metabolic syndrome with non-alcoholic steato-hepatitis (NASH), are long-term cooperators or independent factors fostering the onset of HCC and enhancing disease heterogeneity. Though HCC is known to develop in 90% of cases of cirrhosis (Llovet et al., 2021), its onset and clinical outcome, in terms of phenotypes and speed of progression, are highly variable from one patient to another. Despite the identification of several potential therapeutic targets, most drugs have failed to exceed the efficacy of currently available compounds. Treatments with tyrosine kinase inhibitors (TKIs) for instance lead to short-term, unavoidable relapse (Llovet et al., 2018), whereas treatment with immune check-points inhibitors, such as atezolizumab, or growth factors inhibitors, such as bevacizumab, currently provide some hope for only a minority of patients with unresectable HCC (Llovet et al., 2021).

Hepatologists and researchers are thus seeking alternative/novel targetable HCC players, by shedding light on unexplored features of the disease. In this respect, cellular/tissular structures linking the general pathophysiology of the patient with HCC may be of interest, as they are patient-specific and may uncover novel ways of defining stratification criteria. In line with such notions, several recent original papers (Thaker et al., 2006) (Magnon et al., 2013) (Hayakawa et al., 2017) (Renz et al., 2018a; Renz et al., 2018b) and related commentaries (Monje et al., 2020; Venkatesh and Monje, 2017) highlighted the relevance of studying cancer neurosciences of peripheral organs. In that context, pathological innervation and ANS involvement or dysregulation have been identified in ovarian (Thaker et al., 2006), prostate (Magnon et al., 2013), gastric (Hayakawa et al., 2017) and pancreatic (Renz et al., 2018a; Renz et al., 2018b) cancers, nurturing tumor stroma and conferring stronger carcinogenic properties. Moreover, ANS post-synaptic receptors have been shown to be favorably actionable in some experimental conditions in cancer (Magnon et al., 2013; Renz et al., 2018a; Renz et al., 2018b).

The autonomic nervous system (ANS) comprises the sympathetic (adrenergic signaling) and parasympathetic (cholinergic signaling) arms that relay signals both ways along the brain-liver neural axis in order to regulate involuntary functions of the body by adjusting its internal functions, after an external stimulus. The liver is an innervated organ that hosts autonomic afferent and efferent ANS nerves, in constant communication with the central nervous system (CNS) through the brainstem (Jensen et al., 2013). Afferent and efferent nerves are made of adrenergic (relies on epinephrine or norepinephrine as its

91 neurotransmitter, stress signal) and cholinergic (relies on acetylcholine as its neurotransmitter)
92 fibers that each convey signals to regulate liver functions in real-time.
93 As a consequence, these signals also regulate several processes that may directly or
94 indirectly impact HCC onset and growth. However, data on the association between HCC and
95 neural factors are scarce and sometimes conflicting. It was reported that portal hypertension,
96 a recognized risk factor for HCC development and recurrence (Ganne-Carrie et al., 1996;
97 Ripoll et al., 2009), is correlated with ANS dysfunction (Dumcke and Moller, 2008). In addition,
98 proliferation of hepatocytic progenitors, instrumental in HCC, is impaired by adrenergic
99 signaling (Oben et al., 2003). Conversely, cholinergic signaling was shown to attenuate
100 apoptosis in the mouse liver (Hiramoto et al., 2008; Nishio et al., 2017), and liver angiogenesis
101 is under positive sympathetic regulation (Bennett et al., 1982). Interestingly, human liver ANS
102 innervation is more developed than in rodents. Indeed, it extends deeper into the lobule
103 (Jensen et al., 2013), increasing its capacities of regulation. This latter notion suggests that
104 ANS-related mechanisms observed in animals may play even more important roles in humans.
105 Here, we characterized several ANS markers of HCC samples by Western blot (WB)
106 and immunohistochemistry (IHC), unveiling a predominant parasympathetic signaling
107 compared to normal liver tissue. The definition of two neuroclasses based on levels of
108 adrenergic or cholinergic receptor transcripts, one cholinergic and one adrenergic, enabled the
109 stratification of tumors with more or less aggressiveness, respectively. Our findings shed light
110 on, as yet, unexplored characteristics of the disease and thus offer a realistic outlook for
111 considering alternative HCC investigations and treatment strategies, given the diversity and
112 safety of currently approved ANS-targeting drugs.

Neurogenesis of parasympathetic orientation in a cirrhosis-associated HCC rat model

Emerging evidence suggests a potential dysregulation of ANS signaling in several cancers in humans and in animal models (Hayakawa et al., 2017; Magnon et al., 2013; Renz et al., 2018a; Renz et al., 2018b; Thaker et al., 2006). To our knowledge, neuroregulation in HCC has never been investigated *in vivo*. HCC occurs in a cirrhotic background in 90% of cases. A rat model that allows HCC growth on genuine cirrhosis exists (Roth et al., 2017). It has been characterized and shows documented clinical relevance in particular with respect to the proliferative class of HCC (Kurma et al., 2021). In this context, we herein evaluated the ability of this diethylnitrosamine (DEN)-treated HCC rat model to recapitulate such processes by monitoring the same neural markers as those used for clinical samples. The methodology used for the experimental induction of HCC is shown in **Figure 1A.** To characterize HCC innervation, the following neuron markers were considered: NeuN (RBFOX3) as a mature neuron marker, DCX and INA as immature neurons markers, TH (TYR3H) and VAChT (SLC18A3) as specific ANS neuron markers for adrenergic and cholinergic signals, respectively. Total NeuN signals increased throughout disease progression. Interestingly, signals related to the DCX progenitor marker increased transiently, yet sharply, in samples harboring early HCC. In the case of ANS-specific markers, though levels of the TH marker (adrenergic) remained unaltered throughout disease progression, an increase in the cholinergic VAChT marker was observed in rats suffering from HCC. Degradation of β-tubulin was correlated with DEN-treatment and was likely derived from hepatic cytolysis and release of cytosolic contents, due to DEN-related, neoantigen-targeting, immune activation (**Figure 1B**). Intriguingly, a tight correlation was observed between DCX expression and β-tubulin degradation throughout progression of HCC-predisposing chronic liver disease (CLD) (**Figure 1C**). This suggests that HCC neural remodeling occurs as a consequence of cytolysis or parenchymal remodeling, as recently demonstrated in NASH (Adori et al., 2021). This prompted us to analyze the quantitative evolution of neural markers during CLD and HCC progression, which confirmed neo-neurogenesis, the parasympathetic neural features of HCC in the rat (**Figure 1D-H**), features pertinent to the human phenotype described herein. Of note, consistently, this model was recently shown to recapitulate features of clinical lesions of poorer outcomes (Kurma et al., 2021). Altogether, such data led to the identification of a cirrhosis-bearing HCC animal model with adequate features for HCC neurological research.

Infiltration of neural progenitors of parasympathetic orientation in human HCC samples

Given that the human liver ANS innervation extends deeper into the lobule (Jensen et al., 2013) than in rodents, we then investigated by immunoblotting the presence of ANS neural markers in paired peritumoral and tumoral clinical HCC samples. These samples, obtained from the French National HCC biobank, were evenly distributed across the main four HCC

etiologies (HBV, HCV, ALD, NASH; 24-26% each). The main characteristics of the patients are provided in the **Suppl. Table 1**. For optimal comparability between samples of each etiology, the HBV RNA and HCV RNA intrahepatic viral loads were limited to a maximum of 2 log_{10} difference.

We first considered by immunoblotting the presence of ANS neural markers in normal livers (both uninfected and F0, see Materials & Methods) versus HCC samples. Western blotting highlighted specific DCX and INA positivity in HCC samples, with a slight decrease in mature neural marker NeuN expression in HCC, indicating the presence of immature neurons. In addition, HCC samples displayed a profound depletion of the adrenergic marker TH at the benefit of the cholinergic neural marker VAchT (**Figure 2A**), prompting the analysis of HCC patient-derived specimens. We then compared the expression levels of such markers after technical validation of the antibodies of interest (**Suppl. Fig. 1**) at the peritumoral (cirrhotic/F4 stage) and tumoral levels in samples of the main HCC etiologies ((HBV (n = 14), HCV (n = 9), ALD (n = 14) and NASH (n = 14), total of 51 patients), which revealed no marked difference between peritumoral and tumoral samples (**Suppl. Fig. 2-6**). The intensity of neural markers was heterogeneous between etiologies. Only two clinico-biological features were significantly different between peritumoral and tumoral tissue: DCX enrichment in HBV+ samples and TH depletion in NASH samples ($p < 0.05$) (**Figure 2B-C**). When focusing on tumor differentiation, we then observed that well differentiated HCC samples were inversely correlated with mature innervation (NeuN+) in HBV-related tumors (**Figure 2D**). Overall, the important heterogeneity in neural markers observed across all tumors (significance is summarized in **Suppl. Table 2**), reflects, and maybe even affects, the well-known heterogeneity of HCC. Our data indicate that neo-neurogenesis occurs in all HCC etiologies, and that NASH is the primary etiology able to drive associations with neural markers. Importantly, such data also indicate that neurogenesis and its related alterations precedes HCC *per se* since no significant difference in the expression of markers could be observed in several instances between F4 and HCC.

Next, we sought to gain insight into the localization of neural signals in human samples. A set of 24 HCC patient samples derived from the four main etiologies ((HBV (n = 7), HCV (n = 4), ALD (n = 9), NASH (n = 4)) were subjected to Masson's trichrome staining to expose tissue architecture, and to NeuN, DCX, TH and VAChT immunostaining coupled with DAPI staining. INA signals could not be validated by IHC. The technical validations for NeuN, DCX, TH and VAChT staining are provided in the **Suppl. Fig. 7.** Whereas normal liver samples exhibited no signal, capsule-bearing or fibrosis septa-lined tumors were positive for DCX, NeuN and VAChT (**Suppl. Fig. 7)**. TH staining was negligible in both frequency and intensity throughout samples (**Figure 3A-F**). Importantly, DCX could be found in the tumor bulk where it co-stained with VAChT (**Figure 3G-J**), NeuN was never detected in the tumor bulk, suggesting that intra-tumoral neurogenesis is more immature and dynamic than its capsular counterpart. As

observed by WB, the predominant ANS co-labeling was specific for immature DCX+ fibers and parasympathetic neurons, suggesting that HCC neo-neurogenesis is largely parasympathetic, a notion in line with previous data on NASH (Adori et al., 2021). Such observations were unrelated to any specific HCC etiology, and confirmed findings on other solid malignancies (Hayakawa et al., 2017; Magnon et al., 2013; Renz et al., 2018a; Renz et al., 2018b; Thaker et al., 2006) that these tumors host nerves with migrating potential, likely enabling their interaction with post-synaptic receptors.

Modulation of ANS receptor transcripts from cirrhosis to HCC and tumor-specific uncoupling between pre- and post-synaptic orientations

Transduction of neural signals in the diseased tissue implicate postsynaptic ANS receptors. As a consequence, we compared the expression of several transcripts encoding ANS receptors in paired cirrhosis/F4 and HCC samples in the same cohort from the French National HCC biobank. Neural presynaptic mRNA markers such as *RBFOX3*, *DCX*, *TYR3H*, and *SLC18A3* could not be amplified by RT-qPCR using ad hoc neural controls (not shown), likely due to limited amounts of mRNAs in the distal, hepatic extremity of the axon. Post-synaptic neural markers belonging to detectable and well-characterized factors from the adrenergic group (*ADRA1A*, *ADRA1B*, *ADRA1D*, *ADRB1*, *ADRB2*, *ADRB3*) and from the cholinergic group (*CHRNA4*, *CHRNA7*, *CHRM3*) were quantified by RT-qPCR. *ADRA1A*, *ADRB2* and *CHRNA4* were the most highly expressed. Transcript abundance is shown for both groups in **Figure 4A**. Data indicate the regulation of several receptor transcripts in tumors, using peritumoral (F4) areas as our reference. Within the adrenergic group, *ADRA1A* and *ADRB1* displayed a down-regulation of more than 2-fold, whereas *ADRA1D* and *ADRB2* were up-regulated by 3.2-fold and 2-fold, respectively. Within the cholinergic group of transcripts, the nicotinic receptor mRNA *CHRNA4* was profoundly depleted (> 10-fold) in HCC versus F4 samples, while the muscarinic receptor *CHRM3* was up-regulated by 3-fold. Modulated transcripts *ADRA1A*, *ADRB2* and *CHRNA4* were also the most highly expressed (> 1,000-fold in comparison with the others) and therefore also likely participated in ANS-regulated phenotypes concomitant to the F4-to-HCC transition. Altogether, such data suggest ANS-driven changes to parenchymal signaling during the F4 to HCC transition. Regulation of these receptors may arise from the remodeling of ANS neurons, as identified in other types of cancers (Hayakawa et al., 2017; Magnon et al., 2013; Renz et al., 2018a; Renz et al., 2018b; Thaker et al., 2006).

In order to gain insight into the likelihood of HCC-related abnormal interactions between the neural and hepatic compartments, we compared the evolution of the ANS orientation of both compartments at the peritumoral and tumoral levels in the 51 above mentioned clinical specimens. Again, neural TH and VAChT were quantified by WB. At the post-synaptic level,

the three most highly expressed transcripts were used (*ADRA1A*, *ADRB1*, *ADRB2* for the adrenergic polarity and *CHRNA4*, *CHRNA7*, *CHRM3* for the cholinergic polarity). Shifts of ratios defined by adrenergic over cholinergic signals remained homogenous across paired specimens when comparing neural markers and post-synaptic markers in F4 peritumoral samples ($p < 0.0001$). In stark contrast, in HCC, shifts were unpredictable across samples, and even contradictory with respect to F4 features (**Figure 4B** and **Suppl. Figure 8**). Altogether, such data suggest that hepatic tumorigenesis is correlated with the empowerment of the tumor, ignoring neural polarities observed in the non-tumoral, cirrhotic, tissue. This indicates that neural control mediated by the ANS is likely active in cirrhosis, albeit disrupted in HCC.

Bioinformatics illuminates the pathogenic implication of the parasympathetic orientation in HCC evolution using an adrenergic/cholinergic transcriptomic signature

General sample characterization

We then sought to decipher the potential implication of the ANS in HCC phenotypes and stratification, through bioinformatics. In order to charter the interplay between autonomic functions and HCC in the least possibly biased manner, we performed a multisectional bioinformatics study on the previously published HCC TCGA dataset (Cancer Genome Atlas Research Network. Electronic address and Cancer Genome Atlas Research, 2017).

The adrenergic/cholinergic signal balance defines a unified ANS output in each innervated organ. We first defined a signature encompassing adrenergic and cholinergic receptor transcripts considering all mRNAs belonging to both categories. All these receptors ($n = 24$) are listed in the **Suppl. Table 3.** Adrenergic and cholinergic gene set normalized scores were established and the difference between adrenergic and cholinergic scores was then calculated. Based on the resulting score, samples were split into two classes: those with a higher difference than median were named adrenergic and those with a lower difference than median were named cholinergic (see the Materials and methods section). The mathematical formula used, distribution diagram of obtained values and PCA representation of those two classes, thereafter named 'neuroclasses', define two clearly separated populations and are shown in **Figure 5A-C.** We then generated data describing normalized expression levels of all adrenergic and cholinergic receptors in HCC, in all TCGA samples, at the level of specific etiologies and tumor differentiation statuses. Differential expression analysis revealed that *ADRA1A, ADRA1B, ADRA1D, ADRB1, ADRB2, CHRM1, CHRM4, CHRNA1, CHRNA3, CHRNA5, CHRNA6, CHRNA7, CHRNA9*, *CHRNB2*, *CHRNB4* were expressed at various levels in both neuroclasses. In general, as expected, ADRAx and ADRBx receptors were better expressed by the adrenergic neuroclass, while CHRNAx and CHRNBx receptors were better expressed in the cholinergic neuroclass. (**Figure 5D** and **Suppl. Table 3**).

In order to identify a potential association between a given ANS polarity (sympathetic or parasympathetic) and classically considered clinico-biological parameters in the HCC field, we implemented two-dimensional PCA on these data with respect to gender, ethnicity, etiology, obesity and mutational profile (*hTERT, TP53, CTNNB1*) (**Suppl. Fig. 9**). Importantly, no association could be seen between neuroclasses and gender, ethnicity, obesity, family history, or any of the four main HCC etiologies (HBV, HCV, NASH, ALD). *CTNNB1* mutations and age >60 emerged as positively associated with the adrenergic neuroclass. *TP53* mutations emerged as positively associated with the cholinergic neuroclass (padj $\leq$ 0.05). Of note, mutated *CTNNB1* samples positively correlated with the adrenergic neuroclass, yet at the significance threshold of 0.05 (**Figure 5E**). A Fisher's exact test comparing each neuroclass signature to each variable was constructed (**Suppl. Table 4**). This suggests that the classes defined by this ANS-based signature, conditioned by the interaction of the global pathophysiology of each patient with the liver, may enrich the stratification of HCC heterogeneity.

Differential Gene Expression and Pathway Enrichment Analysis

To identify which HCC phenotypes clustered with the ANS features of the tumor, we performed a differential gene expression analysis (padj < 0.01 and absolute Log2 fold-change > 0.58), the results of which are illustrated in a Volcano plot (**Figure 6**). Data related to the 100 most significantly up- and down-regulated genes for the adrenergic and cholinergic signatures are shown in the **Suppl. Tables 5-6,** respectively. Several mRNAs up-regulated in the cholinergic signature are of pathological significance: (i) *LGALS14* transcript (8-fold Log_2), which encodes a protein fostering apoptosis of T cells, (ii) *CT55* (cancer testis antigen, ranked 3rd; +6-fold Log_2) (iii) *BMP7*, ranked 5th (+6-fold Log_2), is a growth factor of the TGF-β family, *CEACAM7* (carcinoembryonic antigen-related cell adhesion molecule 7, ranked 7th; +5-fold Log_2) and *MAGEA4* as well as *MAGEA10* (ranked 10th and 30th; +4-fold Log_2 each ; both related to MAGEA3, a novel HCC progression driver), XAGE2 (ranked 44th; +4-fold Log_2), a fetal / reproductive tissue tumor-related antigen, and GAGE2A, (76th; +3-fold Log_2) a germ-cell and tumor antigen. CEA, MAGE, XAGE and GAGE antigens are related to colorectal cancer, melanoma and fetal/reproductive tissue tumors, respectively, suggesting a link between cholinergic orientation and general cancer markers. Likewise, *AFP* (+4-fold), ranked 33rd in terms of positive association with the cholinergic signature, encodes a widely used protein for HCC diagnosis, as well as tumor size and differentiation evaluation (**Suppl. Table 5**). In contrast, one alcohol dehydrogenase (ALDH3A1; +3-fold) and three major CYP450 isoforms (1A1, 3A4, 1A2), as well as CYP2A13, 2A7P1 and 3F36P, several of which known to be xenobiotic-inducible hepatocytic differentiation markers, were enriched (2 to 3-fold Log_2) within the transcripts significantly associated with the adrenergic neuroclass (**Suppl. Table 6).** The

β-catenin control target *GLUL*, but not *LGR5*, was also positively associated with this adrenergic neuroclass (+1.52 Log_2; padj = 4.6E-8, rank 241). In contrast, no CYP450 mRNA was found in the cholinergic neuroclass. Altogether, such data support that the cholinergic signature may be correlated with less differentiated HCC tumors.

Pathways associated with ANS polarities by overrepresentation analysis

Next, to accurately document how ANS features of the tumor are integrated within the current landscape of signatures in HCC, we performed an overrepresentation analysis (Hanzelmann et al., 2013) for both neuroclasses using ClusterProfiler (Yu et al., 2012) and the msigdbr R package (Subramanian et al., 2005) to access Molecular Signature Databases for gene sets H, C2, and C5. The lists of genes obtained from differential gene expression were used as inputs. A total of 956 and 604 pathways were correlated with adrenergic and cholinergic signaling, respectively (padj < 0.01, **Suppl. Tables 7-8**). We first sought to validate the approach by probing the presence of known recognized adrenergic and cholinergic processes in both cases. Pathways obtained from overrepresentation analysis of the adrenergic neuroclass contained 24 pathways related to cardiac or heart processes, and none related to nausea or vomiting, hallmarks of parasympathetic activation. Within the analysis pertaining to the cholinergic orientation, two signatures were related to nausea and vomiting, triggered by parasympathetic activation, while none were associated with cardiac pathophysiology.

We then deciphered the most relevant differences between overrepresentation pathways of adrenergic and cholinergic tumors, unveiling striking results. Pathways shared by all cancers (chosen keywords were 'cancer' and 'tumor') were more associated with the adrenergic neuroclass (82 (57%) pathways for adrenergic tumors vs 63 (43%) for cholinergic tumors), (**Figure 7A-B**). In contrast, HCC-specific pathways were enriched in the cholinergic neuroclass of tumors (70% of the total number of HCC pathways identified herein versus 30% in the adrenergic group). Significance of the pathways was also higher in the cholinergic neuroclass, as illustrated by the frequency diagram (**Figure 7C-D**). In the case of adrenergic signaling in HCC, a stronger association was also found with immunological functions (72% vs 28%, **Figure 7E-F**). These tumors displayed a much higher level (98%) of neural pathways (that include many axonal guidance pathways enabling neurogenesis), versus 2% in the cholinergic class (**Figure 7G-H**). Strikingly again, 97% of energetic pathways, representing functions fostering general proliferation, were correlated to cholinergic tumors (**Figure 7I-J**), whereas, as seen in overrepresentation pathways data, specific pathways linked to *CTNNB1* mutations were associated with the adrenergic tumor class.

We finally sought to identify within both classes the recognized HCC-specific signatures known to be related to good or poor prognosis pathways, including those identified by Chiang (Chiang et al., 2008), Hoshida (Hoshida et al., 2009), Lee (Lee et al., 2004) and Boyault (Boyault et al.,

2007) that are regularly considered for classification (Llovet et al., 2021). The adrenergic neuroclass was associated with 18 known signatures, 17 of which were in functional agreement with the transcriptomics of this neuroclass, i.e. related to better prognosis. The cholinergic neuroclass was closer to 8 signatures, of which 7 were in agreement with the transcriptomics of this neuroclass, that is, related to poor prognosis (**Table 1**). Of note, statistical associations were much stronger between cholinergic samples and their pathways than was the case for adrenergic samples (**Figure 8A**), strengthening the link between cholinergic polarity and poor outcome. In addition, the adrenergic neuroclass was correlated with longer overall survival (OS) and progression-free interval (PFI) than its cholinergic counterpart within a timeframe of two years post-diagnosis when performing a Cox model (**Figure 8B-C** and **Suppl. Table 9**), corroborating our findings that the cholinergic neuroclass is associated with more aggressive tumors.

To interpret these data at the level of multigenic functions, we performed a single sample non-parametric, unsupervised gene set variation analysis (GSVA method ssGSEA) for each sample, using the *Hallmarks of Cancer* signatures (Liberzon et al., 2015). As shown in **Figure 9**, the adrenergic neuroclass was correlated with *CTNNB1* mutation-associated metabolic functions, such as oxidative phosphorylation, adipogenesis, peroxisomal activity, xenobiotic detoxication, bile acid functions, and fatty acid metabolism (padj < 0.05). In contrast, the cholinergic neuroclass showed a clear association with mitogenic processes, E2F, MYC, TGF-β signaling, EMT, angiogenesis, NOTCH, Hedgehog, KRAS, TNF-α/NF-KB, IL6/STAT3, P53, hypoxia and PI3K/Akt/mTOR signaling pathways (padj < 0.05) (**Suppl. Table 10**). Hence, adrenergic signaling was correlated with several metabolic functions defining the non-proliferative class, whereas cholinergic signaling was correlated with features defining the proliferative class of HCC tumors (Llovet et al., 2018). Again, these findings argue in favor of a poorer evolution for HCC patients with higher cholinergic signaling.

Correlation between ANS orientation and immune response

Having observed that the number of immune pathways linked to adrenergic tumors was higher than to cholinergic tumors, and given the known impact of HCC immunology on clinical outcome, we then considered potential associations between ANS features and intra-tumoral immune markers, deciphered using the xCell enrichment method (Aran et al., 2017). Interestingly, neither global immune infiltrates nor T CD8+ leucocytic populations were correlated with either neuroclass. However, an axis composed of hematopoietic stem cells (+1.4-fold) and NK cells (+1.3-fold) were enriched in adrenergic tumors. Instead, CD4+ T cells (naïve, +2.5-fold), gamma/delta T cells (+1.5-fold) and several types of B cells (composed of total (+2.7-fold), naive (+29-fold) and class-switched (+2.3-fold) subpopulations) as well as myeloid dendritic cells (+1.7-fold) were significantly enriched in the cholinergic neuroclass.

Total and M2 macrophages were somewhat unexpectedly enriched (+1.2 and +1.4-fold respectively) in the adrenergic neuroclass (padj < 0.05) (**Figure 10 and Suppl. Table 11).** Overall, such data suggest that a B cell orientation, known to foster immunotolerance, is associated with the cholinergic polarity of the tumor. Vagal cholinergic signaling conveys systemic anti-inflammatory signaling (Borovikova et al., 2000) as well as in the gastrointestinal tract (Bonaz et al., 2018; Bonaz and Bernstein, 2013). These findings identify cholinergic signaling as a potential contributor or intrinsic signature of specific pro-tumoral or exhausted immune subsets, likely implicating B cells, which are newly identified and debated players in HCC (Bruno, 2020; Calderaro et al., 2019; Finkin et al., 2015; Shalapour et al., 2017). Accordingly, we investigated the association between each neuroclass and current immunotherapeutic targets of HCC. A hit was found linking one altered PD1 levels-associated pathway and the adrenergic neuroclass (GSE26495_PD1HIGH_VS_PD1LOW_CD8_TCELL_UP, padj = 3.5E-3, see **Suppl. Table 7**). This indicates that the transcriptome of adrenergic tumors is enriched in specific genes that are themselves correlating with variations of PD1 levels. Overall, these bioinformatics data suggest that adrenergic signaling is correlated with immune processes that may better impede pathology progression.

Discussion

The involvement of the ANS in the pathophysiology of many diseases is now recognized and links the CNS, which is unique to each patient, to disease-specific peripheral processes. HCC, a highly heterogeneous cancer at the genetic and pathological levels, remained undocumented with respect to the participation of the ANS. Local neo-neurogenesis and the involvement of the ANS has been identified in ovarian (Thaker et al., 2006), prostate (Magnon et al., 2013), gastric (Hayakawa et al., 2017) and pancreatic (Renz et al., 2018a; Renz et al., 2018b) cancers. In prostate cancer, a study revealed cancer-associated neo-neurogenesis with DCX marker expression, and predominant parasympathetic (cholinergic) features of *de novo* grown intra-tumoral nerves (Mauffrey et al., 2019). In gastric and pancreatic cancers, vagal nerves regulate cholinergic receptors in favor of oncogenesis initiation and progression. In breast cancers, in contrast, a study showed that parasympathetic nerves reduced cancer growth and progression (Kamiya et al., 2019). In the case of HCC, DCX/VAChT staining immune localization, as well as Western blots advocate for an association between the parasympathetic features of the liver ANS and the disease. As was shown recently in NASH (Adori et al., 2021), sympathetic innervation of HCC seems to be weaker if existent. Drastic enrichment of neurogenetic pathways in the adrenergic neuroclass identified in our work could thus be interpreted as compensatory with the aim of reestablishing sympathetic neural control in the neuro-emancipated diseased tissue. Indeed, it would be interesting to know whether HCC-correlating neurogenic netrin-1 (Plissonnier et al., 2016) as well as NGF and neurotrophin 5 (increased in NASH (Liu et al., 2021)) are associated with the adrenergic neuroclass. Herein, we identify parasympathetic innervation as dominant over sympathetic innervation in human, as well as in cirrhotic rat HCC. In addition, we demonstrate that cholinergic tumors are associated with higher *AFP* transcript levels and many poor prognosis-related pathways. Immune tumor infiltrates are correlated with better prognosis in HCC (Sia et al., 2017; Wada et al., 1998). The cholinergic class also seems to be partly depleted of cytotoxic immune or immunotherapy-related markers, suggesting their partially weakened or exhausted immune status. The liver is innervated by vagal outputs, which bear anti-inflammatory properties in several instances including the gastrointestinal tract (Pavlov and Tracey, 2012). This could provide an explanation for higher aggressiveness of cholinergic tumors, as cholinergic/vagal mitigation of local immunity, as suggested by the data herein, could obstruct proper mounting of anti-tumoral responses. In average, *CTNNB1*-mutated specimens that correlate with adrenergic polarity herein are in fact known to be rather immune-excluded (Llovet et al., 2021). This is suggesting that a somewhat heterogenous group of adrenergic tumor subtypes, not yet stratified, may account for the observed association between *CTNNB1*^{mut} and adrenergic tumors. Indeed, this association only reaches the null hypothesis threshold of 0.05 and

implicates the *GLUL* control transcripts enrichment but not the *LGR5* control transcript enrichment, suggesting its moderate significance. Most importantly, our data both further validate and enrich the current landscape of predictive transcriptomic signatures, showing, once again the intensified association between adrenergic features and a series of transcriptomic signatures linked to better prognosis.

The novelty of our findings reside in the implication that the systemic regulation of each patient influences the features of their tumor. In the liver, the *fight-or-flight* model, that is generally accepted for describing ANS functions (Jansen et al., 1995), would predict that adrenergic signaling would mobilize intracellular hepatocytic energy pools for peripheral energetic needs, whereas cholinergic signaling would foster intrahepatic storage of nutrients and related processes, such as liver expansion. This model seems pertinent to the HCC context. Liver expansion implicates liver cell size/mass increase as a condition for organ growth, both being dependent on mTOR functions (Guri et al., 2017; Sengupta et al., 2010), a pathway that is correlated with cholinergic tumors in our study. Frequent comorbidities associated with liver carcinogenesis are excessive BMI and alcohol intake (an underestimated but important energetic source), suggesting that parasympathetic signals aiming at fostering liver expansion could be highjacked by the tumor in a context of excessive nutrient availability. The likely protective and adverse roles of coffee (Schulze et al., 2015) and tobacco (Kolly et al., 2017; Schulze et al., 2015), respectively, as adrenergic and cholinergic agonists, are also in support of our findings.

This study provides the first body of evidence with respect to neural implication in human HCCs and in their stratification, using ANS functions unique to each patient's pathophysiology. This work opens new perspectives in investigating the rich diversity and safety profiles of approved compounds with anticholinergic or antimuscarinic activity for the treatment of HCC.

Acknowledgements

Non-TCGA clinical samples were used thanks to the participation of the French Liver Biobanks network (INCa, BB-0033-00085). This work was supported by INCA (PRT-K 19-033), La Ligue contre le cancer (Comité du Rhône, #R19147CC) and the DevWeCan Laboratories of Excellence network (ANR-LABX-061). IC is the recipient of an ANRS predoctoral fellowship (ECTZ63958).

Materials and Methods

Liver samples

Hepatocellular carcinoma samples used in this study were from the French Liver Biobanks network (INCa, BB-0033-00085, under IRB agreement of Inserm Ethics Committee (CEEI, #1862) and the TCGA Research Network (https://www.cancer.gov/tcga) HCC-LIHC cohort (Cancer Genome Atlas Research Network, 2017). The table presenting data expression was downloaded with the tool TCGA biolinks http://bioconductor.org/packages/release/bioc/html/TCGAbiolinks.html Data were crossed with previously reported metadata to obtain a cohort of 193 patients. Normal liver samples (French South-East region IRB agreement #A16-207) obtained from safety margins of hepatic resections of colorectal cancer metastasis, were histologically normal and devoid of HBV or HCV infection.

Western blotting

Immunoblotting was performed using 40 µg of RIPA (50 mM Tris HCl (pH 8.0), 150 mM NaCl, 1% NP-40, 0.5% sodium deoxycholate, 0.1% SDS, 10 mM sodium fluoride, 50 mM orthovanadate, 1x protease inhibitor cocktail (Roche))-processed cell lysates, then resolved on 8% or 10% SDS-PAGE, blotted onto nitrocellulose membranes (Amersham Biosciences, Saclay, France), blocked using 5% low fat dried milk in TBS Tween 0.1% for 1 h at room temperature (RT) and probed overnight at 4°C with corresponding antibodies listed in the **Suppl. Table 12**. After three washes in TBS-Tween 0.1%, membranes were incubated for 1 h at RT with secondary antibodies coupled to HRP (1/5,000, Sigma-Aldrich, St-Quentin, France) prior to chemiluminescence-based visualization using the Clarity Western ECL substrate (Bio-Rad, Versailles, France).

Total RNA extraction and RT-qPCR

Total RNA was extracted using Trizol (Invitrogen). One µg of RNA was DNAse I-digested (Promega, Charbonnières, France) and reverse transcribed using SuperScript VILO reverse transcriptase (ThermoFischer, Les Ulis, France) according to the manufacturer's instructions. Quantitative real-time PCR was performed on 1/5th diluted samples on a LightCycler 96 device (Roche, Meylan, France) using the No Rox qPCR mix (Bioline, Paris, France). PCR primer sequences (5′-3′) and qPCR conditions are listed in **Suppl. Table 13**. Specificity of all primers was assessed by melting curve analyses and agarose gel electrophoresis. Efficiency of all primers was quantified using 3-fold serial dilutions of target templates.

Immunohistochemistry

All reagents were from Sigma-Aldrich (St. Quentin Fallavier, France) unless otherwise stated. Samples where fixed for 24 h in 4% formaldehyde (pH 7.0). Progressive dehydration was performed using ethanol and xylene through 70%, 80%, and 95% ethanol (45 min each), followed by 3 changes of 100% ethanol (1 h each). Tissue was cleared through 2 changes of xylene, for 1 h each. Tissue was then immersed in 3 changes of paraffin, for 1 h each. Inclusion was automatically performed in a Histocentre3 Shandon (Loughborough, United Kingdom) device prior to cutting 4 µm-thick sections, transferred to SuperFrost slides (Euromedex, Souffelweyersheim, France), and dehydrated at 56°C for 1 h. For Masson's trichrome staining, the whole procedure was performed in a Leica ST5020 (Jena, Germany) apparatus. Paraffin removal was done using xylene and ethanol (backwards compared to protocol depicted above), followed by water rinsing. Gill hematoxylin was then added for 10 min followed by water rinsing. Saturated lithium carbonate was then used for 5 s before rinsing in water. Chlorhydric water (0.5%) was then added for a few seconds to stain specimens in pink before another cycle of lithium carbonate. Fuschin Ponceau was then added for 5 min, and phosphomolybdic acid was added for 10 s before 5 min incubation. Lastly, a Light Green staining was done for 5 min, followed by acetified water for 30 s. Slides were finally dehydrated and mounted as depicted above. Final acquisition of images was done using the NanoZoomer Digital Pathology software (Hamamatsu, Massy, Japan). For immunofluorescence *per se*, the Discovery Ultra device (Roche, Illkirch, France) was used. Paraffin removal was done for 8 min (75°C) using the EZPrep reagent (Roche, Illkirch, France), followed by antigen retrieval (8 min / 95°C then 28 min / 100°C in Tris EDTA pH 8.0), followed by incubations of primary antibodies (**Suppl. Table 12)**, prior to washing three times with PBS / 0.1% Tween and incubation of secondary antibodies (60 min, 37°C, see figure legend) and identical washing. The Discovery DCC Kit 455 (Roche), the Discovery FAM Kit 505 (Roche), the Discovery Cy5 Kit 660 (Roche), and the Opal Polaris 780 Reagent (Akoya) were used. Counterstaining was performed using DAPI (250 ng/mL) before mounting on SuperFrost slides (Euromedex, Souffelweyersheim, France). Final acquisition of images was done using the NanoZoomer Digital Pathology software (Hamamatsu, Massy, France).

Statistics

All statistical analyses and statistical tests pertaining to the bioinformatics analysis were carried out with the R software (version 3.6.1). Heatmaps were generated with ComplexeHeatmap, principal component analysis was completed with ade4, and plotted with factoextra or ggplot. Gaussian finite models were performed with Cluster and ClusterProfiler. Figures were created using the R software. Statistics on samples derived from the French National HCC biobank

were done as follows. Normal distribution of data was first assassed using the Shapiro-Wilk test. The associations between receptor transcript levels and clinico-pathological variables were determined in multiple comparison by Kruskal-Wallis test, Mann-Whitney test and Spearman correlation. We considered a Bonferroni-corrected *p*-value of 0.05/30 variables = 0.0017 as the threshold. Kaplan-Meier plots and log-rank tests were used to evaluate the prognostic value of the receptors by univariate Cox proportional hazards regression model.

Neuronal receptor score calculation and cohort classification

ssGSEA scores were computed through clusterProfiler R package. Gene set scores were calculated with the ssgsea method (Barbie et al., 2009) from the GSVA package (Hanzelmann et al., 2013). ssGSEA is a variation of Gene Set Enrichment Analysis (GSEA) that calculates enrichment scores for each pairing of gene set and sample. ssGSEA transforms data to a higher space level, from individual genes to genes sets (a list of functionally related genes) or pathways. As other methods, this analysis identifies enriched or overrepresented gene sets among a list of ranked genes providing the advantage that ssGSEA enrichment scores reflect the activity level of the biological process in which the genes of a particular gene set are coordinately up- or down-regulated within a sample. This transformation allows the interpretation of cell status through activity levels of biological processes and pathways rather than through the expression levels of individual genes. Here, two ssGSEA scores were calculated from both signatures, one including all adrenergic receptor genes, and the other including all cholinergic receptor genes in order to obtain an adrenergic score (AEs) and a cholinergic score (ChEs), respectively. To obtain a global neurotransmitter receptor score (NRs), the difference based on the adrenergic score minus the cholinergic score was calculated for each sample. Samples were split in two neuroclasses defined by receptor expression: those with higher NRs than median were named adrenergic while those with lower NRs than median were named cholinergic.

Differential Gene Expression:

Differential gene expression was performed with DESeq2 Bioconductor R package (Love et al., 2014) using as contrast previous clustering (neuroclasses by synaptic receptor, adrenergic-cholinergic signature). padj was set to 0.01 and Log2 Fold Change abs > 0.58. “High” (adrenergic) neuroclass was considered as reference.

Pathway enrichment analysis

All pathway-enrichment analyses were conducted using MSigDB gene sets H, C2, and C5 from msigdbr R package (Subramanian et al., 2005). Overrepresentation analysis of pathways

560 was performed with enricher from clusterProfiler (Yu et al., 2012) using as input over-
561 expressed and down-expressed genes previously obtained by differential gene expression
562 analysis.

563 **Survival analysis**

564 The survival data (OS, PFI) were extracted from Liu et al. (Liu et al., 2018). Survival analyses
565 were conducted with survival R packages (Therneau, 2021; Therneau TM, 2000) and
566 survminer (Kassambara). The survival analysis was performed at 2, 3, 5 and 10 years. $p <$
567 0.05 was considered significant.

568 **Microenvironmental analysis**

569 Estimation of immune and non-immune cell fractions from the tumor microenvironment were
570 determined through gene expression analysis using Immunedeconv R package (Sturm et al.,
571 2019) together with xCell enrichment method (Aran et al., 2017). This method allows sample
572 to sample comparisons and to determine stroma, immune and microenvironment scores.

Figure legends

Figure 1.

Evolution towards HCC and hepatic remodeling are correlated with neurogenesis and parasympathetic orientation in the cirrhotic rat.

A. Experimental outline. 6-week-old Fischer 334 rats were given DEN at 50 mg/kg weekly from day 0 to week 14, allowing progression of chronic liver disease to fibrosis, cirrhosis, decompensated cirrhosis and HCC. **B.** Immunoblotting of NeuN (mature neurons), DCX (immature neurons), TH (adrenergic) and VAChT (cholinergic) neural markers. **C.** DCX induction is correlated with parenchymal remodeling. DCX levels were plotted against ratios of full-length versus degraded tubulin signals shown in panel B. Spearman test (*** $p < 0.001$). **C-H.** Signal quantification was done using the Fiji software on non-saturated images, using whole lane Ponceau S fluorescence (540 nm) for normalization, prior to statistical plotting using the Mann-Whitney test (* $p < 0.05$, ** $p < 0.01$). Five to eight rats were used per time point.

Figure 2.

Expression of mature and progenitor neural markers in human HCC.

A. Immunoblotting of NeuN (mature neurons), DCX and INA (immature neurons), TH (adrenergic) and VAChT (cholinergic) neural markers carried out on normal liver and HCC samples. **B-D.** Signal quantification of data presented in **Suppl. Fig. 2-6** was done using the Fiji software on non-saturated images, using whole lane Ponceau S fluorescence (540 nm) for normalization, prior to statistical plotting using the Mann-Whitney test (* $p < 0.05$). Quantifications conducted prior to (B-C) and after (D-G) patient segregation according to the differentiation grade of the disease. HCC: Hepatocellular carcinoma; HCV: Hepatitis C Virus; HBV: Hepatitis B Virus; ALD: Alcoholic Liver Disease; NAFLD: non-alcoholic fatty liver disease. Peritumoral: cirrhotic; Tumoral: HCC; HCC differentiation grade: Low/moderate or High.

Figure 3.

Human HCCs harbor DCX+ neurogenesis with predominant parasympathetic features.

A panel of 24 HCC samples derived from all four main etiologies (HBV: n = 7; HCV: n = 4; ALD: n = 9; NASH: n = 4) was probed for immunolocalization of NeuN, DCX, TH and VAChT by multiplex IHC. **A-F**. Masson's trichrome and IHC staining of a representative capsule-bearing tumor. **G-J.** Staining of a representative tumoral bulk. Nuclei appear as grey. Cap: capsule; Tu: tumoral bulk. Scale bars = 50 µm.

Figure 4.

Uncoupling of ANS receptors and ANS polarity in HCC upon comparison with non-tumoral paired tissues.

A. Adrenergic (ADR) and cholinergic (CHR) receptor abundance and expression in peritumoral tissue (F4) and HCC. 166 pairs of liver tissues were analyzed. Mann-Whitney test (* $p < 0.05$, ** $p < 0.01$, *** $p < 0.001$). **B.** Relationship between neuronal pre-synaptic marker and post-synaptic marker expression. TH and VAChT expression levels in peri-tumoral and tumoral samples (n = 51 HCC cases) were evaluated by immunoblotting with specific antibodies and normalized against Ponceau S staining. Gene expression levels of adrenergic and cholinergic receptors was evaluated by qPCR and normalized against *GUS* expression. Adrenergic/cholinergic ratio was calculated for each patient as follows: (ADRA1A+ADRB2+ADRA1B) / (CHRNA4+CHRNA7+CHRM3), where those six targets correspond to the most expressed of both categories in patient samples. Mann-Whitney test (* $p < 0.05$, ** $p < 0.01$, *** $p < 0.001$).

Figure 5.

Neurosignature based on adrenergic and cholinergic receptors in HCC.

A. Neuronal receptor score (NRs) calculation: adrenergic and cholinergic enrichment scores (AEs and ChEs, respectively) were calculated based on corresponding receptors gene set signatures for each sample, then cholinergic scores were subtracted from adrenergic scores. Samples were grouped in cholinergic and adrenergic classes depending on whether their ssGSEA score values (NRs) were below or above the calculated median, respectively. **B.** Histogram of NRs calculated by ssGSEA for HCC tumors. **C.** Sample distribution after dimensional reduction (PCA) based on the 10 per cent most variable genes (normalized values). Cholinergic neuroclass in blue and adrenergic neuroclass in red are contrasted. **D.** Heatmap of relative expression levels of all adrenergic and cholinergic receptors in HCC tumor samples. Once samples were classified in cholinergic and adrenergic receptor expression classes based on previously obtained signature scores, differential expression analysis was performed and expression values normalized (variance stabilization transformation) and shown in the heatmap. Older60: patients older than 60. HBV: Hepatitis B Virus; HCV: Hepatitis C Virus; ALD: Alcoholic Liver Disease; NAFLD: non-alcoholic fatty liver disease. Mutations: TP53, CTNNB1, TERT; wt: wild type. na: no information available. **E**. Associations between neuroclasses and main HCC clinico-biological features. Fisher test's adjusted *p*-values per variable (** $p < 0.01$, *** $p < 0.001$).

Figure 6.

Transcriptomic features of adrenergic and cholinergic signatures analyzed by DGE. Volcano plot showing differentially-expressed genes in the cholinergic neuroclass compared to the adrenergic neuroclass. Genes with lowest adjusted p-value are indicated. The horizontal red bar represents the adjusted p-value threshold at 0.01. The higher the location of a gene, the stronger its association with a low adjusted p-value (significance). The more a gene is located to the right or left, the stronger its association with a high absolute Log2 fold-change. Increased and decreased genes were considered if absolute Log2 fold-change value was higher than 0.58 and adjusted p-value < than 0.01.

Figure 7.

HCC- and neurally-relevant pathways correlated with each neuroclass as identified by Gene Set Enrichment Analysis (GSEA).

From up-regulated (derived from adrenergic tumors) and down-regulated (derived from cholinergic tumors) transcripts obtained by differential gene expression analysis, enriched pathways were identified. Pathways with adjusted p-value < 0.01 were selected. **A,C,E,G,I**. Pathway allocation to each neuroclass. **B,D,F,H,J**. Statistical significance of both groups of pathways. The higher the pathway on the plot (low *p*-value then (-Log)-transformed), the stronger its association with the neuroclass of interest. The key-words used for the search are the following: Cancer terms: CANCER|TUMOR. HCC terms: HEPATOCELLULAR_CARCINOMA|HCC Immune terms: IMMUN|MACROPHAGE|PHAGO|IGM|ANTIGEN|LEUKO|CYTO|TREG|LYMPHOCYTE|CHEMOKINE|INTERLEUKIN|MONOCYTE|T_CELL|NEUTROPHIL|MACROPHAGE|CD8|CD4|REGULATORY_T|DENDRITIC|B_CELL|NK_CELL|NATURAL_KILLER|INFECTION|INFLAMATION. Neuronal terms: NEUR|SYNAP|AXON|NERV. Metabolic terms: METAB|ANAB|CATAB

Figure 8.

Adrenergic orientation of HCC is of better prognosis than cholinergic orientation.

A. Statistical significance of adrenergic (red circles) and cholinergic (blue circles) tumor-associated HCC signatures. Attention needs to be paid to their actual biological significance extracted from the MSigDB database, listed in **Suppl. Table 9**, before drawing conclusions with respect to pathology. **B-C.** Kaplan-Meier representation of the predictive value of both neuroclasses with respect to overall survival (OS) and progression-free interval (PFI) in HCC.

Figure 9.

Adrenergic and cholinergic-associated hallmark pathways determined by single sample Gene Set Enrichment Analysis (ssGSEA).

ssGSEA scores were calculated for each sample. Pathways comparison between neuroclasses was performed with the Wilcoxon Test and significant pathways (padj < 0.05) selected. Older60: patients older than 60. HBV: Hepatitis B Virus; HCV: Hepatitis C Virus; ALD: Alcoholic Liver Disease; NAFLD: non-alcoholic fatty liver disease. Mutations: TP53, CTNNB1, TERT; wt wild type. na: no information available.

Figure 10.

Immune infiltration in HCC tumor samples determined by the xCell method.

To determine statistical differences for each cell type between neuroclasses, a Wilcoxon Test was performed on 36 immune subpopulations using the immune Xcell score. Significant data obtained on 10 of them are shown (panels **A-J**). Differences in immune cell types were defined by padj < 0.05.

Table 1. ssGSEA HCC signatures correlated with adrenergic (left columns) and cholinergic (right columns) neuroclasses of tumors belonging to the TCGA dataset. Pathways are listed by decreasing order of significance. Besides signature names listed in this table ($p < 0.01$ Wilcoxon Test), attention needs to be paid to their expanded biological significance extracted from the ssGSEA database, listed **in Suppl. Table 9**, before drawing conclusions with respect to pathology.

Adrenergic tumor pathways		Cholinergic tumor pathways	
Prognosis agreement over adrenergic transcriptomic features	**Prognosis discordance with over adrenergic transcriptomic features**	**Prognosis agreement over cholinergic transcriptomic features**	**Prognosis discordance over cholinergic transcriptomic features**
CHIANG_LIVER_CANCER_SUBCLASS_PROLIFERATION_DN Padj = 8.2E-117	CHIANG_LIVER_CANCER_SUBCLASS_INTERFERON_DN Padj = 8.3E-4	CHIANG_LIVER_CANCER_SUBCLASS_PROLIFERATION_UP Padj = 2.2E-90	None
HOSHIDA_LIVER_CANCER_SUBCLASS_S3 Padj = 1.5E-75		DESERT_STEM_CELL_HEPATOCELLULAR_CARCINOMA_SUBCLASS_UP Padj = 9.7E-35	
LEE_LIVER_CANCER_SURVIVAL_UP Padj = 1.4E-53		VILLANUEVA_LIVER_CANCER_KRT19_UP Padj = 1.6E-26	
CHIANG_LIVER_CANCER_SUBCLASS_CTNNB1_UP Padj = 5.7E-49		WOO_LIVER_CANCER_RECURRENCE_UP Padj = 2.2E-19	
WOO_LIVER_CANCER RECURRENCE_DN Padj = 5.58E-42		LEE_LIVER_CANCER_SURVIVAL_DN Padj = 5.3E-8	
VILLANUEVA_LIVER_CANCER_KRT19_DN Padj = 1.1E-32		CHIANG_LIVER_CANCER_SUBCLASS_CTNNB1_DN Padj = 1.3E-6	
DESERT_PERIPORTAL_HEPATOCELLULAR_CARCINOMA_SUBCLASS_UP Padj = 3.9E-28		HOSHIDA_LIVER_CANCER_SUBCLASS_S1 Padj = 7.3E-5	
BOYAULT_LIVER_CANCER_SUBCLASS_G123_DN Padj = 9.2E-27		HOSHIDA_LIVER_CANCER_SURVIVAL_UP Padj = 8.7E-3	
ANDERSEN_LIVER_CANCER_KRT19_DN Padj = 6.5E-24			

YAMASHITA_LIVER_CANCER_STEM_CELL_DN Padj = 2.6E-24
KIM_LIVER_CANCER_POOR_SURVIVAL_DN Padj = 2.3E-21
BOYAULT_LIVER_CANCER_SUBCLASS_G6_UP Padj = 4.0E-16
BOYAULT_LIVER_CANCER_SUBCLASS_G1_DN Padj = 5.8E-9
CHIANG_LIVER_CANCER_SUBCLASS_POLYSOMY7_UP Padj = 8.3E-9
HOSHIDA_LIVER_CANCER_SURVIVAL_DN Padj = 3.3E-8
BOYAULT_LIVER_CANCER_SUBCLASS_G12_DN Padj = 2.0E-6
HOSHIDA_LIVER_CANCER_LATE_RECURRENCE_DN Padj = 9.0E-3
BOYAULT_LIVER_CANCER_SUBCLASS_G56_UP Padj = 1.8E-3

699

Supplementary figures

Supplementary Figure 1.

Validation of anti-NeuN, DCX, INA, TH and VAChT antibodies by Western Blot.

A. Extracts from neonate mouse brain, SKNSH, PHH, and human HCC lines belonging to transcriptomic classes 1, 2 and 3 (Caruso et al., 2019) were processed for detection of the indicated targets. **B.** The same strategy was used for the validation of an anti-DCX antibody specifically suitable for rat epitopes.

Supplementary Figure 2.

Quantification of mature and progenitor neural markers in human HCC of all etiologies.

A-L. Signal quantification was done using the Fiji software on non-saturated images, using whole lane Ponceau S fluorescence (540 nm) for normalization, prior to statistical plotting using the Mann-Whitney test (n = 51 patients, n.s). Quantification before (A-F) and after (G-L) patient stratification based on the 'low/moderate' or 'well' level of differentiation.

Supplementary Figure 3.

Expression of mature and progenitor neural markers in human HCC of HBV etiology.

A. Immunoblotting on neural markers using antibodies against NeuN, DCX, TH and VAChT neural markers and β-tubulin as an internal control. **B-G.** Signal quantification was done using the Fiji software on non-saturated images, using whole lane Ponceau S fluorescence (540 nm) for normalization, prior to statistical plotting using the Mann-Whitney test (n = 14 patients, * $p < 0.05$, ** $p < 0.01$, *** $p < 0.001$).

Supplementary Figure 4.

Expression of mature and progenitor neural markers in human HCC of HCV etiology.

A. Immunoblotting on neural markers using the above-mentioned antibodies. **B-G.** Signal quantification was done using the Fiji software on non-saturated images, using whole lane Ponceau S fluorescence (540 nm) for normalization, prior to statistical plotting using the Mann-Whitney test (n = 9 patients, * $p < 0.05$, ** $p < 0.01$, *** $p < 0.001$).

Supplementary Figure 5.

Expression of mature and progenitor neural markers in human HCC of NASH etiology.

A. Immunoblotting on neural markers using the above-mentioned antibodies. **B-G.** Signal quantification was done using the Fiji software on non-saturated images, using whole lane Ponceau S fluorescence (540 nm) for normalization, prior to statistical plotting using the Mann-Whitney test (n = 14 patients, * $p < 0.05$, ** $p < 0.01$, *** $p < 0.001$).

Supplementary Figure 6.

Expression of mature and progenitor neural markers in human HCC of ALD etiology.

A. Immunoblotting on neural markers using the above-mentioned antibodies. **B-G.** Signal quantification was done using the Fiji software on non-saturated images, using whole lane Ponceau S fluorescence (540 nm) for normalization, prior to statistical plotting using the Mann-Whitney test (n = 14 patients, * $p < 0.05$, ** $p < 0.01$, *** $p < 0.001$).

Supplementary Figure 7.

Validation of antibodies used by IHC. Anti-NeuN, DCX, TH and VAChT antibodies were validated by immunofluorescence on ad hoc human tissue samples prior to their use on HCC specimens. **A.** Cerebellum. **C.** Parotid gland lesion. **E.** Surrenal gland. **G.** Cerebral cortex. **B,D,F,H.** Normal liver (hepatocytic areas). Nuclei were stained with DAPI (grey signal). Antigens of interest are shown in green. Scale bar = 100 µm.

Supplementary Figure 8.

Relationship between neuronal pre-synaptic marker and post-synaptic marker expression after etiology-based stratification.

TH and VAChT expression levels in peri-tumoral and tumoral samples (n = 51 HCC cases) were evaluated by immunoblotting with specific antibodies and normalized against Ponceau S staining. Gene expression levels of adrenergic and cholinergic receptors were evaluated by qPCR and normalized against *GUS* expression. Adrenergic/cholinergic ratio was calculated for each patient as follows: (ADRA1A+ADRB2+ADRA1B) / (CHRNA4+CHRNA7+CHRM3), where those six targets are the most expressed of both categories in patient samples. Mann-Whitney test (* $p < 0.05$, ** $p < 0.01$, *** $p < 0.001$).

Supplementary Figure 9.

HCC neuroclasses are unrelated to many HCC clinico-biological parameters except age>60, *CTNNB1* and *TP53* mutational status. PCAs comparing signature classes with gender, ethnicity, obesity, family history, or any of the four main HCC etiologies (HBV, HCV, NASH, ALD), or main mutational profiles *IDH, TP53, TERT, CTNNB1* mutations.

Supplementary Tables

Supplementary Table 1.

Characteristics of paired F4/HCC samples used in the study.

Supplementary Table 2.

Significance assessment of neural features in HCC.

Supplementary Table 3.

Differential gene expression (by DESeq2) of adrenergic and cholinergic receptors in TCGA samples grouped by neuroclass.

Supplementary Table 4.

Association levels between neuroclasses and major HCC-related clinico-biological variables. Fisher test. $p<0.01$.

Supplementary Table 5.

List of the 100 genes most correlated with the cholinergic neuroclass.

Supplementary Table 6.

List of the 100 genes most correlated with the adrenergic neuroclass.

Supplementary Table 7.

Pathways enriched in the adrenergic neuroclass. Over Representation Analysis with hypergeometric test. $p < 0.01$.

Supplementary Table 8.

Pathways enriched in the cholinergic neuroclass. Over Representation Analysis with hypergeometric test. $p < 0.01$.

Supplementary Table 9.

Biological descriptions of prognosis pathways associated with both HCC neuroclasses.

Supplementary Table 10.

Significance of hallmark pathways. Wilcoxon Test $p < 0.05$.

Supplementary Table 11.

Significance of immune alterations. Wilcoxon Test $p < 0.05$.

Supplementary Table 12.

Antibodies used in this study.

Supplementary Table 13.

Human qPCR primers.

812 **References**

813

814 Adori, C., Daraio, T., Kuiper, R., Barde, S., Horvathova, L., Yoshitake, T., Ihnatko, R.,
815 Valladolid-Acebes, I., Vercruysse, P., Wellendorf, A. M., *et al.* (2021). Disorganization and
816 degeneration of liver sympathetic innervations in nonalcoholic fatty liver disease revealed by
817 3D imaging. Sci Adv *7*.
818 Aran, D., Hu, Z., and Butte, A. J. (2017). xCell: digitally portraying the tissue cellular
819 heterogeneity landscape. Genome Biol *18*, 220.
820 Barbie, D. A., Tamayo, P., Boehm, J. S., Kim, S. Y., Moody, S. E., Dunn, I. F., Schinzel, A. C.,
821 Sandy, P., Meylan, E., Scholl, C., *et al.* (2009). Systematic RNA interference reveals that
822 oncogenic KRAS-driven cancers require TBK1. Nature *462*, 108-112.
823 Bennett, T. D., MacAnespie, C. L., and Rothe, C. F. (1982). Active hepatic capacitance
824 responses to neural and humoral stimuli in dogs. Am J Physiol *242*, H1000-1009.
825 Bonaz, B., Sinniger, V., and Pellissier, S. (2018). Vagus Nerve Stimulation at the Interface of
826 Brain-Gut Interactions. Cold Spring Harb Perspect Med.
827 Bonaz, B. L., and Bernstein, C. N. (2013). Brain-gut interactions in inflammatory bowel
828 disease. Gastroenterology *144*, 36-49.
829 Borovikova, L. V., Ivanova, S., Zhang, M., Yang, H., Botchkina, G. I., Watkins, L. R., Wang,
830 H., Abumrad, N., Eaton, J. W., and Tracey, K. J. (2000). Vagus nerve stimulation attenuates
831 the systemic inflammatory response to endotoxin. Nature *405*, 458-462.
832 Boyault, S., Rickman, D. S., de Reynies, A., Balabaud, C., Rebouissou, S., Jeannot, E.,
833 Herault, A., Saric, J., Belghiti, J., Franco, D., *et al.* (2007). Transcriptome classification of HCC
834 is related to gene alterations and to new therapeutic targets. Hepatology *45*, 42-52.
835 Bruno, T. C. (2020). New predictors for immunotherapy responses sharpen our view of the
836 tumour microenvironment. Nature *577*, 474-476.
837 Calderaro, J., Petitprez, F., Becht, E., Laurent, A., Hirsch, T. Z., Rousseau, B., Luciani, A.,
838 Amaddeo, G., Derman, J., Charpy, C., *et al.* (2019). Intra-tumoral tertiary lymphoid structures
839 are associated with a low risk of early recurrence of hepatocellular carcinoma. J Hepatol *70*,
840 58-65.
841 Cancer Genome Atlas Research Network. Electronic address, w. b. e., and Cancer Genome
842 Atlas Research, N. (2017). Comprehensive and Integrative Genomic Characterization of
843 Hepatocellular Carcinoma. Cell *169*, 1327-1341 e1323.
844 Caruso, S., Calatayud, A. L., Pilet, J., La Bella, T., Rekik, S., Imbeaud, S., Letouze, E.,
845 Meunier, L., Bayard, Q., Rohr-Udilova, N., *et al.* (2019). Analysis of Liver Cancer Cell Lines
846 Identifies Agents With Likely Efficacy Against Hepatocellular Carcinoma and Markers of
847 Response. Gastroenterology *157*, 760-776.
848 Chiang, D. Y., Villanueva, A., Hoshida, Y., Peix, J., Newell, P., Minguez, B., LeBlanc, A. C.,
849 Donovan, D. J., Thung, S. N., Sole, M., *et al.* (2008). Focal gains of VEGFA and molecular
850 classification of hepatocellular carcinoma. Cancer Res *68*, 6779-6788.
851 Dumcke, C. W., and Moller, S. (2008). Autonomic dysfunction in cirrhosis and portal
852 hypertension. Scand J Clin Lab Invest *68*, 437-447.
853 Finkin, S., Yuan, D., Stein, I., Taniguchi, K., Weber, A., Unger, K., Browning, J. L., Goossens,
854 N., Nakagawa, S., Gunasekaran, G., *et al.* (2015). Ectopic lymphoid structures function as
855 microniches for tumor progenitor cells in hepatocellular carcinoma. Nat Immunol *16*, 1235-
856 1244.
857 Ganne-Carrie, N., Chastang, C., Chapel, F., Munz, C., Pateron, D., Sibony, M., Deny, P.,
858 Trinchet, J. C., Callard, P., Guettier, C., and Beaugrand, M. (1996). Predictive score for the
859 development of hepatocellular carcinoma and additional value of liver large cell dysplasia in
860 Western patients with cirrhosis. Hepatology *23*, 1112-1118.
861 Guri, Y., Colombi, M., Dazert, E., Hindupur, S. K., Roszik, J., Moes, S., Jenoe, P., Heim, M.
862 H., Riezman, I., Riezman, H., and Hall, M. N. (2017). mTORC2 Promotes Tumorigenesis via
863 Lipid Synthesis. Cancer Cell *32*, 807-823 e812.
864 Hanzelmann, S., Castelo, R., and Guinney, J. (2013). GSVA: gene set variation analysis for
865 microarray and RNA-seq data. BMC Bioinformatics *14*, 7.

Hayakawa, Y., Sakitani, K., Konishi, M., Asfaha, S., Niikura, R., Tomita, H., Renz, B. W., Tailor, Y., Macchini, M., Middelhoff, M., *et al.* (2017). Nerve Growth Factor Promotes Gastric Tumorigenesis through Aberrant Cholinergic Signaling. Cancer Cell *31*, 21-34.

Hiramoto, T., Chida, Y., Sonoda, J., Yoshihara, K., Sudo, N., and Kubo, C. (2008). The hepatic vagus nerve attenuates Fas-induced apoptosis in the mouse liver via alpha7 nicotinic acetylcholine receptor. Gastroenterology *134*, 2122-2131.

Hoshida, Y., Nijman, S. M., Kobayashi, M., Chan, J. A., Brunet, J. P., Chiang, D. Y., Villanueva, A., Newell, P., Ikeda, K., Hashimoto, M., *et al.* (2009). Integrative transcriptome analysis reveals common molecular subclasses of human hepatocellular carcinoma. Cancer Res *69*, 7385-7392.

Jansen, A. S., Nguyen, X. V., Karpitskiy, V., Mettenleiter, T. C., and Loewy, A. D. (1995). Central command neurons of the sympathetic nervous system: basis of the fight-or-flight response. Science *270*, 644-646.

Jensen, K. J., Alpini, G., and Glaser, S. (2013). Hepatic nervous system and neurobiology of the liver. Compr Physiol *3*, 655-665.

Kamiya, A., Hayama, Y., Kato, S., Shimomura, A., Shimomura, T., Irie, K., Kaneko, R., Yanagawa, Y., Kobayashi, K., and Ochiya, T. (2019). Genetic manipulation of autonomic nerve fiber innervation and activity and its effect on breast cancer progression. Nat Neurosci *22*, 1289-1305.

Kassambara, A. K., M.; Biecek, P. Survminer: Drawing Survival Curves using 'ggplot2'. R package *Version 0.4.9*.

Kolly, P., Knopfli, M., and Dufour, J. F. (2017). Effect of smoking on survival of patients with hepatocellular carcinoma. Liver Int *37*, 1682-1687.

Kurma, K., Manches, O., Chuffart, F., Sturm, N., Gharzeddine, K., Zhang, J., Mercey-Ressejac, M., Rousseaux, S., Millet, A., Lerat, H., *et al.* (2021). DEN-Induced Rat Model Reproduces Key Features of Human Hepatocellular Carcinoma. Cancers (Basel) *13*.

Lee, J. S., Chu, I. S., Heo, J., Calvisi, D. F., Sun, Z., Roskams, T., Durnez, A., Demetris, A. J., and Thorgeirsson, S. S. (2004). Classification and prediction of survival in hepatocellular carcinoma by gene expression profiling. Hepatology *40*, 667-676.

Liberzon, A., Birger, C., Thorvaldsdottir, H., Ghandi, M., Mesirov, J. P., and Tamayo, P. (2015). The Molecular Signatures Database (MSigDB) hallmark gene set collection. Cell Syst *1*, 417-425.

Liu, J., Lichtenberg, T., Hoadley, K. A., Poisson, L. M., Lazar, A. J., Cherniack, A. D., Kovatich, A. J., Benz, C. C., Levine, D. A., Lee, A. V., *et al.* (2018). An Integrated TCGA Pan-Cancer Clinical Data Resource to Drive High-Quality Survival Outcome Analytics. Cell *173*, 400-416 e411.

Liu, K., Yang, L., Wang, G., Liu, J., Zhao, X., Wang, Y., Li, J., and Yang, J. (2021). Metabolic stress drives sympathetic neuropathy within the liver. Cell Metab *33*, 666-675 e664.

Llovet, J. M., Kelley, R. K., Villanueva, A., Singal, A. G., Pikarsky, E., Roayaie, S., Lencioni, R., Koike, K., Zucman-Rossi, J., and Finn, R. S. (2021). Hepatocellular carcinoma. Nat Rev Dis Primers *7*, 6.

Llovet, J. M., Montal, R., Sia, D., and Finn, R. S. (2018). Molecular therapies and precision medicine for hepatocellular carcinoma. Nat Rev Clin Oncol *15*, 599-616.

Love, M. I., Huber, W., and Anders, S. (2014). Moderated estimation of fold change and dispersion for RNA-seq data with DESeq2. Genome Biol *15*, 550.

Magnon, C., Hall, S. J., Lin, J., Xue, X., Gerber, L., Freedland, S. J., and Frenette, P. S. (2013). Autonomic nerve development contributes to prostate cancer progression. Science *341*, 1236361.

Mauffrey, P., Tchitchek, N., Barroca, V., Bemelmans, A. P., Firlej, V., Allory, Y., Romeo, P. H., and Magnon, C. (2019). Progenitors from the central nervous system drive neurogenesis in cancer. Nature *569*, 672-678.

Monje, M., Borniger, J. C., D'Silva, N. J., Deneen, B., Dirks, P. B., Fattahi, F., Frenette, P. S., Garzia, L., Gutmann, D. H., Hanahan, D., *et al.* (2020). Roadmap for the Emerging Field of Cancer Neuroscience. Cell *181*, 219-222.

Nishio, T., Taura, K., Iwaisako, K., Koyama, Y., Tanabe, K., Yamamoto, G., Okuda, Y., Ikeno, Y., Yoshino, K., Kasai, Y., *et al.* (2017). Hepatic vagus nerve regulates Kupffer cell activation via alpha7 nicotinic acetylcholine receptor in nonalcoholic steatohepatitis. J Gastroenterol *52*, 965-976.

Oben, J. A., Roskams, T., Yang, S., Lin, H., Sinelli, N., Li, Z., Torbenson, M., Huang, J., Guarino, P., Kafrouni, M., and Diehl, A. M. (2003). Sympathetic nervous system inhibition increases hepatic progenitors and reduces liver injury. Hepatology *38*, 664-673.

Pavlov, V. A., and Tracey, K. J. (2012). The vagus nerve and the inflammatory reflex--linking immunity and metabolism. Nat Rev Endocrinol *8*, 743-754.

Plissonnier, M. L., Lahlali, T., Michelet, M., Lebosse, F., Cottarel, J., Beer, M., Neveu, G., Durantel, D., Bartosch, B., Accardi, R., *et al.* (2016). Epidermal Growth Factor Receptor-Dependent Mutual Amplification between Netrin-1 and the Hepatitis C Virus. PLoS Biol *14*, e1002421.

Renz, B. W., Takahashi, R., Tanaka, T., Macchini, M., Hayakawa, Y., Dantes, Z., Maurer, H. C., Chen, X., Jiang, Z., Westphalen, C. B., *et al.* (2018a). beta2 Adrenergic-Neurotrophin Feedforward Loop Promotes Pancreatic Cancer. Cancer Cell *33*, 75-90 e77.

Renz, B. W., Tanaka, T., Sunagawa, M., Takahashi, R., Jiang, Z., Macchini, M., Dantes, Z., Valenti, G., White, R. A., Middelhoff, M. A., *et al.* (2018b). Cholinergic Signaling via Muscarinic Receptors Directly and Indirectly Suppresses Pancreatic Tumorigenesis and Cancer Stemness. Cancer Discov *8*, 1458-1473.

Ripoll, C., Groszmann, R. J., Garcia-Tsao, G., Bosch, J., Grace, N., Burroughs, A., Planas, R., Escorsell, A., Garcia-Pagan, J. C., Makuch, R., *et al.* (2009). Hepatic venous pressure gradient predicts development of hepatocellular carcinoma independently of severity of cirrhosis. J Hepatol *50*, 923-928.

Roth, G. S., Macek Jilkova, Z., Zeybek Kuyucu, A., Kurma, K., Ahmad Pour, S. T., Abbadessa, G., Yu, Y., Busser, B., Marche, P. N., Leroy, V., and Decaens, T. (2017). Efficacy of AKT Inhibitor ARQ 092 Compared with Sorafenib in a Cirrhotic Rat Model with Hepatocellular Carcinoma. Mol Cancer Ther *16*, 2157-2165.

Schulze, K., Imbeaud, S., Letouze, E., Alexandrov, L. B., Calderaro, J., Rebouissou, S., Couchy, G., Meiller, C., Shinde, J., Soysouvanh, F., *et al.* (2015). Exome sequencing of hepatocellular carcinomas identifies new mutational signatures and potential therapeutic targets. Nat Genet *47*, 505-511.

Sengupta, S., Peterson, T. R., Laplante, M., Oh, S., and Sabatini, D. M. (2010). mTORC1 controls fasting-induced ketogenesis and its modulation by ageing. Nature *468*, 1100-1104.

Shalapour, S., Lin, X. J., Bastian, I. N., Brain, J., Burt, A. D., Aksenov, A. A., Vrbanac, A. F., Li, W., Perkins, A., Matsutani, T., *et al.* (2017). Inflammation-induced IgA+ cells dismantle anti-liver cancer immunity. Nature *551*, 340-345.

Sia, D., Jiao, Y., Martinez-Quetglas, I., Kuchuk, O., Villacorta-Martin, C., Castro de Moura, M., Putra, J., Camprecios, G., Bassaganyas, L., Akers, N., *et al.* (2017). Identification of an Immune-specific Class of Hepatocellular Carcinoma, Based on Molecular Features. Gastroenterology *153*, 812-826.

Sturm, G., Finotello, F., Petitprez, F., Zhang, J. D., Baumbach, J., Fridman, W. H., List, M., and Aneichyk, T. (2019). Comprehensive evaluation of transcriptome-based cell-type quantification methods for immuno-oncology. Bioinformatics *35*, i436-i445.

Subramanian, A., Tamayo, P., Mootha, V. K., Mukherjee, S., Ebert, B. L., Gillette, M. A., Paulovich, A., Pomeroy, S. L., Golub, T. R., Lander, E. S., and Mesirov, J. P. (2005). Gene set enrichment analysis: a knowledge-based approach for interpreting genome-wide expression profiles. Proc Natl Acad Sci U S A *102*, 15545-15550.

Sung, H., Ferlay, J., Siegel, R. L., Laversanne, M., Soerjomataram, I., Jemal, A., and Bray, F. (2021). Global Cancer Statistics 2020: GLOBOCAN Estimates of Incidence and Mortality Worldwide for 36 Cancers in 185 Countries. CA Cancer J Clin *71*, 209-249.

Thaker, P. H., Han, L. Y., Kamat, A. A., Arevalo, J. M., Takahashi, R., Lu, C., Jennings, N. B., Armaiz-Pena, G., Bankson, J. A., Ravoori, M., *et al.* (2006). Chronic stress promotes tumor growth and angiogenesis in a mouse model of ovarian carcinoma. Nat Med *12*, 939-944.

Therneau, T. (2021). A Package for Survival Analysis in R. In R package

975 Therneau TM, G. P. (2000). Modeling Survival Data: Extending the Cox Model. Springer, New-
976 York.
977 Venkatesh, H., and Monje, M. (2017). Neuronal Activity in Ontogeny and Oncology. Trends
978 Cancer *3*, 89-112.
979 Wada, Y., Nakashima, O., Kutami, R., Yamamoto, O., and Kojiro, M. (1998).
980 Clinicopathological study on hepatocellular carcinoma with lymphocytic infiltration. Hepatology
981 *27*, 407-414.
982 Yu, G., Wang, L. G., Han, Y., and He, Q. Y. (2012). clusterProfiler: an R package for comparing
983 biological themes among gene clusters. OMICS *16*, 284-287.
984

Figures

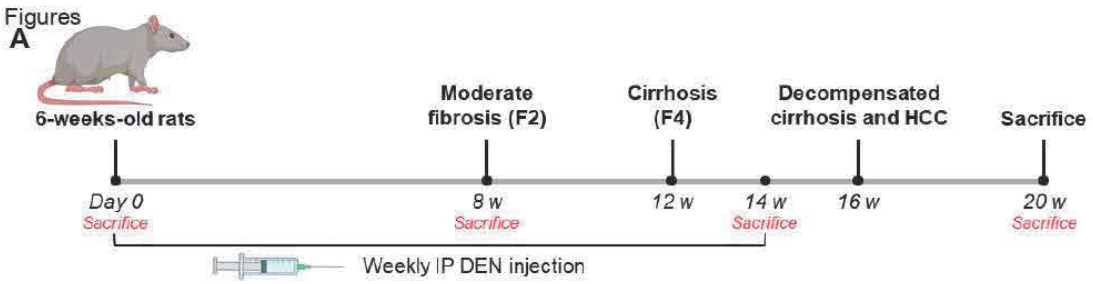
A
6-weeks-old rats
Moderate fibrosis (F2)
Cirrhosis (F4)
Decompensated cirrhosis and HCC
Sacrifice
Day 0
Sacrifice
8 w
Sacrifice
12 w
14 w
Sacrifice
16 w
20 w
Sacrifice
Weekly IP DEN injection

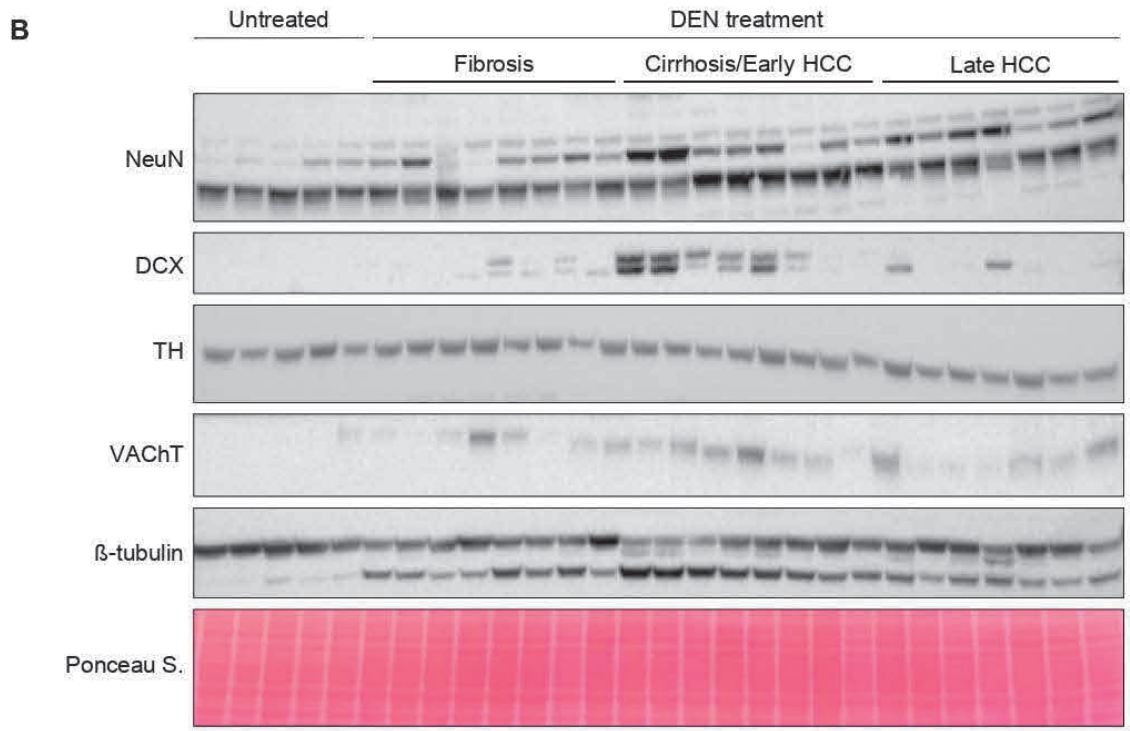
B
Untreated
DEN treatment
Fibrosis
Cirrhosis/Early HCC
Late HCC
NeuN
DCX
TH
VAChT
ß-tubulin
Ponceau S.

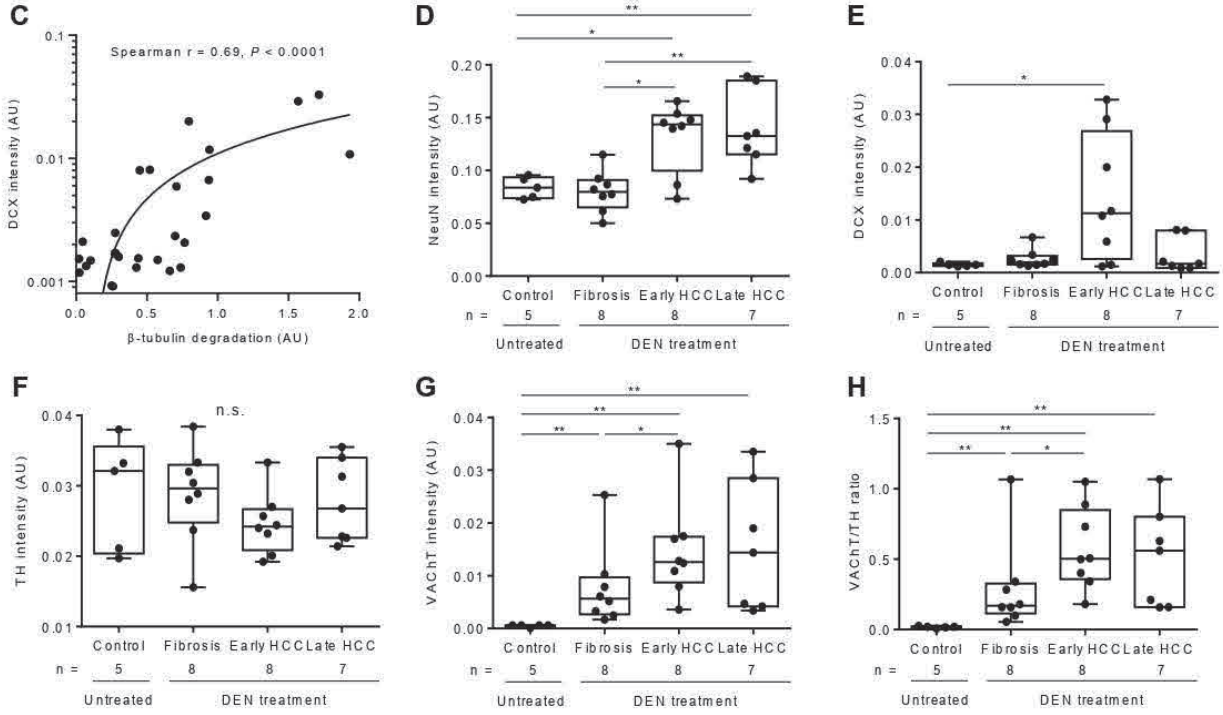
C
Spearman r = 0.69, P < 0.0001
DCX intensity (AU)
β-tubulin degradation (AU)
D
NeuN intensity (AU)
E
DCX intensity (AU)
F
TH intensity (AU)
n.s.
G
VAChT intensity (AU)
H
VAChT/TH ratio
Control
Fibrosis
Early HCC
Late HCC
n =
5
8
8
7
Untreated
DEN treatment

Figure 1.

Evolution towards HCC and hepatic remodeling are correlated with neurogenesis and parasympathetic orientation in the cirrhotic rat.

A. Experimental outline. 6-week-old Fischer 334 rats were given DEN at 50 mg/kg weekly from day 0 to week 14, allowing progression of chronic liver disease to fibrosis, cirrhosis, decompensated cirrhosis and HCC. **B.** Immunoblotting of NeuN (mature neurons), DCX (immature neurons), TH (adrenergic) and VAChT (cholinergic) neural markers. **C.** DCX induction is correlated with parenchymal remodeling. DCX levels were plotted against ratios of full-length versus degraded tubulin signals shown in panel B. Spearman test (*** $p < 0.001$). **C-H.** Signal quantification was done using the Fiji software on non-saturated images, using whole lane Ponceau S fluorescence (540 nm) for normalization, prior to statistical plotting using the Mann-Whitney test (* $p < 0.05$, ** $p < 0.01$). Five to eight rats were used per time point.

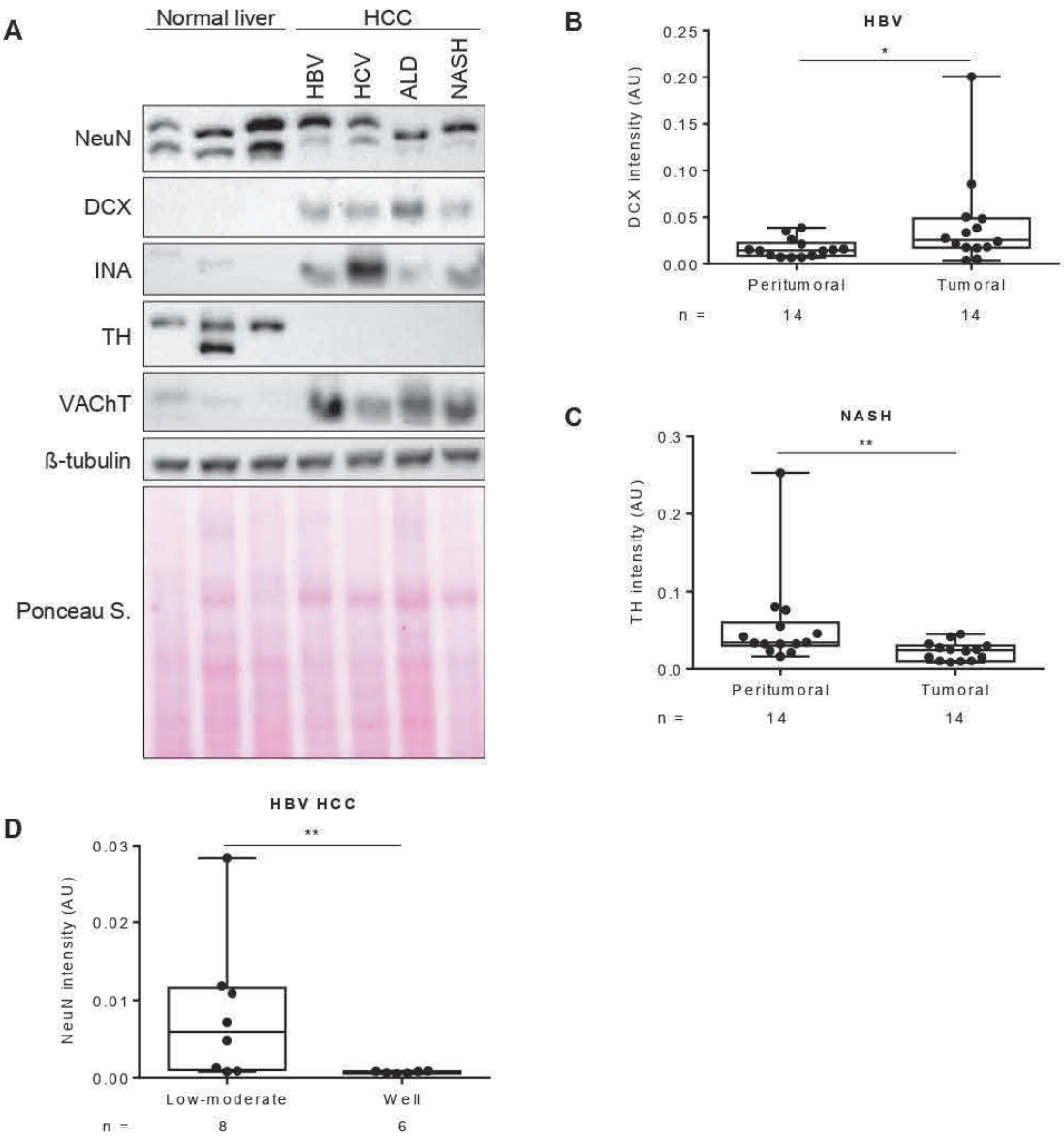

Figure 2.

Expression of mature and progenitor neural markers in human HCC.

A. Immunoblotting of NeuN (mature neurons), DCX and INA (immature neurons), TH (adrenergic) and VAChT (cholinergic) neural markers carried out on normal liver and HCC samples. **B-D.** Signal quantification of data presented in **Suppl. Fig. 2-6** was done using the Fiji software on non-saturated images, using whole lane Ponceau S fluorescence (540 nm) for normalization, prior to statistical plotting using the Mann-Whitney test (* $p < 0.05$). Quantifications conducted prior to (B-C) and after (D-G) patient segregation according to the differentiation grade of the disease. HCC: Hepatocellular carcinoma; HCV: Hepatitis C Virus; HBV: Hepatitis B Virus; ALD: Alcoholic Liver Disease; NAFLD: non-alcoholic fatty liver disease. Peritumoral: cirrhotic; Tumoral: HCC; HCC differentiation grade: Low/moderate or High.

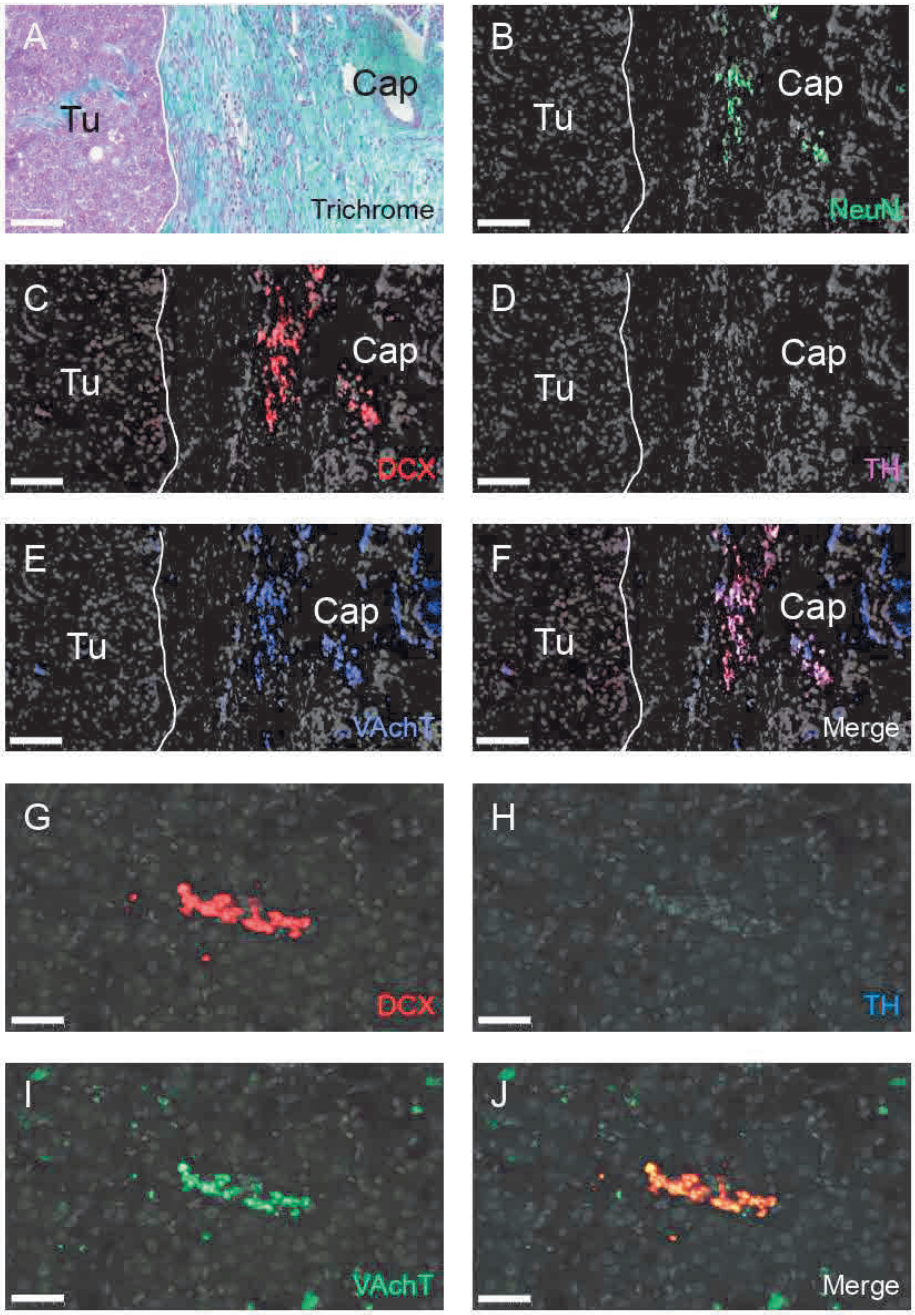

Figure 3.

Human HCCs harbor DCX+ neurogenesis with predominant parasympathetic features. A panel of 24 HCC samples derived from all four main etiologies (HBV: n = 7; HCV: n = 4; ALD: n = 9; NASH: n = 4) was probed for immunolocalization of NeuN, DCX, TH and VAChT by multiplex IHC. **A-F**. Masson's trichrome and IHC staining of a representative capsule-bearing tumor. **G-J.** Staining of a representative tumoral bulk. Nuclei appear as grey. Cap: capsule; Tu: tumoral bulk. Scale bars = 50 µm

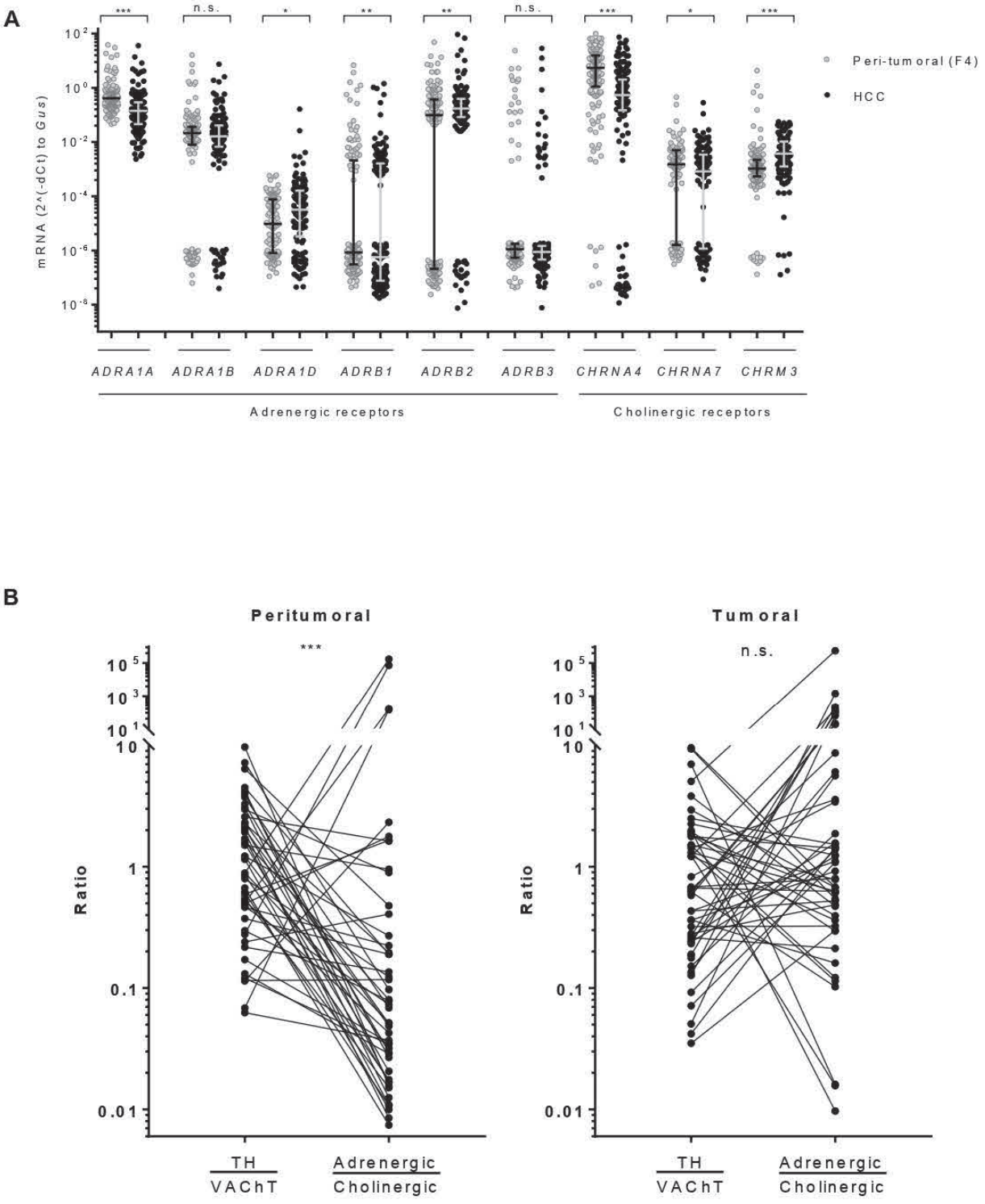
A
***
n.s.
*
**
**
n.s.
***
*
***
mRNA (2^(-dCt) to Gus)
Peri-tumoral (F4)
HCC
ADRA1A
ADRA1B
ADRA1D
ADRB1
ADRB2
ADRB3
CHRNA4
CHRNA7
CHRM3
Adrenergic receptors
Cholinergic receptors
B
Peritumoral
Tumoral
***
n.s.
Ratio
TH
VAChT
Adrenergic
Cholinergic

Figure 4.

Uncoupling of ANS receptors and ANS polarity in HCC upon comparison with non-tumoral paired tissues.

A. Adrenergic (ADR) and cholinergic (CHR) receptor abundance and expression in peritumoral tissue (F4) and HCC. 166 pairs of liver tissues were analyzed. Mann-Whitney test (* $p < 0.05$, ** $p < 0.01$, *** $p < 0.001$). **B.** Relationship between neuronal pre-synaptic marker and post-synaptic marker expression. TH and VAChT expression levels in peri-tumoral and tumoral samples (n = 51 HCC cases) were evaluated by immunoblotting with specific antibodies and normalized against Ponceau S staining. Gene expression levels of adrenergic and cholinergic receptors was evaluated by qPCR and normalized against *GUS* expression. Adrenergic/cholinergic ratio was calculated for each patient as follows: (*ADRA1A+ADRB2+ADRA1B*) / (*CHRNA4+CHRNA7+CHRM3*), where those six targets correspond to the most expressed of both categories in patient samples. Mann-Whitney test (* $p < 0.05$, ** $p < 0.01$, *** $p < 0.001$).

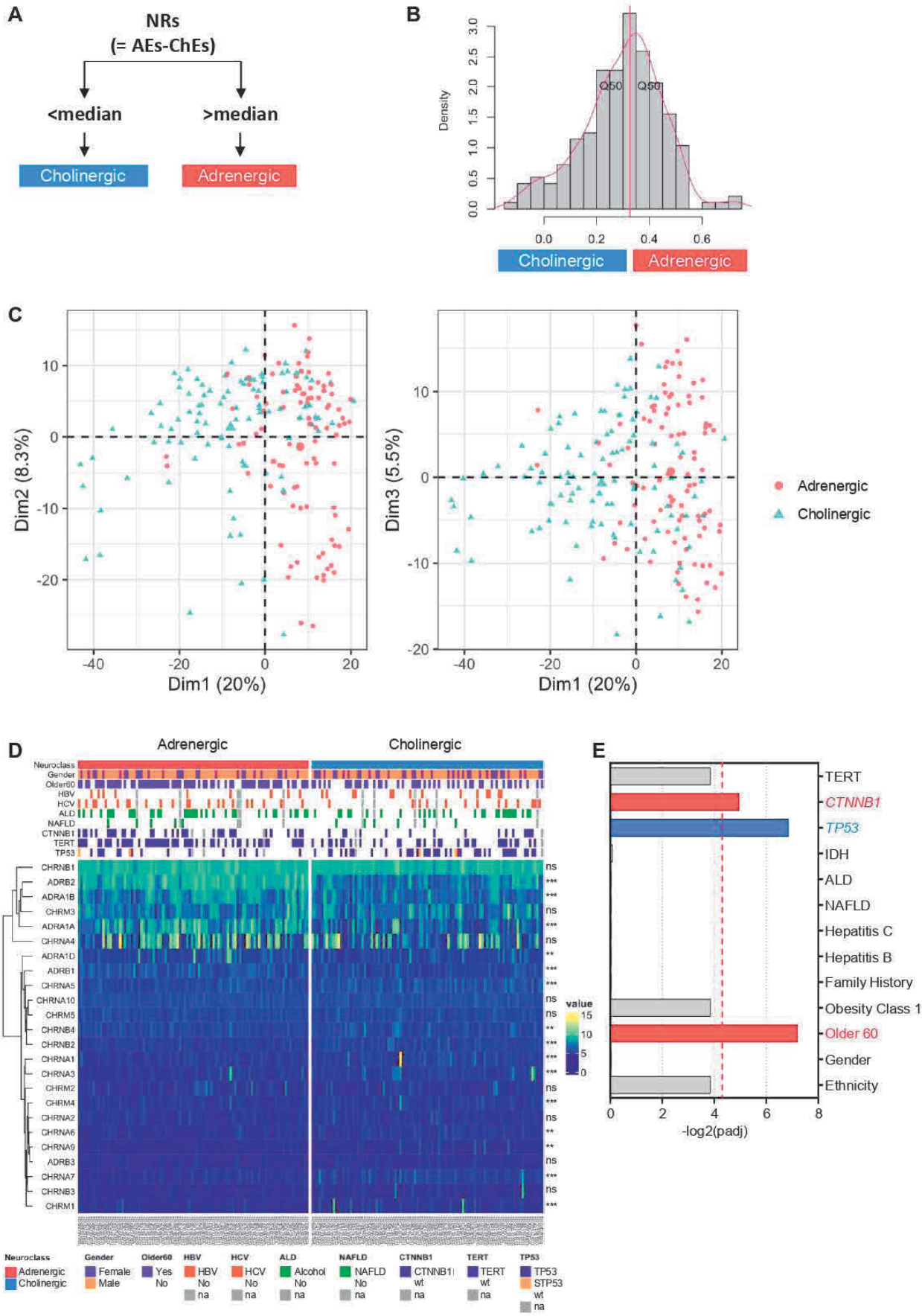
A
NRs
(= AEs-ChEs)
<median
>median
Cholinergic
Adrenergic
B
Density
Q50
Q50
Cholinergic
Adrenergic
C
Dim2 (8.3%)
Dim1 (20%)
Dim3 (5.5%)
Dim1 (20%)
Adrenergic
Cholinergic
D
Adrenergic
Cholinergic
Neuroclass
Gender
Older60
HBV
HCV
ALD
NAFLD
CTNNB1
TERT
TP53
CHRNB1
ADRB2
ADRA1B
CHRM3
ADRA1A
CHRNA4
ADRA1D
ADRB1
CHRNA5
CHRNA10
CHRM5
CHRNB4
CHRNB2
CHRNA1
CHRNA3
CHRM2
CHRM4
CHRNA2
CHRNA6
CHRNA9
ADRB3
CHRNA7
CHRNB3
CHRM1
value
Neuroclass
Adrenergic
Cholinergic
Gender
Female
Male
Older60
Yes
No
HBV
No
na
HCV
No
na
ALD
Alcohol
No
na
NAFLD
No
na
CTNNB1
wt
na
TERT
wt
na
TP53
STP53
wt
na
E
TERT
CTNNB1
TP53
IDH
ALD
NAFLD
Hepatitis C
Hepatitis B
Family History
Obesity Class 1
Older 60
Gender
Ethnicity
-log2(padj)

Figure 5.

Neurosignature based on adrenergic and cholinergic receptors in HCC.

A. Neuronal receptor score (NRs) calculation: adrenergic and cholinergic enrichment scores (AEs and ChEs, respectively) were calculated based on corresponding receptors gene set signatures for each sample, then cholinergic scores were subtracted from adrenergic scores. Samples were grouped in cholinergic and adrenergic classes depending on whether their ssGSEA score values (NRs) were below or above the calculated median, respectively. **B.** Histogram of NRs calculated by ssGSEA for HCC tumors. **C.** Sample distribution after dimensional reduction (PCA) based on the 10 per cent most variable genes (normalized values). Cholinergic neuroclass in blue and adrenergic neuroclass in red are contrasted. **D.** Heatmap of relative expression levels of all adrenergic and cholinergic receptors in HCC tumor samples. Once samples were classified in cholinergic and adrenergic receptor expression classes based on previously obtained signature scores, differential expression analysis was performed and expression values normalized (variance stabilization transformation) and shown in the heatmap. Older60: patients older than 60. HBV: Hepatitis B Virus; HCV: Hepatitis C Virus; ALD: Alcoholic Liver Disease; NAFLD: non-alcoholic fatty liver disease. Mutations: TP53, CTNNB1, TERT; wt: wild type. na: no information available. **E**. Associations between neuroclasses and main HCC clinico-biological features. Fisher test's adjusted *p*-values per variable (** $p < 0.01$, *** $p < 0.001$).

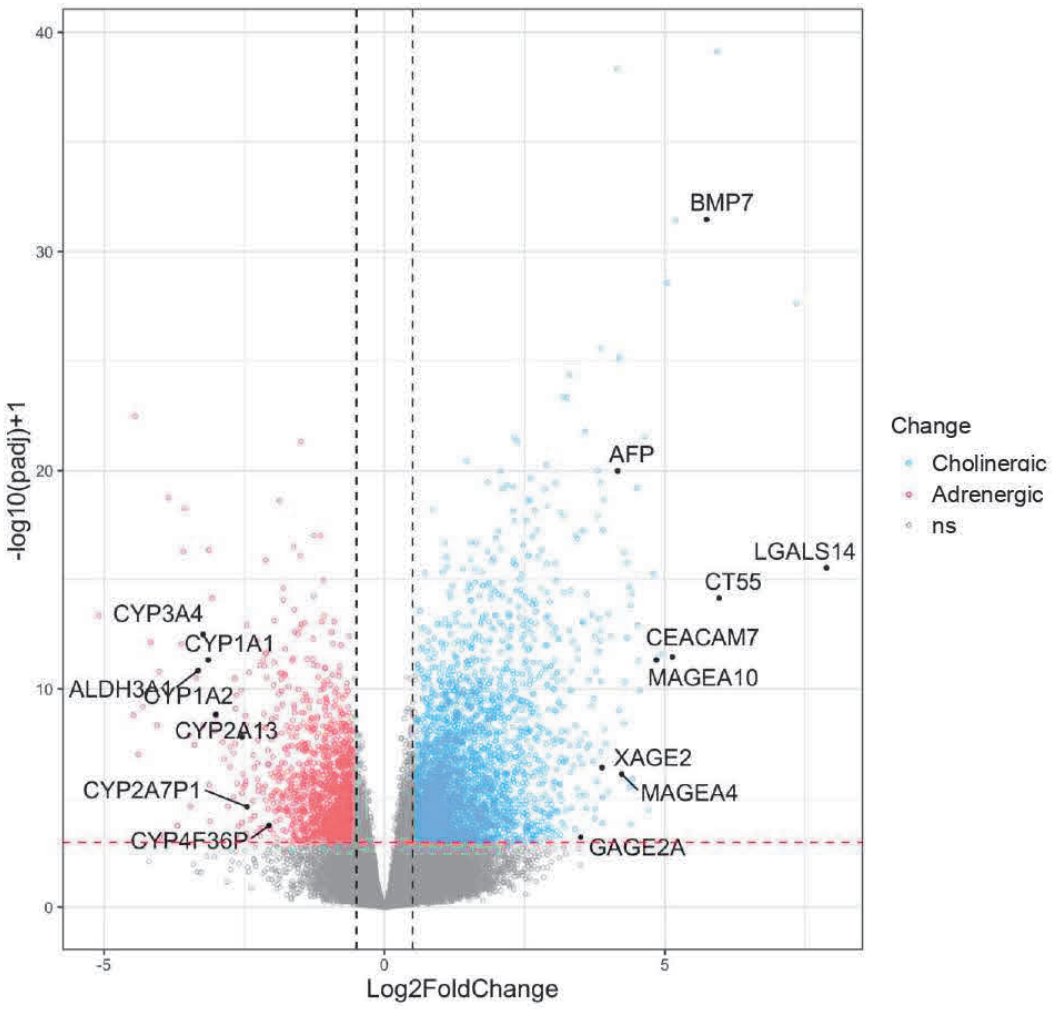

Figure 6.

Transcriptomic features of adrenergic and cholinergic signatures analyzed by DGE. Volcano plot showing differentially-expressed genes in the cholinergic neuroclass compared to the adrenergic neuroclass. Genes with lowest adjusted p-value are indicated. The horizontal red bar represents the adjusted p-value threshold at 0.01. The higher the location of a gene, the stronger its association with a low adjusted p-value (significance). The more a gene is located to the right or left, the stronger its association with a high absolute Log2 fold-change. Increased and decreased genes were considered if absolute Log2 fold-change value was higher than 0.58 and adjusted p-value < than 0.01.

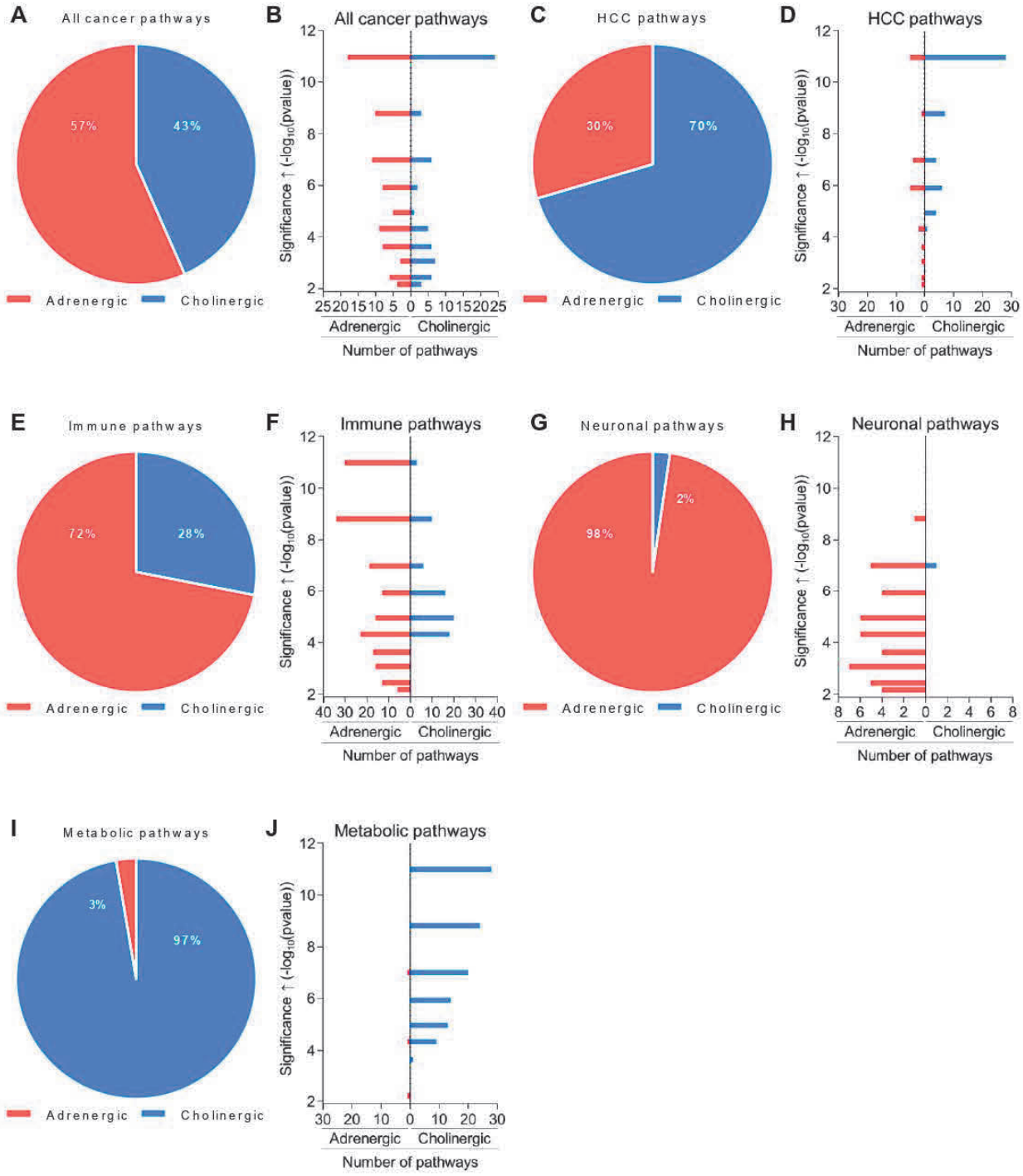
A
All cancer pathways
57%
43%
Adrenergic
Cholinergic
B
All cancer pathways
Significance ↑ (-log10(pvalue))
Adrenergic
Cholinergic
Number of pathways
C
HCC pathways
30%
70%
Adrenergic
Cholinergic
D
HCC pathways
Significance ↑ (-log10(pvalue))
Adrenergic
Cholinergic
Number of pathways
E
Immune pathways
72%
28%
Adrenergic
Cholinergic
F
Immune pathways
Significance ↑ (-log10(pvalue))
Adrenergic
Cholinergic
Number of pathways
G
Neuronal pathways
98%
2%
Adrenergic
Cholinergic
H
Neuronal pathways
Significance ↑ (-log10(pvalue))
Adrenergic
Cholinergic
Number of pathways
I
Metabolic pathways
3%
97%
Adrenergic
Cholinergic
J
Metabolic pathways
Significance ↑ (-log10(pvalue))
Adrenergic
Cholinergic
Number of pathways

Figure 7.

HCC- and neurally-relevant pathways correlated with each neuroclass as identified by Gene Set Enrichment Analysis (GSEA).

From up-regulated (derived from adrenergic tumors) and down-regulated (derived from cholinergic tumors) transcripts obtained by differential gene expression analysis, enriched pathways were identified. Pathways with adjusted p-value < 0.01 were selected. **A,C,E,G,I**. Pathway allocation to each neuroclass. **B,D,F,H,J**. Statistical significance of both groups of pathways. The higher the pathway on the plot (low *p*-value then (-Log)-transformed), the stronger its association with the neuroclass of interest. The key-words used for the search are the following: Cancer terms: CANCER|TUMOR. HCC terms: HEPATOCELLULAR_CARCINOMA|HCC Immune terms: IMMUN|MACROPHAGE|PHAGO|IGM|ANTIGEN|LEUKO|CYTO|TREG|LYMPHOCYTE|CHEMOKINE|INTERLEUKIN|MONOCYTE|T_CELL|NEUTROPHIL|MACROPHAGE|CD8|CD4|REGULATORY_T|DENDRITIC|B_CELL|NK_CELL|NATURAL_KILLER|INFECTION|INFLAMATION. Neuronal terms: NEUR|SYNAP|AXON|NERV. Metabolic terms: METAB|ANAB|CATAB

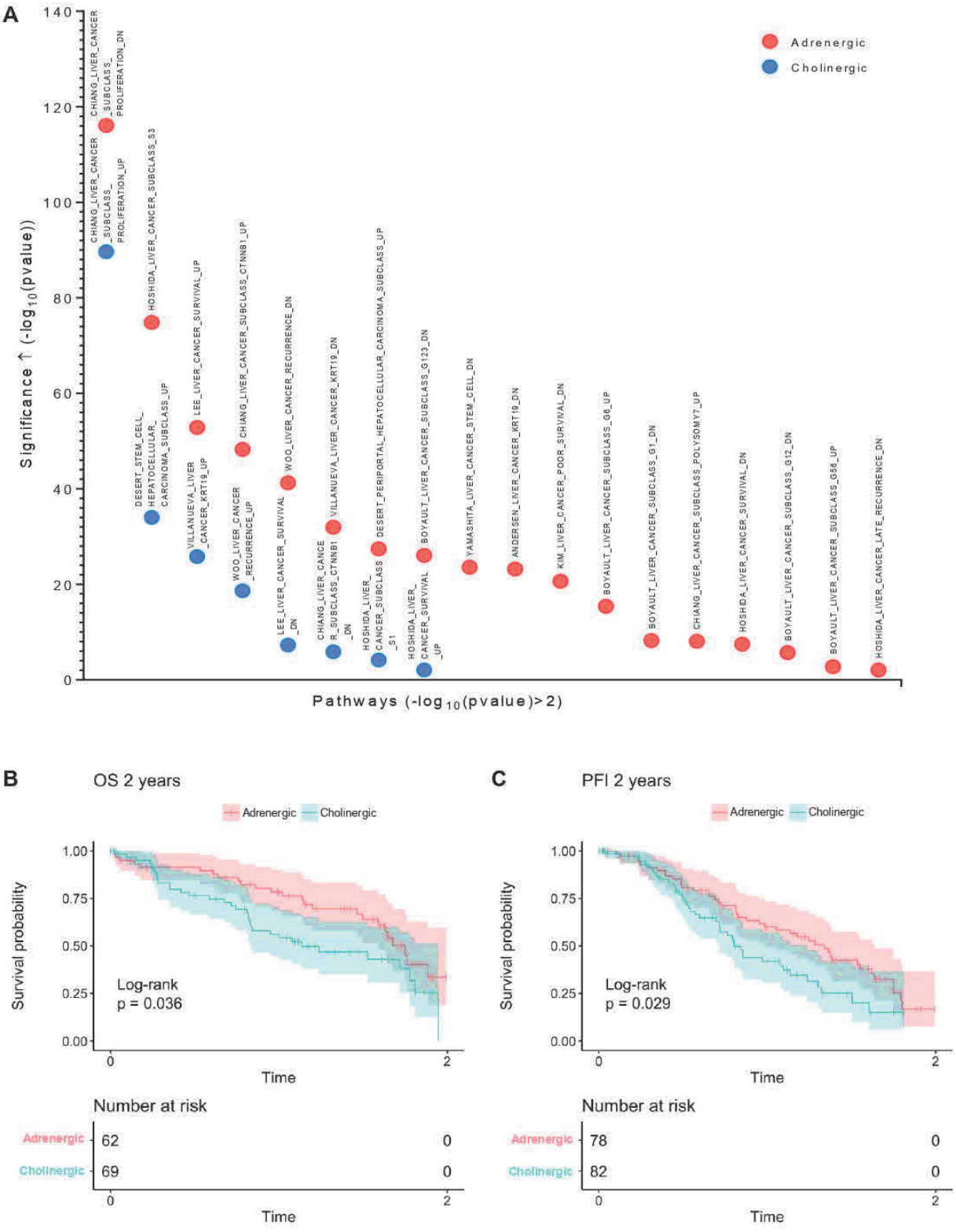
A
Adrenergic
Cholinergic
Significance ↑ (-log10(pvalue))
Pathways (-log10(pvalue)>2)
CHIANG_LIVER_CANCER_SUBCLASS_PROLIFERATION_DN
CHIANG_LIVER_CANCER_SUBCLASS_PROLIFERATION_UP
HOSHIDA_LIVER_CANCER_SUBCLASS_S3
DESERT_STEM_CELL_HEPATOCELLULAR_CARCINOMA_SUBCLASS_UP
LEE_LIVER_CANCER_SURVIVAL_UP
VILLANUEVA_LIVER_CANCER_KRT19_UP
CHIANG_LIVER_CANCER_SUBCLASS_CTNNB1_UP
WOO_LIVER_CANCER_RECURRENCE_UP
WOO_LIVER_CANCER_RECURRENCE_DN
LEE_LIVER_CANCER_SURVIVAL_DN
VILLANUEVA_LIVER_CANCER_KRT19_DN
CHIANG_LIVER_CANCER_SUBCLASS_CTNNB1_DN
DESERT_PERIPORTAL_HEPATOCELLULAR_CARCINOMA_SUBCLASS_UP
HOSHIDA_LIVER_CANCER_SUBCLASS_S1
BOYAULT_LIVER_CANCER_SUBCLASS_G123_DN
HOSHIDA_LIVER_CANCER_SURVIVAL_UP
YAMASHITA_LIVER_CANCER_STEM_CELL_DN
ANDERSEN_LIVER_CANCER_KRT19_DN
KIM_LIVER_CANCER_POOR_SURVIVAL_DN
BOYAULT_LIVER_CANCER_SUBCLASS_G6_UP
BOYAULT_LIVER_CANCER_SUBCLASS_G1_DN
CHIANG_LIVER_CANCER_SUBCLASS_POLYSOMY7_UP
HOSHIDA_LIVER_CANCER_SURVIVAL_DN
BOYAULT_LIVER_CANCER_SUBCLASS_G12_DN
BOYAULT_LIVER_CANCER_SUBCLASS_G56_UP
HOSHIDA_LIVER_CANCER_LATE_RECURRENCE_DN
B
OS 2 years
Adrenergic
Cholinergic
Survival probability
Log-rank
p = 0.036
Time
Number at risk
Adrenergic 62 0
Cholinergic 69 0
C
PFI 2 years
Log-rank
p = 0.029
Number at risk
Adrenergic 78 0
Cholinergic 82 0

Figure 8.

Adrenergic orientation of HCC is of better prognosis than cholinergic orientation.

A. Statistical significance of adrenergic (red circles) and cholinergic (blue circles) tumor-associated HCC signatures. Attention needs to be paid to their actual biological significance extracted from the MSigDB database, listed in **Suppl. Table 9**, before drawing conclusions with respect to pathology. **B-C.** Kaplan-Meier representation of the predictive value of both neuroclasses with respect to overall survival (OS) and progression-free interval (PFI) in HCC.

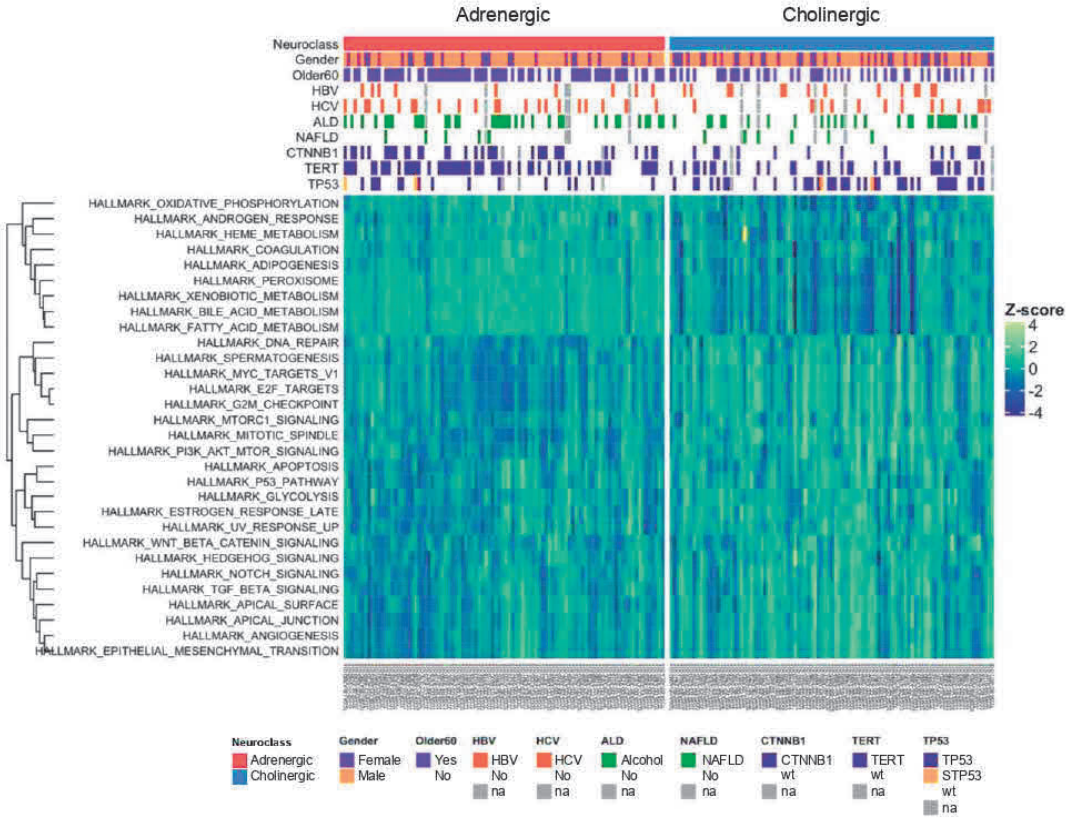

Figure 9.

Adrenergic and cholinergic-associated hallmark pathways determined by single sample Gene Set Enrichment Analysis (ssGSEA).

ssGSEA scores were calculated for each sample. Pathways comparison between neuroclasses was performed with the Wilcoxon Test and significant pathways (padj < 0.05) selected. Older60: patients older than 60. HBV: Hepatitis B Virus; HCV: Hepatitis C Virus; ALD: Alcoholic Liver Disease; NAFLD: non-alcoholic fatty liver disease. Mutations: TP53, CTNNB1, TERT; wt wild type. na: no information available.

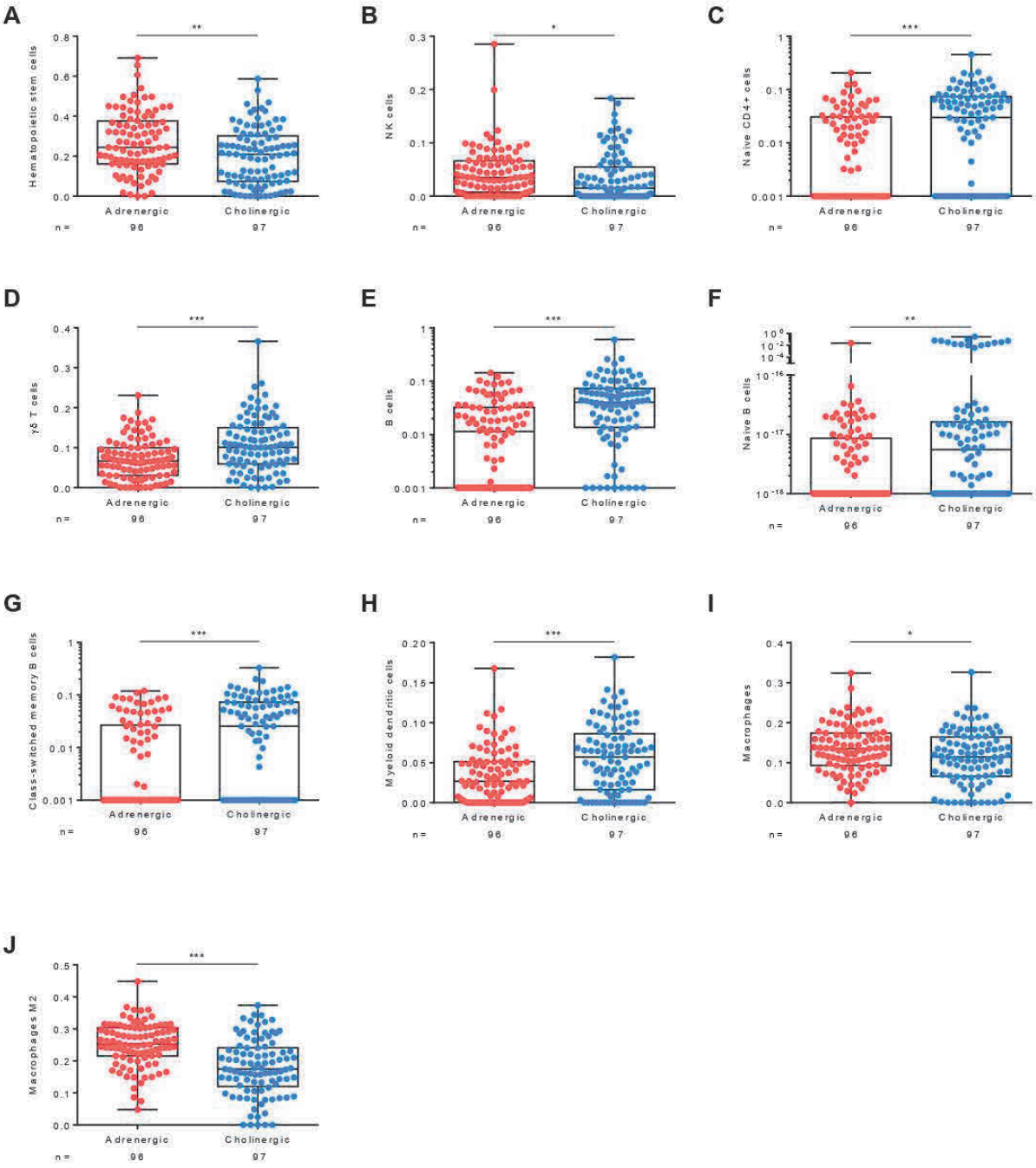

Figure 10.

Immune infiltration in HCC tumor samples determined by the xCell method.

To determine statistical differences for each cell type between neuroclasses, a Wilcoxon Test was performed on 36 immune subpopulations using the immune Xcell score. Significant data obtained on 10 of them are shown (panels **A-J**). Differences in immune cell types were defined by padj < 0.05.

Supplementary Table 1. Characteristics of paired F4/HCC samples used in the study.

Median ± SD is shown for all qualitative data

Variable	Available data (Total: 166)	Values
Age, *y* ± SD	166	69 ± 10
Gender (male/female)	166	140 (84%)/26 (16%)
Etiology (%)	166	
Alcoholic liver disease		36 (21%)
Hepatitis B virus		46 (28%)
Hepatitis C virus		39 (24%)
Non-alcoholic steato-hepatitis		45 (27%)
Serum alpha-fetoprotein, >100 ng/mL	111	17 (16%)
Child-Pugh score (A/B/C) (%)	87	72 (83%)/9 (11%)/6 (6%)
Prothrombin, % ± SD	146	81 ± 22
Bilirubin, µMol/L ± SD	137	14 ± 75
Albumin, g/L ± SD	100	36 ± 7
Platelet count, G/L ± SD	149	131 ± 102
Encephalopathy (%)	164	18 (11%)
Ascites (%)	164	37 (3%)
Jaundice (%)	162	22 (14%)
Esophageal varices (%)	156	62 (40%)
Histological and gross features of the tumors		
Tumor size, *mm* ± SD	165	34 ± 31
Tumor localization (left liver/right liver/double)	165	47 (29%)/112 (68%)/6 (4%)
Intact tumor capsule (%)	143	91 (64%)
Satellite nodules (%)	165	34 (21%)
Macrovascular invasion, Microvascular invasion (%)	151	22 (15%), 81 (52%)
Differentiation grade (poor/moderately/well) (%)	165	15 (9%)/74 (45%)/76 (46%)
Architectural pattern (%)	136	
Trabecular		104 (76%)
Pseudoglandular		10 (7%)
Compact		5 (4%)
Clear cells		4 (3%)
Others		13 (9%)
Tumoral steatosis (%)	165	108 (66%)
Tumoral necrosis (%)	150	84 (56%)
Liver fibrosis score METAVIR (F4) (%)	166	166 (100%)
Inflammation activity score (%)	137	
METAVIR 0		51 (37%)
METAVIR 1		55 (40%)

METAVIR 2	23 (17%)
METAVIR 3	8 (6%)

Supplementary Table 2.

Significance assessment of neural features in HCC. Significance calculated after Western blot and subsequent quantification (stratification based on etiology or Edmonson differentiation grade). Mann-Whitney test (n = 51 patients total, * $p < 0.05$, ** $p < 0.01$, *** $p < 0.001$).

Comparison *tumoral* over *peritumoral*	HBV	HCV	NASH	ALD
NeuN	ns	ns	ns	ns
DCX	*	ns	ns	ns
INA	ns	ns	ns	ns
TH	ns	ns	**	ns
VAChT	ns	ns	ns	ns
VAChT/TH ratio	ns	ns	ns	ns

Comparison *high* over *low-medium*	HBV	HCV	NASH	ALD
NeuN	*	ns	ns	ns
DCX	ns	ns	ns	ns
INA	ns	ns	*	*
TH	ns	ns	ns	ns
VAChT	ns	ns	*	ns
VAChT/TH ratio	ns	ns	ns	ns

Supplementary Table 9.

Biological descriptions of prognosis pathways associated with both HCC neuroclasses.

Standard name	Brief description	Systematic name
ANDERSEN_LIVER_CANCER_KRT19_DN	Genes under-expressed in KRT19-positive [GeneID=3880] hepatocellular carcinoma.	M424
BOYAULT_LIVER_CANCER_SUBCLASS_G1_DN	Down-regulated genes in hepatocellular carcinoma (HCC) subclass G1, defined by unsupervised clustering	M1883
BOYAULT_LIVER_CANCER_SUBCLASS_G12_DN	Down-regulated genes in hepatocellular carcinoma (HCC) subclass G12, defined by unsupervised clustering	M12228
BOYAULT_LIVER_CANCER_SUBCLASS_G123_DN	Down-regulated genes in hepatocellular carcinoma (HCC) subclass G123, defined by unsupervised clustering.	M2218
BOYAULT_LIVER_CANCER_SUBCLASS_G6_UP	Up-regulated genes in hepatocellular carcinoma (HCC) subclass G6, defined by unsupervised clustering.	M4342
CHIANG_LIVER_CANCER_SUBCLASS_CTNNB1_DN	Top 200 marker genes down-regulated in the 'CTNNB1' subclass of hepatocellular carcinoma (HCC); characterized by activated CTNNB1 [GeneID=1499].	M8689
CHIANG_LIVER_CANCER_SUBCLASS_CTNNB1_UP	Top 200 marker genes up-regulated in the 'CTNNB1' subclass of hepatocellular carcinoma (HCC); characterized by activated CTNNB1 [GeneID=1499].	M16496
CHIANG_LIVER_CANCER_SUBCLASS_INTERFERON_DN	All marker genes down-regulated in the 'interferon' subclass of hepatocellular carcinoma (HCC).	M14353
CHIANG_LIVER_CANCER_SUBCLASS_POLYSOMY7_UP	Marker genes up-regulated in the 'chromosome 7 polysomy' subclass of hepatocellular carcinoma (HCC); characterized by polysomy of chromosome 7 and by a lack of gains of chromosome 8q.	M834
CHIANG_LIVER_CANCER_SUBCLASS_PROLIFERATION_DN	Top 200 marker genes down-regulated in the 'proliferation' subclass of hepatocellular carcinoma (HCC); characterized by increased proliferation, high levels of serum AFP [GeneID=174], and chromosomal instability.	M16932
CHIANG_LIVER_CANCER_SUBCLASS_PROLIFERATION_UP	Top 200 marker genes up-regulated in the 'proliferation' subclass of hepatocellular carcinoma (HCC); characterized by increased proliferation, high levels of serum AFP [GeneID=174], and chromosomal instability.	M3268
DESERT_PERIPORTAL_HEPATOCELLULAR_CARCINOMA_SUBCLASS_UP	Genes up-regulated in the periportal-type subclass of hepatocellular carcinomas.	M34031

DESERT_STEM_CELL_HEPATOCELLULAR_CARCINOMA_SUBCLASS_UP	Genes up-regulated in the stem cell-type subclass of hepatocellular carcinomas.	M34034
HOSHIDA_LIVER_CANCER_LATE_RECURRENCE_DN	Genes whose expression correlated with lower risk of late recurrence of hepatocellular carcinoma (HCC).	M13658
HOSHIDA_LIVER_CANCER_SUBCLASS_S1	Genes from 'subtype S1' signature of hepatocellular carcinoma (HCC): aberrant activation of the WNT signaling pathway.	M5311
HOSHIDA_LIVER_CANCER_SUBCLASS_S3	Genes from 'subtype S3' signature of hepatocellular carcinoma (HCC): hepatocyte differentiation.	M1286
HOSHIDA_LIVER_CANCER_SURVIVAL_DN	Survival signature genes defined in adjacent liver tissue: genes correlated with good survival of hepatocellular carcinoma (HCC) patients.	M5451
HOSHIDA_LIVER_CANCER_SURVIVAL_UP	Survival signature genes defined in adjacent liver tissue: genes correlated with poor survival of hepatocellular carcinoma (HCC) patients.	M6939
KIM_LIVER_CANCER_POOR_SURVIVAL_DN	Genes under-expressed in hepatocellular carcinoma (HCC) with poor survival	M534
LEE_LIVER_CANCER_SURVIVAL_DN	Genes highly expressed in hepatocellular carcinoma with worse survival.	M7987
LEE_LIVER_CANCER_SURVIVAL_UP	Genes highly expressed in hepatocellular carcinoma with better survival.	M6145
VILLANUEVA_LIVER_CANCER_KRT19_DN	Genes under-expressed in KRT19-positive [GeneID=3880] hepatocellular carcinoma (HCC).	M373
VILLANUEVA_LIVER_CANCER_KRT19_UP	Genes over-expressed in KRT19-positive [GeneID=3880] hepatocellular carcinoma (HCC).	M336
WOO_LIVER CANCER RECURRENCE_DN	Genes negatively correlated with recurrence free survival in patients with hepatitis B-related (HBV) hepatocellular carcinoma (HCC).	M9911
WOO_LIVER_CANCER_RECURRENCE_UP	Genes positively correlated with recurrence free survival in patients with hepatitis B-related (HBV) hepatocellular carcinoma (HCC).	M12602
YAMASHITA_LIVER_CANCER_STEM_CELL_DN	Genes down-regulated in hepatocellular carcinoma (HCC) cells with hepatic stem cell properties.	M9206

Supplementary Table 12.

Antibodies used in this study.

Antigen	Ig Species	Cat. Number & supplier	Antibody registry (RRID) #
Beta-tubulin	Rabbit polyclonal	Ab6046, Abcam	AB_2210370
NeuN	Mouse monoclonal	MAB377, Millipore	AB_2298772
DCX	Mouse monoclonal Rabbit polyclonal	Ab18723, Abcam (WB) MABN707, Millipore (IHC)	AB_732011 ND
Alpha-internexin	Mouse monoclonal	MAB5224, Millipore	AB_2127486
TH	Rabbit polyclonal Rabbit polyclonal	AB152, Millipore (WB) Ab112, Abcam (IHC)	AB_390204 AB_297840
VAChT	Mouse monoclonal Rabbit polyclonal	SAB5200240, Sigma (WB) PA5-85782, Invitrogen (IHC)	ND AB_2992918
Anti-mouse-HRP	Goat polyclonal	A4416, Sigma	AB_258167
Anti-Rabbit-HRP	Goat polyclonal	A6154, Sigma	AB_258284

Supplementary Table 13.

Human qPCR primers.

Gene symbol	Genbank acc. #	Primer sequences (5'-3', F/R)	PCR conditions	Amplicon length, bp
GUS	NM_001293105	CGTGGTTGGAGAGCTCATTTGGAA TTCCCCAGCACTCTCGTCGGT	Denaturing, 95°C; annealing, 55°C	72
CHRM3	NM_000740	TACCTGGAACAGGTGGAGC GATCCCGGCATAGGACAGAG	Denaturing, 95°C; annealing, 60°C	73
CHRNA4	NM_000744.7	CTCCGAGCTCATCTGGCG TCCCCGTCAGCATTGTTGTA	Denaturing, 95°C; annealing, 60°C	72
CHRNA7	NM_000746.6	GCTGGTCAAGAACTACAATCCC CTCATCCACGTCCATGATCTG	Denaturing, 95°C; annealing, 60°C	106
ADRA1A	NM_000680.4	CCAAGACGGATGGCGTTTG TGGACACTGTAATCCTGGCAG	Denaturing, 95°C; annealing, 60°C	75
ADRA1B	NM_000679.4	TGGGGCGGATCTTCTGTGA GTGACCAGCGTGGGATACTG	Denaturing, 95°C; annealing, 60°C	136
ADRA1D	NM_000678.4	GCCGCTCGGCTCCTTG GGCTGGAACAGGGGTAGATG	Denaturing, 95°C; annealing, 60°C	116
ADRB1	NM_000684.3	ATCGAGACCCTGTGTGTCATT GTAGAAGGAGACTACGGACGAG	Denaturing, 95°C; annealing, 60°C	267
ADRB2	NM_000024.6	TGGTGTGGATTGTGTCAGGC GGCTTGGTTCGTGAAGAAGTC	Denaturing, 95°C; annealing, 60°C	128
ADRB3	NM_000025.3	GACCAACGTGTTCGTGACTTC GCACAGGGTTTCGATGCTG	Denaturing, 95°C; annealing, 60°C	175

Supplementary figures

Click here to access/download;Supplemental Text and Figures;Supplementary figures neuro hcc.pptx

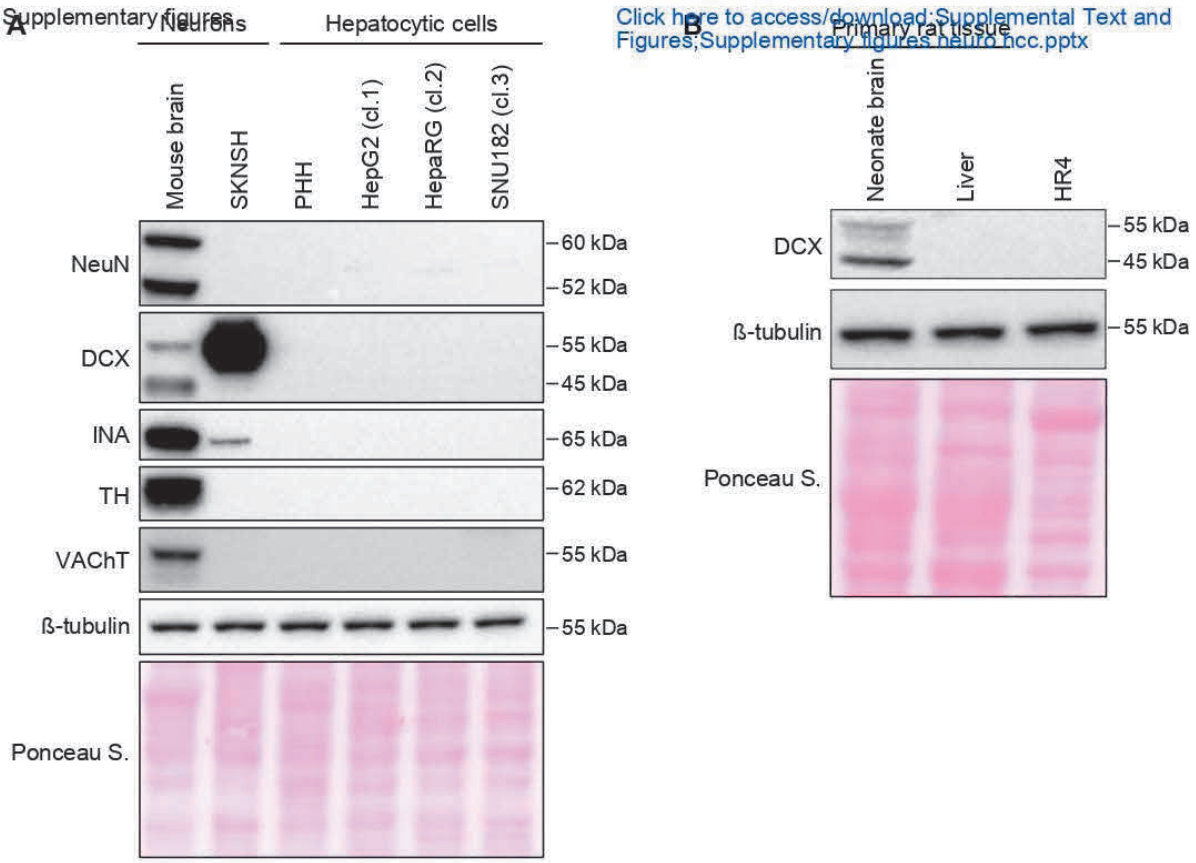

Supplementary Figure 1.

Validation of anti-NeuN, DCX, INA, TH and VAChT antibodies by Western Blot.

A. Extracts from neonate mouse brain, SKNSH, PHH, and human HCC lines belonging to transcriptomic classes 1, 2 and 3 (Caruso et al., 2019) were processed for detection of the indicated targets. **B.** The same strategy was used for the validation of an anti-DCX antibody specifically suitable for rat epitopes.

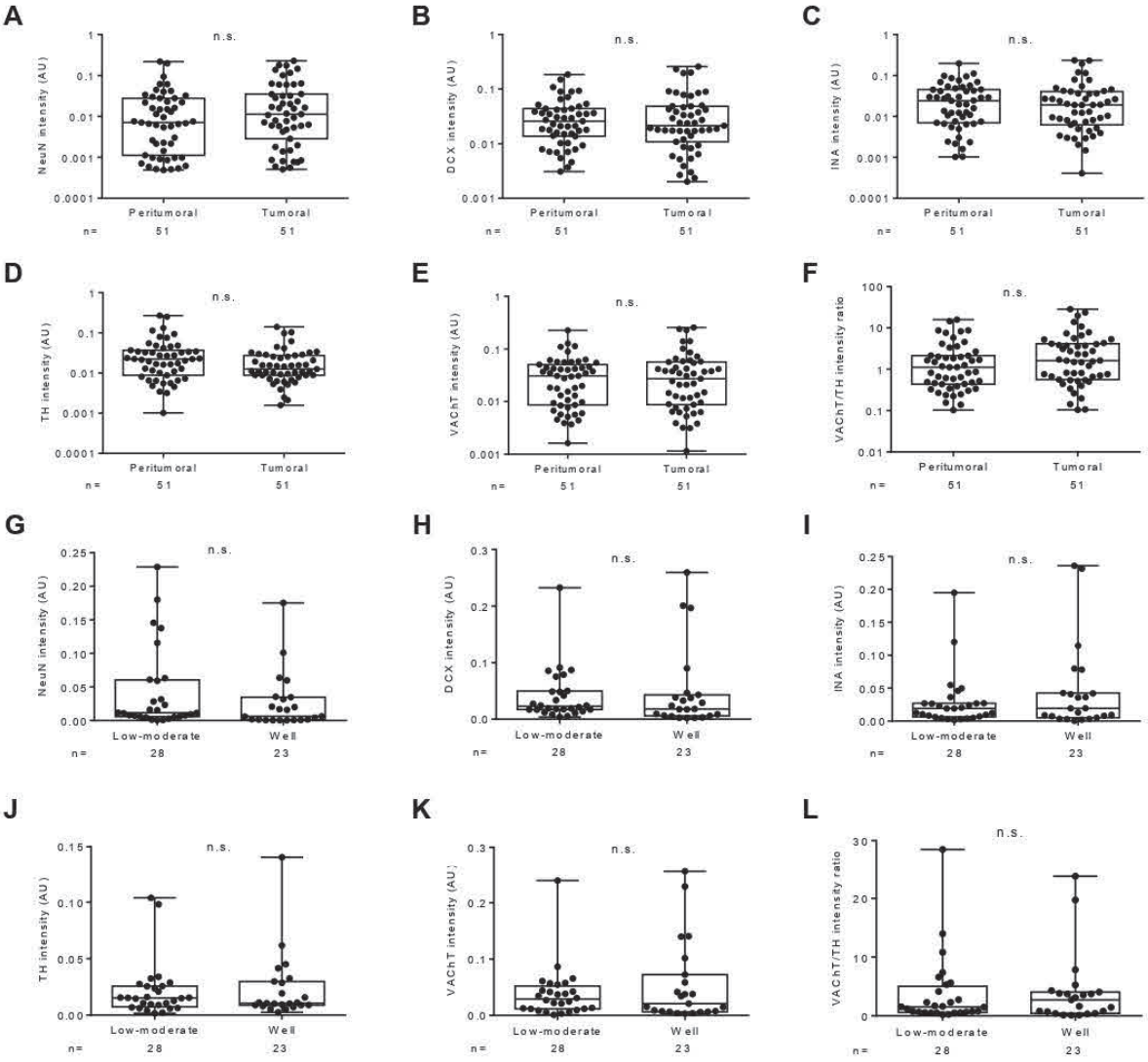

Supplementary Figure 2.

Quantification of mature and progenitor neural markers in human HCC of all etiologies.

A-L. Signal quantification was done using the Fiji software on non-saturated images, using whole lane Ponceau S fluorescence (540 nm) for normalization, prior to statistical plotting using the Mann-Whitney test (n = 51 patients, n.s). Quantification before (A-F) and after (G-L) patient stratification based on the 'low/moderate' or 'well' level of differentiation.

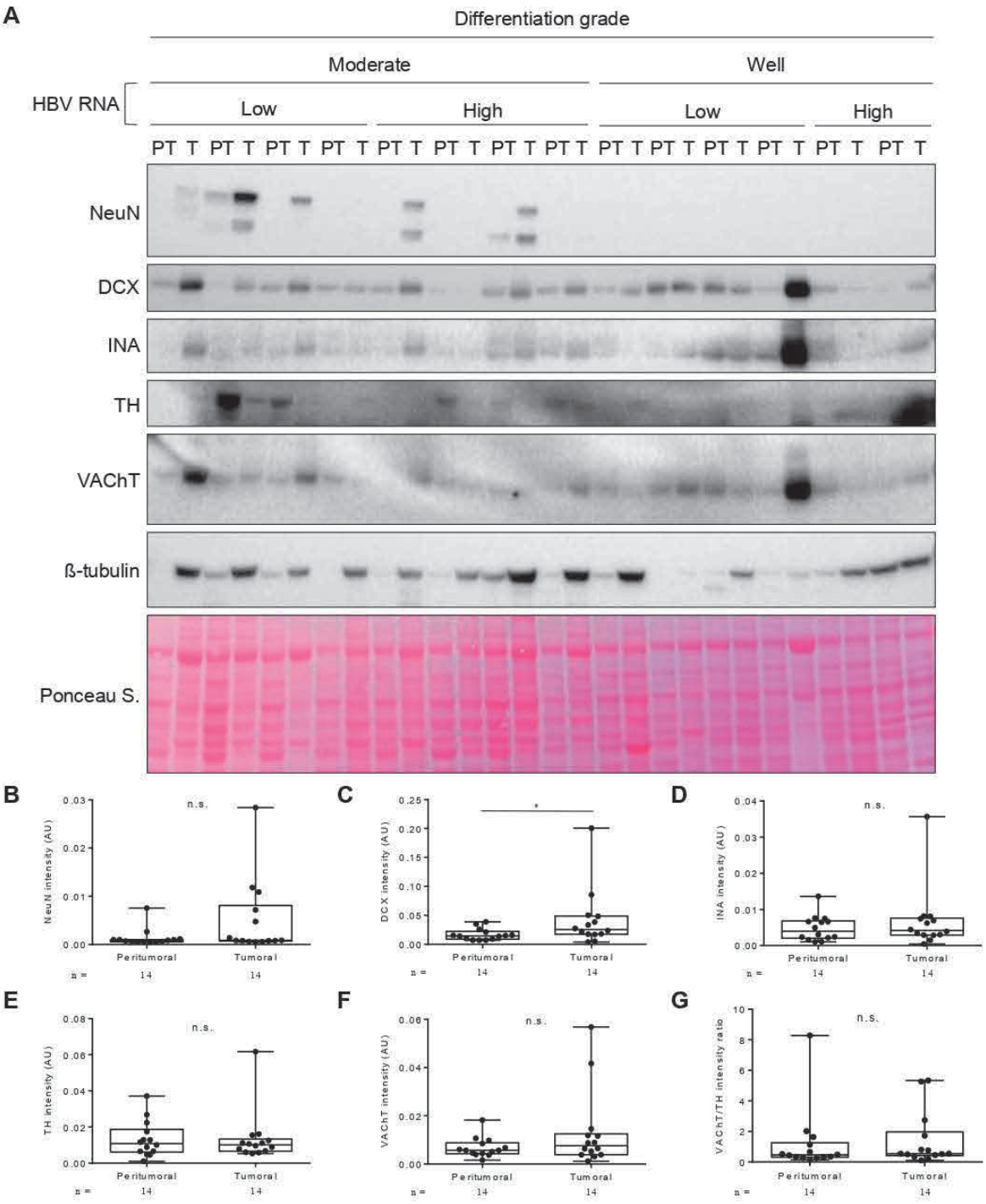

Supplementary Figure 3.

Expression of mature and progenitor neural markers in human HCC of HBV etiology.

A. Immunoblotting on neural markers using antibodies against NeuN, DCX, TH and VAChT neural markers and *β*-tubulin as an internal control. **B-G.** Signal quantification was done using the Fiji software on non-saturated images, using whole lane Ponceau S fluorescence (540 nm) for normalization, prior to statistical plotting using the Mann-Whitney test (n = 14 patients, * $p < 0.05$, ** $p < 0.01$, *** $p < 0.001$).

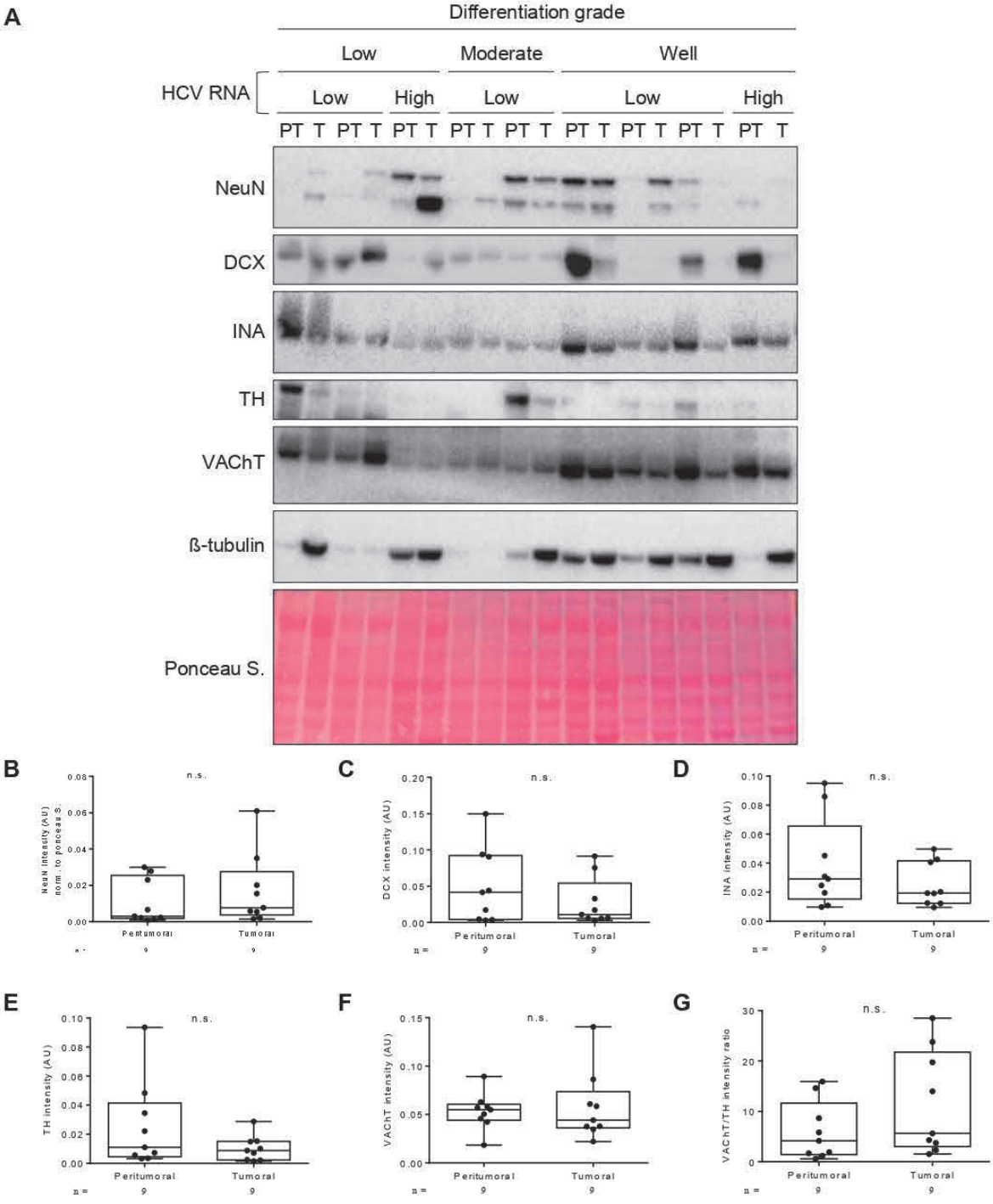

Supplementary Figure 4.

Expression of mature and progenitor neural markers in human HCC of HCV etiology.

A. Immunoblotting on neural markers using the above-mentioned antibodies. **B-G.** Signal quantification was done using the Fiji software on non-saturated images, using whole lane Ponceau S fluorescence (540 nm) for normalization, prior to statistical plotting using the Mann-Whitney test (n = 9 patients, * $p < 0.05$, ** $p < 0.01$, *** $p < 0.001$).

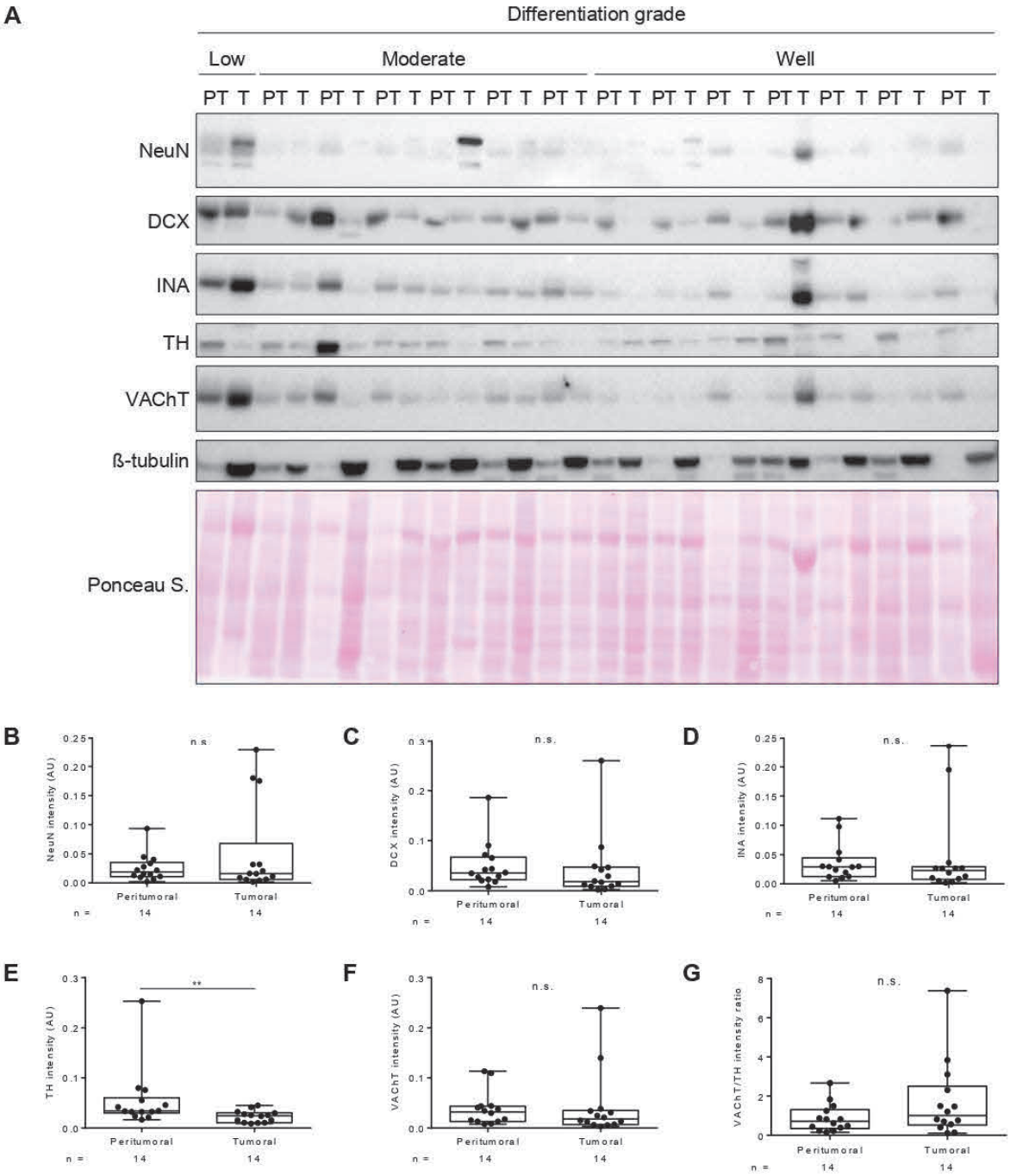

Supplementary Figure 5.

Expression of mature and progenitor neural markers in human HCC of NASH etiology.

A. Immunoblotting on neural markers using the above-mentioned antibodies. **B-G.** Signal quantification was done using the Fiji software on non-saturated images, using whole lane Ponceau S fluorescence (540 nm) for normalization, prior to statistical plotting using the Mann-Whitney test (n = 14 patients, * $p < 0.05$, ** $p < 0.01$, *** $p < 0.001$).

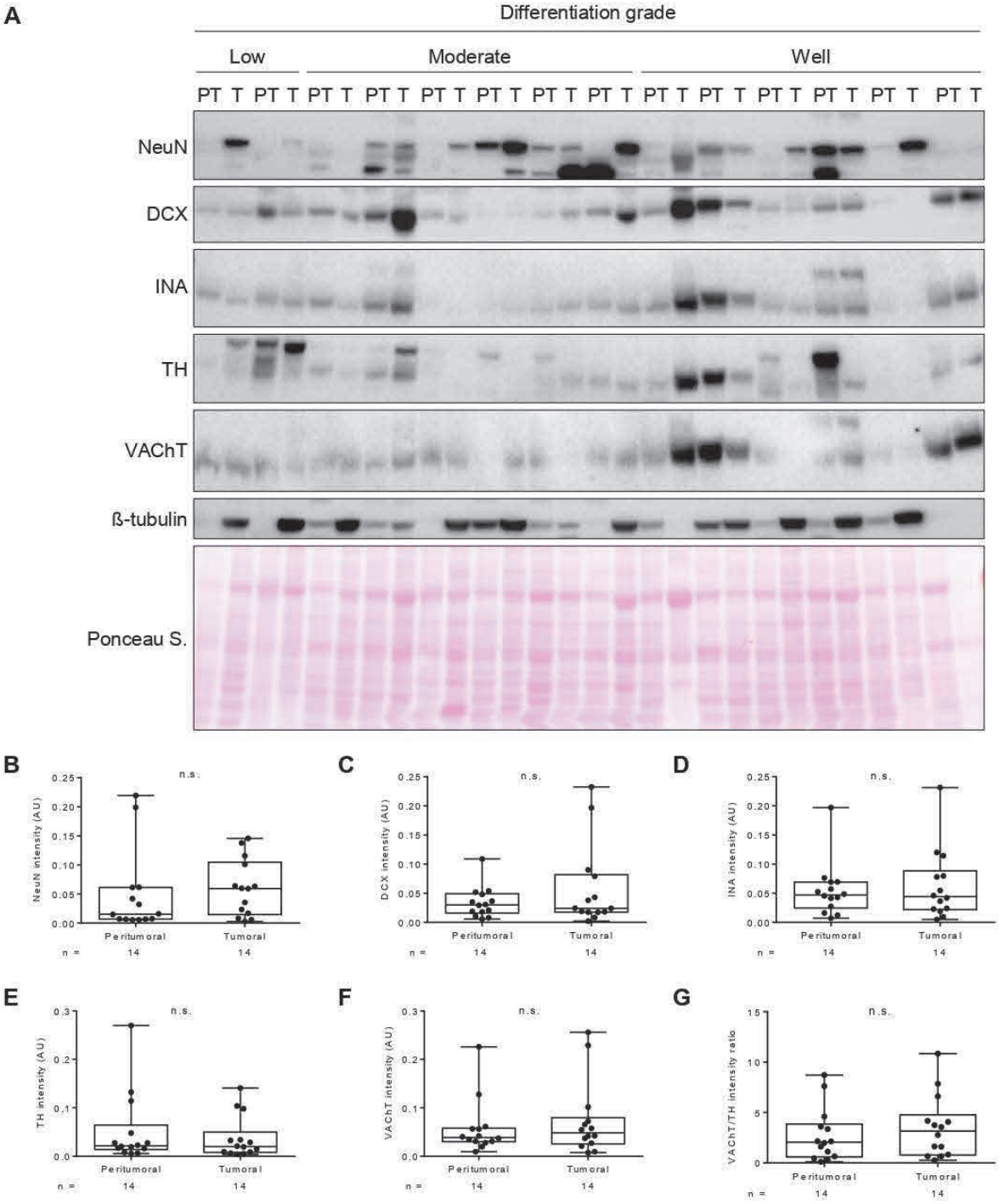

Supplementary Figure 6.

Expression of mature and progenitor neural markers in human HCC of ALD etiology.

A. Immunoblotting on neural markers using the above-mentioned antibodies. **B-G.** Signal quantification was done using the Fiji software on non-saturated images, using whole lane Ponceau S fluorescence (540 nm) for normalization, prior to statistical plotting using the Mann-Whitney test (n = 14 patients, * $p < 0.05$, ** $p < 0.01$, *** $p < 0.001$).

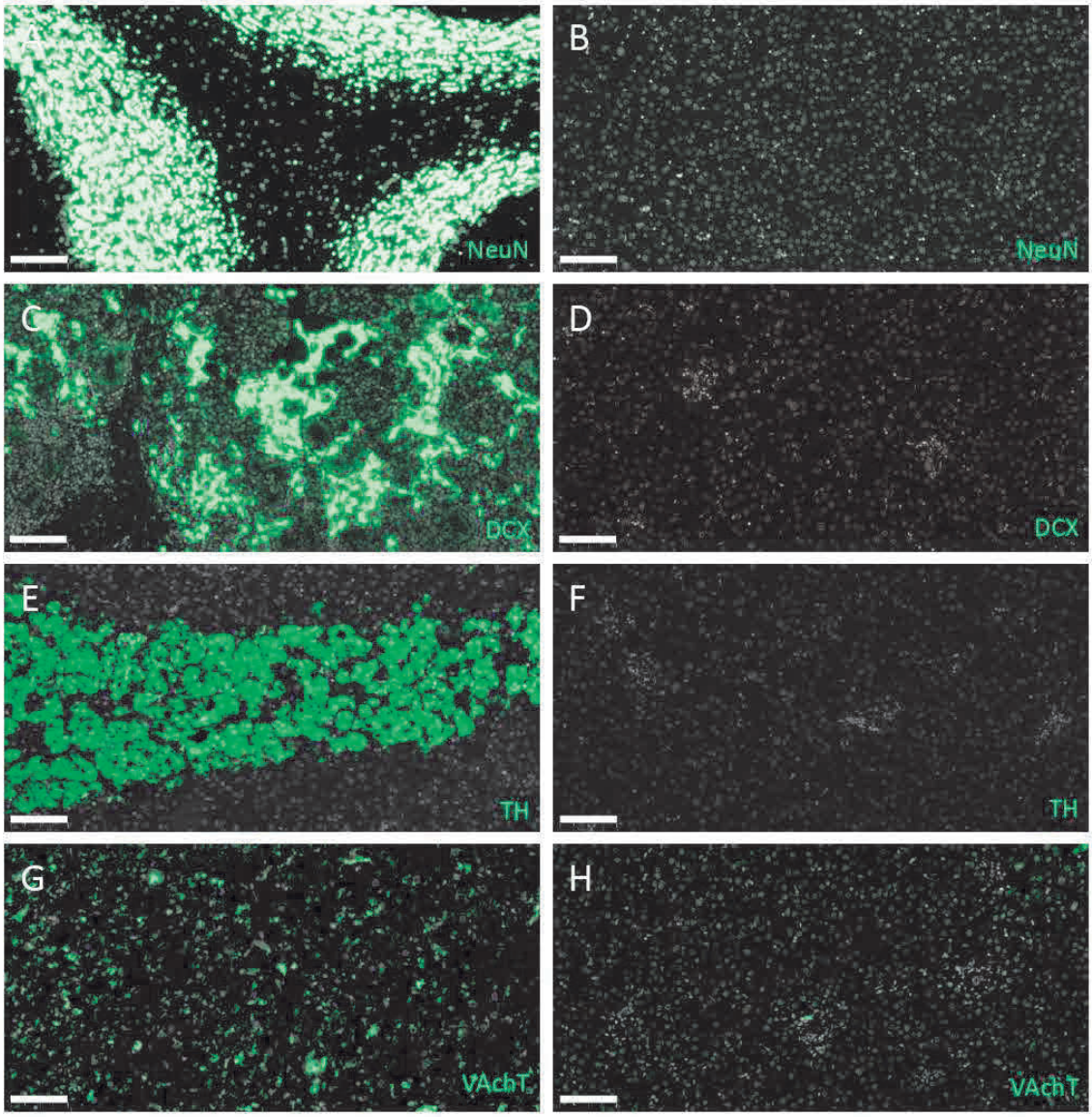

Supplementary Figure 7.

Validation of antibodies used by IHC. Anti-NeuN, DCX, TH and VAChT antibodies were validated by immunofluorescence on ad hoc human tissue samples prior to their use on HCC specimens. **A.** Cerebellum. **C.** Parotid gland lesion. **E.** Surrenal gland. **G.** Cerebral cortex. **B,D,F,H.** Normal liver (hepatocytic areas). Nuclei were stained with DAPI (grey signal). Antigens of interest are shown in green. Scale bar = 100 µm.

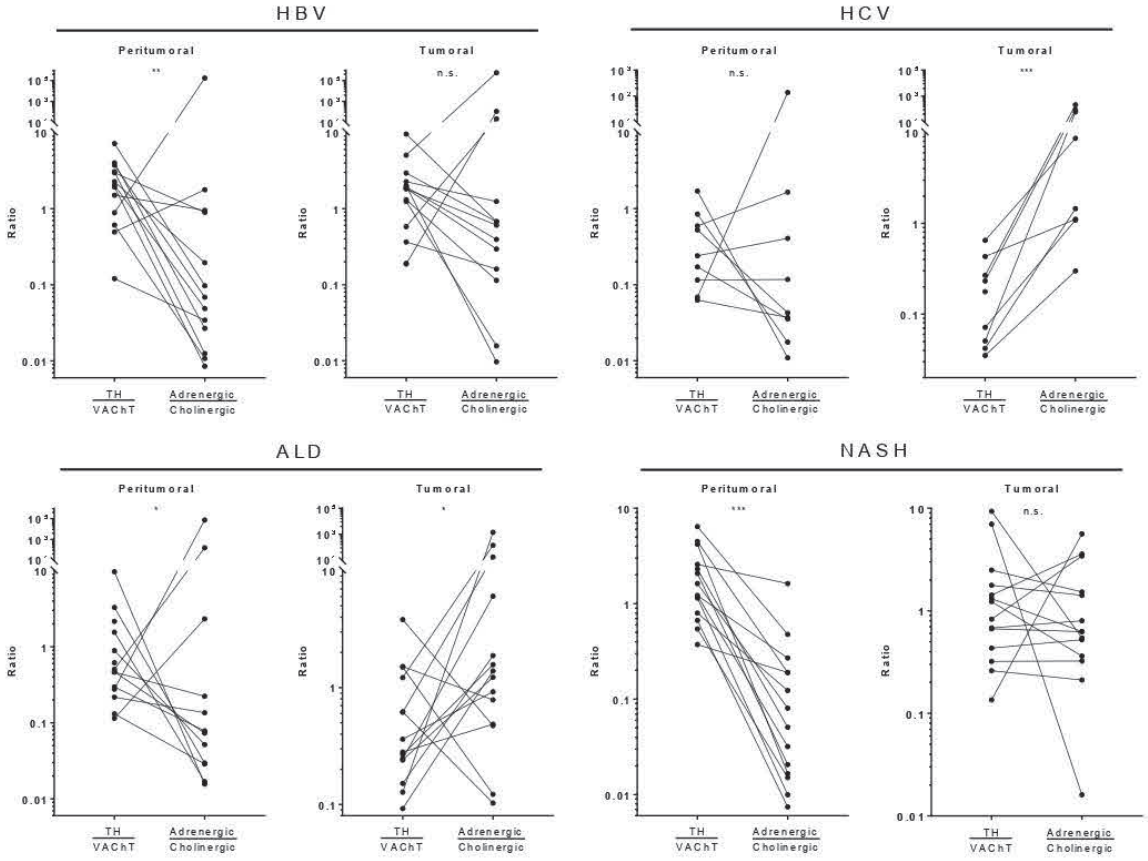

Supplementary Figure 8.

Relationship between neuronal pre-synaptic marker and post-synaptic marker expression after etiology-based stratification.

TH and VAChT expression levels in peri-tumoral and tumoral samples (n = 51 HCC cases) were evaluated by immunoblotting with specific antibodies and normalized against Ponceau S staining. Gene expression levels of adrenergic and cholinergic receptors were evaluated by qPCR and normalized against *GUS* expression. Adrenergic/cholinergic ratio was calculated for each patient as follows: (ADRA1A+ADRB2+ADRA1B) / (CHRNA4+CHRNA7+CHRM3), where those six targets are the most expressed of both categories in patient samples. Mann-Whitney test (* $p < 0.05$, ** $p < 0.01$, *** $p < 0.001$).

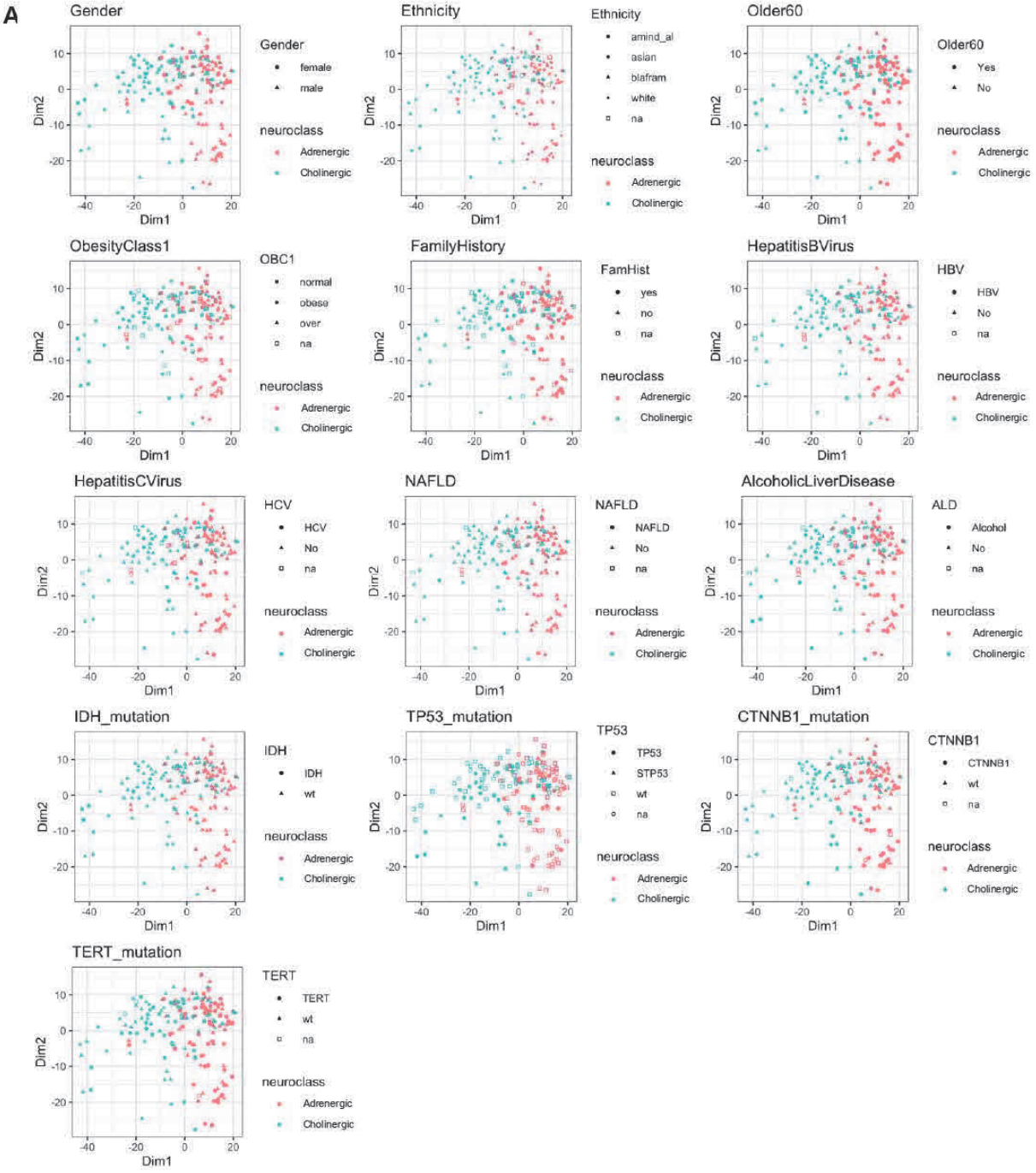

Supplementary Figure 9.

HCC neuroclasses are unrelated to many HCC clinico-biological parameters except age>60, *CTNNB1* and *TP53* mutational status. PCAs comparing signature classes with gender, ethnicity, obesity, family history, or any of the four main HCC etiologies (HBV, HCV, NASH, ALD), or main mutational profiles *IDH, TP53, TERT, CTNNB1* mutations.

Received: 2 November 2021 | Revised: 16 February 2022 | Accepted: 17 February 2022

DOI: 10.1002/hep.32446

ORIGINAL ARTICLE

Hepatic inflammation elicits production of proinflammatory netrin-1 through exclusive activation of translation

Romain Barnault[1,2,3,4,5] | **Claire Verzeroli**[1,2,3,4,5] | **Carole Fournier**[6] | **Maud Michelet**[1,2,3,4,5] | **Anna Rita Redavid**[2,3,4,5,7] | **Ievgeniia Chicherova**[1,2,3,4,5] | **Marie-Laure Plissonnier**[2,3,4,5,8] | **Annie Adrait**[9] | **Olga Khomich**[1,2,3,4,5] | **Fleur Chapus**[10] | **Mathieu Richaud**[2,3,4,5,7] | **Maëva Hervieu**[2,3,4,5,7] | **Veronika Reiterer**[11] | **Federica Grazia Centonze**[11] | **Julie Lucifora**[1,2,3,4,5] | **Birke Bartosch**[1,2,3,4,5] | **Michel Rivoire**[12,13] | **Hesso Farhan**[11] | **Yohann Couté**[9] | **Valbona Mirakaj**[14] | **Thomas Decaens**[6] | **Patrick Mehlen**[2,3,4,5,7] | **Benjamin Gibert**[2,3,4,5,7] | **Fabien Zoulim**[1,2,3,4,5,15] | **Romain Parent**[1,2,3,4,5]

[1]Pathogenesis of Chronic Hepatitis B and C Laboratory - LabEx DEVweCAN, Inserm U1052, Cancer Research Centre of Lyon, Lyon, France

[2]University of Lyon, Lyon, France

[3]University Lyon 1, Institut des Sciences Pharmaceutiques et Biologiques, Lyon, France

[4]CNRS UMR5286, Lyon, France

[5]Centre Léon Bérard, Lyon, France

[6]Institute for Advanced Biosciences, Inserm U1209, University of Grenoble-Alpes, La Tronche, France

[7]Apoptosis, Cancer and Development Laboratory - LabEx DEVweCAN, Inserm U1052, Cancer Research Centre of Lyon, Lyon, France

[8]Inserm U1052, Cancer Research Centre of Lyon, Lyon, France

[9]University of Grenoble-Alpes, Inserm, CEA, UMR BioSanté U1292, CNRS CEA FR2048, Grenoble, France

[10]Single Cell Dynamics Group, Epigenetics and Stem Cell Biology Laboratory, National Institute of Environmental Health Sciences, Research Triangle Park, Durham, North Carolina, USA

[11]Institute of Pathophysiology, Medical University of Innsbruck, Innsbruck, Austria

[12]Léon Bérard Cancer Center, Lyon, France

[13]Université Lyon 1, Lyon, France

[14]Department of Anesthesiology and Intensive Care Medicine, University Hospital of Tuebingen, Eberhard-Karls University, Tuebingen, Germany

[15]Service of Hepato-Gastroenterology, Hospices Civils de Lyon, Lyon, France

Correspondence
Romain Parent, Inserm Unit 1052, 151 cours Albert Thomas, F-69424-Lyon Cedex 03, France.
Email: romain.parent@inserm.fr

Abstract

Background and Aims: Netrin-1 displays protumoral properties, though the pathological contexts and processes involved in its induction remain understudied. The liver is a major model of inflammation-associated cancer development, leading to HCC.

Abbreviations: Arg, arginine; CLD, chronic liver disease; dsRNA, double-stranded RNA; ECM, extracellular matrix; ER, endoplasmic reticulum; FSL-1, Pam2CGDPKHPKSF; HMW, high molecular weight; HRP, horseradish peroxidase; IHC, immunohistochemistry; LPS, lipopolysaccharide; Lys, lysine; *NTN1*, netrin-1; Pam3CSK4, Pam3CysSerLys4; PDI, protein dissulfide isomerase; PHH, primary human hepatocytes; poly(I:C), polyinosinic:polycytidylic acid; RIG-I, retinoic acid-inducible gene I; RT-qPCR, reverse transcription quantitative polymerase chain reaction; STAU1, Staufen-1; TLR, toll-like receptor; UTR, untranslated region.

Romain Barnault and Claire Verzeroli contributed equally to this work.

Funding information
Romain Barnault and Ievgeniia Chicherova are recipients of a DevWeCan Labex (Laboratories of Excellence Network, ANR-LABX-061) and Agence Nationale de la Recherche sur le Sida et les Hepatites Virales (ECTZ63958) predoctoral fellowships, respectively. Funding was obtained through the same Labex consortium (ANR-LABX-061) and the French National Cancer Institute (Inca PRT-K 19-033). Proteomic experiments were partially supported by the French National Research Agency under projects ProFI (Proteomics French Infrastructure, ANR-10-INBS-08) and GRAL, a program from the Chemistry Biology Health Graduate School of University of Grenoble-Alps (ANR-17-EURE-0003)

Approach and Results: A panel of cell biology and biochemistry approaches (reverse transcription quantitative polymerase chain reaction, reporter assays, run-on, polysome fractionation, cross linking immunoprecipitation, filter binding assay, subcellular fractionation, western blotting, immunoprecipitation, stable isotope labeling by amino acids in cell culture) on in vitro–grown primary hepatocytes, human liver cell lines, mouse samples and clinical samples was used. We identify netrin-1 as a hepatic inflammation-inducible factor and decipher its mode of activation through an exhaustive eliminative approach. We show that netrin-1 up-regulation relies on a hitherto unknown mode of induction, namely its exclusive translational activation. This process includes the transfer of *NTN1* (netrin-1) mRNA to the endoplasmic reticulum and the direct interaction between the Staufen-1 protein and this transcript as well as netrin-1 mobilization from its cell-bound form. Finally, we explore the impact of a phase 2 clinical trial-tested humanized anti-netrin-1 antibody (NP137) in two distinct, toll-like receptor (TLR) 2/TLR3/TLR6-dependent, hepatic inflammatory mouse settings. We observe a clear anti-inflammatory activity indicating the proinflammatory impact of netrin-1 on several chemokines and Ly6C+ macrophages.
Conclusions: These results identify netrin-1 as an inflammation-inducible factor in the liver through an atypical mechanism as well as its contribution to hepatic inflammation.

INTRODUCTION

Chronic liver diseases (CLDs) affect more than 1 billion people worldwide. They represent the main etiological conditions for the onset of liver injury, impaired liver function (cirrhosis), and HCC.[1] Though CLDs exhibit a high degree of diversity in terms of causal effects, including infectious (HBV and HCV), metabolic, toxic, and genetic, they all converge toward hepatic inflammation and represent a pertinent model for its study. Inflammation in turn drives hepatocyte turnover, extracellular matrix (ECM) accumulation, histological worsening, and the long-term induction of tumorigenic mediators such as IL-6, eventually leading to the development of HCC.[2] A clear understanding of the onset of this inflammatory response and of its outcome in the hepatic tissue is hampered by biologically opposite functions, as it favors viral and dead cell clearance, as well as histological wound healing, but exacerbates fibrogenesis, thus inducing cirrhosis and oncogenesis. Hence, the identification of factors involved in the harmful consequences of inflammation may lead to its clinical improvement.

Netrin-1 is well known for preventing cellular apoptosis through its binding to "dependence receptors,"[3–5] and we demonstrated that it is HBV-HCV induced[6] and endowed hepatocytes with resistance to apoptosis during the unfolded protein response (UPR),[7] a hallmark of CLDs and cirrhosis. Owing to the causal link between inflammation, cancer in general, and HCC, we hypothesized that hepatic inflammation and netrin-1 may be reciprocal influencers in the liver. However, conflicting data currently depict the implication of netrin-1 in inflammation by either exacerbating[8,9] or dampening[10–12] the inflammatory response according to the setting studied. This prompted us to test its inducibility and inflammatory contribution in the liver in the context of previous descriptions in inflammatory bowel disease and colorectal cancer.[13,14]

MATERIALS AND METHODS

For better reproducibility, methods that have necessitated in-depth in-house development describing transfection, preparative and analytical biochemistry, generation of Netrin-1 Crispr cell lines, flow cytometry analysis, netrin-1 IHC, ImmunoPrecipitation, and mass spectrometry (MS) are exhaustively described in Supporting Information 8.

Clinical samples

Clinical liver samples were used under the French Institutional Review Board (IRBAQ61) "CPP South-East IV" approval #A16/207 (2016) related to the Inserm unit 1052 Hepatology biobank, France (#DC2008-235).

Commercial TMAs used (US Biomax) were the following: LV2084, LV2081, LV8011a, LV2085, and LV2086, of which 34 normal and chronic hepatitis samples were analyzed. Written informed consent was obtained from each patient and conformed to the ethics guidelines of the 1975 Declaration of Helsinki. All activity scores were determined by the pathology department of the Lyon University Hospital.

Animal housing, treatment, and sample harvest

All trials were performed under the French Lyon IRB agreement #CECCAP_CLB_2014_015 as previously described.[50] All the mice received humane care according to the criteria outlined in the NIH Guide for the care and use of laboratory animals, and all the treatments were approuved by the institutional animal care and use committee. Eight-week-old C57BL/6J mice (Janvier Labs, Saint-Berthevin, France) were injected intraperitoneally with NP001 or NP137 antibodies (10 mg/kg; circulating half-life of 48 h in the mouse) and poly(I:C) or FSL-1 (Pam2CGDPKHPKSF) (30 µg/mouse and 1 µg/mouse, respectively, Invivogen, Toulouse, France) at indicated doses or vehicle control for 16 h and sacrificed before liver harvest. Due to liver zonation considerations, all analyses were performed after selection on ice of the median hepatic lobe of all animals.

Statistics

Normal distribution of data was first assayed using the Shapiro-Wilk test. All quantitative data were tested using the two-way ANOVA with Tukey's multiple comparisons test or with the Mann-Whitney test. Slope data were analyzed using the Mann-Whitney test.

RESULTS

Inflammation fosters netrin-1 protein, but not mRNA, up-regulation in clinical samples, in vitro, and in mice

Data related to clinical samples can be found in the Supporting Information 1. In order to probe the robustness of these correlative clinical data, we investigated the potential impact of experimentally induced inflammation using a panel of toll-like receptor (TLR) ligands, namely Pam3CysSerLys4 (Pam3CSK4) as a TLR1/2 agonist, lipopolysaccharide (LPS) as a TLR4 agonist, flagellin as a TLR5 agonist, FSL-1 as a TLR2/6 agonist, Riboxxol (molecularly defined TLR3 agonist), and finally low or high molecular weight (HMW) polyinosinic:polycytidylic acid [poly(I:C)] as TLR3, RIG-I (retinoic acid-inducible gene I), and melanoma differentiation–associated protein 5 agonists. Experiments were carried out on HepaRG cells[15] and in primary human hepatocytes (PHH). RIG-I was also probed as a control. Pam3CSK4, LPS, FSL-1, Riboxxol, and HMW poly(I:C) induced netrin-1, suggesting its relevance in the hepatic environment. Inducibility was confirmed in PHH for Pam3CSK4, LPS, Riboxxol, and HMW poly(I:C) (Figure 1A). Chronic viral liver infections represent one of the major etiologies of CLDs, and, though still controversial for HBV, HBV and HCV have been reported to be direct inducers of double-stranded RNA (dsRNA)-based responses,[16,17] which in turn unleash an inflammatory response in hepatocytes. TLR3 signaling may be activated by a variety of ligands derived from HCV infection or other viral motifs,[18] commensal bacteria[19] or hepatotoxicity.[20] We hereafter focused on the dsRNA analogue poly(I:C) of HMW as a viral mimetic and TLR3 agonist and robust netrin-1 inducer.

We initially assayed inflammation-related netrin-1 induction in the liver in vivo. To achieve this, C57BL/6J male and female mice were challenged with HMW poly(I:C), before harvesting their liver. Although poly(I:C) injection did not increase ALT levels in mouse serum in females and marginally in males (Figure S3A), several other markers of inflammation (*chemokine [C-X-C motif] ligand 10*, *IL-1B*, *IL-6*, *KC*) were induced in both sexes. Interestingly, the inducibility of inflammation was higher in females (Figure S3B). Though *NTN1* (netrin-1) mRNA induction was not observed within total RNA populations, a western blot and immunohistochemistry (IHC) approach uncovered netrin-1 induction, which appeared to a greater extent in female mice (Figure 1B–E). Such data suggest a causal link between inflammation, inflammation intensity, and netrin-1 induction. By IHC, netrin-1 staining yielded a homogenous, and therefore most likely hepatocytic as well, staining pattern, similar to previous data obtained in human liver.[6]

To gain further insight into the mechanisms of netrin-1 production, we conducted a set of in vitro experiments using HepaRG cells[15] as well as PHH, where poly(I:C) led to netrin-1 protein induction in a dose- and time-dependent manner (56- and 7-fold increase in HepaRG and PHH after 72 h, respectively). The RIG-I inducible marker was monitored to verify poly(I:C) activity (Figure 2A). As a laminin-related protein, netrin-1 is secreted and may accumulate at the extracellular surface of the plasma membrane. We thus tested netrin-1 signals by immunoprecipitation after heparin-based release of plasma membrane-bound netrin-1. Data indicate that the previously observed netrin-1 up-regulation concerns the plasma membrane-bound netrin-1 pool in both cell types (Figure 2B). Importantly, netrin-1 up-regulation by inflammation was unrelated to cell death protection (Supporting Information 2).

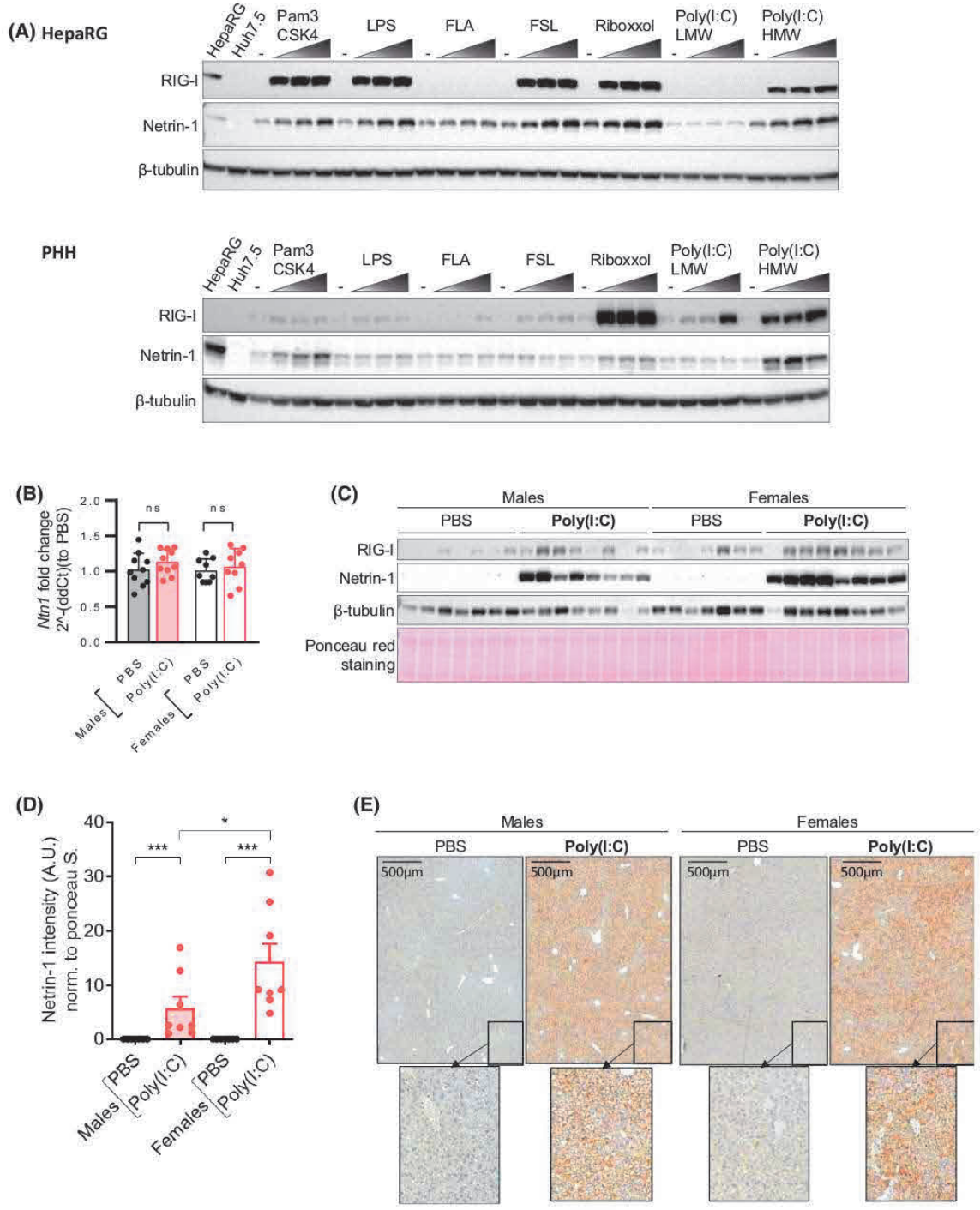

FIGURE 1 Netrin-1 induction in vivo and in vitro. (A) Netrin-1 expression levels were evaluated by immunoblotting (n = 3). (B) Levels of *NTN1* mRNA in total RNA extracts processed from mouse livers were quantified by RT-qPCR. (C) The same liver extracts were probed for immunoblotting. (D) Densitometric quantification of netrin-1 on mice blots. (E) IHC on netrin-1 using the same antibody. Data are representative of a total of 40 mice [10 females, 10 males, ± poly(I:C), Mann-Whitney test (n.s)]

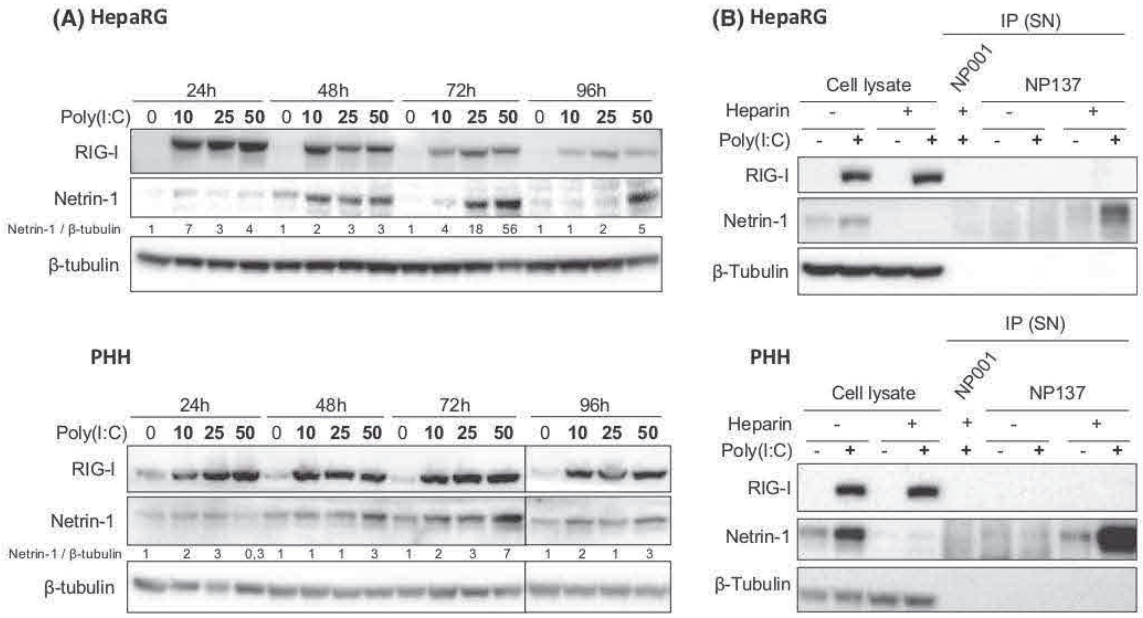

FIGURE 2 Cell-associated and soluble netrin-1 levels are up-regulated by poly(I:C) in HepaRG cells and in PHH. (A) Netrin-1 expression levels were evaluated by immunoblotting. (B) Netrin-1 expression levels were evaluated by immunoblotting in total cell lysates or after immunoprecipitation in supernatants, with or without heparin pretreatment. NP001, isotype control; NP137, anti-netrin-1 Ig. RIG-I was used as a poly(I:C) activity control (n = 3, HepaRG; and n = 3 distinct PHH batches in both panels)

Netrin-1 up-regulation is translational and differs in immortalized/dedifferentiated cells versus primary hepatocytes

We have first demonstrated that netrin-1 induction does not rely on transcription, RNA splicing, or RNA stability (Supporting Information 3). Following the next step in the biogenetic processing of netrin-1, we then considered translational regulation as a potential contributor to netrin-1 protein induction. We first submitted HepaRGs as amenable cells for mechanistic studies, PHHs, and mouse livers to total polysomal fractionation using sucrose gradient-based isopycnic ultracentrifugation followed by gradient trace monitoring, RNA extraction, and reverse transcription quantitative polymerase chain reaction (RT-qPCR) on the *NTN1* transcript. Adequate fractionation could be evidenced using gradient UV traces. The presence of the peak of free RNA, followed by the 40S, 60S, and 80S ribosomal subunits and preceding the typical oscillating profile of successive polyribosomes, was identified (Figure 3A, black and red traces). As expected, translation was more active in HepaRG cells than in resting, optimally differentiated, PHH, or mouse livers. Moreover, for HepaRG cells, the percentage of polysome-bound *NTN1* mRNA signals versus total *NTN1* signals remained unchanged on poly(I:C) treatment (87.9% versus 86.0% in treated cells), whereas in PHH, a major shift of the *NTN1* signal could be observed toward the polysomal compartment of the gradient (46% versus 89%) (Figure 3B–C). The polysomal association of the netrin-1 transcript in mouse livers led to a clear shift of *NTN1* toward heavy polysomes (fractions 13–17) that are associated with strong translational activity. In order to confirm this, an EDTA release control experiment[21] was carried out in all types of samples. EDTA induces polysomal collapse through Mg^{2+} and Ca^{2+} chelation, enabling the evaluation of the genuine polysomal origin of the RT-qPCR signals, and reinforced these results (Figure 3A–C). Our data advocate for distinct modes of regulation of netrin-1 induction in HepaRG hepatocyte-like cells and fully differentiated environments such as PHH and mice livers. Unlike in HepaRGs, mouse livers and PHH appear to activate total polysome-based translation of the *NTN1* transcript for the final induction of the protein. Yet, netrin-1 biogenesis mechanisms remain uncharted at this stage of the study in HepaRG cells, which are representative of late stage CLD.[15]

Because translational propensity of a transcript may be to some extent uncoupled from its level of association to polysomes, intensities of *de novo* synthesis of the netrin-1 protein in inflammatory conditions and in naïve HepaRG cells were then quantified. Nascent proteins were labeled with heavy amino acids on treatment or not with poly(I:C) using a pulsed stable isotope labeling by amino acids in cell culture method before netrin-1 immunoprecipitation and MS-based proteomic analyses. This strategy indicated a 4.5-fold increase

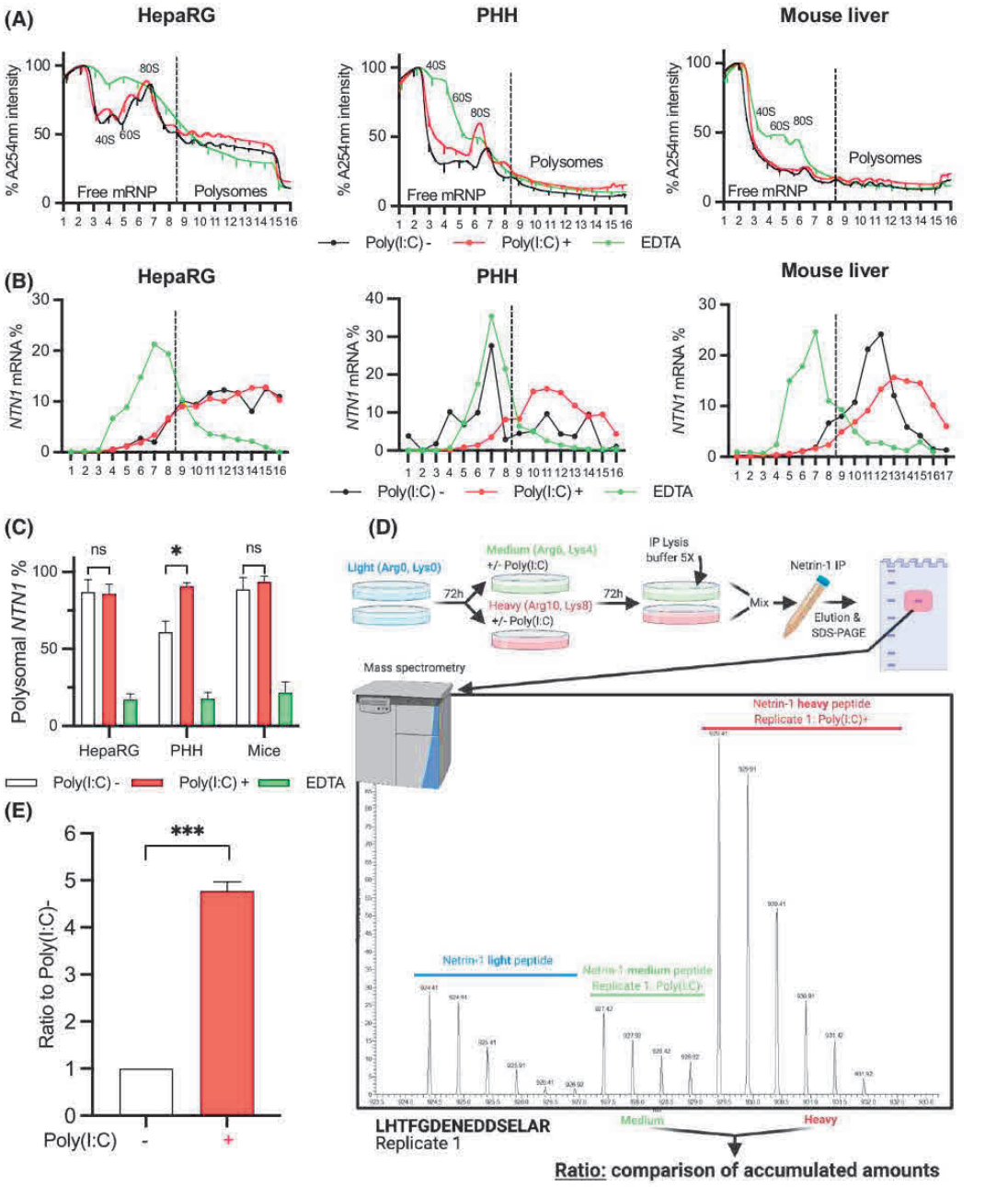

FIGURE 3 Inflammation activates translation of the *NTN1* transcript in HepaRG cells, PHH, and mouse livers. Samples were homogenized in polysome lysis buffer and loaded onto a linear sucrose gradient before isopycnic ultracentrifugation. (A) Representative profile of UV gradient traces. (B) *NTN1* distribution profile. Total polyribosomes were processed for *NTN1* ($n = 3$, HepaRG; $n = 3$ distinct PHH donors, $n = 6$ female mice). Mann-Whitney test, $^{*}p < 0.05$. (A,B) An EDTA release control assay was performed by adding EDTA to lysates before ultracentrifugation (green values). (C) Quantification of corresponding signals. (D) Total lysates and supernatants (and labeled with medium or heavy lysine [Lys] or arginine [Arg] isotopes supplemented in Lys/Arg-free William's E medium) were lysed, quantified for total protein amounts, and mixed 1:1 before netrin-1 immunoprecipitation. (E) Immunoprecipitated material was run onto SDS-PAGE and submitted to tryptic digestion and isotope-specific mass spectrometry-based quantification ($n = 3$ independent experiments). Diagram used the BioRender software. Mann-Whitney test, $^{***}p < 0.001$

in *de novo* synthesis of netrin-1 in inflammatory conditions versus naïve cells (Figure 3D,E). These data suggest that if ribosomal loading by the *NTN1* transcript *per se* is not modulated in HepaRG cells, as observed after polysomal fractionation, processes increasing the susceptibility of the *NTN1* transcript to translation are strong candidates.

Staufen-1 mediates netrin-1 induction through direct interaction with the *NTN1* transcript

Netrin-1 is a secreted protein, and its translation should naturally take place in association with endoplasmic reticulum (ER) membranes so that cotranslational translocation of the nascent peptide across the ER membrane may occur through the transient association of the peptide's signal sequence with the translocon.[22] Therefore, netrin-1 translation is conditioned by two distinct events: association with polyribosomes and accumulation of the transcript at the ER level for subsequent transfer of the native peptide to the secretory pathway. Given the pathophysiological relevance of dedifferentiated cells in CLD, we took into consideration this process in order to determine divergences between HepaRG cells and PHH for netrin-1 induction. Based on the so-called "sequential extraction" method,[23] which allows the investigation of mRNA partitioning between cytosol and microsomes, we verified netrin-1 mRNA enrichment following poly(I:C) treatment using three protein markers (RIG-I and caspase-3 as cytosolic proteins and the ER-associated PDI (protein dissulfide isomerase)/P4HD protein; Figure 4A). Whereas no significant alteration in cytosolic or membrane-bound levels of *NTN1* transcripts was evidenced on poly(I:C) treatment in PHH, the level of *NTN1* transcript enrichment in membrane-bound versus cytosolic fractions

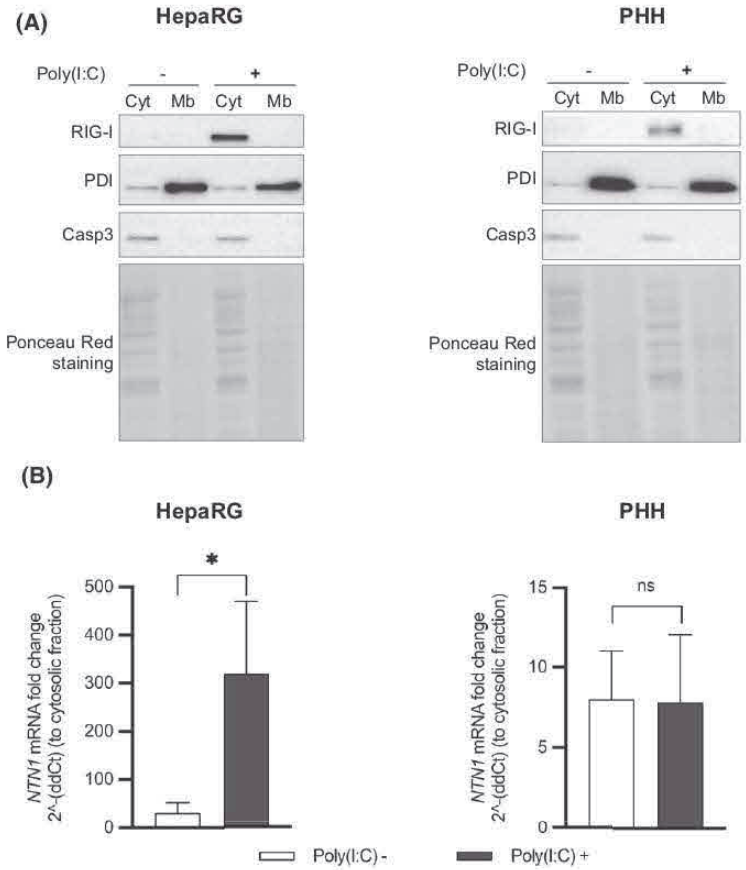

FIGURE 4 *NTN1* accumulates in membrane/ER-positive fractions on poly(I:C) treatment in HepaRG cells. (A) Adequate partitioning was verified by Western blotting on PDI (internal membrane contents) and caspase-3 (cytosolic contents). RIG-I (cytosolic location) was also probed as a poly(I:C) activity control. The Stephens et al.[23] sequential extraction method was used. (B) *NTN1* transcripts were monitored for their partitioning. Mann-Whitney test, $*p < 0.05$ [$n = 3$ (HepaRG), and $n = 3$ distinct PHH batches in both panels]

increased by 7-fold in inflammatory HepaRG cells (Figure 4B). These findings indicate that translational induction of netrin-1 occurs through the transfer of the *NTN1* transcript to the ER before its active translation in HepaRG cells. We then identified that this phenotype was not sensitive to altered differentiation in vitro (Supporting Information 4).

We then focused on *NTN1* mRNA relocalization by conducting a bibliographic search for proteins participating in transport and translational regulation of highly structured, GC (guanine-cytosine)-rich mRNAs in their 5′ ends, which the *NTN1* transcript belongs to.[7] The RNA-binding protein Staufen-1 (STAU1) shuttles between the cytosol and the ER thanks to its association with microtubules through its tubulin binding domain.[24] STAU1 is implicated in translational activation through GC-rich, structured 5′ untranslated regions (UTRs)[25] and was proposed to bind to the *NTN1* transcript in high throughput experiments.[26,27] In resting HepaRG cells, STAU1 displayed a granular staining also observed in other studies, where it associates with RNA granules before or after movement on microtubules.[28,29] Interestingly, poly(I:C) triggered the reconfiguration of STAU1 signals from a granular to a microtubule-like filamentous pattern, also in accordance with other studies.[30] The number of STAU1-positive granular foci per cell decreased 11-fold and the percentage of STAU1 filamentous staining-positive cells increased 9-fold with poly(I:C) (Figure 5A,B). STAU1 staining also displayed an increased overlap with PDI+ (ER) areas, quantified using the Li colocalization coefficient. (Figure 5C). Accumulation of STAU1 at these ER+ areas on poly(I:C) treatment was verified by immunoblotting after subcellular fractionation using previously described markers (Figure 5D). Such data suggest that STAU1 may be involved in netrin-1 induction.

Direct interaction between STAU1 and netrin-1 mRNA promotes its transfer to the ER and its subsequent translation

In order to test interactions between STAU1 and the full length netrin-1 mRNA in our biological context, we set up a cross linking immunoprecipitation assay in UV cross-linked HepaRG cells using a variety of relevant positive and negative control transcripts.[26,27] Immunoprecipitation conditions for STAU1 were first defined (Figure 6A). Data depicted in the following panel show significant increase in STAU1-bound *NTN1* levels versus several other transcripts, in addition to a specific and positive impact of poly(I:C) *per se* on these *NTN1* binding levels to STAU1. Percentages of transcript inputs are indicated in poly(I:C)-treated or untreated conditions in Figure 6B.

To further probe the likelihood of a direct interaction between STAU1 and *NTN1*, we carried out a filter binding assay using recombinant STAU1 and in vitro transcribed *NTN1* 5′UTR, which provides information on the affinity of both partners and on their class of interaction dynamics downstream of collected STAU1-bound, RNA-conjugated, biotin-avidin-horseradish peroxidase (HRP) signals. Based on the profiles obtained, filter binding data were fit to a sigmoidal equation to determine binding constants and to estimate the degree of binding cooperativity. Calculation of Kd led to a value of 1.17 ± 0.11 nM. Calculation of the Hill constant was done using the formula Log (81) / Log (EC_{50}/EC_{10})[31] and led to a value of 1.9 ± 0.28, suggesting a moderately cooperative interaction. As a control, no interaction between an HBV epsilon loop RNA sequence and STAU1 was observed. In competition experiments, incubation of increasing concentrations of unlabeled *NTN1* 5′UTR led to displacement of the prebound labeled *NTN1* 5′UTR RNA, whereas, again, no reversion of STAU1-*NTN1* 5′UTR complex-derived signals could be achieved using HBV control RNA Figure 6C,D. Altogether, such data suggest that the RNA-binding protein STAU1 directly associates with the 5′UTR of the netrin-1 transcript. This finding corroborates the accumulation of STAU1 at the ER level for enhanced translational susceptibility of the mRNA of this secreted protein.

In order to functionally confirm the implication of STAU1 in the accumulation of the *NTN1* transcript at ER sites for netrin-1 protein induction, we tested the effect of RNAi-mediated STAU1 depletion on poly(I:C)-induced *NTN1* accumulation at the ER and on netrin-1 induction. Both approaches showed reversion of poly(I:C)-induced netrin-1 signals in HepaRG cells (Figure 6E–G). In order to assess whether dependence of netrin-1 induction toward STAU1 is widespread in dedifferentiated hepatocytic contexts, we depleted STAU1 in the Hep3B cell line and in PHH as a control. We observed that netrin-1 induction was also reversed by STAU1 depletion in Hep3B cells but not in PHH, which is data consistent with the abovementioned *NTN1* mRNA transfer-independent phenotype of the latter (Figure S11). Altogether, these mechanistic data indicated that STAU1-dependent transcript transfer to the ER in dedifferentiated hepatocytic cells determined netrin-1 induction. A comparison of results obtained in hepatocytic lines and PHH suggests that mRNA relocalization and translational activation *per se* seem to be mutually exclusive mechanisms across both cell environments yet, importantly, converging and enabling netrin-1 induction. We finally also demonstrated that netrin-1 induction does not rely on posttranslational steps (Supporting Information 5), providing final evidence that netrin-1 induction occurs through exclusive translational activation.

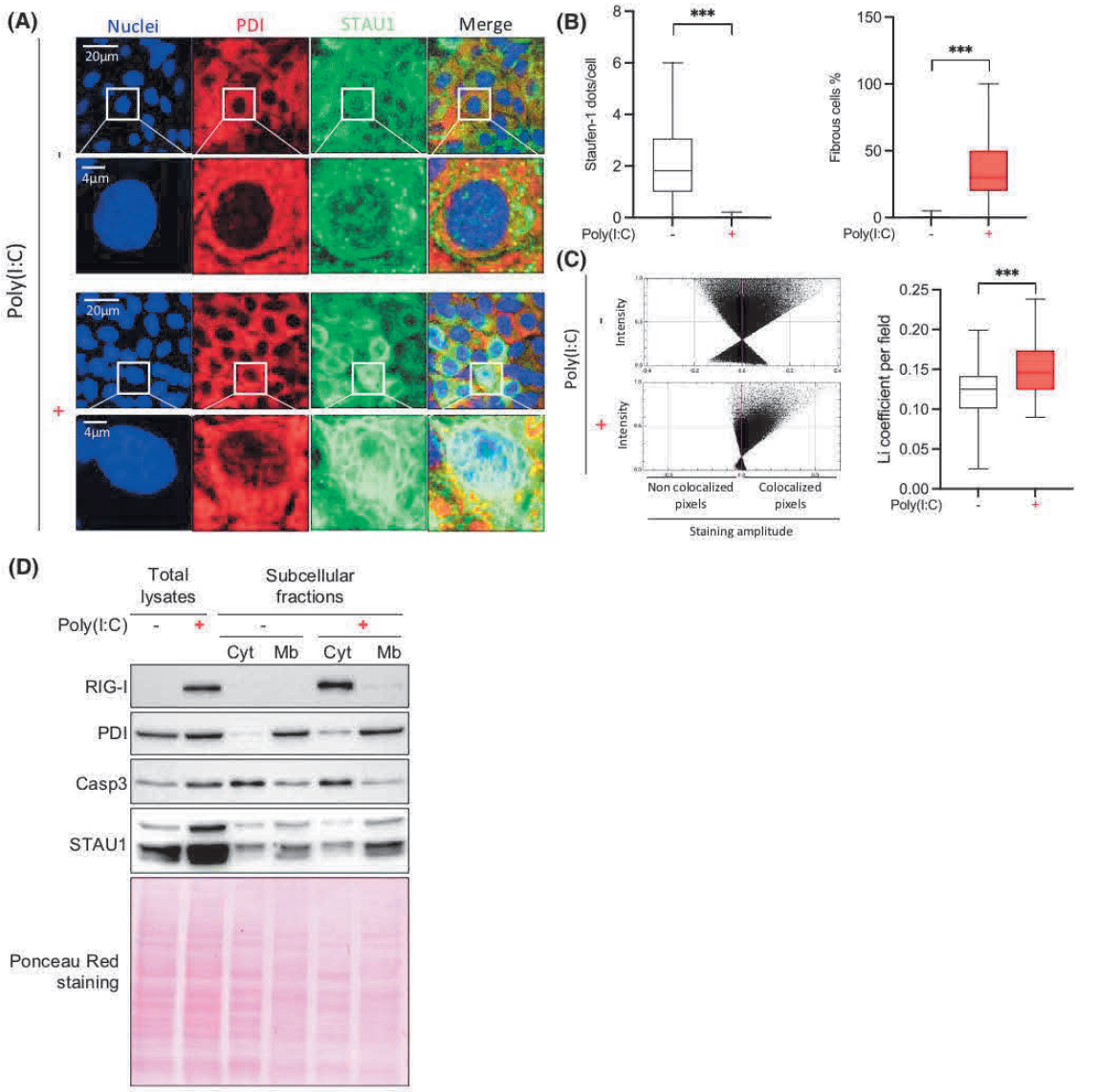

FIGURE 5 Poly(I:C) induces STAU1 relocalization and accumulation at the ER. (A) Representative immunofluorescence-based localization of PDI (red) and STAU1 (green). (B) Number of STAU1-positive dots per cell and percentage of fibrillar STAU1-positive cells versus total cells are shown. Mann-Whitney test after Shapiro-Wilk test (*$p < 0.05$, $n = 3$ independent experiments). (C) Li diagrams coefficient calculations for PDI and STAU1 colocalization quantification, respectively, using the JACop plugin from the ImageJ software. Twenty random fields were acquired per biological sample ($n = 3$ independent experiments). (D) STAU1 transfer to the ER on inflammation assessed by immunoblotting. Markers used are depicted in Figure 4A ($n = 3$ independent experiments)

A phase 2 trial-validated antibody enabling netrin-1 capture unravels its contribution to hepatic inflammation in mice

We first identified netrin-1 as a diffusible factor during inflammation (Supporting Information 6). Considering that this diffusible status corroborated previously known tissular effects of netrin-1,[8,9,32,33] we treated C57BL/6J mice with the clinically used and well-tolerated anti-netrin-1 antibody NP137 (NCT02977195)[34] or its NP001 isotypic control 32 h before challenging them with poly(I:C) for 16 h and liver harvest (Figure 7A). Treatment with the former dampened poly(I:C)-induced netrin-1 levels (Figure 7B,C)

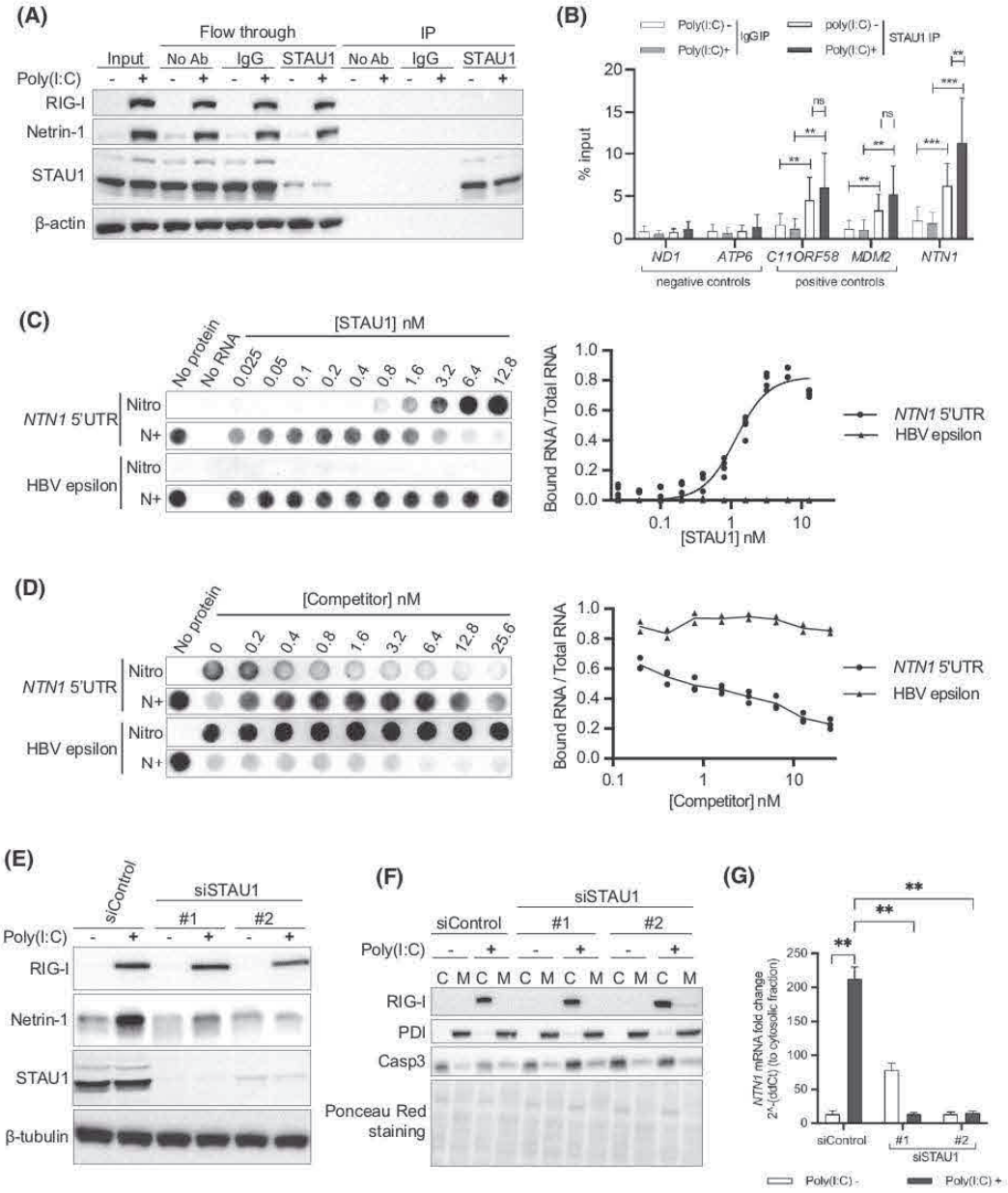

FIGURE 6 STAU1 interacts with *NTN1* mRNA through its 5′UTR and conditions *NTN1* transcript relocalization as well as netrin-1 induction in HepaRG cells. (A) cross linking immunoprecipitation/STAU1 immunoprecipitation. HepaRG cell lysates were immunoprecipitated before elution and one-dimensional SDS-PAGE. (B) Negative control (mitochondrial) transcripts, positive control transcripts for STAU1 binding,[26] and *NTN1* were quantified on immunoprecipitated materials relatively to inputs. Mann-Whitney test, $***p < 0.01$ ($n = 5$ independent experiments). (C) Filter binding assay. The ability of the biotin-labeled *NTN1* 5′UTR RNA to bind STAU1 was assessed by measuring the ratio of HRP signals between the upper nitrocellulose (Nitro) membrane (adsorbing complexes) and the lower nylon (N+) membrane (adsorbing unbound RNA). HBV RNA epsilon loop was a negative control. (D) Competition experiments using the filter assay approach. Prebound STAU1-*NTN1* 5′UTR biotin(+) complexes were submitted to increased concentrations of unlabeled competitors (*NTN1* 5′UTR or HBV epsilon RNAs). Corresponding quantification of HRP signals and obtained parameters derived from one representative experiment are shown ($n = 5$ independent experiments). (E) Impact of STAU1 depletion by immunoblotting. (F) Adequate partitioning in control and STAU1-depleted cells between cytosolic (C) and membrane (M) fractions was addressed by Western blotting on PDI (internal membrane contents) and caspase-3 (cytosolic contents). RIG-I (cytosolic location) was probed. (G) *NTN1* was then quantified by RT-qPCR in both fractions. Mann-Whitney test, $**p < 0.01$ ($n = 3$ independent experiments)

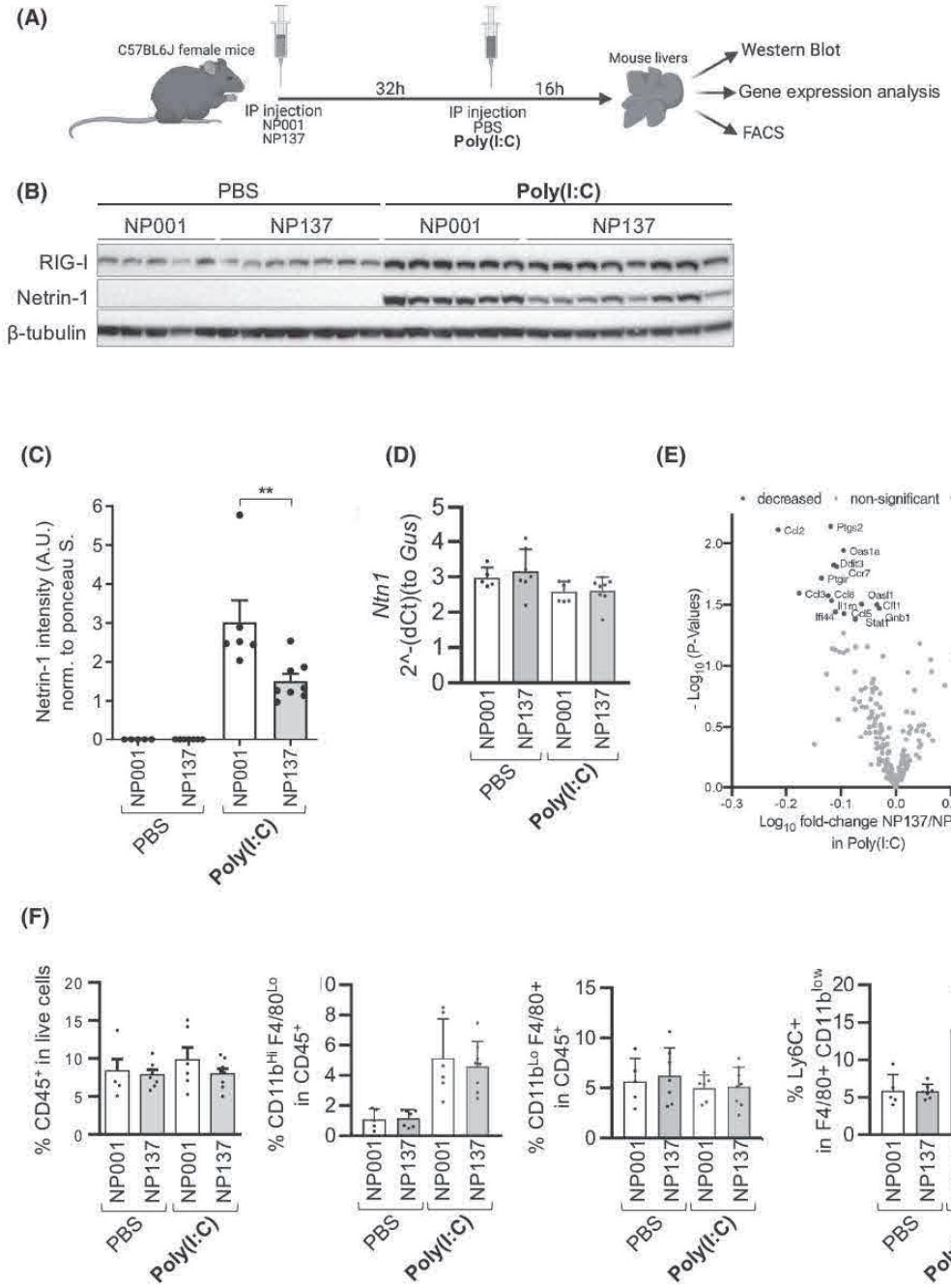

FIGURE 7 Netrin-1 capture by a clinically used antibody dampens hepatic inflammation in mice. (A) Workflow created with Biorender.com. (B) Hepatic netrin-1 levels in mice were measured by western blotting. (C) Quantification of signals. (D) *Ntn1* was quantified by RT-qPCR. (E) Transcripts conditioned by netrin-1 levels. (F) Percentage of positive live (DsRed) cells against CD45, CD11b, F4/80, and Ly6C markers are indicated (n = 5–8 mice per group). Mann-Whitney test. *$p < 0.05$, **$p < 0.01$, ***$p < 0.001$

in addition to its netrin-1 capture activity.[34] Such events occurred again independently of *NTN1* RNA up-regulation in all instances (Figure 7D). Gene expression analysis was conducted on a panel of 248 inflammation-related cytokines. Poly(I:C)-triggered up-regulation of 81 inflammation-related transcripts (Table S7). Our experiment highlighted a causal relationship between netrin-1 inactivation by NP137 and reversion of the induction of 15 transcripts, of which several encode chemokines (chemokine [C-C motif] ligand [*Ccl*] *2*, -1.63-fold*; Ccl3*, -1.51-fold; *Ccl5*, -1.64-fold; *Ccl8,* -1.33-fold). Four actors related to the inflammation-associated interferon system (signal transducer and activator of transcription [*Stat*] *1*, 2',5'-oligoadenylate synthetase 1, 2'-5'-oligoadenylate synthetase like,interferon induced protein 44 were also significantly reversed, albeit more weakly, together with the master regulator of inflammation cyclooxygenase prostaglandin-endoperoxide synthase 2 and its product prostaglandin I2. Consistently, the only NP137-induced transcript out of the 248 analyzed targets encodes an anti-inflammatory kinase, ribosomal protein S6 kinase A5 (+1.44-fold, Figure 7E). In order to further document this phenotype that implicates several chemotactic factors, we performed a flow cytometry analysis to monitor immune cell population regulation. Gating strategies are shown in Figure S15, where the three left panels depict $Ly6C^{+}$ $CD11^{low}$ $F4/80^{hi}$ gatings (from top to bottom: Poly(I:C)+ and NP001, Poly(I:C)+ and NP137, and finally Ly6C fluorescence minus one control on pooled cells from all mice). Monocyte-derived macrophages ($CD45^{+}$ $CD11b^{+}$ $F4/80^{low}$) remained stable. Total Kupffer cells ($CD45^{+}$ $CD11b^{low}$ $F4/80^{hi}$) counts were not regulated. However, the NP137 antibody specifically reversed $Ly6C^{+}$ intrahepatic macrophages counts in inflammatory conditions (Figure 7F), a population that is activated by CCL2, CCL3, and CCL5 in four distinct models of CLD.[35–37] Confirmatory data were obtained in the context of lipopeptide FSL-1–driven inflammation (Supporting Information 7). Hence, such data identify netrin-1 as an amplifier of liver inflammation induced by two unrelated microbial classes of triggers (dsRNA and lipopeptides), in accordance with its role in other organs.[8,9,32]

DISCUSSION

In the present study, we identify a to-date unknown mode of induction of netrin-1 and unveil the implication of STAU1 during inflammation. Transcriptional regulation is considered to be a hallmark regulatory step in liver differentiation processes,[38] and regulation of netrin-1 has been repeatedly identified as transcription dependent through hypoxia inducible factor 1 alpha subunit or NF-kB transcriptional complexes,[10,13,39] suggesting this work's timeliness. However, increasing evidence suggests that processes that need swift temporal regulation in highly remodeled tissues, such as during inflammation, and, more generally, oncogenic processes and associated resistance, also rely on translational modulation.[40,41]

For instance, hepatocytic differentiation is strongly associated with important down-regulation of a majority of transcripts at the total RNA level and a concomitant up-regulation in polysomal fractions of a subset of hepatocytic differentiation-related mRNAs.[42] Experimental activation of the mTOR pathway, which is present in half of HCC cases, impairs hepatocytic differentiation and impedes the translation of transcripts moderating lipid homeostasis and cell growth.[43] Following the UPR, netrin-1 translation is selectively favored during global translation shutdown, together with internal ribosome entry site–bearing transcripts implicated in cell survival and transformation.[7] Moreover, the liver is one of the most, if not the most, active secretory and metabolic organs in human physiology, as well as being exposed to real-time needs for metabolic and hence secretory regulation (acute phase, postprandial phases). It is thus conceivable that the biogenesis of secreted factors such as netrin-1 are more often constrained by swift regulatory processes such as translational control in the liver than in other organs. The present data, to be interpreted as a confirmation of the particular susceptibility of netrin-1 to posttranscriptional regulation, strengthen the need for more frequent molecular analyses of inflammatory processes using total RNA-unrelated enrichment methods, such as polysomal profiling, at least at the level of the liver.

Moreover, we have shown, depending on the cell system of interest, i.e., undifferentiated HepaRG or PHH, that netrin-1 biogenesis under inflammation was specifically regulated at the mRNA localization level in the former but at the translational level *per se* in the latter case. The presence of these mechanisms is of interest, because it appears that two distinct modes of posttranscriptional regulation actually converge toward a single phenotypic outcome, i.e., netrin-1 increase. Pathophysiological needs for delivering this final phenotype therefore seem to override cell type-specific functional singularities, suggesting that induced netrin-1 conveys important functions in the liver, either immunomodulatory[8,9,32,33] or, in the long term, merging with hepatoprotection as an antiapoptotic factor.[3–5,44]

This phenotype relies on the RNA-binding protein STAU1, the implication of which is to-date undocumented in inflammation. However, STAU1 has recently been shown to foster gastric cancer progression in a cyclin- and kinase-dependent manner[45] and also to take part in an enhancer Of zeste 2 polycomb repressive complex 2 subunit-related, HCC-promoting pathway,[46] suggesting the relevance of further studies aiming at characterizing its implication in end-stage liver disease, possibly through netrin-1. Interestingly, STAU1 regulates cortical neurogenesis, a process that is highly dependent on netrin-1 as well.[47]

This work suggests a potential link between hepatic inflammation and liver disease progression through netrin-1. Direct cross-talks between inflammation and HCC have been notably defined through the IL-6/glycoprotein 130/STAT3 axis and lymphotoxin beta.[48] Our study improves the understanding of the potential implication of inflammation in the evolution of CLDs and identifies an actionable target for its modulation. Chronic inflammation of a given tissue is counterbalanced by ECM growth. As mentioned before, netrin-1 is a laminin-related protein that shares several structural features with ECM-constituting proteins. As a consequence, one may hypothesize that netrin-1 could participate in ECM growth. A recent study featuring netrin-1 as a fibrosis promoter in the inflammatory lung[49] strengthens the likelihood of this hypothesis. Finally, the humanized anti-netrin capture antibody NP137 developed by the authors[34] (US Clinical Trials #02977195) displays anti-inflammatory activity in the present setting and identifies netrin-1 as a previously unknown proinflammatory factor in CLD.

ACKNOWLEDGMENTS

We thank B. Bancel (pathologist, Lyon U. Hospital) for determining the activity scores; M. Ressejac for help with FACS processing; A. Paradisi for the netrin-1 promoter reporter plasmid; the CIQLE and Anipath platforms for assistance with confocal microscopy and IHC, respectively; and B. Manship for editing.

CONFLICT OF INTEREST

Dr. Mehlen owns stock in Netris Pharma.

AUTHOR CONTRIBUTIONS

Substantial contribution to conception and design, acquisition of data, or analysis and interpretation of data: Romain Barnault, Claire Verzeroli, Carole Fournier, Maud Michelet, Anna Rita Redavid, Ievgeniia Chicherova, Marie-Laure Plissonnier, Annie Adrait, Olga Komich, Fleur Chapus, Mathieu Richaud, Maëva Hervieu, Veronika Reiterer, Federica Grazia, Centonze, Julie Lucifora, Birke Bartosch, Michel Rivoire, Hesso Farhan, Yohann Couté, Thomas Decaens, Patrick Mehlen, Benjamin Gibert, Romain Parent. Drafting the article or revising it critically for important intellectual content: Romain Barnault, Claire Verzeroli , Carole Fournier, Julie Lucifora , Hesso Fahran, Yohann Couté, Benjamin Gibert, Fabien Zoulim, Romain Parent. Final approval of the version to be published: Romain Barnault, Claire Verzeroli, Romain Parent, Fabien Zoulim.

ORCID

Romain Barnault https://orcid.org/0000-0003-1671-3251
Claire Verzeroli https://orcid.org/0000-0001-5728-0363
Carole Fournier https://orcid.org/0000-0001-5735-0472
Maud Michelet https://orcid.org/0000-0002-5607-7889
Anna Rita Redavid https://orcid.org/0000-0002-1332-2792
Ievgeniia Chicherova https://orcid.org/0000-0002-0764-9641
Marie-Laure Plissonnier https://orcid.org/0000-0003-4879-4586
Annie Adrait https://orcid.org/0000-0002-1565-2859
Olga Khomich https://orcid.org/0000-0001-5172-199X
Fleur Chapus https://orcid.org/0000-0001-6611-9547
Mathieu Richaud https://orcid.org/0000-0002-7472-9019
Veronika Reiterer https://orcid.org/0000-0002-7734-1255
Federica Grazia Centonze https://orcid.org/0000-0002-2124-443X
Julie Lucifora https://orcid.org/0000-0003-0482-7809
Birke Bartosch https://orcid.org/0000-0001-6354-4660
Hesso Farhan https://orcid.org/0000-0002-0889-8463
Yohann Couté https://orcid.org/0000-0003-3896-6196
Valbona Mirakaj https://orcid.org/0000-0002-6907-6455
Thomas Decaens https://orcid.org/0000-0003-0928-0048
Patrick Mehlen https://orcid.org/0000-0003-1743-5417
Benjamin Gibert https://orcid.org/0000-0002-5295-3124
Fabien Zoulim https://orcid.org/0000-0002-2245-0083
Romain Parent https://orcid.org/0000-0002-3645-7008

REFERENCES

1. El-Serag HB. Epidemiology of viral hepatitis and hepatocellular carcinoma. Gastroenterology. 2012;142(6):1264–73.e1.
2. Lee UE, Friedman SL. Mechanisms of hepatic fibrogenesis. Best Pract Res Clin Gastroenterol. 2011;25(2):195–206.
3. Llambi F, Causeret F, Bloch-Gallego E, Mehlen P. Netrin-1 acts as a survival factor via its receptors UNC5H and DCC. EMBO J. 2001;20(11):2715–22.
4. Fitamant J, Guenebeaud C, Coissieux MM, Guix C, Treilleux I, Scoazec JY, et al. Netrin-1 expression confers a selective advantage for tumor cell survival in metastatic breast cancer. Proc Natl Acad Sci USA. 2008;105(12):4850–5.
5. Paradisi A, Creveaux M, Gibert B, Devailly G, Redoulez E, Neves D, et al. Combining chemotherapeutic agents and netrin-1 interference potentiates cancer cell death. EMBO Mol Med. 2013;5(12):1821–34.
6. Plissonnier ML, Lahlali T, Michelet M, Lebossé F, Cottarel J, Beer M, et al. Epidermal growth factor receptor-dependent mutual amplification between netrin-1 and the hepatitis C virus. PLoS Biol. 2016;14(3):e1002421.

7. Lahlali T, Plissonnier ML, Romero-López C, Michelet M, Ducarouge B, Berzal-Herranz A, et al. Netrin-1 protects hepatocytes against cell death through sustained translation during the unfolded protein response. Cell Mol Gastroenterol Hepatol. 2016;2(3):281–301.e9.
8. Hadi T, Boytard L, Silvestro M, Alebrahim D, Jacob S, Feinstein J, et al. Macrophage-derived netrin-1 promotes abdominal aortic aneurysm formation by activating MMP3 in vascular smooth muscle cells. Nat Commun. 2018;9(1):5022.
9. van Gils JM, Derby MC, Fernandes LR, Ramkhelawon B, Ray TD, Rayner KJ, et al. The neuroimmune guidance cue netrin-1 promotes atherosclerosis by inhibiting the emigration of macrophages from plaques. Nat Immunol. 2012;13(2):136–43.
10. Rosenberger P, Schwab JM, Mirakaj V, Masekowsky E, Mager A, Morote-Garcia JC, et al. Hypoxia-inducible factor-dependent induction of netrin-1 dampens inflammation caused by hypoxia. Nat Immunol. 2009;10(2):195–202.
11. Mirakaj V, Thix CA, Laucher S, Mielke C, Morote-Garcia JC, Schmit MA, et al. Netrin-1 dampens pulmonary inflammation during acute lung injury. Am J Respir Crit Care Med. 2010;181(8):815–24.
12. Aherne CM, Collins CB, Masterson JC, Tizzano M, Boyle TA, Westrich JA, et al. Neuronal guidance molecule netrin-1 attenuates inflammatory cell trafficking during acute experimental colitis. Gut. 2012;61(5):695–705.
13. Paradisi A, Maisse C, Bernet A, Coissieux MM, Maccarrone M, Scoazec JY, et al. NF-kappaB regulates netrin-1 expression and affects the conditional tumor suppressive activity of the netrin-1 receptors. Gastroenterology. 2008;135(4):1248–57.
14. Paradisi A, Maisse C, Coissieux MM, Gadot N, Lépinasse F, Delloye-Bourgeois C, et al. Netrin-1 up-regulation in inflammatory bowel diseases is required for colorectal cancer progression. Proc Natl Acad Sci USA. 2009;106(40):17146–51.
15. Parent R, Marion MJ, Furio L, Trepo C, Petit MA. Origin and characterization of a human bipotent liver progenitor cell line. Gastroenterology. 2004;126(4):1147–56.
16. Saito T, Owen DM, Jiang F, Marcotrigiano J, Gale M Jr. Innate immunity induced by composition-dependent RIG-I recognition of hepatitis C virus RNA. Nature. 2008;454(7203):523–27.
17. Sato S, Li K, Kameyama T, Hayashi T, Ishida Y, Murakami S, et al. The RNA sensor RIG-I dually functions as an innate sensor and direct antiviral factor for hepatitis B virus. Immunity. 2015;42(1):123–32.
18. Yu P, Lübben W, Slomka H, Gebler J, Konert M, Cai C, et al. Nucleic acid-sensing Toll-like receptors are essential for the control of endogenous retrovirus viremia and ERV-induced tumors. Immunity. 2012;37(5):867–79.
19. Kawashima T, Kosaka A, Yan H, Guo Z, Uchiyama R, Fukui R, et al. Double-stranded RNA of intestinal commensal but not pathogenic bacteria triggers production of protective interferon-beta. Immunity. 2013;38(6):1187–97.
20. Cavassani KA, Moreira AP, Habiel D, Ito T, Coelho AL, Allen RM, et al. Toll like receptor 3 plays a critical role in the progression and severity of acetaminophen-induced hepatotoxicity. PLoS One. 2013;8(6):e65899.
21. del Prete MJ, Vernal R, Dolznig H, Mullner EW, Garcia-Sanz JA. Isolation of polysome-bound mRNA from solid tissues amenable for RT-PCR and profiling experiments. RNA. 2007;13(3):414–21.
22. Chen Q, Jagannathan S, Reid DW, Zheng T, Nicchitta CV. Hierarchical regulation of mRNA partitioning between the cytoplasm and the endoplasmic reticulum of mammalian cells. Mol Biol Cell. 2011;22(14):2646–58.
23. Stephens SB, Nicchitta CV. In vitro and tissue culture methods for analysis of translation initiation on the endoplasmic reticulum. Methods Enzymol. 2007;431:47–60.
24. Wickham L, Duchaine T, Luo M, Nabi IR, DesGroseillers L. Mammalian Staufen is a double-stranded-RNA- and tubulin-binding protein which localizes to the rough endoplasmic reticulum. Mol Cell Biol. 1999;19(3):2220–30.
25. Dugre-Brisson S, Elvira G, Boulay K, Chatel-Chaix L, Mouland AJ, DesGroseillers L. Interaction of Staufen1 with the 5' end of mRNA facilitates translation of these RNAs. Nucleic Acids Res. 2005;33(15):4797–812.
26. Ricci EP, Kucukural A, Cenik C, Mercier BC, Singh G, Heyer EE, et al. Staufen1 senses overall transcript secondary structure to regulate translation. Nat Struct Mol Biol. 2014;21(1):26–35.
27. Furic L, Maher-Laporte M, DesGroseillers L. A genome-wide approach identifies distinct but overlapping subsets of cellular mRNAs associated with Staufen1- and Staufen2-containing ribonucleoprotein complexes. RNA. 2008;14(2):324–35.
28. Kohrmann M, Luo M, Kaether C, DesGroseillers L, Dotti CG, Kiebler MA. Microtubule-dependent recruitment of Staufen-green fluorescent protein into large RNA-containing granules and subsequent dendritic transport in living hippocampal neurons. Mol Biol Cell. 1999;10(9):2945–53.
29. Fang J, Pietzsch C, Ramanathan P, Santos RI, Ilinykh PA, Garcia-Blanco MA, et al. Staufen1 interacts with multiple components of the Ebola virus ribonucleoprotein and enhances viral RNA synthesis. MBio. 2018;9(5):e01771-18.
30. Marion RM, Fortes P, Beloso A, Dotti C, Ortin J. A human sequence homologue of Staufen is an RNA-binding protein that is associated with polysomes and localizes to the rough endoplasmic reticulum. Mol Cell Biol. 1999;19(3):2212–9.
31. Taketa K, Pogell BM. Allosteric inhibition of rat liver fructose 1,6-diphosphatase by adenosine 5'-monophosphate. J Biol Chem. 1965;240(2):651–62.
32. Mediero A, Wilder T, Ramkhelawon B, Moore KJ, Cronstein BN. Netrin-1 and its receptor Unc5b are novel targets for the treatment of inflammatory arthritis. FASEB J. 2016;30(11):3835–44.
33. Schlegel M, Kohler D, Korner A, Granja T, Straub A, Giera M, et al. The neuroimmune guidance cue netrin-1 controls resolution programs and promotes liver regeneration. Hepatology. 2016;63(5):1689–705.
34. Grandin M, Meier M, Delcros JG, Nikodemus D, Reuten R, Patel TR, et al. Structural decoding of the netrin-1/UNC5 interaction and its therapeutical implications in cancers. Cancer Cell. 2016;29(2):173–85.
35. Ambade A, Lowe P, Kodys K, Catalano D, Gyongyosi B, Cho Y, et al. Pharmacological inhibition of CCR2/5 signaling prevents and reverses alcohol-induced liver damage, steatosis, and inflammation in mice. Hepatology. 2019;69(3):1105–21.
36. Baeck C, Wei X, Bartneck M, Fech V, Heymann F, Gassler N, et al. Pharmacological inhibition of the chemokine C-C motif chemokine ligand 2 (monocyte chemoattractant protein 1) accelerates liver fibrosis regression by suppressing Ly-6C(+) macrophage infiltration in mice. Hepatology. 2014;59(3):1060–72.
37. Baeck C, Wehr A, Karlmark KR, Heymann F, Vucur M, Gassler N, et al. Pharmacological inhibition of the chemokine CCL2 (MCP-1) diminishes liver macrophage infiltration and steatohepatitis in chronic hepatic injury. Gut. 2012;61(3):416–26.
38. Odom DT, Zizlsperger N, Gordon DB, Bell GW, Rinaldi NJ, Murray HL, et al. Control of pancreas and liver gene expression by HNF transcription factors. Science. 2004;303(5662):1378–81.
39. Berg NK, Li J, Kim B, Mills T, Pei G, Zhao Z, et al. Hypoxia-inducible factor-dependent induction of myeloid-derived netrin-1 attenuates natural killer cell infiltration during endotoxin-induced lung injury. FASEB J. 2021;35(4):e21334.
40. Knight JRP, Alexandrou C, Skalka GL, Vlahov N, Pennel K, Officer L, et al. MNK inhibition sensitizes KRAS-mutant colorectal cancer to mTORC1 inhibition by reducing eIF4E phosphorylation and c-MYC expression. Cancer Discov. 2021;11(5):1228–47.
41. Boussemart L, Malka-Mahieu H, Girault I, Allard D, Hemmingsson O, Tomasic G, et al. eIF4F is a nexus of

resistance to anti-BRAF and anti-MEK cancer therapies. Nature. 2014;513(7516):105–9.
42. Parent R, Beretta L. Translational control plays a prominent role in the hepatocytic differentiation of HepaRG liver progenitor cells. Genome Biol. 2008;9(1):R19.
43. Parent R, Kolippakkam D, Booth G, Beretta L. Mammalian target of rapamycin activation impairs hepatocytic differentiation and targets genes moderating lipid homeostasis and hepatocellular growth. Can Res. 2007;67(9):4337–45.
44. Guenebeaud C, Goldschneider D, Castets M, Guix C, Chazot G, Delloye-Bourgeois C, et al. The dependence receptor UNC5H2/B triggers apoptosis via PP2A-mediated dephosphorylation of DAP kinase. Mol Cell. 2010;40(6):863–76.
45. Xu TP, Wang YF, Xiong WL, Ma P, Wang WY, Chen WM, et al. E2F1 induces TINCR transcriptional activity and accelerates gastric cancer progression via activation of TINCR/STAU1/CDKN2B signaling axis. Cell Death Dis. 2017;8(6):e2837.
46. Xu F, Li CH, Wong CH, Chen GG, Lai PBS, Shao S, et al. Genome-wide screening and functional analysis identifies tumor suppressor long noncoding RNAs epigenetically silenced in hepatocellular carcinoma. Cancer Res. 2019;79(7):1305–17.
47. Serafini T, Kennedy TE, Galko MJ, Mirzayan C, Jessell TM, Tessier-Lavigne M. The netrins define a family of axon outgrowth-promoting proteins homologous to C. elegans UNC-6. Cell. 1994;78(3):409–24.
48. Haybaeck J, Zeller N, Wolf MJ, Weber A, Wagner U, Kurrer MO, et al. A lymphotoxin-driven pathway to hepatocellular carcinoma. Cancer Cell. 2009;16(4):295–308.
49. Gao R, Peng X, Perry C, Sun H, Ntokou A, Ryu C, et al. Macrophage-derived netrin-1 drives adrenergic nerve-associated lung fibrosis. J Clin Invest. 2021;131(1):e136542.
50. Jiang S, Richaud M, Vieugué P, Rama N, Delcros JG, Siouda M, et al. Targeting netrin-3 in small cell lung cancer and neuroblastoma. EMBO Mol Med. 2021;13(4):e12878.

SUPPORTING INFORMATION

Additional supporting information may be found in the online version of the article at the publisher's website.

How to cite this article: Barnault R, Verzeroli C, Fournier C, Michelet M, Redavid AR, Chicherova I, et al. Hepatic inflammation elicits production of proinflammatory netrin-1 through exclusive activation of translation. Hepatology. 2022;00:1–15. doi:10.1002/hep.32446

Remerciements

Je voudrais remercier mon mari **Roman** qui a vécu ma thèse avec moi et qui était là pour me soutenir, mes enfants **George**, **Marcel** et **Edouard**, sans qui cette expérience ne serait pas aussi sportive, ma maman **Elena**, ma sœur **Olya** et mon frère **Alexandre** pour leur soutien malgré la distance physique qui nous sépare.

Merci à mon directeur de thèse **Romain.** Je te suis très reconnaissante pour ta confiance, l'autonomie et la liberté que j'avais pendant ma thèse. Je n'étais peut-être pas la thésarde exemplaire mais j'ai toujours fait de mon mieux. Pour moi le but primaire de cette expérience avant tout était de devenir une scientifique, raisonner comme une scientifique, s'exprimer comme une scientifique et poser de bonnes questions. Je te remercie pour ton encadrement et j'ai l'impression que cette expérience est plutôt réussite.

Merci à **Patrick Mehlen**, de me soutenir dans mon projet avec les imprévus et les obstacles.

Merci à **Pierre Nahon** pour l'expertise clinique.

Merci à **Mathieu Richaud**, pour ta disponibilité et ton aide dans les études in vivo.

Merci à **Benjamin Gibert** pour tes conseils, à **Benjamin Ducarouge** et **David Neves** pour le support dans les études in vivo.

Merci à **Zuzana Macek-Jilkova** pour notre collaboration et les balades ensemble à Prague en 2020.

Merci à **Marie-Agnes Vittoz**, qui a été mon support dans les périples burocratiques.

Merci à **Alexia**, j'espère de pouvoir garder l'amitié créée sur 4 ans passés ensemble dans notre bureau. Merci à **Francesca**, le soleil italien.

Merci à **Chloé Goldsmith**, qui m'inspirait et égayait les journées grises, à **Claire Verzeroli**, le soutien quotidien au laboratoire, toujours en forme, souriante et dynamique, à **Romain Barnault** pour tes conseils, à **Guada Martinez** pour ton sourire et ton expertise en génétique, à **Damien Cohen** pour tes conseils en séquençage et ta bonne humeur.

Merci à **Margot, Jennifer, Yasmina, Marie-Laure, Andres, Christophe, Isabelle, Françoise, Léa, Boyan, Charlotte** et **Mailys,** mais aussi à **Aurore** et **François-Xavier, Michelle** et **Jean-Pierre**.